Interferon-stimulated Genes and Their Role in Controlling Hepatitis E Virus

Lei Xu

The studies presented in this thesis were performed at the Laboratory of Gastroenterology and Hepatology, Erasmus MC-University Medical Center Rotterdam, the Netherlands.

The research was funded by:

- Netherlands Organization for Scientific Research (NWO)
- Dutch Digestive Foundation (MLDS)
- Daniel den Hoed Foundation

Financial support for printing of this thesis was provided by:
Erasmus Postgraduate School Molecular Medicine

Cover design: DAOSI Advertising Design, Xi'an, China. Layout design: the author of this thesis.

Printed by: Ridderprint BV, Ridderkerk, the Netherlands

ISBN: 978-94-6299-624-3

Interferon-stimulated Genes and Their Role in Controlling Hepatitis E Virus

Interferon gestimuleerde genen en hun rol bij de controle van hepatitis E virus

Thesis

to obtain the degree of Doctor from the
Erasmus University Rotterdam
by command of the
rector magnificus

Prof. dr. H.A.P. Pols

and in accordance with the decision of the Doctorate Board

The public defense shall be held on

Tuesday 27th June 2017 at 15:30

by

Lei Xu

born in Yangling, Shaanxi Province, China

Erasmus University Rotterdam

Doctoral Committee

Promoter:

Prof. dr. M.P. Peppelenbosch

Inner Committee:

Prof. dr. R.A. de Man

Prof. dr. R.A.M. Fouchier

Prof. dr. P.J. Coffer

Copromoter:

Dr. Q. Pan

CONTENTS

Chapter 1

General Introduction and Outline of This Thesis

During the early 1980s, waterborne hepatitis outbreak was reported and later denominated as Hepatitis E [1, 2]. Hepatitis E virus (HEV) was first discovered in a feces sample in 1983 [3] and molecularly cloned in 1990 [3]. However, due to the lack of culture system, studies of HEV life cycle, pathogenesis, genome variability and other molecular characteristics were substantial hampered. HEV is a positive-strand RNA virus, its genome contains a 7.2 kb RNA that typically contains three open reading frames (ORFs) [4]. The diameter of HEV virions is around 27 - 34 nm [4].

HEV belongs to the *Orthohepevirus* genus within the *Hepeviridae* family [5]. With the development of the sequencing technology, genetically different HEV strains were identified, the *Hepeviridae* family can be classified as genera: genus *Orthohepevirus* (all mammalian and avian HEV isolates) and genus *Piscihepevirus* (cutthroat trout virus) [6, 7]. Within the *Orthohepevirus* species, at least four genotypes (gts) are known have the ability to infect humans and all belong to a single serotype. Gt1 HEV mainly causes large outbreaks in Asia. Gt2 can also cause large outbreaks and is mainly restricted in Mexico and some African countries [7]. Gt3 HEV infection can cause chronic hepatitis in specific population such as immunocompromised patients in industrialized countries [8, 9]. Gt4 HEV infection is mainly prevalent in China and Japan [10-12]. Both gt3 and gt4 HEV are zoonotically transmitted and animal reservoirs play important roles during transmission and epidemiology [7].

Course of HEV infection

Acute infection

Gt1 and gt2 HEV are the main HEV genotypes that could cause the waterborne outbreak of acute HEV infection in developing countries [13-15]. Therefore, to control the HEV infection, basic sanitation is thought to be the first strategy against HEV infection. Both gt1 and gt2 HEV are strictly restricted to humans. Importantly, gt1 infection is particularly dangerous for pregnant women: infected expecting mothers display severe symptoms and an extremely high mortality, up to 25% [16-18]. Currently, in Nepal and China, large-scale randomized, double-blind studies are performed based on a recombinant-produced vaccine against gt1 HEV [19-21]. However, only one vaccine named Hecolin has been licensed in China since 2012.

Gt3 and gt4 HEV have a broad host range including wild animals and domestic animals. Pigs and game are thought to be the main reservoirs. Zoonotic foodborne transmission is the most common route of sporadic infection [13]. However, other

transmission routes can not be ruled out. The detection of HEV RNA in milk from infected cows provides us new clue that how the zoonotic transmission occurred [11]. The seroprevalence rate of HEV in developed countries is diverse, ranging from 5% to 20% and the highest seropositive rate has been reported in southwest France [22]. In the Netherlands, the HEV seropositive rate in general population is around 30% and the prevalence increase with age [23, 24]. A small group of study among hospital-associated patients indicates that HEV also plays an important role in causing acute hepatitis in this specific population in the Netherlands as well [25].

Chronic infection

Chronic HEV infection is mainly caused by gt3 HEV [4]. In European countries, chronic HEV infections are mainly found in immunocompromised patients, for example in transplantation recipients, HIV patients and patients under chemotherapy [8, 9, 26-28]. Chronic HEV infection confers a high risk for developing into to cirrhosis and in transplantation patients also causing graft loss, eventually leading to a requirement for new transplantation [4, 8, 9]. Interestingly, most of the chronic infections in organ transplant recipients were reported in European countries, whereas only a limited number of cases have been reported from the North America. This may probably due to the lack of standard diagnostic test approved for clinical use in this region.

Anti-HEV treatment

Usually, acute HEV infection is a self-limiting disease and the antiviral treatment is not necessary. In some cases, such as in pregnant women and immunocompromised patients, antiviral therapies are required. Pegylated (PegIFN-α) or ribavirin monotherapy or a combination have been used in this respect [29-32]. Although both antiviral treatments have strong antiviral potential, as evident from *in vitro* study [33-35], ribavirin as monotherapy has been more widely used recently. The reason is that most chronic infections HEV occurred in organ transplantation patients and thereby the use of IFN-α is associated with side effects that sometimes lead to graft rejections. Therefore, ribavirin has become the best choice in this respect and its efficacy has been proven [36]. Meanwhile, ribavirin also shows its clinical effectiveness when treating severe acute HEV infection [37, 38].

Although ribavirin is effective in most acute and chronic patients, there were cases had been reported that recurrence was found during or after ribavirin treatment [39]. A

sequencing study found a G1634R mutation in the HEV RdRp domain (Fig. 1) may associate with the treatment failure [39]. A similar mutation was also observed in a different study [40]. Interestingly, both studies showed that this mutation did not alter the sensitivity towards ribavirin treatment [39, 40]. Instead, the replication fitness of HEV was improved when introducing this G1634R mutation into the wide-type virus. Recently, more mutations were identified to be associated with the ribavirin resistance. For instance, Y1320H, G1634R mutations and an insertion in the hypervariable region were found to be related to the increase replication of HEV, while the K1383N mutation was found related to decrease replication and conferred enhanced sensitivity to ribavirin [41]. A recent study found that the 1634R variant has lower prevalence in patients that achieve sustained virological response (SVR) as compared to patients with treatment failure [42]. However, even in the presence of this 1634R mutation, a second ribavirin treatment still has therapeutic effects [42]. Therefore, whether there is clinical potential to use this mutation as a biomarker to predict the ribavirin treatment outcome still needs further exploration [42].

The combination of ribavirin related viral resistance and IFN-α related severe side effect create an urgency to develop new antiviral therapies. Sofosbuvir, an HCV polymerase inhibitor, was shown has the ability to inhibit gt3 HEV replication *in vitro* [43], but some inconsistent results have also been reported [44]. Interestingly, this drug failed in clearing HEV viremia in a patient that was co-infection with both HCV and HEV [45]. Thus, more studied are required to evaluate the anti-HEV potential of this drug. In our recent study, we have found that the activation of protein kinase C alpha (PKCα) and its downstream pathway strongly inhibits HEV replication [46]. In addition, the nucleotides synthesis pathway also constitutes a potential anti-HEV target. We have proven that the inhibition of the pyrimidine pathway exerted strong anti-HEV effect [47]. Interestingly, we observed that the gene expression of many ISGs is up-regulated when this pathway is blocked and importantly, this happens in an IFN-JAK-STAT axis independent manner. However, whether this up-regulation of ISG expression contributes to the antiviral ability of these nucleotide synthesis inhibitors is still unclear [47]. Taken together, all these studies provide new ideas to develop novel antiviral drugs against HEV infection and encourage investigation in this respect.

Most chronic HEV infection happens in immunocompromised patients, therefore, it is important to assess the effect of different immunosuppressive drugs [48]. *In vitro* studies from our group have shown that mTOR inhibitors (rapamycin, everolimus) and calcineurin

inhibitors (cyclosporin A, tacrolimus) enhance HEV replication in cell culture models [49, 50]. In contrast, mycophenolic acid (MPA) effectively suppresses HEV replication [50]. Although these important findings give some clues that different immunosuppressive drugs may affect the propagation of HEV, there are only limited studies available reporting the effect of these drugs in patients. A recently study showed that patients received mTOR inhibitor treatment have higher HEV RNA levels as compared to those had calcineurin inhibitors treatment [51], whereas the treatment of mycophenolic acid had no influence on the effect of ribavirin [51]. *In toto*, a picture emerges in which different type of immunosuppressive interacts with the HEV infectious process. Studies focus on the interaction details shall be continued.

Molecular organization of HEV

The HEV genomic RNA is 7-methylguanylate (m^7G) capped at the 5' end and has a poly-A tail at the 3' end [4]. It is generally believed that the HEV RNA contains three open reading frames (ORFs) [4, 13, 52]. ORF1 encodes a nonstructural protein is essential for RNA replication [53]. ORF2 protein is the viral capsid protein [4]. ORF3 is a small protein that may play a poorly defined role during the viral secretion step [4]. Recently, a novel ORF4 was defined in gt1 HEV [54]. Usually, two different HEV RNAs are produced during the HEV life cycle, a 7.2 kb full-length RNA and a 2.2 kb subgenomic RNA (Fig. 1).

ORF1 is the largest ORF in HEV genome which constitutes almost 70% of the genomic length [4]. ORF1 translates into a polyprotein [4]. Employing computer-assisted alignments, in ORF1, eight putative domains are discerned based on the similarity with other viruses [55]. The main functional domains including an RNA-dependent RNA polymerase (RdRp) domain, a Y domain (Y), a methyltransferase (MeT), a macro, a papain-like cysteine protease (PCP) and an RNA helicase (Hel) domain (Fig. 1) [56]. The function of each domain still needs further investigations.

The putative PCP domain of ORF1 has some homology with the protease of Rubella virus [55]. However, the function of the PCP during HEV replication is still controversial. Generally, positive-strand RNA virus expresses proteases for processing viral polyproteins or host proteins to foster the infectious process. Many studies support the idea that HEV PCP also processes the ORF1 polyprotein [57-62]. However, the absence of processing activity by ORF1 PCP has also been reported [63-65]. Further studies should continue to address this issue since a clear understanding of this question and this will open novel avenues for developing

new anti-HEV drugs that directly target this protein. Such studies would also extend our knowledge on the HEV life cycle and pathogenesis in general.

Hel domain exerts NTPase and RNA unwinding activities [66]. Meanwhile, Hel also plays important roles during cap formation [67]. Thus, HEV may employ this protein to initiate the synthesis of 5' cap RNA [67]. Therefore, HEV helicase may exert two functions in one protein, a strategy common to viruses, which are under evolutionary pressure to encode multiple viral proteins in a relatively small genome.

The Met domain is at the N-terminus of the ORF1 polyprotein. Computer-assisted sequence analysis revealed AA (amino acids) residues 56-240 was predicted as the putative Met domain [55]. The RdRp domain is located at the end of HEV ORF1 [4]. RdRp is a viral protein that is required for all positive-stranded RNA viruses and plays an essential role during RNA replication. Purified recombinant HEV RdRp protein has the ability to bind to the 3' end of viral RNA, which is a potential location for a replication start site [68]. The expression of GFP-tagged RdRp protein demonstrates that it locates to the endoplasmic reticulum, where it might be colocalized with the negative-stranded RNA synthesis [69]. Importantly, the recently reported above-mentioned ribavirin-related HEV mutations mainly emerge in this domain [39, 41, 42, 70, 71].

The ORF2 encodes capsid is a 72 KD protein constituting of 660 AA (Fig. 1). It can be glycosylated at Asn 132, Asn 310 and Asn 562 sites [72-74]. However, it is not clear whether these glycosylation sites exert any biological function for HEV infection since it is not common for the non-enveloped viruses to have their capsid proteins glycosylated. Mutagenesis studies revealed that the elimination of potential glycosylation sites will lead to the loss of infectious ability of the virus particles [75]. HEV that derived from cell culture medium has a lipid envelope [76] and the non-enveloped and quasi-enveloped HEV have a distinct entry mechanism [77]. However, whether there is any relation between the glycosylation of ORF2 and the lipid envelope still requires further study. The HEV capsid protein contains three linear domains named as S domain (AA 129-319), M domain (AA 320-455) and P domain (AA 456-606) that constitute a neutralizing epitope [78-81]. With the 3.5-A resolution crystal structure of HEV VPL (viral-like particles), it showed that the HEV VPL structure is consistent by 60 subunits capsid protein [81]. Meanwhile, a mutation study showed that the P domain plays important roles with regard to the binding to the host cells, and that, as said, it contains some epitopes for antibody-mediated neutralization [81].

The ORF3 partially overlaps with ORF2 and it is the smallest ORF of HEV. The ORF3 protein encodes a product of 13 KD (VP13) and constitutes of 113 AA (gt3) or 114 AA (gt1, 2 and 4) [4]. It contains a phosphorylation site (Ser71) that can be phosphorylated by MAPK (mitogen-activated protein kinase) [82]. Based on a hybridization study, ORF3 was suggested to may play a regulatory in the signal transduction pathway [83]. An early study showed that the ORF3 protein associates with cytoskeletal fraction via its hydrophobic N-terminal domain [82]. In a subsequent study, GFP-tagged ORF3 was shown to interact with microtubules and to have the ability to modulate its dynamics [84]. In a recent *in vivo* study, the ORF3 protein was found to be mainly located near to the apical membrane and within the bile canaliculi, which suggests that this protein plays some roles during HEV egress and viral secretion into the bile [85]. *In vitro* studies also demonstrated that ORF3 is required for the egress of HEV [86, 87]. Apart from these cellular functions, the ORF3 protein was also reported to interact with HEV viral proteins such as Hel, PCP and Met, suggesting it plays important roles during HEV replication as well [88]. However, the exact function and structure of HEV ORF3 protein still need further investigations.

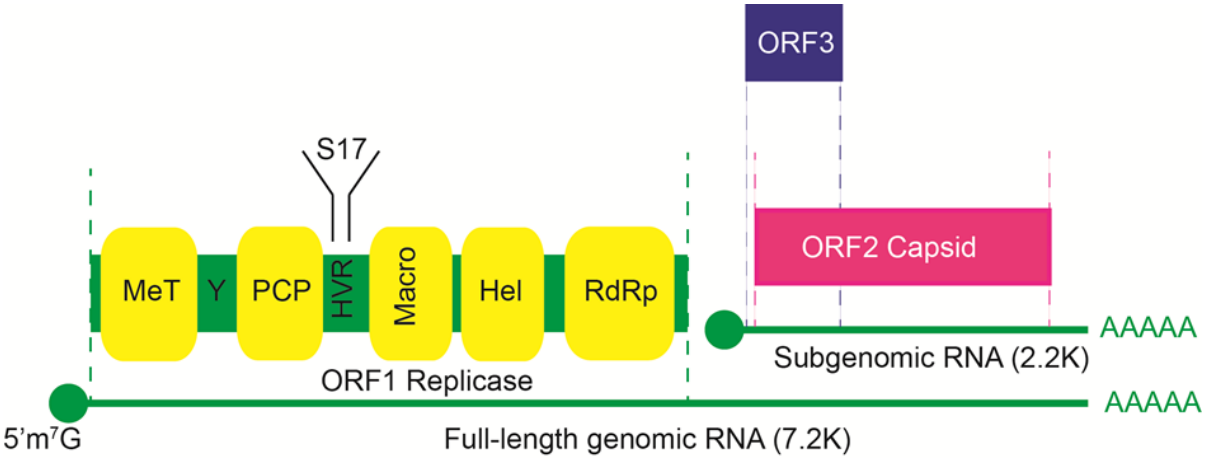

Figure 1. Molecular organization of HEV RNA.

The HEV genome is a 7.2 kb, single-stranded positive RNA. It has a 7-methylguanylate (m^7G) at the 5' end and a poly-A tail at the 3' end. Usually, it has three open reading frames (ORFs). It is generally believed that two HEV RNA are produced during replication, a 7.2 kb full-length RNA and a 2.2 kb subgenomic RNA. ORF1 is a polyprotein translated from the 7.2 kb full-length RNA. It has several domains including methyltransferase (Met), Y domain (Y), papain-like cysteine protease (PCP), hypervariable region (HVR), Macro, RNA helicase (Hel), RNA-dependent RNA polymerase (RdRp). ORF2 is the capsid protein and ORF3 partially overlaps with ORF2. Both of them are translated from the 2.2 kb subgenomic RNA. An insertion of human sequences (S17) into the HVR domain increases cell culture adaptation.

Recently, a novel viral protein ORF4 was identified in gt1 HEV [54]. Interestingly, unlike other HEV viral proteins, it is a protein that induced by endoplasmic reticulum (ER) stress via

the internal initiation mediated translation to promote gt1 HEV infection [54]. This unique protein interacts with multiple viral and cellular proteins [54]. Together with host eEF1α1 (eukaryotic elongation factor 1 isoform-1), ORF4 increases HEV RdRp activity to enhance viral replication and an ORF4 stably expressed human hepatoma cells have higher HEV replication level [54]. This novel ORF4 protein was only found in gt1 HEV [54]. Whether this protein is related to the higher pathogenicity of gt1 HEV is still unclear and needs further investigation.

HEV cell culture models

Since the discovery of HEV virus, great efforts have been taken to propagate this virus in cell culture systems. However, such cell culture mediated production is still relatively inefficient and seems ineffective. With regard to producing infectious virus, as a surrogate, a virus that is also a member of *Hepeviridae* family, Cutthroat trout virus (CTV) is developed as an alternative virus model to study the replication cycle of HEV [89]. Gt3 and gt4 HEV have been successfully cultured under laboratory conditions. However, until now, there is only one study that reported a successful culture of patient serum-derived gt1 HEV without transfection RNA directly into host cells [90]. An attempt to infect swine kidney cells with gt1 HEV revealed that the HEV infectivity was inhibited at multiple steps [91].

For single-stranded positive RNA viruses, the direct transfection of RNA into host cells is a commonly used strategy, in which the thus-delivered RNA is able to start the translation of viral protein just after transfection. *In vitro* transfection of plasmid-derived capped HEV RNA in two different cell lines, PLC/PRF/5 and Huh7 cells were shown to support HEV replication and the production of infectious virions [92]. A better replication result of gt1 HEV (Sar55) was observed in a subclone of the Huh7 cell, S10-3 cell [93]. Nevertheless, all these studies required the delivery of HEV RNA into the host cell that may not totally recapitulate the real infection progress and thus, the host response.

Gt3 HEV from an acute hepatitis patient can be cultured in PLC/PRF/5 cells [94] and A549 cells [95]. Interestingly, a gt3 HEV strain named Kernow-C1 was isolated from a chronic patient and had the ability to infect different human and animal cell lines such as pig and deer cells [93]. They also observed an insertion of human sequences into the HEV viral genome (ORF1, HRV) (Fig. 1) [93]. Since this insertion was noticed after six passages, this strain was denominated as Kernow-C1 p6. The following study demonstrated that this 171-

nucleotide insertion is important for the enhanced replication ability of this p6 strain [96]. The gt3 HEV Kernow-C1 p6 is a widely used cell culture system by different research groups [39, 41, 96-98]. In the present thesis, I also used this gt3 Kernow-C1 p6 strain. The observation that gt3 HEV has the ability to the complete life cycle in pluripotent stem cell (PSC)-derived hepatocytes may provide new ideas for developing novel HEV cell culture system [99]. Gt4 HEV from the feces of experimentally infected monkeys can be effectively cultured in the PLC/PRF/5 and the replication of this strain was inhibited by IFN-α [100].

Animal models

Rabbits are used as a model to recapitulate HEV infection and to evaluate vaccine efficacy [101]. For certain HEV strains, acute infection can even develop to chronic infection in rabbit models [102, 103]. Another widely used experimental model to investigate HEV infection is pigs [104, 105]. Other animals like rat [106] and Mongolian gerbils [107] are also reported to support infection by certain strains of HEV.

Recently, three different groups reported that the human liver chimeric mice could be used for modeling chronic HEV infection [85, 108, 109]. Stool-derived HEV gt1 and gt3 have the ability to establish a long-term HEV infection in the UPA/SCID/beige chimeric mice that have humanized liver [85]. Interestingly, a gt1 HEV-infected mouse can infect naïve humanized mice when they stay in the same cage, indicating that gt1 HEV infection can be transmitted fecal-orally or through direct physical contact route [85]. However, feeding of these mice with HEV contaminated food was not able to create a robust infection. Therefore, the direct physical contact route or the blood route via micro-injuries cannot be ruled out. Of note, compared to gt1 infection, gt3 infection showed a more slow progression and displayed lower viral titers with respect to the latter strain [85]. This appears consistent with the clinical observation that gt1 HEV mainly leads to acute infection, whereas gt3 mainly leads to chronic infection. Importantly, neither gt1 nor gt3 infection induces any liver damage [85]. The commonly used anti-HEV drug ribavirin has convincing antiviral ability in these models against gt1 HEV infection. Nevertheless, the antiviral potential of ribavirin and another commonly used anti-HEV drug, IFN-α should also be evaluated regarding gt3 HEV infection [85].

In another study, in such animals it was demonstrated that cell cultured-derived HEV did not result in a detectable HEV infection, but when the supernatant was treated with

sodium deoxycholic acid and trypsin, the HEV RNA can be detected in some mice, albeit not in all mice. Chimpanzee-derived HEV can infect humanized mice. Stool suspension from gt1 (Sar55) HEV infected chimpanzees was intrasplenically injected and led to robust infection. Viral titer was 10- to 100- fold higher in stool than in plasma. Patient-derived gt3 HEV could also infect this humanized mice model, consistent with the above-mentioned study [85]. It was also observed that a relatively low viral titer was reached in gt3 infection mice as compared to gt1 HEV-infected mice. Gt1 HEV-infected mice display a small up-regulation of host ISG expression, while a large subset of ISG is intact during infection [108].

In a third study, immunocompromised patient-derived gt3 HEV was used to infect chimeric mice that have a humanized with human liver [109]. Interestingly, they also found human feces- or liver-derived HEV has the ability to establish a chronic infection in this mice model. HEV RNA can be detected in all infected mouse livers [109]. It was also noticed that HEV from cell culture medium or patient plasma failed to infect these chimeric mice [109]. In summary, all three studies used humanized chimeric mouse to model chronic HEV infection, feces-derived HEV superior with respect to infection in these models. All these chimeric humanized mouse models provide valuable tools to study the acute and chronic infection of HEV. However, further studies that use these models to evaluate the new anti-HEV therapy should be conducted.

Host response and IFN pathway

Usually, viral infection induces an innate immune response by producing interferons (IFNs), especially the production of type I IFNs [110]. Human type I IFNs is a group of antiviral cytokines than can be divided into many subtypes including IFN-α and IFN-β [111]. This type of IFNs plays essential roles in defending viral infection and human with defected IFN production or receptors are more sensitive to viral infections [112-114]. After viral infection, the production of type I IFNs is mainly triggered via the detection of pathogens by pattern recognition receptors (PRRs) [110]. Viral nucleic acids are important PAMPs that can be sensed by different kinds of PRRs. For example, Toll-like receptor 3 (TLR3) have the ability to recognize ds-RNA (double-stranded RNA) and retinoic acid-inducible gene 1 (RIG-I) detect viral RNA with unique signatures in the cytoplasm [115]. Meanwhile, melanoma differentiation associated protein 5 (MDA5) is also a cellular RNA sensor that has the ability to sense the present of viral RNA in the cytoplasm [116]. For DNA viruses, its nucleic acids

could be detected by DNA sensor, cyclic GMP-AMP synthase (cGAS) [117]. Upon the detection of virus by these PRRs, the downstream pathways will be activated which eventually leading to the production of anti-viral cytokines, especially type I IFNs [110]. More specifically, RIG-I and MDA5 converge on the mitochondrial antiviral signaling protein (MAVS) which located in mitochondrial membrane while cGAS could activate the stimulator of IFN genes (STING) which mainly distributed in the endoplasmic reticulum (ER) [110]. After the stimulation of MAVS and STING, interferon regulatory factor 3 and 7 (IRF3 and IRF7) will be phosphorylated [110] and transported into the nucleus. Meanwhile, the NF-κB pathway will be also activated by IRF3 and 7 [110]. Next, all these transcription factors including IRF3, 7 and NF-κB bind to the promotor region of antiviral cytokines like type I IFNs (Fig. 2) [110]. The binding leads to the gene expression of IFNs genes and eventually protein productions.

Once the IFNs have been produced and secreted, the IFN proteins bind to the cell surface receptors complex such as IFN-α receptor 1 (IFNAR1) and 2 (IFNAR2) [111]. The binding of IFN proteins and receptor chains leads to the activation of STAT (signal transducers and activators of transcription) 1 and 2 via the phosphorylation of JAK1 and TYK2 (Janus kinase 1 and Tyrosine kinase 2) [110]. The phosphorylated STAT1, STAT2 together with IRF9 will form a complex named IFN-stimulated gene factor 3 (ISGF3). This complex will be transported into the nucleus and bind to a unique element named IFN-stimulated response elements (ISRE) and finally leading to the transcriptional regulation of more than 300 IFN-stimulated genes (ISGs) [110]. The products of these genes are thought to be the ultimate effectors of IFN [110, 118, 119]. It has been shown that many of the ISGs exert their antiviral function at different steps of viral life cycles [110, 118, 119]. For instance, IFITM3 and MX2 inhibit viral entry [120-123], IFIT1 inhibits viral protein translation [124], Viperin (also known as RSAD2) inhibits virus at the egress stage [125]. Meanwhile, a large number of ISGs play regulatory roles in pathogen recognition and cellular signaling pathways. Many ISGs are induced by IFNs but also involved in signal transduction such as IRF9 and STAT1, which have the ability to rapidly amplify the IFN-initiated cell cascade [110]. Interestingly, many of the PRRs are also ISGs that constitutively expressed at host cell. After viral infection, these PRRs such as MDA5, RIG-I and cGAS were induced by IFNs, which eventually scaling up the IFN productions [110, 118, 119, 126]. Finally, some ISGs such as SOCS are negative regulators that prevent the excessive expression of IFNs and ISGs, which have pathological outcomes for the host cells [110]. They also help the activated cells back to homeostasis status [110]. Taken

together, the host response to viral infection by producing antiviral IFNs, the IFN establish an antiviral status by the transcriptional regulation of a large number of ISGs. These ISGs form a complicated web that eventually eradicates virus invasion.

Host response to HEV infection

Until now, there are limited studies about the cellular immune response after HEV infection. An RNA-Seq based transcriptome analysis of Huh7 cells infected by gt1 HEV demonstrated that totally 306 genes were affected. Most of the genes were related to immune response and signal transaction [127]. SIRP-α (signal regulator protein α) was strongly stimulated while pIRF3 was down regulated by gt4 HEV infection, which eventually leading to the negative regulation of IFN-β and the host innate immune system [128]. Gt4 HEV infection in A549 cells affects the protein expression of totally 31 proteins, as revealed by a proteomics analysis [100]. Among these 31 proteins, 10 proteins were up-regulated while the rest were down-regulated [100]. In a PLC/PRF/5 cells based monkey feces-derived gt4 HEV cell culture model, HEV infection leads to the up-regulation of many ISGs including IFI27, IFI6, MX1, and CMPK2 [129].

As combat strategies, HEV developed different tools to manipulate the host immune response. HEV was found have the ability to suppress poly (I:C)-initiated immune response and the product of HEV ORF1 was the antagonist [130]. By screening each domain of the ORF1, the author revealed that the PCP domain inhibits IFN-β expression by deubiquitinating RIG-I and TBK-1, which are key components involved to type I IFN expression. Meanwhile, they identified the X domain (macro domain) also play some roles in the suppression of IFN-β expression [130]. In another study done by the same author, ORF3 was found to stimulate poly (I·C)-initiated immune response through the interaction of one important PRR for type I IFN expression, RIG-I [131]. HEV ORF3 protein stimulates RIG-I controlled IFN-β expression by activating RIG-I expression and function [131]. Interestingly, these two studies showed that one virus has different effects on the same host cellular response. What is the exact role of this difference in establishing an infection is still unclear and needs further investigation. In another study, they showed that the IFN-α induced STAT1 phosphorylation and ISG expression were inhibited by HEV infection [132]. They further identified ORF3 alone have the ability to complete this inhibition effect [132]. Similarly, the IFN-initiated ISG expression was suppressed in HEV infected cell. In line with this, in **Chapter 4,** we also observed the similar

results. We demonstrated that the IFN-initiated ISG expression was inhibited by HEV infection [35].

Beside IFN pathway, other cellular pathways were also influenced by the HEV infection. For instance, the transfection of HEV ORF2, but not ORF3 in human hepatoma cells inhibits NF-κB signaling activity by the disruption of IκBα ubiquitination [133]. Meanwhile, an ORF3 protein from a gt1 strain was also reported has the ability to inhibit TNF-α induced NF-κB pathway activation [134]. Furthermore, the ORF3 protein was also reported to regulate the transportation of STAT3, which may affect regulation of the inflammatory response [135]. Altogether, the difference of HEV viral proteins in modulating innate immune response suggests further investigations are required.

Although the cell culture system could reflect the host response after HEV infection, it cannot totally capture the *in vivo* infection course and immune response. Therefore, many studies were performed in animal models and in patients. In a chimpanzees model that infection with gt1 HEV, 58 ISGs were up-regulated in acute HEV infection. However, the induction level was much lower compared to HCV infection, which had a stronger induction of ISG expression [136]. In a study performed in whole blood from patients with chronic HEV infection, they found a total number of 30 genes were stimulated compare to health patients [137]. Interestingly, 25 out of these 30 genes were ISGs and the expression of some ISGs was correlated with HEV persistence [137]. Since HEV infection is more severe in pregnant patients, a study was focused on the relation between cytokines and HEV infection outcomes [14]. They showed that the expression level of many cytokines was much higher in HEV infected women [14]. This suggested the high mortality of HEV infection in pregnant women might due to the high level of cytokine productions [14, 16-18]. Interestingly, the cytokines such as TLR3 and IFN-γ were reported to have a beneficial role during HEV infection [138]. Patients with higher expression levels of TLR3 and IFN-γ are pro to eradicate infection and get full recover [138]. In **Chapter 7,** we revealed that the antiviral ability of IFN-α against HEV and HCV can be enhanced by one important cytokine, TNF-α. We showed that the downstream of TNF-α, NF-κB can directly bind to the ISRE motif in the ISG promoter to drive the transcription of antiviral ISGs [139]. However, the *in vivo* roles of TNF-α are still unclear. It was reported that the polymorphisms of TNF-α are related to HEV infection outcomes, for example, the genotype -308AA was more common found in gt1 HEV infected patients [140]. Taken together, cytokines, especially IFNs play important roles during HEV

infection. Meanwhile, HEV also develops different strategies to combat the host immune response. However, there are limited studies currently about the virus-host interactions, especially the interaction between HEV infection and innate immunity. Further investigations should focus on this field.

Scope of this thesis

As discussed above, IFN-α and ribavirin were used to treat chronic HEV patients [29-32]. However, failures of ribavirin treatment were observed [39, 42, 71] and thereby new antiviral treatments are urgently required. The IFN pathway plays an important role in defending viral infection through the expression of ISGs [110, 118], but little is known about the relation between HEV infection and IFN/ISG pathway. In this thesis, we aimed to investigate anti-HEV activities of IFN pathway and its mechanism-of-action. We first studied the anti-HEV potential of IFNs against HEV in cell culture models. Next, we mainly focused on the anti-HEV ability of many important ISGs and the mechanism-of-action of some key anti-HEV ISGs. Meanwhile, some novel mechanisms that regulate ISG transcription and their role in controlling HEV were also investigated.

Outline of this thesis

IFN-initiated cell signaling is the most important antiviral pathways against viral infection [110]. ISGs are the ultimate antiviral effectors and different cell pathways precisely controlled their expressions. In **Chapter 2,** we comprehensively reviewed the regulation of ISG transcription, including the canonical and non-canonical mechanisms. As mentioned above, many ISGs, especially some IRFs and PRRs were thought to exert their function through the induction of IFNs. In **Chapter 3**, we discussed the IFN-independent antiviral mechanisms of these ISGs in defending viral infections.

In **Chapter 4**, we characterize the antiviral potential of a panel of cytokines against HEV infection and identified IFN-α exert strong antiviral ability. We further comprehensively investigated the antiviral potential different type of IFNs against HEV replication in comparison with HCV. Given the fact that ISGs are ultimate effectors of IFN, in **Chapter 5**, by using an overexpression approach, we screened the anti-HEV potential of many important human ISGs. We identified RIG-I, MDA5 and IRF1 as the potent anti-HEV ISGs. In **Chapter 5**, we mainly focus on the mechanism-of-action of RIG-I. This extends our knowledge about the anti-HEV mechanism of IFNs and paves the avenues for developing new anti-HEV strategies.

In **Chapter 6,** we further investigated the antiviral mechanism of IRF1, which is an important ISG that have broad antiviral activities. The anti-HEV mechanism of IRF1 was investigated in multiple cell lines and the interaction with ribavirin was evaluated. In **Chapter 7**, we focus on another important antiviral cytokine, TNF-α. The antiviral ability of TNF-α and its novel mechanism that involved in the regulation of ISG transcription were investigated. In **Chapter 8**, we explore the mechanisms that allow antiviral ISGs constitutively expressed without IFN treatment. The antiviral potential of these basally expressed ISGs against HEV and HCV replication was evaluated. Since the virus totally relies on the host machinery to complete viral life cycles but little is known upon HEV infection. In **Chapter 9,** we focus on the role of host translation complex played during HEV replication. In **Chapter 10,** we studied whether HEV replication can be influenced by the host protein degradation system. The novel findings of this thesis were summarized and discussed in **Chapter 11.** This may provide a better understanding of the virus-host interaction during HEV infection and may open the gate to develop new antiviral therapies.

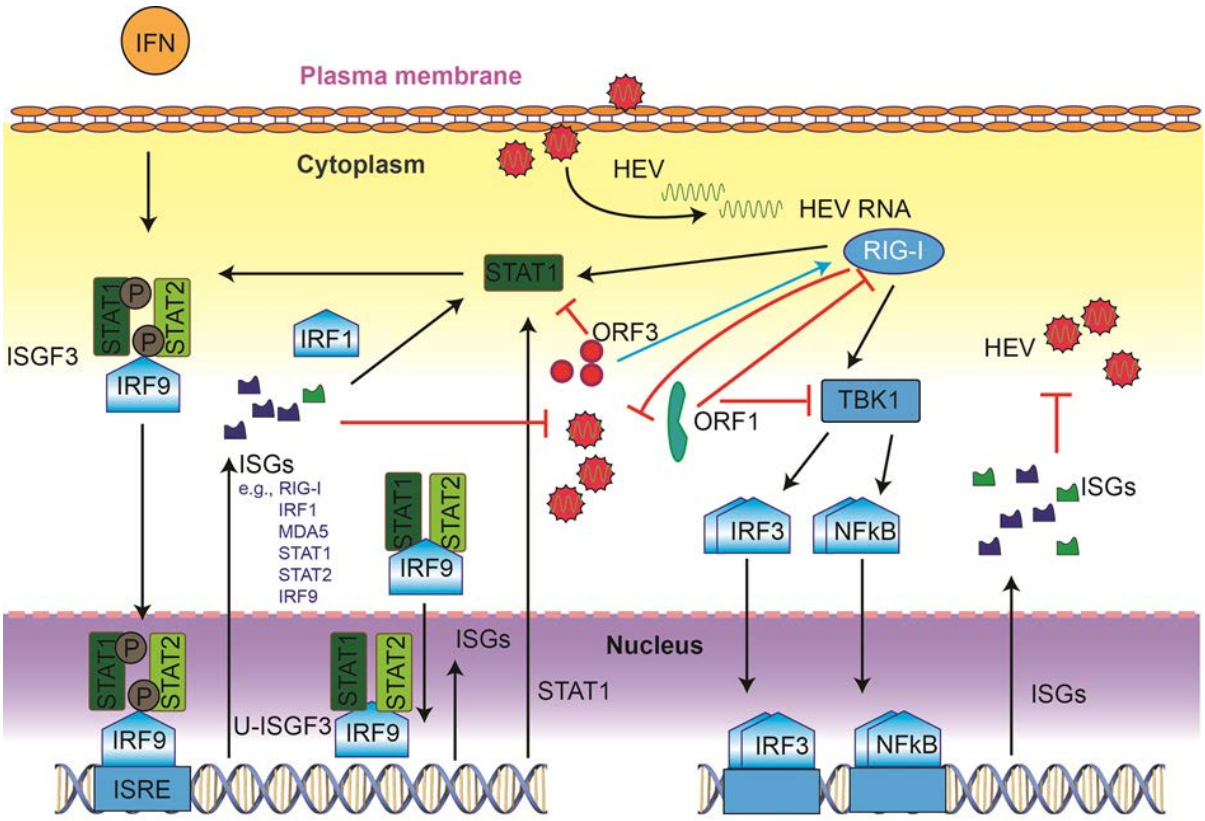

Figure 2. The interferon (IFN) pathway and HEV infection.

The binding of IFN and cell surface receptors leads to the phosphorylation of STAT 1 and 2. Phosphorylated STAT1, STAT2 together with IRF9 form the ISGF3 (IFN-stimulated gene factor 3) complex. This complex binds to ISRE (IFN-stimulated response elements) and then activates the

expression of ISGs (IFN-stimulated genes). HEV ORF1 was reported to inhibit poly (I:C)-initiated IFN expression by deubiquitinating RIG-I and TBK-1 (TANK Binding Kinase 1). Meanwhile, HEV ORF3 was reported to enhance innate immune response by direct interaction with RIG-I. At the same time, ORF3 also binds to STAT1 to prevent its phosphorylation and thereby inhibit IFN-initiated signaling cascades. In **Chapter 4**, we showed IFN-α exert strong anti-HEV ability. In **Chapter 5**, we studied the anti-HEV activity of each individual ISG. RIG-I, MDA5 and IRF1 were identified as the potent anti-HEV ISGs. We further showed RIG-I inhibits HEV replication independent of its IFN production ability, but partially through the phosphorylation of STAT1. In **Chapter 6**, we showed IRF1 inhibits HEV via the activation of the JAK-STAT pathway. In **Chapter 7**, we found TNF-α inhibits HEV replication through the activation of ISG expression. We further revealed that NF-κB, the downstream of TNF-α, have the ability to directly bind to the promoter region of many ISGs. In **Chapter 8**, we reported a novel mechanism that the unphosphorylated ISGF3 (U-ISGF3) complex drives the constitutive expression of ISGs in homeostatic condition. This novel U-ISGF3 complex consists by unphosphorylated STAT1 and STAT2 together with IRF9.

References

1. Khuroo, M.S., Study of an epidemic of non-A, non-B hepatitis. Possibility of another human hepatitis virus distinct from post-transfusion non-A, non-B type. *Am J Med*, 1980. **68**(6): p. 818-24.
2. Wong, D.C., et al., Epidemic and endemic hepatitis in India: evidence for a non-A, non-B hepatitis virus aetiology. *Lancet*, 1980. **2**(8200): p. 876-9.
3. Balayan, M.S., et al., Evidence for a virus in non-A, non-B hepatitis transmitted via the fecal-oral route. *Intervirology*, 1983. **20**(1): p. 23-31.
4. Debing, Y., et al., Update on Hepatitis E Virology:Implications for Clinical Practice. *J Hepatol*, 2016.
5. Emerson, S.U., et al., Hepevirus. *Virus taxonomy*, 2004. p. 853-857.
6. Smith, D.B., et al., Consensus proposals for classification of the family Hepeviridae. *J Gen Virol*, 2014. **95**(Pt 10): p. 2223-32.
7. Meng, X.J., Expanding Host Range and Cross-Species Infection of Hepatitis E Virus. *PLoS Pathog*, 2016. **12**(8): p. e1005695.
8. Behrendt, P., et al., The impact of hepatitis E in the liver transplant setting. *J Hepatol*, 2014. **61**(6): p. 1418-29.
9. Kamar, N., et al., Hepatitis E virus and chronic hepatitis in organ-transplant recipients. *N Engl J Med*, 2008. **358**(8): p. 811-7.
10. Zhang, L., et al., Prevalence of hepatitis E virus infection among blood donors in mainland China: a meta-analysis. *Transfusion*, 2016.
11. Huang, F., et al., Excretion of infectious hepatitis E virus into milk in cows imposes high risks of zoonosis. *Hepatology*, 2016. **64**(2): p. 350-9.
12. Nakano, T., et al., Investigating the origin and global dispersal history of hepatitis E virus genotype 4 using phylogeographical analysis. *Liver Int*, 2016. **36**(1): p. 31-41.
13. Kamar, N., et al., Hepatitis E. *Lancet*, 2012. **379**(9835): p. 2477-88.
14. Kumar, A., et al., Association of cytokines in hepatitis E with pregnancy outcome. *Cytokine*, 2014. **65**(1): p. 95-104.
15. Hakim, M.S., et al., The global burden of hepatitis E outbreaks: a systematic review. *Liver Int*, 2016.
16. Khuroo, M.S., et al., Incidence and severity of viral hepatitis in pregnancy. *Am J Med*, 1981. **70**(2): p. 252-5.
17. Patra, S., et al., Maternal and fetal outcomes in pregnant women with acute hepatitis E virus infection. *Ann Intern Med*, 2007. **147**(1): p. 28-33.
18. Krain, L.J., et al., Fetal and neonatal health consequences of vertically transmitted hepatitis E virus infection. *Am J Trop Med Hyg*, 2014. **90**(2): p. 365-70.
19. Shrestha, M.P., et al., Safety and efficacy of a recombinant hepatitis E vaccine. *N Engl J Med*, 2007. **356**(9): p. 895-903.
20. Zhu, F.C., et al., Efficacy and safety of a recombinant hepatitis E vaccine in healthy adults: a large-scale, randomised, double-blind placebo-controlled, phase 3 trial. *Lancet*, 2010. **376**(9744): p. 895-902.
21. Zhang, J., et al., Long-term efficacy of a hepatitis E vaccine. *N Engl J Med*, 2015. **372**(10): p. 914-22.
22. Mansuy, J.M., et al., Hepatitis E virus antibodies in blood donors, France. *Emerg Infect Dis*, 2011. **17**(12): p. 2309-12.
23. van Gageldonk-Lafeber, A.B., et al., Hepatitis E virus seroprevalence among the general population in a livestock-dense area in the Netherlands: a cross-sectional population-based serological survey. *BMC Infect Dis*, 2017. **17**(1): p. 21.
24. Hogema, B.M., et al., Past and present of hepatitis E in the Netherlands. *Transfusion*, 2014. **54**(12): p. 3092-6.

25. Tholen, A.T., et al., Hepatitis E virus as a Cause of Acute Hepatitis in The Netherlands. *PLoS One*, 2016. **11**(2): p. e0146906.
26. Colson, P., et al., Hepatitis E in an HIV-infected patient. *J Clin Virol*, 2009. **45**(4): p. 269-71.
27. Kamar, N., et al., Factors associated with chronic hepatitis in patients with hepatitis E virus infection who have received solid organ transplants. *Gastroenterology*, 2011. **140**(5): p. 1481-9.
28. Geng, Y., et al., Persistent hepatitis e virus genotype 4 infection in a child with acute lymphoblastic leukemia. *Hepat Mon*, 2014. **14**(1): p. e15618.
29. Kamar, N., et al., Pegylated interferon-alpha for treating chronic hepatitis E virus infection after liver transplantation. *Clin Infect Dis*, 2010. **50**(5): p. e30-3.
30. Mallet, V., et al., Brief communication: case reports of ribavirin treatment for chronic hepatitis E. *Ann Intern Med*, 2010. **153**(2): p. 85-9.
31. Dalton, H.R., et al., Treatment of chronic hepatitis E in a patient with HIV infection. *Ann Intern Med*, 2011. **155**(7): p. 479-80.
32. Kamar, N., et al., Ribavirin therapy inhibits viral replication on patients with chronic hepatitis e virus infection. *Gastroenterology*, 2010. **139**(5): p. 1612-8.
33. Debing, Y., et al., Ribavirin inhibits in vitro hepatitis E virus replication through depletion of cellular GTP pools and is moderately synergistic with alpha interferon. *Antimicrob Agents Chemother*, 2014. **58**(1): p. 267-73.
34. Todt, D., et al., Antiviral activity of different interferon (sub-) types against hepatitis E virus replication. *Antimicrob Agents Chemother*, 2016.
35. Zhou, X., et al., Disparity of basal and therapeutically activated interferon signalling in constraining hepatitis E virus infection. *J Viral Hepat*, 2016. **23**(4): p. 294-304.
36. Kamar, N., et al., Ribavirin for chronic hepatitis E virus infection in transplant recipients. *N Engl J Med*, 2014. **370**(12): p. 1111-20.
37. Pischke, S., et al., Ribavirin treatment of acute and chronic hepatitis E: a single-centre experience. *Liver Int*, 2013. **33**(5): p. 722-6.
38. Robbins, A., et al., Severe acute hepatitis E in an HIV infected patient: Successful treatment with ribavirin. *J Clin Virol*, 2014. **60**(4): p. 422-3.
39. Debing, Y., et al., A mutation in the hepatitis E virus RNA polymerase promotes its replication and associates with ribavirin treatment failure in organ transplant recipients. *Gastroenterology*, 2014. **147**(5): p. 1008-11 e7; quiz e15-6.
40. Todt, D., et al., In vivo evidence for ribavirin-induced mutagenesis of the hepatitis E virus genome. *Gut*, 2016. **65**(10): p. 1733-43.
41. Debing, Y., et al., Hepatitis E virus mutations associated with ribavirin treatment failure result in altered viral fitness and ribavirin sensitivity. *J Hepatol*, 2016. **65**(3): p. 499-508.
42. Lhomme, S., et al., Mutation in the Hepatitis E Virus Polymerase and Outcome of Ribavirin Therapy. *Antimicrob Agents Chemother*, 2016. **60**(3): p. 1608-14.
43. Dao Thi, V.L., et al., Sofosbuvir Inhibits Hepatitis E Virus Replication In Vitro and Results in an Additive Effect When Combined With Ribavirin. *Gastroenterology*, 2016. **150**(1): p. 82-85 e4.
44. Wang, W., et al., Distinct Antiviral Potency of Sofosbuvir against Hepatitis C and E Viruses. *Gastroenterology*, 2016.
45. Donnelly, M.C., et al., Sofosbuvir and Daclatasvir Anti-Viral Therapy Fails to Clear HEV Viremia and Restore Reactive T Cells in a HEV/HCV Co-Infected Liver Transplant Recipient. *Gastroenterology*, 2017. **152**(1): p. 300-301.
46. Wang, W., et al., Biological or pharmacological activation of protein kinase C alpha constrains hepatitis E virus replication. *Antiviral Res*, 2017. **140**: p. 1-12.
47. Wang, Y., et al., Cross Talk between Nucleotide Synthesis Pathways with Cellular Immunity in Constraining Hepatitis E Virus Replication. *Antimicrob Agents Chemother*, 2016. **60**(5): p. 2834-48.
48. Wang, Y., et al., Chronic hepatitis E in solid-organ transplantation: the key implications of immunosuppressants. *Curr Opin Infect Dis*, 2014. **27**(4): p. 303-8.

49. Zhou, X., et al., Rapamycin and everolimus facilitate hepatitis E virus replication: revealing a basal defense mechanism of PI3K-PKB-mTOR pathway. *J Hepatol*, 2014. **61**(4): p. 746-54.
50. Wang, Y., et al., Calcineurin inhibitors stimulate and mycophenolic acid inhibits replication of hepatitis E virus. *Gastroenterology*, 2014. **146**(7): p. 1775-83.
51. Kamar, N., et al., An Early Viral Response Predicts the Virological Response to Ribavirin in Hepatitis E Virus Organ Transplant Patients. *Transplantation*, 2015. **99**(10): p. 2124-31.
52. Wu, C., Y. Nan, and Y.-J. Zhang, New insights into hepatitis E virus virus–host interaction: interplay with host interferon induction. *Future Virology*, 2015. **10**(4): p. 439-448.
53. Nan, Y. and Y.J. Zhang, Molecular Biology and Infection of Hepatitis E Virus. *Front Microbiol*, 2016. **7**: p. 1419.
54. Nair, V.P., et al., Endoplasmic Reticulum Stress Induced Synthesis of a Novel Viral Factor Mediates Efficient Replication of Genotype-1 Hepatitis E Virus. *PLoS Pathog*, 2016. **12**(4): p. e1005521.
55. Koonin, E.V., et al., Computer-assisted assignment of functional domains in the nonstructural polyprotein of hepatitis E virus: delineation of an additional group of positive-strand RNA plant and animal viruses. *Proc Natl Acad Sci U S A*, 1992. **89**(17): p. 8259-63.
56. Ahmad, I., R.P. Holla, and S. Jameel, Molecular virology of hepatitis E virus. *Virus Res*, 2011. **161**(1): p. 47-58.
57. Paliwal, D., et al., Hepatitis E virus (HEV) protease: a chymotrypsin-like enzyme that processes both non-structural (pORF1) and capsid (pORF2) protein. *J Gen Virol*, 2014. **95**(Pt 8): p. 1689-700.
58. Karpe, Y.A. and K.S. Lole, Deubiquitination activity associated with hepatitis E virus putative papain-like cysteine protease. *J Gen Virol*, 2011. **92**(Pt 9): p. 2088-92.
59. Karpe, Y.A. and X.J. Meng, Hepatitis E virus replication requires an active ubiquitin-proteasome system. *J Virol*, 2012. **86**(10): p. 5948-52.
60. Parvez, M.K., Molecular characterization of hepatitis E virus ORF1 gene supports a papain-like cysteine protease (PCP)-domain activity. *Virus Res*, 2013. **178**(2): p. 553-6.
61. Ropp, S.L., et al., Expression of the hepatitis E virus ORF1. *Arch Virol*, 2000. **145**(7): p. 1321-37.
62. Sehgal, D., et al., Expression and processing of the Hepatitis E virus ORF1 nonstructural polyprotein. *Virol J*, 2006. **3**: p. 38.
63. Perttila, J., P. Spuul, and T. Ahola, Early secretory pathway localization and lack of processing for hepatitis E virus replication protein pORF1. *J Gen Virol*, 2013. **94**(Pt 4): p. 807-16.
64. Suppiah, S., Y. Zhou, and T.K. Frey, Lack of processing of the expressed ORF1 gene product of hepatitis E virus. *Virol J*, 2011. **8**: p. 245.
65. Ansari, I.H., et al., Cloning, sequencing, and expression of the hepatitis E virus (HEV) nonstructural open reading frame 1 (ORF1). *J Med Virol*, 2000. **60**(3): p. 275-83.
66. Karpe, Y.A. and K.S. Lole, NTPase and 5' to 3' RNA duplex-unwinding activities of the hepatitis E virus helicase domain. *J Virol*, 2010. **84**(7): p. 3595-602.
67. Karpe, Y.A. and K.S. Lole, RNA 5'-triphosphatase activity of the hepatitis E virus helicase domain. *J Virol*, 2010. **84**(18): p. 9637-41.
68. Agrawal, S., D. Gupta, and S.K. Panda, The 3' end of hepatitis E virus (HEV) genome binds specifically to the viral RNA-dependent RNA polymerase (RdRp). *Virology*, 2001. **282**(1): p. 87-101.
69. Rehman, S., et al., Subcellular localization of hepatitis E virus (HEV) replicase. *Virology*, 2008. **370**(1): p. 77-92.
70. Testoni, B., et al., Ribavirin restores IFNalpha responsiveness in HCV-infected livers by epigenetic remodelling at interferon stimulated genes. *Gut*, 2015.
71. Todt, D., et al., Mutagenic Effects of Ribavirin on Hepatitis E Virus-Viral Extinction versus Selection of Fitness-Enhancing Mutations. *Viruses*, 2016. **8**(10).
72. Zafrullah, M., et al., Mutational analysis of glycosylation, membrane translocation, and cell surface expression of the hepatitis E virus ORF2 protein. *J Virol*, 1999. **73**(5): p. 4074-82.

73. Jameel, S., et al., Expression in animal cells and characterization of the hepatitis E virus structural proteins. *J Virol*, 1996. **70**(1): p. 207-16.
74. Torresi, J., et al., Only the non-glycosylated fraction of hepatitis E virus capsid (open reading frame 2) protein is stable in mammalian cells. *J Gen Virol*, 1999. **80 (Pt 5)**: p. 1185-8.
75. Graff, J., et al., Mutations within potential glycosylation sites in the capsid protein of hepatitis E virus prevent the formation of infectious virus particles. *J Virol*, 2008. **82**(3): p. 1185-94.
76. Qi, Y., et al., Hepatitis E Virus Produced from Cell Culture Has a Lipid Envelope. *PLoS One*, 2015. **10**(7): p. e0132503.
77. Yin, X., et al., Distinct Entry Mechanisms for Nonenveloped and Quasi-Enveloped Hepatitis E Viruses. *J Virol*, 2016. **90**(8): p. 4232-42.
78. Guu, T.S., et al., Structure of the hepatitis E virus-like particle suggests mechanisms for virus assembly and receptor binding. *Proc Natl Acad Sci U S A*, 2009. **106**(31): p. 12992-7.
79. Casey, B.J., et al., Behavioral and neural correlates of delay of gratification 40 years later: Proc. Natl. Acad. Sci. U.S.A. 2011, Vol 108 No. 36:14998-5003. *Ann Neurosci*, 2012. **19**(1): p. 27-8.
80. Xing, L., et al., Structure of hepatitis E virion-sized particle reveals an RNA-dependent viral assembly pathway. *J Biol Chem*, 2010. **285**(43): p. 33175-83.
81. Yamashita, T., et al., Biological and immunological characteristics of hepatitis E virus-like particles based on the crystal structure. *Proc Natl Acad Sci U S A*, 2009. **106**(31): p. 12986-91.
82. Zafrullah, M., et al., The ORF3 protein of hepatitis E virus is a phosphoprotein that associates with the cytoskeleton. *J Virol*, 1997. **71**(12): p. 9045-53.
83. Tyagi, S., S. Jameel, and S.K. Lal, Self-association and mapping of the interaction domain of hepatitis E virus ORF3 protein. *J Virol*, 2001. **75**(5): p. 2493-8.
84. Kannan, H., et al., The hepatitis E virus open reading frame 3 product interacts with microtubules and interferes with their dynamics. *J Virol*, 2009. **83**(13): p. 6375-82.
85. Allweiss, L., et al., Human liver chimeric mice as a new model of chronic hepatitis E virus infection and preclinical drug evaluation. *J Hepatol*, 2016.
86. Nagashima, S., et al., Tumour susceptibility gene 101 and the vacuolar protein sorting pathway are required for the release of hepatitis E virions. *J Gen Virol*, 2011. **92**(Pt 12): p. 2838-48.
87. Nagashima, S., et al., The membrane on the surface of hepatitis E virus particles is derived from the intracellular membrane and contains trans-Golgi network protein 2. *Arch Virol*, 2014. **159**(5): p. 979-91.
88. Osterman, A., et al., The Hepatitis E virus intraviral interactome. *Sci Rep*, 2015. **5**: p. 13872.
89. von Nordheim, M., et al., Cutthroat Trout Virus-Towards a Virus Model to Support Hepatitis E Research. *Viruses*, 2016. **8**(10).
90. Takahashi, M., et al., Hepatitis E Virus (HEV) strains in serum samples can replicate efficiently in cultured cells despite the coexistence of HEV antibodies: characterization of HEV virions in blood circulation. *J Clin Microbiol*, 2010. **48**(4): p. 1112-25.
91. Nguyen, H.T., et al., Hepatitis E virus genotype 1 infection of swine kidney cells in vitro is inhibited at multiple levels. *J Virol*, 2014. **88**(2): p. 868-77.
92. Emerson, S.U., et al., In Vitro Replication of Hepatitis E Virus (HEV) Genomes and of an HEV Replicon Expressing Green Fluorescent Protein. *J Virol*, 2004. **78**(9): p. 4838-4846.
93. Shukla, P., et al., Cross-species infections of cultured cells by hepatitis E virus and discovery of an infectious virus-host recombinant. *Proc Natl Acad Sci U S A*, 2011. **108**(6): p. 2438-43.
94. Tanaka, T., et al., Development and evaluation of an efficient cell-culture system for Hepatitis E virus. *J Gen Virol*, 2007. **88**(Pt 3): p. 903-11.
95. Okamoto, H., Culture systems for hepatitis E virus. *J Gastroenterol*, 2013. **48**(2): p. 147-58.
96. Shukla, P., et al., Adaptation of a genotype 3 hepatitis E virus to efficient growth in cell culture depends on an inserted human gene segment acquired by recombination. *J Virol*, 2012. **86**(10): p. 5697-707.

97. Kenney, S.P. and X.J. Meng, The lysine residues within the human ribosomal protein S17 sequence naturally inserted into the viral nonstructural protein of a unique strain of hepatitis E virus are important for enhanced virus replication. *J Virol*, 2015. **89**(7): p. 3793-803.
98. Xu, L., et al., IFN regulatory factor 1 restricts hepatitis E virus replication by activating STAT1 to induce antiviral IFN-stimulated genes. *FASEB J*, 2016. **30**(10): p. 3352-3367.
99. Helsen, N., et al., Stem cell-derived hepatocytes: A novel model for hepatitis E virus replication. *J Hepatol*, 2016. **64**(3): p. 565-73.
100. Shen, Q., et al., Changes in the cellular proteins of A549 infected with hepatitis E virus by proteomics analysis. *BMC Vet Res*, 2014. **10**: p. 188.
101. Cheng, X., et al., Rabbit as a novel animal model for hepatitis E virus infection and vaccine evaluation. *PLoS One*, 2012. **7**(12): p. e51616.
102. Han, J., et al., SPF rabbits infected with rabbit hepatitis E virus isolate experimentally showing the chronicity of hepatitis. *PLoS One*, 2014. **9**(6): p. e99861.
103. Wang, L., et al., Experimental infection of rabbits with genotype 3 hepatitis E virus produced both chronicity and kidney injury. *Gut*, 2016.
104. Tang, Z.M., et al., The Bama miniature swine is susceptible to experimental HEV infection. *Sci Rep*, 2016. **6**: p. 31813.
105. Rogee, S., et al., Quantitative proteomics identifies host factors modulated during acute hepatitis E virus infection in the swine model. *J Virol*, 2015. **89**(1): p. 129-43.
106. Debing, Y., et al., A rat model for hepatitis E virus. *Dis Model Mech*, 2016.
107. Yang, Y., et al., Effect of swine hepatitis E virus on the livers of experimentally infected Mongolian gerbils by swine hepatitis E virus. *Virus Res*, 2015. **208**: p. 171-9.
108. Sayed, I.M., et al., Study of hepatitis E virus infection of genotype 1 and 3 in mice with humanised liver. *Gut*, 2016.
109. van de Garde, M.D., et al., Hepatitis E Virus (HEV) Genotype 3 Infection of Human Liver Chimeric Mice as a Model for Chronic HEV Infection. *J Virol*, 2016. **90**(9): p. 4394-401.
110. Schneider, W.M., M.D. Chevillotte, and C.M. Rice, Interferon-stimulated genes: a complex web of host defenses. *Annu Rev Immunol*, 2014. **32**: p. 513-45.
111. Heim, M.H., Interferons and hepatitis C virus. *Swiss Med Wkly*, 2012. **142**: p. w13586.
112. Andersen, L.L., et al., Functional IRF3 deficiency in a patient with herpes simplex encephalitis. *J Exp Med*, 2015. **212**(9): p. 1371-9.
113. Ciancanelli, M.J., et al., Infectious disease. Life-threatening influenza and impaired interferon amplification in human IRF7 deficiency. *Science*, 2015. **348**(6233): p. 448-53.
114. Hwang, S.Y., et al., A null mutation in the gene encoding a type I interferon receptor component eliminates antiproliferative and antiviral responses to interferons alpha and beta and alters macrophage responses. *Proc Natl Acad Sci U S A*, 1995. **92**(24): p. 11284-8.
115. Schlee, M. and G. Hartmann, Discriminating self from non-self in nucleic acid sensing. *Nat Rev Immunol*, 2016. **16**(9): p. 566-80.
116. Rodriguez, K.R., A.M. Bruns, and C.M. Horvath, MDA5 and LGP2: accomplices and antagonists of antiviral signal transduction. *J Virol*, 2014. **88**(15): p. 8194-200.
117. Chen, Q., L. Sun, and Z.J. Chen, Regulation and function of the cGAS-STING pathway of cytosolic DNA sensing. *Nat Immunol*, 2016. **17**(10): p. 1142-9.
118. Schoggins, J.W., et al., A diverse range of gene products are effectors of the type I interferon antiviral response. *Nature*, 2011. **472**(7344): p. 481-5.
119. Schoggins, J.W., et al., Pan-viral specificity of IFN-induced genes reveals new roles for cGAS in innate immunity. *Nature*, 2014. **505**(7485): p. 691-5.
120. Bulli, L., et al., Complex Interplay between HIV-1 Capsid and MX2-Independent Alpha Interferon-Induced Antiviral Factors. *J Virol*, 2016. **90**(16): p. 7469-80.
121. Kane, M., et al., MX2 is an interferon-induced inhibitor of HIV-1 infection. *Nature*, 2013. **502**(7472): p. 563-6.
122. Liu, Z., et al., The interferon-inducible MxB protein inhibits HIV-1 infection. *Cell Host Microbe*, 2013. **14**(4): p. 398-410.

123. Gorman, M.J., et al., The interferon-stimulated gene IFITM3 restricts West Nile virus infection and pathogenesis. *J Virol*, 2016.
124. Reynaud, J.M., et al., IFIT1 Differentially Interferes with Translation and Replication of Alphavirus Genomes and Promotes Induction of Type I Interferon. *PLoS Pathog*, 2015. **11**(4): p. e1004863.
125. Helbig, K.J., et al., The antiviral protein viperin inhibits hepatitis C virus replication via interaction with nonstructural protein 5A. *Hepatology*, 2011. **54**(5): p. 1506-17.
126. Paludan, S.R., Innate Antiviral Defenses Independent of Inducible IFNalpha/beta Production. *Trends Immunol*, 2016. **37**(9): p. 588-96.
127. Jagya, N., et al., RNA-seq based transcriptome analysis of hepatitis E virus (HEV) and hepatitis B virus (HBV) replicon transfected Huh-7 cells. *PLoS One*, 2014. **9**(2): p. e87835.
128. Huang, F., et al., Hepatitis E virus infection activates signal regulator protein alpha to down-regulate type I interferon. *Immunol Res*, 2016. **64**(1): p. 115-22.
129. Zhang, F., et al., Hepatitis E genotype 4 virus from feces of monkeys infected experimentally can be cultured in PLC/PRF/5 cells and upregulate host interferon-inducible genes. *J Med Virol*, 2014. **86**(10): p. 1736-44.
130. Nan, Y., et al., Hepatitis E virus inhibits type I interferon induction by ORF1 products. *J Virol*, 2014. **88**(20): p. 11924-32.
131. Nan, Y., et al., Enhancement of interferon induction by ORF3 product of hepatitis E virus. *J Virol*, 2014. **88**(15): p. 8696-705.
132. Dong, C., et al., Suppression of interferon-alpha signaling by hepatitis E virus. *Hepatology*, 2012. **55**(5): p. 1324-32.
133. Surjit, M., B. Varshney, and S.K. Lal, The ORF2 glycoprotein of hepatitis E virus inhibits cellular NF-kappaB activity by blocking ubiquitination mediated proteasomal degradation of IkappaBalpha in human hepatoma cells. *BMC Biochem*, 2012. **13**: p. 7.
134. Xu, J., et al., Open reading frame 3 of genotype 1 hepatitis E virus inhibits nuclear factor-kappaappa B signaling induced by tumor necrosis factor-alpha in human A549 lung epithelial cells. *PLoS One*, 2014. **9**(6): p. e100787.
135. Chandra, V., et al., The hepatitis E virus ORF3 protein modulates epidermal growth factor receptor trafficking, STAT3 translocation, and the acute-phase response. *J Virol*, 2008. **82**(14): p. 7100-10.
136. Yu, C., et al., Pathogenesis of hepatitis E virus and hepatitis C virus in chimpanzees: similarities and differences. *J Virol*, 2010. **84**(21): p. 11264-78.
137. Moal, V., et al., Chronic hepatitis E virus infection is specifically associated with an interferon-related transcriptional program. *J Infect Dis*, 2013. **207**(1): p. 125-32.
138. Majumdar, M., et al., Role of TLR gene expression and cytokine profiling in the immunopathogenesis of viral hepatitis E. *J Clin Virol*, 2015. **73**: p. 8-13.
139. Wang, W., et al., Convergent Transcription of Interferon-stimulated Genes by TNF-alpha and IFN-alpha Augments Antiviral Activity against HCV and HEV. *Sci Rep*, 2016. **6**: p. 25482.
140. Mishra, N. and V.A. Arankalle, Association of polymorphisms in the promoter regions of TNF-alpha (-308) with susceptibility to hepatitis E virus and TNF-alpha (-1031) and IFN-gamma (+874) genes with clinical outcome of hepatitis E infection in India. *J Hepatol*, 2011. **55**(6): p. 1227-34.

Chapter 2

Transcriptional Regulation of Antiviral Interferon-stimulated Genes

Wenshi Wang[1], **Lei Xu[1]**, Junhong Su[2], Maikel P. Peppelenbosch[1] and Qiuwei Pan[1]

[1]Department of Gastroenterology and Hepatology, Erasmus MC-University Medical Center and Postgraduate School Molecular Medicine, Rotterdam, the Netherlands

[2]Medical Faculty, Kunming University of Science and Technology, Kunming, PR China

Trends in Microbiology. 2017. In Press

Abstract

Interferon-stimulated genes (ISGs) are a group of gene products that coordinately combat pathogen invasions, in particular viral infections. Transcription of ISGs rapidly occurs upon pathogen invasion, and this is classically provoked via activation of the Janus kinase/signal transducer and activator of transcription (JAK-STAT) pathway, mainly by interferons (IFNs). However, plethoras of recent studies have reported a variety of non-canonical mechanisms regulating ISG transcription. These new studies are extremely important for understanding the quantitative and temporal differences in ISG transcription under specific circumstances. Because these canonical and non-canonical regulatory mechanisms are essential for defining the nature of host defense and associated detrimental pro-inflammatory effects, we comprehensively review the state of this rapidly evolving field and the clinical implications of recently acquired knowledge in this respect.

Keywords: IFN; ISG; transcription

Outstanding Questions

- Although signaling through the same receptor, there are many type I IFNs in the genome. How the cells dynamically control the production of the particular members of these type I IFNs?
- Upon IFNλ binding, which types of modification (*e.g.* phosphorylation, acetylation) happened to IFNλRs to kick off ISG transcription?
- Generally, HAT activity transforms chromatin into a more relaxed structure, while HDAC activity organizes chromatin into higher order nucleosomes. Counterintuitively, HDAC activity has been reported to be required for ISG transcription. How this mechanistically works?
- How exactly the nucleotide synthesis pathways mediate ISG transcription?
- Will ISG-based antiviral strategy circumvent the issue of side effects caused by IFN treatment, but retain the therapeutic potency in patients?

Trends Box

- Transcriptional regulation of interferon-stimulated genes (ISGs) defines the state of host anti-pathogen defense.
- In light of the recently identified regulatory elements and mechanisms of the IFN-JAK-STAT pathway, new insights have been gained into this classical cascade in regulating ISG transcription.
- A variety of non-canonical mechanisms have been recently revealed that coordinately regulate ISG transcription.
- With regards to the adverse effects of IFNs in clinic, ISG-based antiviral strategy could be the next promising frontier in drug discovery.

Host antiviral defense

IFN-mediated innate immune response forms a forward line of cell-autonomous defense against pathogens. Virus invasion (*e.g.* the presence of single-stranded RNA in endosomes or cytosolic double-stranded RNA) triggers the host cells to recognize the infection through pattern recognition receptors, that in turn mediates production of IFNs [1]. The thus-released IFN molecules bind to cell surface receptors and initiate signal transduction prominently involving the Janus kinase signal transducer and activator of transcription (JAK-STAT) pathway. This activates the transcription of hundreds of so-called IFN-stimulated genes (ISGs) that are the effectors of cell-autonomous antiviral defense. The representative well-studied ISG members in this respect with specific or broad antiviral activities include RIG-I, MDA5, MX2, IRF1, IRF3, IRF7, IRF9, IFITM3, ISG15 and OASL [2]. ISGs act at different stages of the viral life cycle, from entry, replication, assembly to release. This leads to a remarkable antiviral state that provides adequate cellular immunity against positive-, negative-, and double-stranded RNA viruses, DNA viruses, and even intracellular bacteria and parasites.

Although the JAK-STAT pathway plays key roles in regulating ISG transcription, a far more complex cell signaling network with both canonical and non-canonical mechanisms is involved [3]. The signaling strength, kinetics and specificity of regulatory pathways on ISG transcription are modulated at various levels by distinct mechanisms in conjunction. Understanding the different mechanisms of ISG transcription and how their mode-of-action relates to clinically used antiviral medications will reveal new insights of virus-host interactions and provide novel avenues for antiviral drug development. Therefore, we aim to comprehensively review the classical and non-classical mechanisms in regulating ISG transcription and to emphasize their clinical implications.

Classical mechanisms of regulating ISG transcription: the IFN-JAK-STAT pathway

Upon IFN binding to its cognate cell surface receptors, a signal is transmitted through the membrane into the cell via the JAK-STAT pathway, leading to rapid transcriptional activation of ISGs [4]. Decades of dedicated efforts have elucidated this classical regulatory network, as we have outlined here (Figure 1).

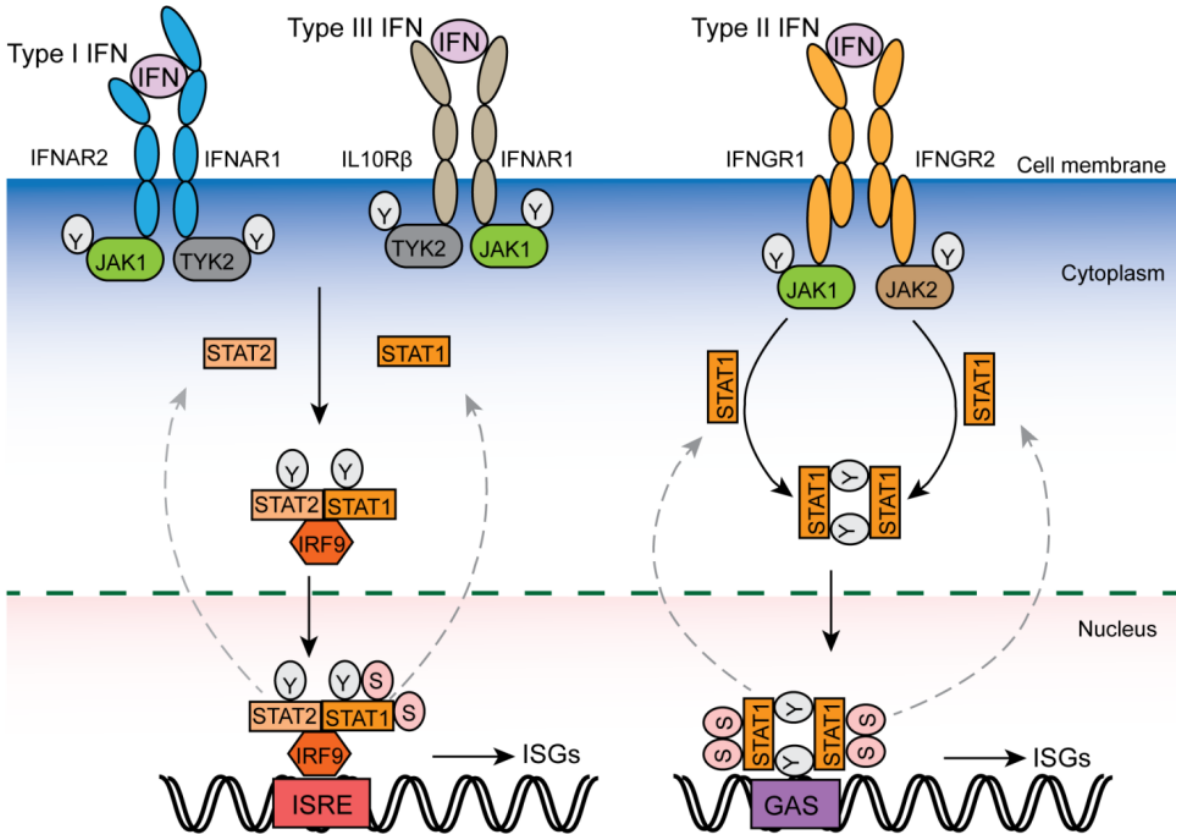

Figure 1. The classical IFN signaling pathways in regulating ISG transcription.

The three different classes of IFNs signal through their corresponding receptor complexes, leading to the phosphorylation of preassociated Janus kinases. For type I and III IFNs, the phosphorylated Janus kinase 1 (JAK1) and tyrosine kinase 2 (TYK2) in turn phosphorylate the receptors at specific intracellular tyrosine residues. This leads to the recruitment and phosphorylation of signal transducers and activators of transcription 1 and 2 (STAT1 and STAT2) at specific tyrosine residues. Then, STAT1 and 2 recruits IRF9 to form the IFN-stimulated gene factor 3 (ISGF3). For type II IFNs, the phosphorylated JAK1 and JAK2 tyrosine kinases phosphorylate the receptor chains, leading to tyrosine phosphorylation and homodimerization of STAT1. Both ISGF3 and STAT1 homodimer translocate to the nucleus to get further phosphorylation at specific serine residues of STAT1, achieving fully activation. Consequently, IFN-stimulated genes (ISGs) are transcriptionally activated upon the binding of ISGF3 and STAT1 homodimer to IFN-stimulated response elements (ISRE) and gamma-activated sequence (GAS) promoter elements, respectively. Conversely, the specific phosphatases in the nucleus dephosphorylate STAT1 and STAT2 to avoid excessive and detrimental responses.

IFNs and their receptors-dependent regulation

Genes encoding IFNs and their receptors have been duplicated extensively throughout vertebrate evolution, indicating substantial evolutionary pressure on this system in combating pathogens [5]. Up to now, more than twenty distinct IFN genes/proteins have been identified. Based on the type of receptor through which they signal, the multitude of different IFNs in mammalian genome are classified into three major types: Type I, II and III.

In humans, type I IFNs include IFN-α (which can be further subdivided into 13 different subtypes), IFN-β, IFN-δ, IFN-ε, IFN-κ, IFN-ζ and IFN-ω1-3. All type I IFNs bind to a common cell-surface receptor, the type I IFN heterodimeric receptor complexes comprising two subunits: IFN-α receptor 1 (IFNAR1) and IFN-α receptor 2 (IFNAR2). Unlike type I IFNs, there is only one type II IFN, IFN-γ. It has no marked structural homology with type I IFNs. IFN-γ binds to a different cell surface receptor comprised of two subunits: IFNGR1 and IFNGR2. Type III IFN family is composed of four genes: IFNλ1 (IL29), IFNλ2 (IL28A), IFNλ3 (IL28B) and IFNλ4 (frameshift variant of IL28B). They signal through the IFNλ receptor (IFNλR) which is composed of two subunits: IFNλR1 (IL28Rα) and IL10Rβ.

Type II IFN signaling leads to STAT1 phosphorylation, followed by homodimerization, nuclear translocation, and DNA binding at gamma-activated sequence (GAS) elements located within promoter regions of IFN-γ-induced genes. While both type I and III IFN signaling activate similar intracellular JAK-STAT pathway forming the transcription complex, ISGF3, to transcribe ISGs, although they utilize distinct receptor complexes for signaling [6]. However, IFNAR is ubiquitously expressed in all nucleated cells; whereas IFNλR1 is only expressed on specific tissues/cells of epithelial origin [7], suggesting a selectivity of type III IFNs compared with type I IFNs.

For optimal activation, signaling through the IFN receptor complex depends on tyrosine phosphorylation, serine phosphorylation and acetylation on IFN receptors (Table 1) [8-10]. Nevertheless, negative regulation is also essential for balancing its beneficial antiviral versus detrimental pro-inflammatory effects. Primarily, this is achieved by (i) phosphorylation induced IFN receptor ubiquitination and degradation [11]; (ii) blocking the interaction between IFNAR and downstream signaling elements, such as the function of USP18, ISG15 and SOCS1 [12-16]; (iii) receptor-mediated ligand internalization/degradation [17]; and (iv) modulating cell surface IFN receptor level [18, 19].

JAK kinases (JAKs)-dependent regulation

The JAKs comprises 4 members, three of them (JAK1, JAK2 and TYK2) function in IFN signaling and are ubiquitously expressed [20]. They are pre-associated with the corresponding IFN receptor. Upon IFN binding to receptor, they become activated through close proximity trans-phosphorylation (JAK1: $Tyr^{1022,1023}$, JAK2: $Tyr^{1007,1008}$ and TYK2: $Tyr^{1054,1055}$). Subsequently, activated JAKs phosphorylate the cytoplasmic regions of the receptor,

generating docking sites for SH2-domain containing proteins, in particular STAT1 and STAT2 [21]. Activation of JAK enzymatic activity also triggers negative feedback on antiviral immunity. Phosphatases, including T cell protein tyrosine phosphatase (TCPTP), protein tyrosine phosphatases (PTP) 1B and CD45, are the most important negative regulators [22-25]. The SOCS-1 protein also negatively regulates this process through phosphorylation mediated proteasomal degradation of JAK [26]. The critical function of JAKs in cell signaling has made them ideal targets for controlling a range of autoimmune diseases. Several JAK inhibitors have been approved by the FDA or are in clinical trials for the treatment of rheumatoid arthritis, psoriasis, inflammatory bowel disease and ankylosing spondylitis [27].

Table 1. Classical modification of the IFN-JAK-STAT pathway

	Modification site	Modification type[a]	Signal transduction	References
IFNAR1	Tyr^{466}	Phosphorylation	Activation	[28]
IFNAR1	Tyr^{512} and Tyr^{337}	Phosphorylation	Activation	[29]
IFNAR1	Ser^{535}, Ser^{539}	Phosphorylation	Inactivation	[11]
IFNAR1	Lys^{501}, Lys^{525} and Lys^{526}	Ubiquitination	Inactivation	[11]
IFNAR2	Ser^{364}, Ser^{384}	Phosphorylation	Activation	[9]
IFNAR2	Lys^{399}	Acetylation	Activation	[9]
IFNGR1	Pro^{267}	ND	Activation	[30]
IFNGR1	Tyr^{440}	Phosphorylation	Activation	[31]
IFNGR1	$^{270}LI^{271}$	ND	Inactivation	[17]
IFNGR1	Tyr^{441}	Phosphorylation	Inactivation	[16, 31]
IFNGR2	$^{263}PPSIP^{267}$ and $^{270}IEEYL^{274}$	ND	Activation	[10]
JAK1	$Tyr^{1022,1023}$	Phosphorylation	Activation	[21]
JAK2	$Tyr^{1007,1008}$	Phosphorylation	Activation	[21]
TYK2	$Tyr^{1054,1055}$	Phosphorylation	Activation	[21]
STAT1	Tyr^{701}	Phosphorylation	Activation	[32]
STAT1	Ser^{727}	Phosphorylation	Activation	[32]
STAT1	Ser^{708}	Phosphorylation	Activation	[33]
STAT1	Lys^{703}	SUMO-1 Binding	Inactivation	[34]
STAT2	Tys^{690}	Phosphorylation	Activation	[35]
STAT2	Ser^{287}	Phosphorylation	Inactivation	[35]

[a]ND, not determined.

STAT-dependent regulation

There are seven STAT members in mammals, STAT1, STAT2, STAT3, STAT4, STAT5a, STAT5b and STAT6. STAT1 and STAT2 are the most important STATs with respect to IFN signaling [2]. In response to IFNs, STAT1 is phosphorylated on Tyr^{701}, Ser^{708} and Ser^{727}. These sites are all

positively related to signaling transduction [33, 36]. STAT2 acquires transcriptional activation upon tyrosine phosphorylation (Tyr^{690}). Conversely, serine phosphorylation (Ser^{287}) in STAT2 negatively regulates IFN response [21, 35]. Although JAKs play key role in STAT1 phosphorylation and activation, nevertheless, other cellular factors are also required. Tyrosine kinase non-receptor 1 (TNK1) and retinoic acid-inducible gene I (RIG-I) potentiate dual phosphorylation of STAT1 at Tyr^{701} and Ser^{727} positions [37-39]; Nuclear cyclin-dependent kinase 8 (CDK8) phosphorylates Ser^{727} of STAT1 [40, 41]. Protein kinase C family members, PKC-δ or PKC-ε mediates phosphorylation of STAT1 on Ser^{727} (no effect on STAT1 tyrosine phosphorylation) via its upstream phosphatidylinositol 3-kinase (PI3K)-AKT pathway [42-45]. Interestingly, stress signals can also induce phosphorylation of STAT1 (Ser^{727}) via the p38-MAPK pathway [46]. As p38-MAP kinase inhibitors are well tolerated and safe for humans, it is thus tempting to speculate that such inhibitors may be used to mitigate pro-inflammatory effects following IFN-γ-therapy [47].

Evidently, phosphatase-dependent STAT1 dephosphorylation constitutes an important negative-regulatory event that is central in titrating the IFN response. The functional phosphatases include SHP-2 [48, 49], the nuclear isoform of TCPTP, TC45 [50] and SHPTP1 [51]. Phosphatase dysregulation has been reported in cancers and autoimmune disorders, thus representing potential therapeutic targets [52]. A small ubiquitin-related modifier 1 (SUMO-1) was also reported to conjugate at Lys^{703} of STAT1 to inhibit signaling transduction [34]. Thus, a plethora of molecular mechanisms can balance the IFN response through acting on STAT1.

IRF9 is a main DNA binding component of the ISGF3 complex. IRF9 alone binds to DNA and recognizes the specific promotor elements denoted as interferon-stimulated response elements (ISRE), but has no transcriptional activity. Upon its DNA binding, IRF9 provides specific protein-DNA interaction sites for STAT1 and STAT2. Activated STAT1 and STAT2 bind to the ISRE region together with IRF9 to exert strong pro-transcriptional activity [53]. Theoretically, IRF9 (as part of the ISGF3 complex) only involves in type I and III IFN signaling to regulate ISG transcription. However, IFNγ induced ISG activation and antiviral state were severely impaired in the absence of IRF9, indicating that IRF9 may also be involved in type II IFN signaling [54, 55]. More interestingly, IFNγ pretreatment induces high levels of IRF9, which serves as an important subunit of latent precursor to ISGF3. In this way,

IFN-α and IFN-γ synergize to induce the formation of ISGF3 complex, leading to much stronger ISG transcription [56].

Regulation of ISGs at the transcriptional level

In the case of type I and III IFNs, ISGF3 works as the predominant transcriptional factor binding to ISREs within the promoter region of ISGs; whereas for type II IFN, the homodimers or heterodimers of STATs are the determinant binding to GAS elements. However, this is a simplified model and other regulatory elements are also involved (Figure 2).

Chromatin modulators.

Histone octamers bind to DNA and organize chromatin into higher order nucleosomes, prohibiting transcription factor binding and gene expression [57]. As a consequence, the induction of ISGs by IFNs requires chromatin remodeling. The condensed chromatin needs to be transformed into a more relaxed structure. In humans, the nucleosome remodeling complex BAF and PBAF prime ISG promoters by utilizing ATP-derived energy to maintain chromatin in a constitutively open conformation, allowing fast and potent induction of ISGs after IFN exposure [58-61]. Histone acetylation and deacetylation are also essential in chromatin modulation. These reactions are typically catalyzed by enzymes with histone acetyltransferase (HAT) or histone deacetylase (HDAC) activity. HAT activity transforms chromatin into a more relaxed structure, while HDAC activity organizes chromatin into higher order nucleosomes. Therefore, the HAT family members, including p300/CBP and GCN5, are essential for transcriptional activation of ISGs [62, 63]. HATs are positive regulators of transcription in general. However, HDAC activity is also essential for transcriptional induction of ISGs [64-69]. HDAC activity has been reported to be required for recruiting RNA polymerase II to the promoters of ISGs [70], although how HDACs regulate transcriptional activation of ISG remains unclear. In addition, FOXO3 and PI3K/AKT pathway coordinate in chromatin modulation. FOXO3 together with the nuclear co-repressor 2 (NCOR2) and HDAC3 forms a ternary complex to facilitate a closed chromatin structure to limit ISG transcription under basal conditions. However, type I IFN can activate the PI3K/AKT pathway, which in turn leads to FOXO3 degradation and ISG transcription [71].

Co-activators and co-repressors.

Particular co-activators or co-repressors mediate the transcription of ISGs via the interaction with ISGF3 or STAT1 homodimers. The co-activators, such as MCM5 (minichromosome

maintenance) and MCM3 protein complex [72, 73], N-Myc interactor (NMi) [74] and DRIP150 [75], facilitate the transcriptional activation of ISGs. Conversely, co-repressors, such as TAF-1 [76] and the protein inhibitor of activated STAT proteins (PIAS1 and PIASγ [77, 78], negatively suppress the formation of transcription complex on the ISG promoter to limit transcription. Recently, four previously unrecognized regulatory factors (ETV6, ATF3, LYN and TBK1) of ISG transcription have been identified [79]. These efforts have led to a more comprehensive understanding of ISG transcription.

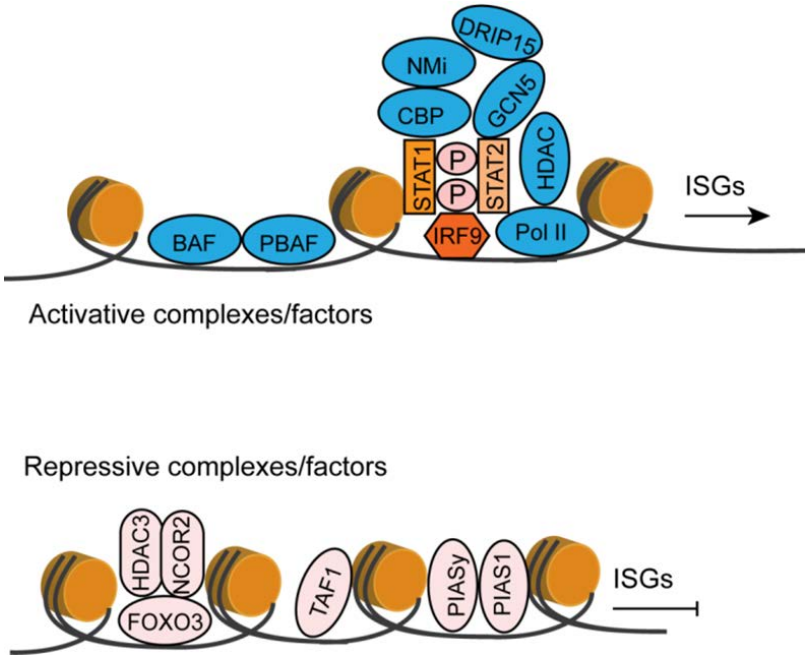

Figure 2. The transcriptional regulation of IFN-stimulated genes (ISGs) involves chromatin remodeling and various co-activators and co-repressors.

Upon IFN stimulation, the IFN-stimulated gene factor 3 (ISGF3) or STAT1 homodimer binds to ISG promoter regions, recruiting various chromatin remodeling factors and transcriptional co-activators. These factors include the nucleosome remodeling complex BAF and PBAF, p300/CBP and GCN5 histone acetyltransferase (HAT), histone deacetylase (HDAC), minichromosome maintenance 3 and 5 (MCM3 and MCM5), N-Myc interactor (NMi), DRIP150 (a subunit of the multimeric mediator coactivator complex). Consequently, the condensed chromatin transforms into a more relaxed structure to facilitate the transcription of ISGs. Conversely, the co-repressor factors could inhibit ISG transcription either via the facilitation of a closed chromatin or interference with the recruitment of STAT1 or ISGF3 to the ISG promoter.

Non-canonical regulation of ISG transcription

All three types of IFNs signal through the JAK-STAT pathway to elicit antiviral activity. Yet, type II IFN is thought to do so only through STAT1 homodimers; whereas type I and III IFNs activate both STAT1 and STAT2 to form ISGF3 together with IRF9. However, accumulating evidence highlights a far more complex process of activation and function beyond this

classical theory. The heterogeneity of the regulatory mechanisms of ISG transcription has been recently highlighted. A substantial fraction of these cascades have little or no link to STAT1/2 and ISGF3, paralleling the existence of non-canonical mechanisms outside of the JAK-STAT axis [79]. Here, we review both JAK-STAT axis dependent and independent non-canonical mechanisms of ISG transcription (Figure 3).

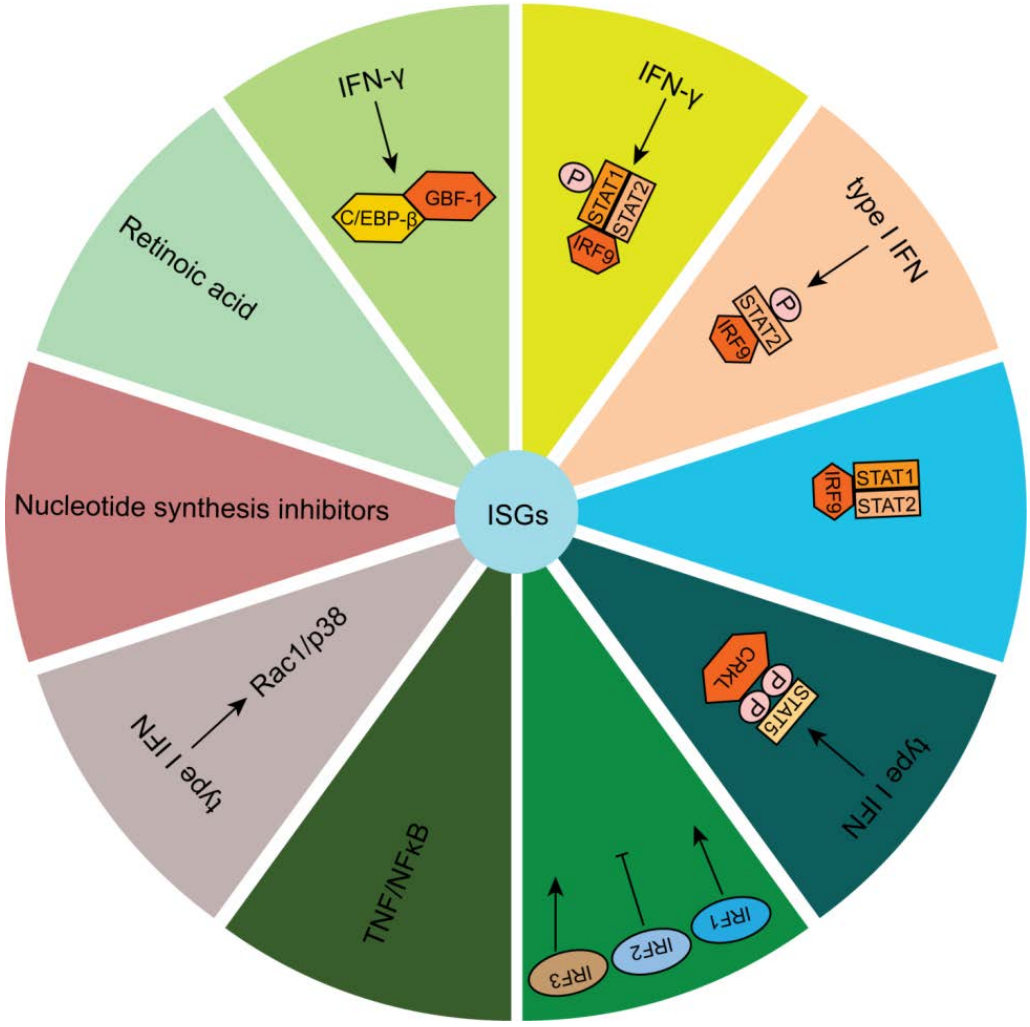

Figure 3. Non-canonical mechanisms in regulating ISG transcription.

Non-canonical mechanisms both within and outside of the IFN-JAK-STAT axis were summarized. Together with canonical mechanisms, they coordinately regulate ISG transcription, thus defining the cellular defense status against pathogen invasion.

Non-canonical ISGF3 complex.

Up to date, three different forms of non-canonical ISGF3 complexes have been identified, including ISGF3^{II}, the STAT2-IRF9 complex and unphosphorylated ISGF3 (U-ISGF3). IFN-γ treatment has been reported to induce the formation of a new manifestation of ISGF3 (ISGF3^{II}) containing phosphorylated STAT1, unphosphorylated STAT2 and IRF9 [80]. In the

absence of STAT1, STAT2 was found to interact with IRF9 to form an ISGF3-like complex to mediate specific ISG transcription [81]. Finally, continuous exposure to a low level of exogenous IFNs, U-ISGF3 formed by IFN induced IRF9 and unphosphorylated STAT1 and STAT2, can lead to increased expression of a subset of ISGs [82, 83].

STAT5-CrkL complex.

Apart from STAT1 and STAT2, STAT5 is also involved in type I IFN induced ISG transcription. STAT5 interacts constitutively with IFN receptor-associated TYK-2. Upon type I IFN stimulation, STAT5 is phosphorylated on both tyrosine and serine sites, thus acting as a docking site for the SH2 domain of CrkL. CrkL and STAT5 then form a complex that translocates to the nucleus and binds to GAS elements to activate type I IFN-dependent gene transcription [3, 84].

IRFs.

IRF1 has been shown to function as a transcription factor. The DNA sequences (IRF-E site) recognized by IRF1 overlap with the ISRE, and in this way IRF1 induces a subset of ISGs. IRF1 can also enhance the levels of both total and phosphorylated STAT1 to amplify ISG transcription via JAK-STAT pathway [85]. Conversely, IRF2 binds to the same IRF-E site to repress IRF1 induced transcription [86, 87]. Upon virus infection, IRF3 is activated and cooperates with NF-κB and ATF-2/c-Jun to form a transcriptionally active enhanceosome complex on the IFN-β promoter. Newly synthesized IFN binds to cognate receptors to activate ISG transcription via the JAK-STAT pathway. Importantly, IRF3 was also been reported to directly induce a subset of ISGs in an IFN-independent manner through the ISREs element on their promoters [88, 89].

Cross-regulation between TNF and IFN signaling.

It is well documented that when combined with TNF-α, type I or II IFN works cooperatively on antiviral ISG induction and exerts synergistic antiviral effects [90-93]. TNF-α has been reported to inhibit hepatitis C virus (HCV) infection-caused degradation of IFNAR2, thus maintaining IFN signaling and ISG expression [93]. TNF-α alone can already moderately induce the transcription of a subset of ISGs [90, 91]. This is mainly through NF-κB protein complex, a key downstream element of the TNF-α signaling. This may explain the antiviral activity of TNF-α on different virus as documented [92, 94-96].

Rac1/p38 pathway.

Rac1/p38 Map kinase signaling regulates IFN induced ISG transcription. Type I IFN treatment results in activation of Rac1 and its downstream effectors including MAP kinase kinase 3 (MKK3), MAP kinase kinase 6 (MKK6) [97, 98] and cytosolic phospholipase A2 [99, 100]. In turn, these events provoke phosphorylation and activation of the p38 MAP kinase, an important mediator of the inflammatory response [101]. p38 MAP kinase activation leads to downstream MapKapK-2 and MapKapK-3 activation, contributing to type I IFN-dependent transcriptional regulation of ISGs. However, Rac1/p38 Map kinase signaling is not required for IFN-dependent phosphorylation of STAT1 on both sites (Ser^{727} and Tyr^{701}) and has no impact on the formation of ISGF3 complex [102, 103]. Histone phosphorylation and chromatin remodeling are possible mechanisms employed by this cascade [102]. Many immune-relevant gene products are subject to post-transcriptional regulation by this signaling [104], but ISGs have not been investigated in this respect.

IFN-γ-activated response element (GATE).

In response to IFN-γ, two factors bind to a unique IFN-γ-activated response element called GATE, the CCAAT/enhancer binding protein C/EBP-β and the GATE binding factor GBF-1. MEK1, ERK1 and ERK2 are the upstream kinases needed to activate C/EBP-β in response to IFN-γ [105]. This novel IFN-γ-activated pathway promotes ISG expression in STAT1-, but not JAK1-dependent manner.

Nucleotide synthesis inhibitor.

Purine and pyrimidine nucleotides are the major cellular energy carriers and constitute subunits of nucleic acids. Nucleotides can be synthesized de novo through a series of enzymatic reactions or recycled through salvage pathways. Interestingly, purine and pyrimidine synthesis inhibitors (such as ribavirin, mycophenolic acid and brequinar) can efficiently induce ISG expression and exert strong and broad antiviral responses [106-108]. However, this process is independent of the classical JAK-STAT cascade, suggesting a non-canonical mechanism that is independent of IFNs [109]. Ribavirin, an inhibitor of the IMPDH enzyme, was shown to reset a subset of ISG promoters to a “ready to be activated” status, thus potentiating ISG activation [110]. However, the crosstalk of nucleotide synthesis and innate immune response remains to be further elucidated.

Retinoic acid.

Retinoic acid (RA) is a metabolite of vitamin A that mediates the functions of vitamin A required for growth and development. RA activates transcriptional status via retinoic acid receptors (RAR) and retinoid X receptors (RXR) heterodimer, which binds to regions in promoters called retinoic acid response elements (RAREs). Numerous studies have reported antiviral activities of RA against a variety of pathogens [111, 112]. Interestingly, intracellular RA increases ISG expression at basal levels and augments ISG induction in response to IFNs [113]. This is consistent with the clinical observation that RA enhances the response to IFN-based antiviral therapy [112, 114]. Strikingly, a bioinformatics study showed that most ISGs regulatory regions contain RARE sequence [113]. This indicates that RA can induce transcriptional activation of these ISGs containing RAREs, facilitating the binding of additional transcription factors to the promoters of these ISGs. Consequently, RA initiates and works synergistically with IFNs to induce ISG expression.

IFNs and ISGs: clinical implications and future perspective

IFNs have been used in various clinical settings to counteract pathogen-related diseases. Because of its robust and broad antiviral activity, IFN-α represents the standard treatment for chronic hepatitis B virus (HBV) or HCV infections for decades. Its application also extends to other virus infections as off-label treatment, *e.g.* hepatitis E virus [115] and severe acute respiratory syndrome [116]. IFN-λ has been shown to play a crucial role in cancer, autoimmune disease and viral infections [117]. The antitumor and anti-infection activities of IFN-γ have been comprehensively evaluated and used in a variety of clinical indications. It has been approved by FDA to treat chronic granulomatous disease and osteopetrosis and is experimentally used for the treatment of idiopathic pulmonary fibrosis and Friedreich's ataxia [118]. But it is unsuccessful for treating viral infections [119, 120]. IFN-λ has been shown specific antiviral activity in both chronic HBV and HCV patients, not superior as compared to IFN-α therapy but with limited side effects [121, 122]. This is because of the fact that IFNλR1 has a more restricted tissue-specific pattern of expression. IFN-λ has also been shown to determine the intestinal epithelial antiviral host defense against rotavirus infection. It acts synergistically with IL-22 for the induction of ISGs and eventually controls rotavirus infection in animal models [123, 124]. Thus, IFN-λ might be an attractive option for the treatment of many viral infections. Although the clinical application of IFNs, in particular for HCV, will be

limited because of the recent launch of direct-acting antiviral agents, it may extend to other devastating viral diseases such as Ebola, Zika or Dengue virus infections.

Mechanistically, for all three different types of IFNs, ISGs are the ultimate antiviral effectors. Recent studies on the function of individual ISG indicate that different viruses are targeted by unique sets of ISGs. Some ISGs possess broad antiviral but others have specific antiviral effects [125]. Thus, characterization of individual ISG with respect to their antiviral spectrum or specificity provides new avenues for improving current antiviral therapies. Interestingly, several ISGs have been reported to paradoxically enhance the replication of certain viruses, illustrating the complexity of the network of mutual interaction between ISGs and viruses [125]. In pre-clinical or clinical studies, the expression pattern of some specific ISGs have been identified as bio-makers to predict treatment responses, disease progression or outcomes in both infectious (*e.g.* HCV and HIV infections) [126-128] and non-infectious human diseases (*e.g.* Aicardi-Goutieres syndrome and systemic lupus erythematosus) [129, 130]. Some ISGs (*e.g.* TLR3, TLR7, RIG-I and MDA5) belong to pattern recognition receptors (PRRs). Attributing to their key roles in innate immune responses, there is a growing interest in targeting PRRs for the prevention and treatment of cancer, autoimmune diseases and infections. Their specific activators are now undergoing preclinical and clinical evaluation for safety and efficacy [131]. With regards to the adverse effects of IFNs in clinic, ISG-based antiviral strategies could be the next promising frontier in drug discovery.

Concluding Remarks

Decades of research has shaped up a picture of the complex network in regulating ISG transcription. This includes both canonical and non-canonical mechanisms within and outside of the IFN-JAK-STAT axis, coordinately defining the cellular defense status against pathogen invasion. We expect that the spectrum of new elements involved in both canonical and non-canonical regulation of ISG transcription will continue to grow and their mechanism-of-actions will be further clarified (see **Outstanding Questions**). Because of their importance in clinical implication, this knowledge is highly relevant in guiding the development of new therapies that promote the eradication of severe pathogen infections, but avoiding autoimmune diseases and toxic effects to the host.

References

1. Wu, J. and Z.J. Chen, Innate immune sensing and signaling of cytosolic nucleic acids. *Annu Rev Immunol*, 2014. **32**: p. 461-88.
2. Schneider, W.M., M.D. Chevillotte, and C.M. Rice, Interferon-stimulated genes: a complex web of host defenses. *Annu Rev Immunol*, 2014. **32**: p. 513-45.
3. Platanias, L.C., Mechanisms of type-I- and type-II-interferon-mediated signalling. *Nat Rev Immunol*, 2005. **5**(5): p. 375-86.
4. Stark, G.R. and J.E. Darnell, Jr., The JAK-STAT pathway at twenty. *Immunity*, 2012. **36**(4): p. 503-14.
5. Krause, C.D. and S. Pestka, Cut, copy, move, delete: The study of human interferon genes reveal multiple mechanisms underlying their evolution in amniotes. *Cytokine*, 2015. **76**(2): p. 480-95.
6. Kotenko, S.V., IFN-lambdas. *Curr Opin Immunol*, 2011. **23**(5): p. 583-90.
7. Galani, I.E., O. Koltsida, and E. Andreakos, Type III interferons (IFNs): Emerging Master Regulators of Immunity. *Adv Exp Med Biol*, 2015. **850**: p. 1-15.
8. Tang, X., et al., Acetylation-dependent signal transduction for type I interferon receptor. *Cell*, 2007. **131**(1): p. 93-105.
9. New, M., H. Olzscha, and N.B. La Thangue, HDAC inhibitor-based therapies: can we interpret the code? *Mol Oncol*, 2012. **6**(6): p. 637-56.
10. Schroder, K., et al., Interferon-gamma: an overview of signals, mechanisms and functions. *J Leukoc Biol*, 2004. **75**(2): p. 163-89.
11. Kumar, K.G., J.J. Krolewski, and S.Y. Fuchs, Phosphorylation and specific ubiquitin acceptor sites are required for ubiquitination and degradation of the IFNAR1 subunit of type I interferon receptor. *J Biol Chem*, 2004. **279**(45): p. 46614-20.
12. Malakhova, O.A., et al., UBP43 is a novel regulator of interferon signaling independent of its ISG15 isopeptidase activity. *EMBO J*, 2006. **25**(11): p. 2358-67.
13. Zhang, X., et al., Human intracellular ISG15 prevents interferon-alpha/beta over-amplification and auto-inflammation. *Nature*, 2015. **517**(7532): p. 89-93.
14. Fenner, J.E., et al., Suppressor of cytokine signaling 1 regulates the immune response to infection by a unique inhibition of type I interferon activity. *Nat Immunol*, 2006. **7**(1): p. 33-9.
15. Linossi, E.M., et al., Suppression of cytokine signaling: the SOCS perspective. *Cytokine Growth Factor Rev*, 2013. **24**(3): p. 241-8.
16. Starr, R., et al., SOCS-1 binding to tyrosine 441 of IFN-gamma receptor subunit 1 contributes to the attenuation of IFN-gamma signaling in vivo. *J Immunol*, 2009. **183**(7): p. 4537-44.
17. Farrar, M.A. and R.D. Schreiber, The molecular cell biology of interferon-gamma and its receptor. *Annu Rev Immunol*, 1993. **11**: p. 571-611.
18. Bernabei, P., et al., Interferon-gamma receptor 2 expression as the deciding factor in human T, B, and myeloid cell proliferation or death. *J Leukoc Biol*, 2001. **70**(6): p. 950-60.
19. Bach, E.A., et al., Ligand-induced autoregulation of IFN-gamma receptor beta chain expression in T helper cell subsets. *Science*, 1995. **270**(5239): p. 1215-8.
20. Babon, J.J., et al., The molecular regulation of Janus kinase (JAK) activation. *Biochem J*, 2014. **462**(1): p. 1-13.
21. Steen, H.C. and A.M. Gamero, STAT2 phosphorylation and signaling. *JAKSTAT*, 2013. **2**(4): p. e25790.
22. Myers, M.P., et al., TYK2 and JAK2 are substrates of protein-tyrosine phosphatase 1B. *J Biol Chem*, 2001. **276**(51): p. 47771-4.
23. Irie-Sasaki, J., et al., CD45 is a JAK phosphatase and negatively regulates cytokine receptor signalling. *Nature*, 2001. **409**(6818): p. 349-54.

24. Yamada, T., et al., CD45 controls interleukin-4-mediated IgE class switch recombination in human B cells through its function as a Janus kinase phosphatase. *J Biol Chem*, 2002. **277**(32): p. 28830-5.
25. Simoncic, P.D., et al., The T cell protein tyrosine phosphatase is a negative regulator of janus family kinases 1 and 3. *Curr Biol*, 2002. **12**(6): p. 446-53.
26. Ali, S., et al., SHP-2 regulates SOCS-1-mediated Janus kinase-2 ubiquitination/degradation downstream of the prolactin receptor. *J Biol Chem*, 2003. **278**(52): p. 52021-31.
27. O'Shea, J.J., et al., Janus kinase inhibitors in autoimmune diseases. *Ann Rheum Dis*, 2013. **72 Suppl 2**: p. ii111-5.
28. Yan, H., et al., Phosphorylated interferon-alpha receptor 1 subunit (IFNaR1) acts as a docking site for the latent form of the 113 kDa STAT2 protein. *EMBO J*, 1996. **15**(5): p. 1064-74.
29. Zhao, W., et al., A conserved IFN-alpha receptor tyrosine motif directs the biological response to type I IFNs. *J Immunol*, 2008. **180**(8): p. 5483-9.
30. Kaplan, D.H., et al., Identification of an interferon-gamma receptor alpha chain sequence required for JAK-1 binding. *J Biol Chem*, 1996. **271**(1): p. 9-12.
31. Qing, Y., et al., Role of tyrosine 441 of interferon-gamma receptor subunit 1 in SOCS-1-mediated attenuation of STAT1 activation. *J Biol Chem*, 2005. **280**(3): p. 1849-53.
32. Sadzak, I., et al., Recruitment of Stat1 to chromatin is required for interferon-induced serine phosphorylation of Stat1 transactivation domain. *Proc Natl Acad Sci U S A*, 2008. **105**(26): p. 8944-9.
33. Ng, S.L., et al., IkappaB kinase epsilon (IKK(epsilon)) regulates the balance between type I and type II interferon responses. *Proc Natl Acad Sci U S A*, 2011. **108**(52): p. 21170-5.
34. Ungureanu, D., et al., SUMO-1 conjugation selectively modulates STAT1-mediated gene responses. *Blood*, 2005. **106**(1): p. 224-6.
35. Steen, H.C., et al., Identification of STAT2 serine 287 as a novel regulatory phosphorylation site in type I interferon-induced cellular responses. *J Biol Chem*, 2013. **288**(1): p. 747-58.
36. Tenoever, B.R., et al., Multiple functions of the IKK-related kinase IKKepsilon in interferon-mediated antiviral immunity. *Science*, 2007. **315**(5816): p. 1274-8.
37. Ooi, E.L., et al., Novel antiviral host factor, TNK1, regulates IFN signaling through serine phosphorylation of STAT1. *Proc Natl Acad Sci U S A*, 2014. **111**(5): p. 1909-14.
38. Jiang, L.J., et al., RA-inducible gene-I induction augments STAT1 activation to inhibit leukemia cell proliferation. *Proc Natl Acad Sci U S A*, 2011. **108**(5): p. 1897-902.
39. Zhang, F., et al., Hepatitis E genotype 4 virus from feces of monkeys infected experimentally can be cultured in PLC/PRF/5 cells and upregulate host interferon-inducible genes. *J Med Virol*, 2014. **86**(10): p. 1736-44.
40. Staab, J., C. Herrmann-Lingen, and T. Meyer, CDK8 as the STAT1 serine 727 kinase? *JAKSTAT*, 2013. **2**(3): p. e24275.
41. Bancerek, J., et al., CDK8 kinase phosphorylates transcription factor STAT1 to selectively regulate the interferon response. *Immunity*, 2013. **38**(2): p. 250-62.
42. Choudhury, G.G., A linear signal transduction pathway involving phosphatidylinositol 3-kinase, protein kinase Cepsilon, and MAPK in mesangial cells regulates interferon-gamma-induced STAT1alpha transcriptional activation. *J Biol Chem*, 2004. **279**(26): p. 27399-409.
43. Nguyen, H., et al., Roles of phosphatidylinositol 3-kinase in interferon-gamma-dependent phosphorylation of STAT1 on serine 727 and activation of gene expression. *J Biol Chem*, 2001. **276**(36): p. 33361-8.
44. Uddin, S., et al., Protein kinase C-delta (PKC-delta) is activated by type I interferons and mediates phosphorylation of Stat1 on serine 727. *J Biol Chem*, 2002. **277**(17): p. 14408-16.
45. Deb, D.K., et al., Activation of protein kinase C delta by IFN-gamma. *J Immunol*, 2003. **171**(1): p. 267-73.
46. Ramsauer, K., et al., p38 MAPK enhances STAT1-dependent transcription independently of Ser-727 phosphorylation. *Proc Natl Acad Sci U S A*, 2002. **99**(20): p. 12859-64.

47. Branger, J., et al., Inhibition of coagulation, fibrinolysis, and endothelial cell activation by a p38 mitogen-activated protein kinase inhibitor during human endotoxemia. *Blood*, 2003. **101**(11): p. 4446-8.
48. Wu, T.R., et al., SHP-2 is a dual-specificity phosphatase involved in Stat1 dephosphorylation at both tyrosine and serine residues in nuclei. *J Biol Chem*, 2002. **277**(49): p. 47572-80.
49. Xu, D. and C.K. Qu, Protein tyrosine phosphatases in the JAK/STAT pathway. *Front Biosci*, 2008. **13**: p. 4925-32.
50. ten Hoeve, J., et al., Identification of a nuclear Stat1 protein tyrosine phosphatase. *Mol Cell Biol*, 2002. **22**(16): p. 5662-8.
51. David, M., et al., Differential regulation of the alpha/beta interferon-stimulated Jak/Stat pathway by the SH2 domain-containing tyrosine phosphatase SHPTP1. *Mol Cell Biol*, 1995. **15**(12): p. 7050-8.
52. He, R.J., et al., Protein tyrosine phosphatases as potential therapeutic targets. *Acta Pharmacol Sin*, 2014. **35**(10): p. 1227-46.
53. Qureshi, S.A., M. Salditt-Georgieff, and J.E. Darnell, Jr., Tyrosine-phosphorylated Stat1 and Stat2 plus a 48-kDa protein all contact DNA in forming interferon-stimulated-gene factor 3. *Proc Natl Acad Sci U S A*, 1995. **92**(9): p. 3829-33.
54. John, J., et al., Isolation and characterization of a new mutant human cell line unresponsive to alpha and beta interferons. *Mol Cell Biol*, 1991. **11**(8): p. 4189-95.
55. Kimura, T., et al., Essential and non-redundant roles of p48 (ISGF3 gamma) and IRF-1 in both type I and type II interferon responses, as revealed by gene targeting studies. *Genes Cells*, 1996. **1**(1): p. 115-24.
56. Levy, D.E., et al., Synergistic interaction between interferon-alpha and interferon-gamma through induced synthesis of one subunit of the transcription factor ISGF3. *EMBO J*, 1990. **9**(4): p. 1105-11.
57. Bell, O., et al., Determinants and dynamics of genome accessibility. *Nat Rev Genet*, 2011. **12**(8): p. 554-64.
58. Cui, K., et al., The chromatin-remodeling BAF complex mediates cellular antiviral activities by promoter priming. *Mol Cell Biol*, 2004. **24**(10): p. 4476-86.
59. Yan, Z., et al., PBAF chromatin-remodeling complex requires a novel specificity subunit, BAF200, to regulate expression of selective interferon-responsive genes. *Genes Dev*, 2005. **19**(14): p. 1662-7.
60. Huang, M., et al., Chromatin-remodelling factor BRG1 selectively activates a subset of interferon-alpha-inducible genes. *Nat Cell Biol*, 2002. **4**(10): p. 774-81.
61. Ni, Z., et al., Apical role for BRG1 in cytokine-induced promoter assembly. *Proc Natl Acad Sci U S A*, 2005. **102**(41): p. 14611-6.
62. Bhattacharya, S., et al., Cooperation of Stat2 and p300/CBP in signalling induced by interferon-alpha. *Nature*, 1996. **383**(6598): p. 344-7.
63. Paulson, M., et al., IFN-Stimulated transcription through a TBP-free acetyltransferase complex escapes viral shutoff. *Nat Cell Biol*, 2002. **4**(2): p. 140-7.
64. Shakespear, M.R., et al., Histone deacetylases as regulators of inflammation and immunity. *Trends Immunol*, 2011. **32**(7): p. 335-43.
65. Chang, H.M., et al., Induction of interferon-stimulated gene expression and antiviral responses require protein deacetylase activity. *Proc Natl Acad Sci U S A*, 2004. **101**(26): p. 9578-83.
66. Gao, B., et al., Inhibition of histone deacetylase activity suppresses IFN-gamma induction of tripartite motif 22 via CHIP-mediated proteasomal degradation of IRF-1. *J Immunol*, 2013. **191**(1): p. 464-71.
67. Nusinzon, I. and C.M. Horvath, Interferon-stimulated transcription and innate antiviral immunity require deacetylase activity and histone deacetylase 1. *Proc Natl Acad Sci U S A*, 2003. **100**(25): p. 14742-7.

68. Falkenberg, K.J. and R.W. Johnstone, Histone deacetylases and their inhibitors in cancer, neurological diseases and immune disorders. *Nat Rev Drug Discov*, 2014. **13**(9): p. 673-91.
69. Klampfer, L., et al., Requirement of histone deacetylase activity for signaling by STAT1. *J Biol Chem*, 2004. **279**(29): p. 30358-68.
70. Sakamoto, S., R. Potla, and A.C. Larner, Histone deacetylase activity is required to recruit RNA polymerase II to the promoters of selected interferon-stimulated early response genes. *J Biol Chem*, 2004. **279**(39): p. 40362-7.
71. Litvak, V., et al., A FOXO3-IRF7 gene regulatory circuit limits inflammatory sequelae of antiviral responses. *Nature*, 2012. **490**(7420): p. 421-5.
72. Zhang, J.J., et al., Ser727-dependent recruitment of MCM5 by Stat1alpha in IFN-gamma-induced transcriptional activation. *EMBO J*, 1998. **17**(23): p. 6963-71.
73. DaFonseca, C.J., F. Shu, and J.J. Zhang, Identification of two residues in MCM5 critical for the assembly of MCM complexes and Stat1-mediated transcription activation in response to IFN-gamma. *Proc Natl Acad Sci U S A*, 2001. **98**(6): p. 3034-9.
74. Zhu, M., et al., Functional association of Nmi with Stat5 and Stat1 in IL-2- and IFNgamma-mediated signaling. *Cell*, 1999. **96**(1): p. 121-30.
75. Lau, J.F., et al., Role of metazoan mediator proteins in interferon-responsive transcription. *Mol Cell Biol*, 2003. **23**(2): p. 620-8.
76. Kadota, S. and K. Nagata, Silencing of IFN-stimulated gene transcription is regulated by histone H1 and its chaperone TAF-I. *Nucleic Acids Res*, 2014. **42**(12): p. 7642-53.
77. Tahk, S., et al., Control of specificity and magnitude of NF-kappa B and STAT1-mediated gene activation through PIASy and PIAS1 cooperation. *Proc Natl Acad Sci U S A*, 2007. **104**(28): p. 11643-8.
78. Liu, B., et al., A transcriptional corepressor of Stat1 with an essential LXXLL signature motif. *Proc Natl Acad Sci U S A*, 2001. **98**(6): p. 3203-7.
79. Mostafavi, S., et al., Parsing the Interferon Transcriptional Network and Its Disease Associations. *Cell*, 2016. **164**(3): p. 564-78.
80. Morrow, A.N., et al., A novel role for IFN-stimulated gene factor 3II in IFN-gamma signaling and induction of antiviral activity in human cells. *J Immunol*, 2011. **186**(3): p. 1685-93.
81. Fink, K. and N. Grandvaux, STAT2 and IRF9: Beyond ISGF3. *JAKSTAT*, 2013. **2**(4): p. e27521.
82. Cheon, H., et al., IFNbeta-dependent increases in STAT1, STAT2, and IRF9 mediate resistance to viruses and DNA damage. *EMBO J*, 2013. **32**(20): p. 2751-63.
83. Sung, P.S., et al., Roles of unphosphorylated ISGF3 in HCV infection and interferon responsiveness. *Proc Natl Acad Sci U S A*, 2015. **112**(33): p. 10443-8.
84. Fish, E.N., et al., Activation of a CrkL-stat5 signaling complex by type I interferons. *J Biol Chem*, 1999. **274**(2): p. 571-3.
85. Xu, L., et al., IFN regulatory factor 1 restricts hepatitis E virus replication by activating STAT1 to induce antiviral IFN-stimulated genes. *FASEB J*, 2016.
86. Harada, H., et al., Structure and regulation of the human interferon regulatory factor 1 (IRF-1) and IRF-2 genes: implications for a gene network in the interferon system. *Mol Cell Biol*, 1994. **14**(2): p. 1500-9.
87. Ivashkiv, L.B. and L.T. Donlin, Regulation of type I interferon responses. *Nat Rev Immunol*, 2014. **14**(1): p. 36-49.
88. Grandvaux, N., et al., Transcriptional profiling of interferon regulatory factor 3 target genes: direct involvement in the regulation of interferon-stimulated genes. *J Virol*, 2002. **76**(11): p. 5532-9.
89. Collins, S.E., R.S. Noyce, and K.L. Mossman, Innate cellular response to virus particle entry requires IRF3 but not virus replication. *J Virol*, 2004. **78**(4): p. 1706-17.
90. Bartee, E., et al., The addition of tumor necrosis factor plus beta interferon induces a novel synergistic antiviral state against poxviruses in primary human fibroblasts. *J Virol*, 2009. **83**(2): p. 498-511.

91. Wang, W., et al., Convergent Transcription of Interferon-stimulated Genes by TNF-alpha and IFN-alpha Augments Antiviral Activity against HCV and HEV. *Sci Rep*, 2016. **6**: p. 25482.
92. Mestan, J., et al., Antiviral activity of tumour necrosis factor. Synergism with interferons and induction of oligo-2',5'-adenylate synthetase. *J Gen Virol*, 1988. **69 (Pt 12)**: p. 3113-20.
93. Lee, J., et al., TNF-alpha Induced by Hepatitis C Virus via TLR7 and TLR8 in Hepatocytes Supports Interferon Signaling via an Autocrine Mechanism. *PLoS Pathog*, 2015. **11**(5): p. e1004937.
94. Ruby, J., H. Bluethmann, and J.J. Peschon, Antiviral activity of tumor necrosis factor (TNF) is mediated via p55 and p75 TNF receptors. *J Exp Med*, 1997. **186**(9): p. 1591-6.
95. Seo, S.H. and R.G. Webster, Tumor necrosis factor alpha exerts powerful anti-influenza virus effects in lung epithelial cells. *J Virol*, 2002. **76**(3): p. 1071-6.
96. Mestan, J., et al., Antiviral effects of recombinant tumour necrosis factor in vitro. *Nature*, 1986. **323**(6091): p. 816-9.
97. Uddin, S., et al., The Rac1/p38 mitogen-activated protein kinase pathway is required for interferon alpha-dependent transcriptional activation but not serine phosphorylation of Stat proteins. *J Biol Chem*, 2000. **275**(36): p. 27634-40.
98. Li, Y., et al., Activation of mitogen-activated protein kinase kinase (MKK) 3 and MKK6 by type I interferons. *J Biol Chem*, 2005. **280**(11): p. 10001-10.
99. Wu, T., et al., Interferon-gamma induces the synthesis and activation of cytosolic phospholipase A2. *J Clin Invest*, 1994. **93**(2): p. 571-7.
100. Peppelenbosch, M.P., et al., Rac mediates growth factor-induced arachidonic acid release. *Cell*, 1995. **81**(6): p. 849-56.
101. Young, P.R., Perspective on the discovery and scientific impact of p38 MAP kinase. *J Biomol Screen*, 2013. **18**(10): p. 1156-63.
102. Li, Y., et al., Role of p38alpha Map kinase in Type I interferon signaling. *J Biol Chem*, 2004. **279**(2): p. 970-9.
103. Uddin, S., et al., Activation of the p38 mitogen-activated protein kinase by type I interferons. *J Biol Chem*, 1999. **274**(42): p. 30127-31.
104. Lee, Y.B., J.W. Schrader, and S.U. Kim, p38 map kinase regulates TNF-alpha production in human astrocytes and microglia by multiple mechanisms. *Cytokine*, 2000. **12**(7): p. 874-80.
105. Hu, J., et al., ERK1 and ERK2 activate CCAAAT/enhancer-binding protein-beta-dependent gene transcription in response to interferon-gamma. *J Biol Chem*, 2001. **276**(1): p. 287-97.
106. Lucas-Hourani, M., et al., Inhibition of pyrimidine biosynthesis pathway suppresses viral growth through innate immunity. *PLoS Pathog*, 2013. **9**(10): p. e1003678.
107. Pan, Q., et al., Mycophenolic acid augments interferon-stimulated gene expression and inhibits hepatitis C Virus infection in vitro and in vivo. *Hepatology*, 2012. **55**(6): p. 1673-83.
108. Chung, D.H., et al., Discovery of a broad-spectrum antiviral compound that inhibits pyrimidine biosynthesis and establishes a type 1 interferon-independent antiviral state. *Antimicrob Agents Chemother*, 2016.
109. Wang, Y., et al., Cross Talk between Nucleotide Synthesis Pathways with Cellular Immunity in Constraining Hepatitis E Virus Replication. *Antimicrob Agents Chemother*, 2016. **60**(5): p. 2834-48.
110. Testoni, B., et al., Ribavirin restores IFNalpha responsiveness in HCV-infected livers by epigenetic remodelling at interferon stimulated genes. *Gut*, 2016. **65**(4): p. 672-82.
111. Neuzil, K.M., et al., Safety and pharmacokinetics of vitamin A therapy for infants with respiratory syncytial virus infections. *Antimicrob Agents Chemother*, 1995. **39**(5): p. 1191-3.
112. Bocher, W.O., et al., All-trans retinoic acid for treatment of chronic hepatitis C. *Liver Int*, 2008. **28**(3): p. 347-54.
113. Cho, N.E., et al., Retinoid regulation of antiviral innate immunity in hepatocytes. *Hepatology*, 2016. **63**(6): p. 1783-95.

114. Bitetto, D., et al., Vitamin A deficiency is associated with hepatitis C virus chronic infection and with unresponsiveness to interferon-based antiviral therapy. *Hepatology*, 2013. **57**(3): p. 925-33.
115. Debing, Y. and J. Neyts, Antiviral strategies for hepatitis E virus. *Antiviral Res*, 2014. **102**: p. 106-18.
116. Loutfy, M.R., et al., Interferon alfacon-1 plus corticosteroids in severe acute respiratory syndrome: a preliminary study. *JAMA*, 2003. **290**(24): p. 3222-8.
117. Lasfar, A., A. Zloza, and K.A. Cohen-Solal, IFN-lambda therapy: current status and future perspectives. *Drug Discov Today*, 2016. **21**(1): p. 167-71.
118. Miller, C.H., S.G. Maher, and H.A. Young, Clinical Use of Interferon-gamma. *Ann N Y Acad Sci*, 2009. **1182**: p. 69-79.
119. Lau, J.Y., et al., A randomised controlled trial of recombinant interferon-gamma in Chinese patients with chronic hepatitis B virus infection. *J Med Virol*, 1991. **34**(3): p. 184-7.
120. Muir, A.J., P.B. Sylvestre, and D.C. Rockey, Interferon gamma-1b for the treatment of fibrosis in chronic hepatitis C infection. *J Viral Hepat*, 2006. **13**(5): p. 322-8.
121. Chan, H.L., et al., Peginterferon lambda for the treatment of HBeAg-positive chronic hepatitis B: A randomized phase 2b study (LIRA-B). *J Hepatol*, 2016. **64**(5): p. 1011-9.
122. Muir, A.J., et al., A randomized phase 2b study of peginterferon lambda-1a for the treatment of chronic HCV infection. *J Hepatol*, 2014. **61**(6): p. 1238-46.
123. Hernandez, P.P., et al., Interferon-lambda and interleukin 22 act synergistically for the induction of interferon-stimulated genes and control of rotavirus infection. *Nat Immunol*, 2015. **16**(7): p. 698-707.
124. Pott, J., et al., IFN-lambda determines the intestinal epithelial antiviral host defense. *Proc Natl Acad Sci U S A*, 2011. **108**(19): p. 7944-9.
125. Schoggins, J.W., et al., A diverse range of gene products are effectors of the type I interferon antiviral response. *Nature*, 2011. **472**(7344): p. 481-5.
126. Asselah, T., et al., Liver gene expression signature to predict response to pegylated interferon plus ribavirin combination therapy in patients with chronic hepatitis C. *Gut*, 2008. **57**(4): p. 516-24.
127. Dill, M.T., et al., Interferon-gamma-stimulated genes, but not USP18, are expressed in livers of patients with acute hepatitis C. *Gastroenterology*, 2012. **143**(3): p. 777-86 e1-6.
128. Crow, Y.J. and N. Manel, Aicardi-Goutieres syndrome and the type I interferonopathies. *Nat Rev Immunol*, 2015. **15**(7): p. 429-40.
129. Bennett, L., et al., Interferon and granulopoiesis signatures in systemic lupus erythematosus blood. *J Exp Med*, 2003. **197**(6): p. 711-23.
130. Mandl, J.N., et al., Divergent TLR7 and TLR9 signaling and type I interferon production distinguish pathogenic and nonpathogenic AIDS virus infections. *Nat Med*, 2008. **14**(10): p. 1077-87.
131. Mullen, L.M., G. Chamberlain, and S. Sacre, Pattern recognition receptors as potential therapeutic targets in inflammatory rheumatic disease. *Arthritis Res Ther*, 2015. **17**: p. 122.

Chapter 3

Non-canonical Antiviral Mechanisms of ISGs: Dispensability of Interferons

Lei Xu[1], Wenshi Wang[1], Maikel P. Peppelenbosch[1], and Qiuwei Pan[1]

[1]Department of Gastroenterology and Hepatology, Erasmus MC-University Medical Center, Rotterdam, the Netherlands

Trends in Immunology. 2017. 38(1):1-2

Type I interferons (IFNs) have broad antiviral activities through the induction of interferon-stimulated genes (ISGs). It is considered to constitute the first line of antiviral defense, but excessive exposure to IFNs provokes tissue damage and other pathological events. In addition to type I IFNs, however, the body has other innate antiviral defenses as well, which were commandingly reviewed by dr. Paludan in a recent issue of *Trends in Immunology* [1]. The article highlights that type I IFN-independent antiviral mechanisms, including alternative antiviral cytokines (*e.g.* IFN-λ or interleukin 22), or the basal expression of particular ISGs that all can mediate early antiviral defenses without evoking the inflammatory damage associated with production of type I IFNs. However, we feel that, while the constitutively expressed IFN regulatory factors (IRFs) and pattern recognition receptors (PRRs) have been largely examined in the context of the scaling of IFN responses, they also mediate important antiviral mechanisms that are independent of IFN induction and, thus, should also be emphasized.

There are hundreds of ISGs that are usually induced by IFNs. Although they are thought to be the ultimate antiviral effectors, only a small subset of ISGs actually have potent antiviral activity as recently demonstrated by a screening of over 380 human ISGs for their antiviral effects [2, 3]. Some ISGs appear to act on specific viruses; whereas others have potent antiviral activity against a broad spectrum of viruses, especially IRFs (*e.g.* IRF1 and IRF2) and PRRs (*e.g.* cGAS, RIG-I and MDA5) [2, 3]. Classically, the induction or/and activation of these broad antiviral ISGs by viruses or IFNs are thought to enhance further IFN production, in turn inducing strong and broad induction of ISGs capable of combating viral infection through positive feedback loop. However, constitutive expression of particular ISGs may provide necessary antiviral defense without the need for IFN production. Especially the observation that, several ISGs have general antiviral effects in human STAT1 deficient fibroblasts, which are deficient in IFN signal transduction, in our view strongly supports this notion [2].

IRFs are transcription factors that indeed can bind to promoter regions of specific IFN genes to drive their transcription. PRRs can recognize specific components of the viral nucleic acid and trigger IFN production through downstream elements including IRF3 and IRF7 [4]. Thus, IFNs are important mediators of their antiviral action. However, accumulating evidence suggest that these broad antiviral ISGs simultaneously function through IFN-independent pathways, as they are capable of inducing transcription of many ISGs

independent of IFN production or signaling [2]. For instance, IRF1 inhibits hepatitis E virus infection through activation of STAT1 transcription and phosphorylation without concomitant IFN production [5]. cGAS can induce a large number of ISGs via a STING-dependent, IRF3-mediated process but functions independent of the canonical IFN signaling [3]. RIG-I has also been demonstrated to induce ISGs by augmenting STAT1 activation but independent of the classical IFN pathway [6]. It has been reported to strengthen STAT1 activation by disruption of the binding of STAT1 to its negative regulator SHP1 [7].

We feel that this idea is further bolstered by the definition of at least some of the other molecular mechanisms that execute type I IFN-independent antiviral defense. RIG-I can directly inhibit viral replication by blocking the binding of viral polymerase to viral RNA [8, 9]. During hepatitis B virus (HBV) infection, RIG-I recognizes and binds the 5'-ε region of the pregenomic viral RNA (pgRNA). It thus prevents the interaction of HBV polymerase with this 5'-ε region, leading to suppression of HBV replication [8]. During influenza A virus infection, RIG-I binds to the nucleocapsids of cytoplasm-invading viruses, resulting in destabilization of the nucleocapsids that hampers viral propagation [9]. Furthermore, RIG-I and MDA5 exert their direct antiviral functions that require intact ATPase activity and involves displacing viral proteins from their pre-bound positions on dsRNA [10]. In response, viruses have also developed sophisticated strategies to counteract host antiviral defense. For instance, herpesvirus can hijack activated RIG-I to avoid antiviral cytokine production [11]. Hepatitis C virus can prevent physical interaction between viral RNA and host PRRs like RIG-I and MDA5 [12]. Nevertheless, constitutive expression of RIG-I and MDA5 can be expected to provide protection against a variety of viruses.

In line with the review by Paludan highlighting the essential role of IFN-independent antiviral response, we now have extended and emphasized the importance of possible IFN-independent mechanisms of these broad antiviral ISGs. However, these non-canonical antiviral mechanisms are largely elusive, thus deserving further investigation, although the IFN-dependent mechanisms also require further clarification (Figure 1). We would thus call upon the scientific community to devote more attention to this under-investigated subject as it appears to constitute a vital component of the defense of the body against viral challenges.

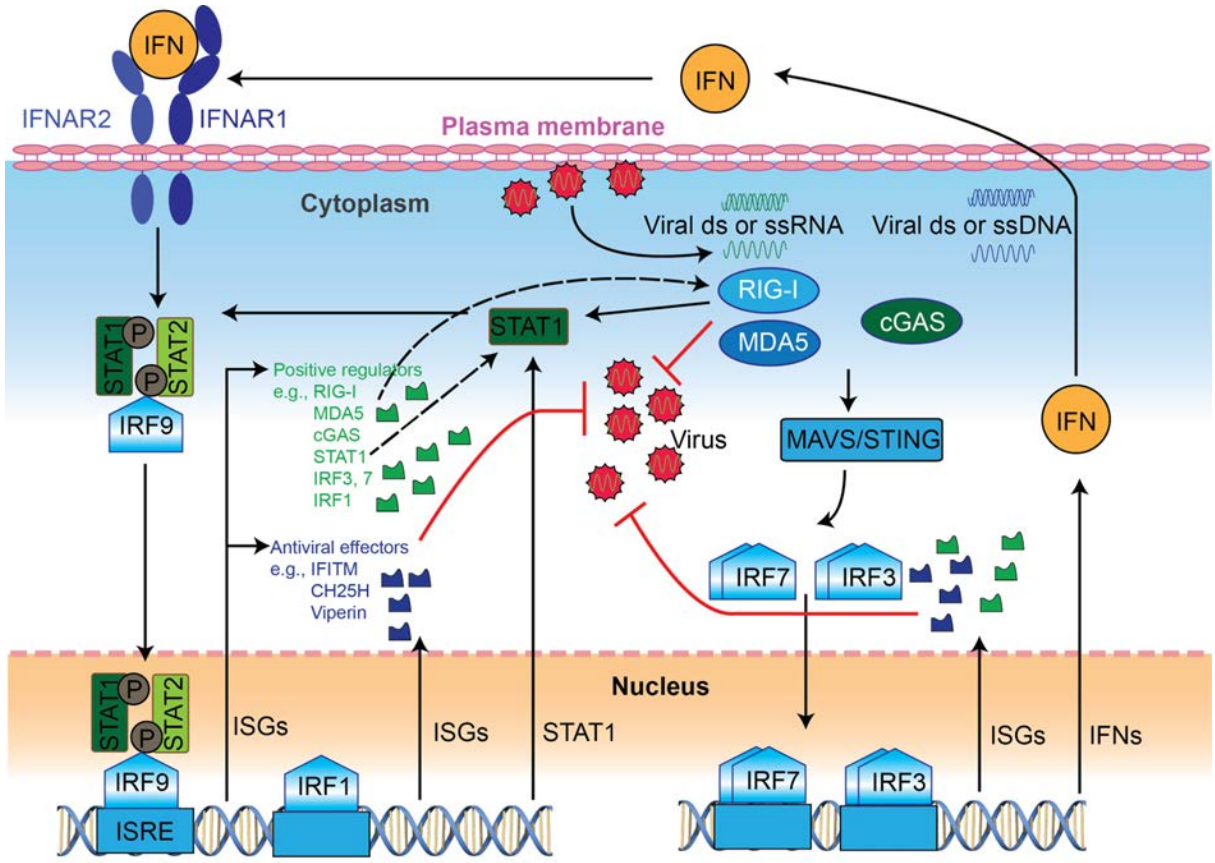

Figure 1. Interferon (IFN)-Dependent and Independent Antiviral Mechanisms of IFN-Stimulated Genes (ISGs).

Classically, Type I IFN induces gene expression via the Janus kinase-signal transducer and activator of transcription (JAK-STAT) pathway, resulting in expression of a range of ISGs that can be mainly divided into antiviral effectors and positive regulators. Some positive regulators, such as retinoic-acid inducible gene I (RIG-I), melanoma differentiation associated protein 5 (MDA5), and cyclic GMP-AMP synthase (cGAS), can recognize viral nucleic acid, triggering expression of IFNs through the IFN regulatory factors IRF3 and IRF7. Many of these positive regulators can activate the transcription of ISGs independently of IFN production. In particular, cGAS can induce ISG expression via a stimulator of IFN genes (STING)-dependent, IRF3-mediated process. RIG-I can induce ISG expression by augmenting STAT1 activation. IRF1 can activate ISG expression via STAT1 activation. Of note, RIG-I and MDA5 also directly inhibit viral propagation. Abbreviations: IFNAR1/2, IFN-α receptor 1/2; ISRE, IFN-stimulated response element. The red line with a blunt end indicates antiviral activity.

References

1. Paludan, S.R., Innate Antiviral Defenses Independent of Inducible IFNalpha/beta Production. *Trends Immunol*, 2016. **37**(9): p. 588-96.
2. Schoggins, J.W., et al., A diverse range of gene products are effectors of the type I interferon antiviral response. *Nature*, 2011. **472**(7344): p. 481-5.
3. Schoggins, J.W., et al., Pan-viral specificity of IFN-induced genes reveals new roles for cGAS in innate immunity. *Nature*, 2014. **505**(7485): p. 691-5.
4. Gurtler, C. and A.G. Bowie, Innate immune detection of microbial nucleic acids. *Trends Microbiol*, 2013. **21**(8): p. 413-20.
5. Xu, L., et al., IFN regulatory factor 1 restricts hepatitis E virus replication by activating STAT1 to induce antiviral IFN-stimulated genes. *FASEB J*, 2016. **30**(10): p. 3352-3367.
6. Jiang, L.J., et al., RA-inducible gene-I induction augments STAT1 activation to inhibit leukemia cell proliferation. *Proc Natl Acad Sci U S A*, 2011. **108**(5): p. 1897-902.
7. Zhang, F., et al., Hepatitis E genotype 4 virus from feces of monkeys infected experimentally can be cultured in PLC/PRF/5 cells and upregulate host interferon-inducible genes. *J Med Virol*, 2014. **86**(10): p. 1736-44.
8. Sato, S., et al., The RNA sensor RIG-I dually functions as an innate sensor and direct antiviral factor for hepatitis B virus. *Immunity*, 2015. **42**(1): p. 123-32.
9. Weber, M., et al., Influenza virus adaptation PB2-627K modulates nucleocapsid inhibition by the pathogen sensor RIG-I. *Cell Host Microbe*, 2015. **17**(3): p. 309-19.
10. Yao, H., et al., ATP-Dependent Effector-like Functions of RIG-I-like Receptors. *Mol Cell*, 2015. **58**(3): p. 541-8.
11. He, S., et al., Viral pseudo-enzymes activate RIG-I via deamidation to evade cytokine production. *Mol Cell*, 2015. **58**(1): p. 134-46.
12. Neufeldt, C.J., et al., The Hepatitis C Virus-Induced Membranous Web and Associated Nuclear Transport Machinery Limit Access of Pattern Recognition Receptors to Viral Replication Sites. *PLoS Pathog*, 2016. **12**(2): p. e1005428.

Chapter 4

Disparity of Basal and Therapeutically Activated Interferon Signaling in Constraining Hepatitis E Virus Infection

Xinying Zhou[1], **Lei Xu[1]**, Wenshi Wang[1], Koichi Watashi[2], Yijin Wang[1], Dave Sprengers[1], Petra E. de Ruiter[3], Luc J.W. van der Laan[3], Herold J. Metselaar[1], Nassim Kamar[4, 5, 6], Maikel P. Peppelenbosch[1] and Qiuwei Pan[1]

[1]Department of Gastroenterology and Hepatology, Erasmus MC-University Medical Center and Postgraduate School Molecular Medicine, Rotterdam, Netherlands

[2]Department of Virology II, National Institute of Infectious Diseases, Shinjuku-ku, Tokyo, Japan;

[3]Department of Surgery, Erasmus MC-University Medical Center and Postgraduate School Molecular Medicine, Rotterdam, Netherlands

[4]Department of Nephrology and Organ Transplantation, CHU Rangueil, TSA, Toulouse cedex 9, France;

[5]INSERM U1043, IFR–BMT, CHU Purpan, Toulouse, France;

[6]Université Paul Sabatier, Toulouse, France

Journal of Viral Hepatitis. 2016. 23(4): 294-304.

Abstract

Hepatitis E virus (HEV) represents one of the foremost causes of acute hepatitis globally. Although there is no proven medication for hepatitis E, pegylated Interferon-α (IFN-α) has been used as off-label drug for treating HEV. However, the efficacy and molecular mechanisms of how IFN signaling interacts with HEV remain undefined. As IFN-α has been approved for treating chronic hepatitis C for decades and the role of interferon signaling has been well studied in hepatitis C virus (HCV) infection, this study aimed to comprehensively investigate virus-host interactions in HEV infection with focusing on the IFN signaling, in comparison to HCV infection. A comprehensive screen of human cytokines and chemokines revealed that IFN-α was the sole humoral factor inhibiting HEV replication. IFN-α treatment exerted a rapid and potent antiviral activity against HCV; whereas it had moderate and delayed anti-HEV effects *in vitro* and in patients. Surprisingly, blocking the basal IFN pathway by inhibiting JAK1 to phosphorylate STAT1 has resulted in drastic facilitation of HEV, but not HCV infection. Gene silencing of the key components of JAK-STAT cascade of the IFN signaling, including JAK1, STAT1 and interferon regulatory factor 9 (IRF9) stimulated HEV infection. In conclusion, compared to HCV, HEV is less sensitive to IFN treatment. In contrast, the basal IFN cascade could effectively restrict HEV infection. This bears significant implications in management of HEV patients and future therapeutic development.

Keyword: Hepatitis E virus; interferon; interferon-stimulated genes; JAK-STAT cascades

Introduction

As an emerging infectious pathogen, hepatitis E virus (HEV) represents the most common cause of acute viral hepatitis [1]. Outbreaks of hepatitis E occur periodically throughout the developing world, which often cause fulminant hepatitis with high mortality (reaching 25%) in the case of pregnant women [2]. In the industrialized countries, HEV usually only causes an acute and self-limiting infection, it however bears a high risk of developing chronic hepatitis in immunocompromised patients with substantial mortality rates [3]. Thus, it is important to understand the underlying mechanisms of the distinct infection courses of different populations upon exposure to HEV. For severely affected patients, there is an urgent need for developing optimal therapies, because no proven antiviral medication is available for hepatitis E.

Cytokines induced by viral infection play a key role in host defense against the infection [4], but their roles in anti-HEV immunity remain largely obscure. HEV provokes the production of a panel of inflammatory cytokines and chemokines with considerable higher levels in experimental models and in patients [4-7]. However, the action of these HEV-induced cytokines on the life-cycle and pathogenesis of HEV infection remain unknown. Interferons (IFNs), pleiotropic cytokines, are of vital importance for the innate defense against viral infection [8]. They are grouped into three classes including type I, II and III, which bind to distinct receptors to stimulate their antiviral responses in host cells [9]. Pegylated IFN-α in combination with ribavirin was considered the standard antiviral therapy for chronic hepatitis C virus (HCV) infection [10]. In addition, type III IFN-lambdas (IFN-λs), which appear to have less side effects than IFN-α, are currently clinically evaluated for the treatment of chronic hepatitis C [11, 12]. Although Pegylated IFN-α, ribavirin or the combination have already been used to treat individual cases or small case series of HEV infection as off-label drugs [13-15], their mechanism-of-actions in the setting of HEV remain poorly investigated.

Intriguingly, basal JAK-STAT signaling in the absence of exogenous IFN stimulation could already serve as a first line of intracellular antiviral defense [16]. In fact, the seroprevalence of HEV is substantially high in both developing and developed countries; whereas majority healthy people have only asymptomatic or self-limiting acute infection. Thus, humans clearly have powerful defense mechanisms against HEV. It is of an intriguing

question whether basal IFN signaling plays a crucial role in the process of HEV resistance or self-limiting.

The absence of robust cell culture models has hampered fundamental and translational research of HEV. Fortunately, subgenomic and infectious models for HEV infection have come available [17] and such models were recently used in studying the infection biology and assessing potential antivirals [18-20]. In this study, we comprehensively characterized the role of cytokines in regulating HEV infection. IFN-α was found the sole humoral factor provoking inhibition of HEV replication. Further investigation identified the essential role of basal IFN signaling and the key components of JAK-STAT cascades in protecting against HEV replication. These results revealed distinct mode-of-actions of basal and treatment activated IFN signaling in controlling HEV infection.

Materials and Methods

Patients

Chronic HEV patients treated with pegylated IFN-α monotherapy at CHU Rangueil, Toulouse, France were selected and 4 cases were identified. Patient 1, 2 and 3 were immunocompromised patients with liver transplantation and patient 4 had hematologic disease. HEV viral kinetics was analyzed in these four patients by retrieving HEV RNA titters (log copies/mL) at day 0, 1, 3, 7, 15, 21 and 30 post-treatment. The study was approved by the institutional review boards of Toulouse Hospital, and all of the patients presented their written informed consent to participate in this study.

Reagents

Cytokines and chemokines (PeproTech or R&D Systems) were used for screening. Human IFNs (Thermo Scientific, Netherlands) were dissolved in culture medium. Stocks of Jak inhibitor I (Santa Cruz Biotech, Santa Cruz, CA) was dissolved in DMSO (Sigma-Aldrich, St Louis, MO) with a final concentration of 5 mg/mL. Stocks of AG-490 and CP 690,550 were dissolved in DMSO with a final concentration of 10 mg/mL. Antibodies including phospho-STAT1, total STAT1, phospho-JAK1, Interferon stimulated factor 9 (IRF9) (Cell Signaling Technology, Netherlands) and β-actin (Santa Cruz Biotech, Santa Cruz, CA); anti-rabbit or anti-mouse IRDye-conjugated secondary antibodies (Stressgen, Glandford Ave, Victoria, BC, Canada) were also used.

Cell culture models

HEV genomic RNA was generated from a plasmid construct containing the full-length HEV genome (Kernow-C1 p6 clone, GenBank Accession Number JQ679013) or a construct containing subgenomic HEV sequence coupled with a *Gaussia* luciferase reporter gene (p6-Luc), using the Ambion MESSAGE MACHINE *in vitro* RNA transcription Kit (Life Technologies Corporation) [17, 21]. The human hepatoma 7 (Huh7) cells were collected and centrifuged for 5 min, 1500 rpm, 4 °C. Supernatant was removed and washed with 4 mL Opti-MEM by centrifuging for 5 min, 1500 rpm, 4 °C. The cell pellet was re-suspended in 100 µL Opti-MEM and mixed with p6 full-length HEV RNA or p6-Luc subgenomic RNA. Electroporation was performed with the Bio-Rad's electroporation systems using the protocol of a designed program (240 volts, pulse length 0.5, number 1 and cuvette 4 mm) [17]. Huh7-ET replicon was based on Huh7 cells containing a subgenomic HCV bicistronic replicon (1389/NS3-3V/LucUbiNeo-ET) and maintained with 250 µg/mL G418. Huh7 cells harboring the full-length JFH1-derived genome was used as an infectious HCV model [22].

Gene knockdown and overexpression by lentiviral vector

Lentiviral vectors (Sigma-Aldrich) targeting JAK1, STAT1, IRF9 or GFP control were obtained from the Erasmus Center for Biomics and produced in HEK 293T cells as previously described [23]. After a pilot study, the shRNA vectors exerting optimal gene knockdown were selected. To generate gene knockdown or overexpression cells, Huh7 cells were transduced with lentiviral vectors. Since the knockdown vectors also express a puromycin resistance gene, transduced cells were subsequently selected by adding 2.5 µg/mL puromycin (Sigma) to the cell culture medium.

Measurement of luciferase activity

For *Gaussia* luciferase, the activity of secreted luciferase in the cell culture medium was measured by BioLux® *Gaussia* Luciferase Flex Assay Kit (New England Biolabs). For *firefly* luciferase, luciferin potassium salt (100 mM; Sigma) was added to cells and incubated for 30 min at 37 °C. Both *Gaussia* and *firefly* Luciferase activity was quantified with a LumiStar Optima luminescence counter (BMG LabTech, Offenburg, Germany).

MTT assay

10 mM 3-(4,5-dimethylthiazol-2-yl)-2,5-diphenyltetrazolium bromide (MTT) (Sigma) was added to cells seeded in 96-well plate and the cells were grew at 37 °C with 5% CO_2 for 3 hrs. The medium was removed and 100 µL of DMSO was added to each well. The absorbance of each well was read on the microplate absorbance readers (BIO-RAD) at wavelength of 490 nm. All measurements were performed in triplicates.

Quantitative real-time polymerase chain reaction

RNA was isolated with a Machery-Nucleo Spin RNA II kit (Bioke, Leiden, Netherlands) and quantified using a Nanodrop ND-1000 (Wilmington, DE, USA). cDNA was prepared from total RNA using a cDNA Synthesis Kit (TAKARA BIO INC). The cDNA was quantified with a SYBR Green-based real-time PCR (MJ Research Opticon, Hercules, CA, USA) according to the manufacturer's instructions. GAPDH was considered as reference gene to normalize gene expression.

Western blot assay

Proteins in cell lysates were heated 5 min at 95 °C followed by loading onto sodium dodecyl sulphate-polyacrylamide gel (SDS-PAGE) and separated by electrophoresis. Proteins were electrophoretically transferred onto PVDF membrane (Invitrogen) for 1.5 hrs with an electric current of 250 mA. Subsequently, the membrane was blocked with blocking buffer. It was followed by incubation with rabbit p-JAK1, p-STAT1, t-STAT1, IRF9 (1: 1000) antibodies overnight at 4 °C. The membrane was washed 3 times and incubated for 1 hrs with anti-rabbit or anti-mouse IRDye-conjugated secondary antibodies (1: 5000) at room temperature. Blots were scanned and quantified by Odyssey infrared imaging (Li-COR Biosciences, Lincoln, NE, USA). Results were visualized and quantitated with Odyssey 3.0 software.

Statistical analysis

All results were presented as mean ± SEM. Comparisons between groups were performed with Mann-Whitney test. Differences were considered significant at a p value less than 0.05 *or 0.01 **.

Results

HEV replication is insensitive to the regulation of cytokines and chemokines

Viral infections often induce various cytokines and chemokines that in turn modulate the infection course [24]. We thus investigated the effects of a panel of cytokines and chemokines

on host susceptibility to HEV infection. To this end, we employed cell culture model of human hepatoma cells (Huh7 cell line) transfected with subgenomic construct of HEV coding sequence in which the 5' portion of ORF2 was replaced with the in-frame *Gaussia* luciferase reporter (p6-Luc) [17]. In parallel, Huh7 cells constitutively expressing a non-secreted *firefly* luciferase are used for normalization of non-specific effects on luciferase signals [18, 20].

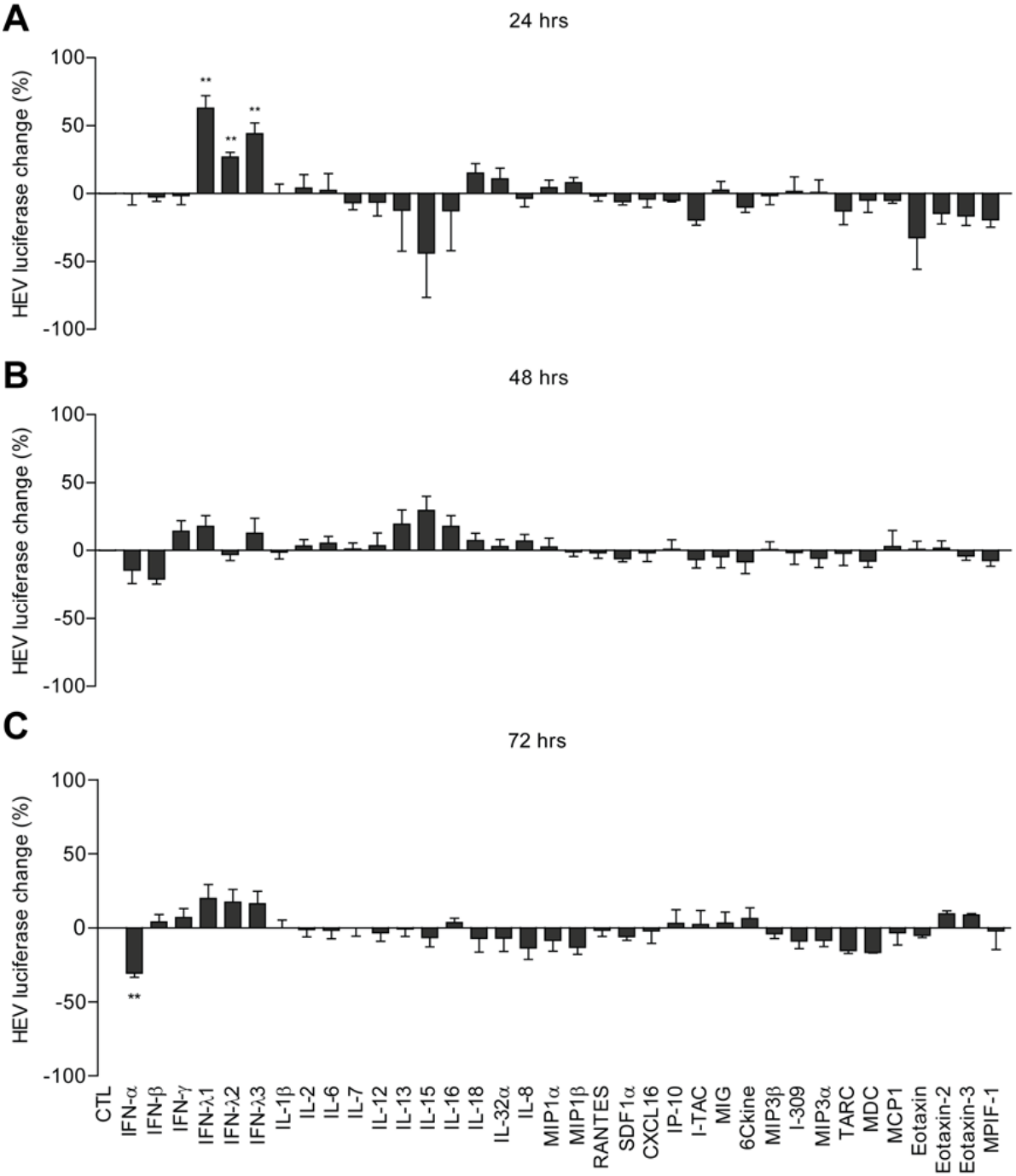

Figure 1. HEV replication was insensitive to the regulation of cytokines and chemokines.

Huh7-p6-Luc cells were treated with cytokines at 100 ng/mL (except for IFN-α and IFN-β at 100 IU /mL) for 24 (A), 48 (B) and 72 hrs (C), and then luciferase activity was measured. (Mean ± SEM, n = 4). ** $P < 0.01$.

Exploiting this experimental system, 36 cytokines and chemokines, including type I, II and III IFNs, interleukins and others, were examined in the HEV replicon, culture medium served as control. MTT assay has shown that these cytokines/chemokines in general did not exert cytotoxicity to host cells (Supplementary Figure 1). However, except for some forms of IFNs, other cytokines and chemokines had no significant effects on HEV replication (Figure 1). Hence, HEV replication is in general insensitive to the regulation of cytokines and chemokines, except for type I interferons, suggesting that antiviral immunity to HEV is mediated through a very specific branch of our immune system.

HEV, compared to HCV, is less sensitive to IFN-α treatment

Based on the results of our profiling of humoral factors involved in anti-HEV immunity, we further investigated the action of IFN-α, the archetypical type I IFN that has been successfully used to treat chronic HCV in the clinic for decades [25]. As expected, treatment of IFN-α resulted in robust inhibition of HCV replication in the Huh7-based subgenomic replicon containing a luciferase reporter (Figure 2A), suggesting that our model system can reflect clinically relevant processes. High dose of IFN-α (10-1000 IU/mL) almost completely suppressed HCV replication as early as after 24 hrs treatment. In contrast, the action of IFN-α, although evidently present, was much less effective in suppressing HEV replication in a similar subgenomic replicon that also contains a luciferase reporter. Moderate inhibitory effects were observed only after 72 hrs treatment with relatively high concentrations (100 IU/mL: 31% ± 8, mean ± SEM, n = 3 independent experiments with each 2 - 3 replicates, $P < 0.01$; 1000 IU/mL: 41% ± 3, mean ± SEM, n = 3 independent experiments with each 2 - 3 replicates, $P < 0.01$) (Figure 2B). Consistently, in the full-length HCV and HEV infectious models, IFN-α had significantly more potent antiviral effects against HCV than HEV (Figure 2C). In apparent agreement, whereas it is well-known that chronic HCV patients who respond to IFN-α therapy often experience a rapid and sharp reduction of viral load within the first few days upon treatment [26, 27], we observed that three out of four chronic HEV patients had only minor fluctuation of viral load within first two weeks of pegylated IFN-α treatment, although all the patients eventually cleared the virus (Figure 2D). These results indicate that IFN-α exerts a moderate and delayed antiviral activity against HEV, in contrast to the rapid and potent effect of this cytokine against HCV, which suggests that their underlying antiviral mechanisms differ.

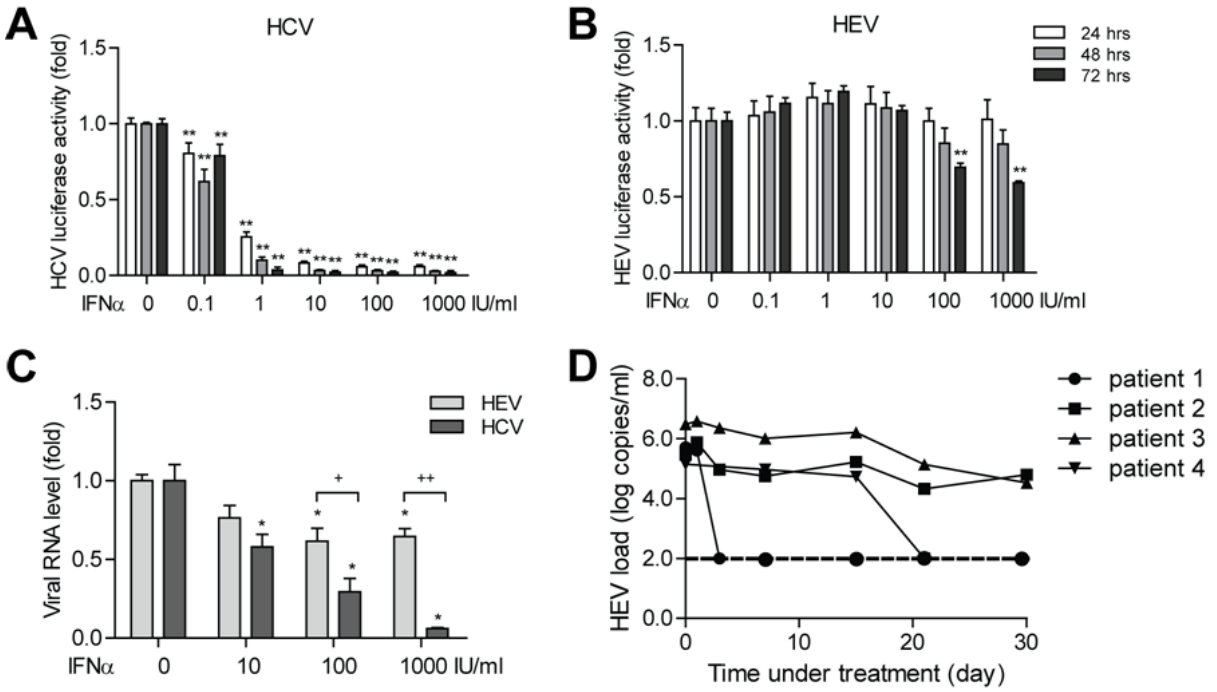

Figure 2. IFN-α exerted moderate but delayed antiviral activity against HEV.

(A) In the Huh7 cell-based subgenomic HCV replicon, treatment with IFN-α dose-dependently decreased viral replication-related luciferase activity. (Mean ± SEM, n = 3 independent experiments with each 2 - 3 replicates). (B) In the Huh7 cell-based subgenomic HEV replicon, treatment with IFN-α moderately inhibited viral replication-related luciferase activity (Mean ± SEM, n = 3 independent experiments with each 2 - 3 replicates). (C) In the full-length HEV and HCV infectious model, IFN-α significantly decreased cellular viral RNA at 48 hrs determined by qRT-PCR (Mean ± SEM, n = 5). Significant differences between level of INF-α antiviral effects were observed. (D) Four chronic HEV patients were treated with monotherapy of INF-α and the viral load was analyzed within 30 days. Treatment time was indicated as 24, 48 or 72 hrs * or + $P < 0.05$; ** or ++ $P < 0.01$.

The notion that anti-viral activity of IFN-α towards HEV is mechanistically different from that against HCV was further supported by experiments in which the anti-viral effect of alternative member of the family of type I, II and III IFNs were investigated. IFN-β and IFN-γ effectively inhibits HCV replication in the replicon model, but did not exert a significant effect on HEV replication (Figure 3A and 3B). IFN-λ is currently under clinical investigation for treating chronic HCV patients and has been shown to possess good anti-HCV antiviral activity but with fewer adverse events as compared to IFN-α [12]. In HCV replicon, IFN-λ1, IFN-λ2 and IFN-λ3 showed significant inhibition on viral replication. Unexpectedly, high dose of IFN-λ1, IFN-λ2 and IFN-λ3 even significantly enhanced viral replication in the HEV replicon after 24 hrs treatment, although the effects were mild (Figure 3C-E). Thus, the anti-HEV activity of type I, II and III IFNs appears mechanistically distinct from that against HCV (Supplementary Figure 2).

HEV replication is sensitive to basal IFN signaling

Although humoral factors do not confer protection action against HEV replication, the only partial exception being IFN-α (Figure 2 and 3), humans appear to have powerful defense mechanisms combating HEV [18], raising questions as to the nature of these mechanisms. The partial activity of IFN-α against HEV replication led us hypotheses that signaling elements, in particular JAK-STAT cascades, involved in IFN-α signal transduction might contribute to anti-HEV defense. Constitutive JAK-STAT signaling is an essential part of the innate immunity for host defense against viruses [16]. To investigate how the endogenous JAK-STAT signaling affects HEV replication, JAK inhibitor I that is known to predominantly inhibit JAK1 (but may also inhibit JAK2 and JAK3) was first tested. As expected, it can effectively inhibit its downstream target, the phosphorylation of STAT1, induced by treatment of IFN-α or IFN-λ (Supplementary Figure 3A). Consistently, it significantly inhibited the stimulation of the IFN response reporter, IFN-stimulated response elements (ISRE)-luciferase transcription reporter (Supplementary Figure 3B). Accordingly, IFN-α triggered induction of ISGs, as represented by four important members RSAD2, ISG15, OAS1 and PKR, were blocked by this inhibitor (Supplementary Figure 3C).

Importantly, treatment of JAK inhibitor I dramatically elevated HEV replication in both subgenomic replicon (Figure 4A) and the infectious model (Figure 4B). Treatment with 10 μM for 72 hrs, increased HEV replication-related luciferase activity by 3.02 ± 0.50-fold (mean ± SEM, n = 3 independent experiments with each 3 replicates, $P < 0.01$) in the replicon (Figure 4A). Similarly, treatment with 10 μM for 48 hrs, it increased viral RNA by 4.78 ± 1.13-fold (mean ± SEM, n = 3, $P < 0.05$) in the infectious model (Figure 4B). In contrast, JAK inhibitor I had only minor effect on HCV replication (Figure 4C). To investigate whether JAK2 (associated with type II IFN) and JAK3 (activated by cytokines with receptors containing the common gamma chain) are also involved, their corresponding inhibitors AG-490 and CP-690550 were tested in both HEV and HCV replicon. As shown in Figure 4D and 4E, both inhibitors had no clear effects on both HEV and HCV replication. Of note, all three inhibitors did have notable effects on cell growth determined by MTT assay (Supplementary Figure 3D). Thus, the basal JAK-STAT pathway could effectively limit HEV infection, although exogenous IFN is ineffective, whereas it is *vice versa* for HCV.

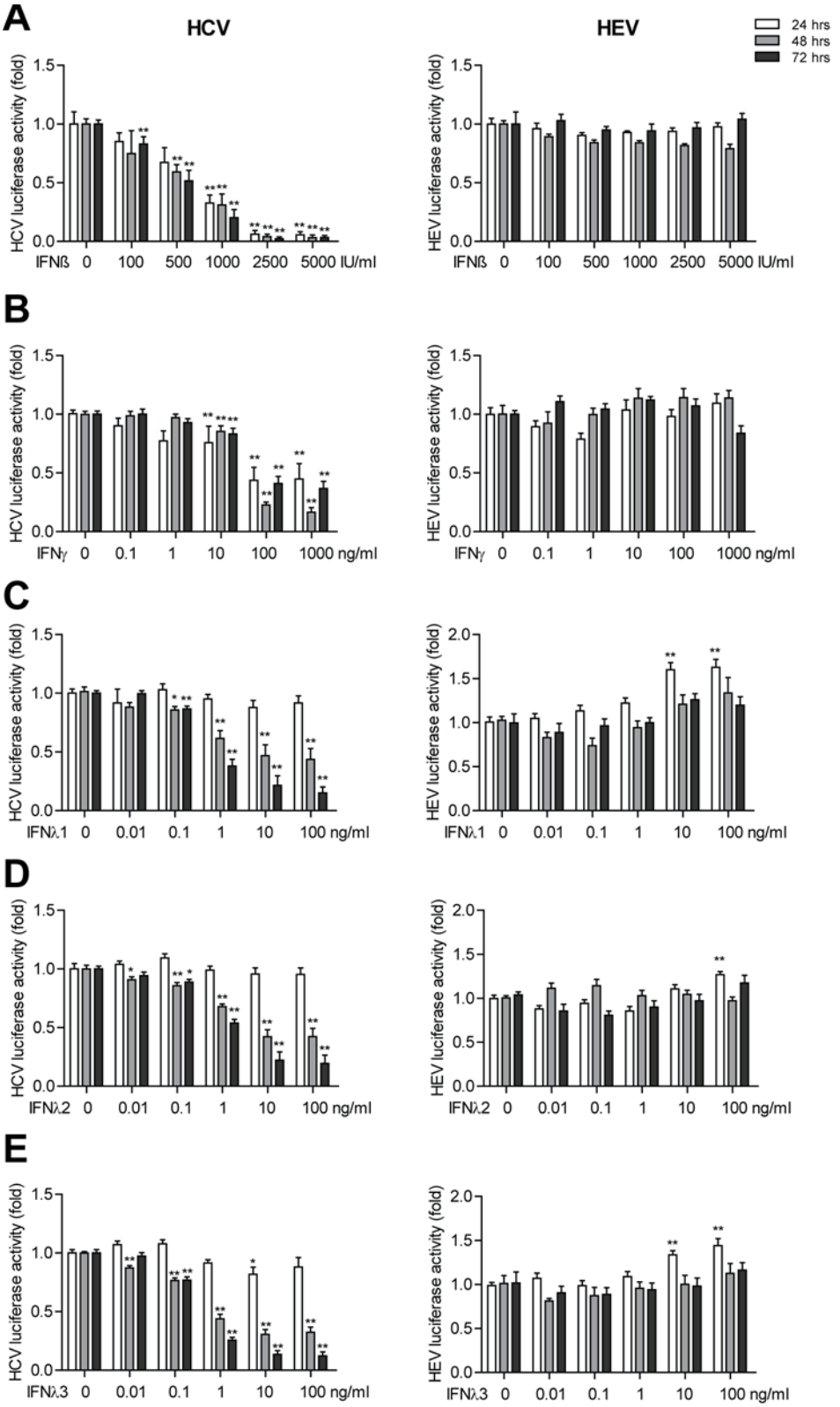

Figure 3. IFN-β, γ and λs had no significant antiviral activity against HEV infection.

In the Huh7 cell-based subgenomic HCV and HEV replicon, viral replication-related luciferase activity determined after dose-dependently treatments with IFN-β (A), IFN-γ (B), IFN-λ1 (C), IFN-λ2 (D) and IFN-λ3 (E) (Mean ± SEM, n = 3 independent experiments with each 3 - 4 replicates). Treatment time was indicated as 24, 48 or 72 hrs. * $P < 0.05$; ** $P < 0.01$.

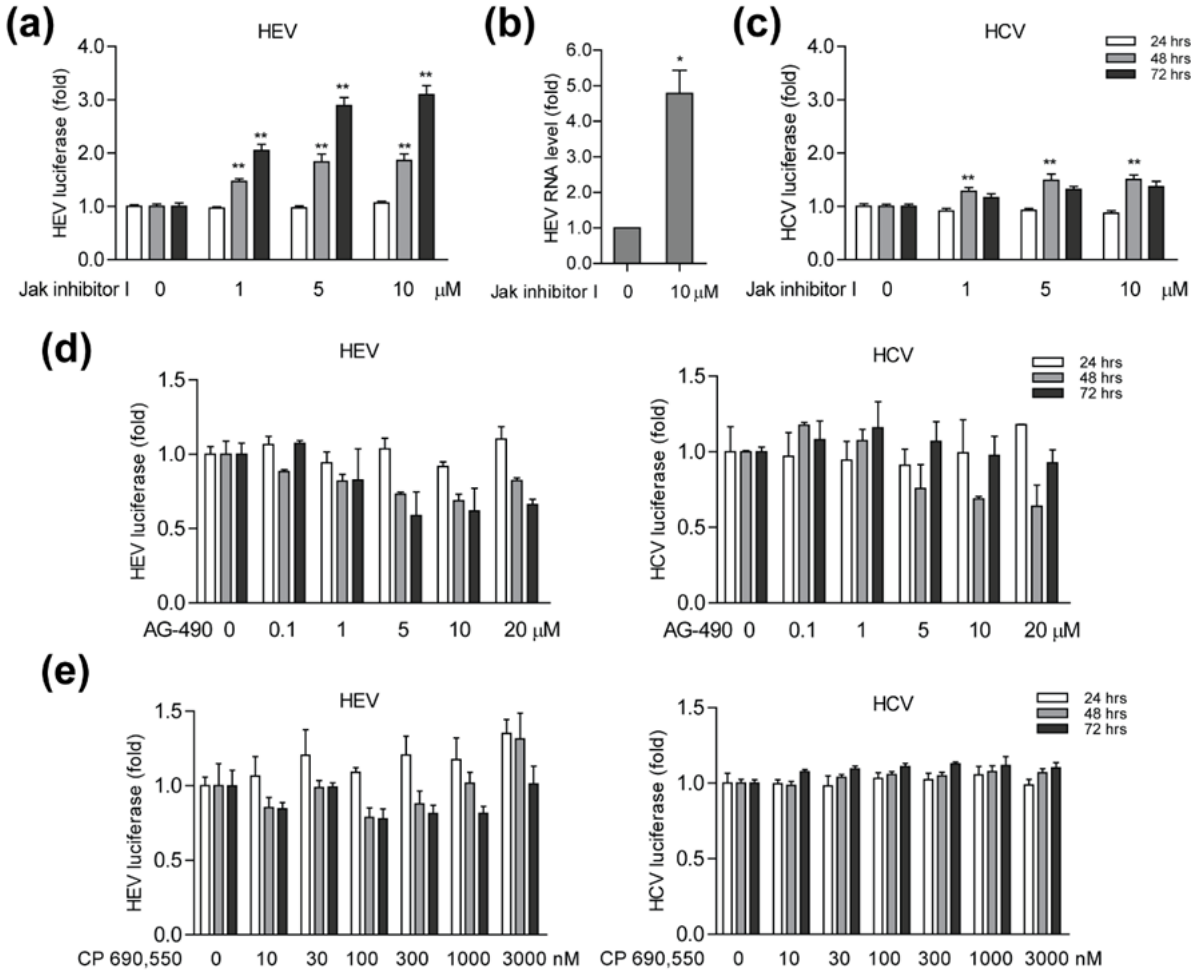

Figure 4. Pharmacological inhibition of JAK1 dramatically stimulated HEV replication.

(A) In the Huh7 cell-based subgenomic HEV replicon, treatment with Jak inhibitor I dose-dependently increased viral replication-related luciferase activity (Mean ± SEM, n = 3 independent experiments with each 3 replicates). (B) In the full-length HEV infectious model, 10 μM Jak inhibitor I significantly increased cellular viral RNA at 48 hrs determined by qRT-PCR (Mean ± SEM, n = 3). (C) In the Huh7 cell-based subgenomic HCV replicon, treatment with Jak inhibitor I did not effectively affect viral replication-related luciferase activity (Mean ± SEM, n = 3 independent experiments with each 3 replicates). (D) AG-490 is an inhibitor of JAK2 signaling and in the Huh7 cell-based subgenomic HEV and HCV replicon, treatment with AG-490 did not affect viral replication-related luciferase activity (Mean ± SEM, n = 3). (E) CP 690550 is an inhibitor of JAK3 signaling and in the Huh7 cell-based subgenomic HEV and HCV replicon, treatment with CP 690550 did not affect viral replication-related luciferase activity (Mean ± SEM, n = 3). Treatment time was indicated as 24, 48 or 72 hrs. * $P < 0.05$; ** $P < 0.01$.

Key components of JAK-STAT cascades restrict HEV infection

Upon binding of IFN-α to its receptor, JAK1 is stimulated, resulting in tyrosine phosphorylation of STAT1 and STAT2. This is followed by the formation and nuclear translocation of the STAT1-STAT2-IRF9, a transcription factor complex known as IFN-stimulated gene factor 3 (ISGF3), which in turn combines to the ISREs in the genome DNA and subsequently drives transcription of ISGs to establish an antiviral status (Figure 5A) [28].

Specific inhibition of the JAK/STAT signaling pathway has been reported to modulate HCV replication [29].

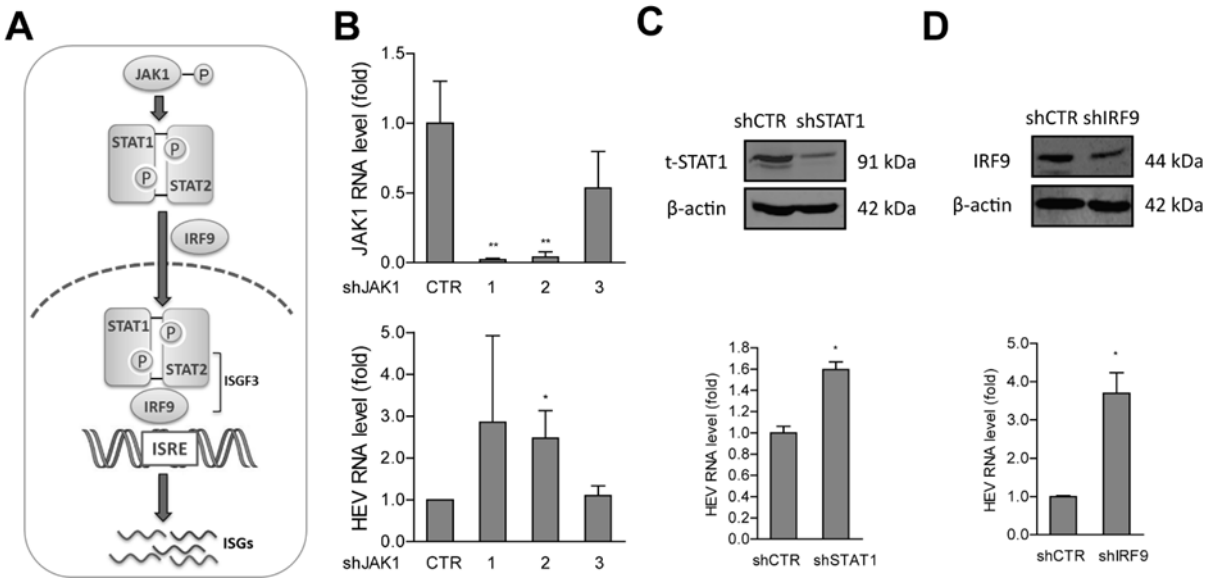

Figure 5. Key components of JAK-STAT cascades restrict HEV infection.

(A) Key components in interferon JAK-STAT signaling. (B) Knockdown of JAK1 by lentiviral shRNA vectors. Compared with the control vector transduced cells, the shJAK1 clone 1 and 2 expert potent silencing capability shown at mRNA level (Mean ± SEM, n = 4). Correspondingly, knockdown of JAK1 of clone 2 resulted in significant increase of cellular HEV RNA level (Mean ± SEM, n = 4). (C) Knockdown of STAT1 by lentiviral shRNA vectors. Western blot assay presented a potent decrease of total STAT1 protein level, correspondingly, silencing of STAT1 led to significant increase of cellular HEV RNA level (Mean ± SEM, n = 4). (D) Knockdown of IRF9 by lentiviral shRNA vectors. Western blot assay presented a potent decrease of total IRF9 protein level, similarly, silencing of IRF9 led to significant increase of cellular HEV RNA level (Mean ± SEM, n = 4). Treatment time was indicated as 24, 48 or 72 hrs. * $P < 0.05$; ** $P < 0.01$.

To evaluate the direct effects of the key components of JAK-STAT pathway including JAK1, STAT1 and IFR9 on HEV infection, Huh7 cells were transduced with integrating lentiviral vectors expressing shRNA specifically targeting JAK1, STAT1, IRF9 or GFP as a control. For JAK1 knockdown cells, two of the tested three shRNA vectors targeting JAK1 exert potent gene silencing capacity, resulted in a profound down-regulation of JAK1 mRNA level (Figure 5B). Correspondingly, JAK1 silencing led to significant increase of cellular HEV RNA level, which was measured by qRT-PCR after inoculation of HEV particles for 72 hrs. For instance, knockdown of shRNA clone 2 in JAK1 led to 2.47 ± 0.66-fold increase of HEV viral RNA (mean ± SEM, n = 4, $P < 0.05$) (Figure 5B). Furthermore, STAT1, which is phosphorylated by JAK1, was successfully silenced by shRNA targeting STAT1 in Huh7 cells with a potent reduction in protein level in shSTAT1 cells (Figure 5C). Consistently, STAT1 silencing could also significantly potentiated cellular HEV RNA level to 1.6 ± 0.13-fold (mean ± SEM, n = 3, P

< 0.05) (Figure 5C). To further determine whether event downstream of JAK-STAT cascades influences HEV replication, IRF9 was silenced with a profound down-regulation of total IRF9 protein level (Figure 5D). Similarly, silencing of IRF9 resulted in 3.70 ± 1.07-fold (mean ± SEM, n = 4, P < 0.05) elevation of cellular HEV RNA level. Therefore, key constituents of JAK-STAT cascades including JAK1, STAT1 and IRF9 play an intrinsic role in restricting HEV infection.

Discussion

Cytokines and chemokines are important components of the immune response for countering invading viruses [30]. With this group of mediators, especially IFNs play a cardinal role, exerting a wide range of pleiotropic effects [25]. Accordingly, IFN-α has become the mainstay for the treatment of chronic HCV and HBV infection, despite the considerable systemic side effects. Whereas IFN-λ shows a potent anti-viral activity as well in phase III clinical trial for treating HCV patients with much less reverse side effects, owing to the tissue-restricted expression of type III IFN receptor [31]. Hitherto, there is no approved medication for hepatitis E. Lessons have learned from standard therapy of chronic hepatitis C that IFN-α, ribavirin, or a combination as off-label drugs have been used to treat individual HEV cases or small case series [3]. As shown in this study (Figure 2D), four chronic hepatitis E patients all eventually cleared the virus after monotherapy of pegylated IFN-α. However, the viral kinetics in responding to IFN-α is very different between chronic hepatitis C and E. In chronic HCV, patients who respond to the therapy often experience a rapid and sharp reduction of viral load within the first few days upon initiation of IFN-α therapy [26, 27, 32]. In contrast, only one out of four chronic HEV patients had a rapid decline of viral load; whereas others had rather minor changes in the first two weeks of treatment. This is in line with our experimental results that HEV has a moderate and delayed responsiveness to IFN-α, compared with HCV in cell culture models. The HEV subgenomic model only mimics viral replication; whereas the HEV infectious cell culture system models the complete life cycle of HEV infection. IFN-α probably interferes HEV infection at various steps. Thus, the infectious clone appears more sensitive to IFN-α compared to the subgenomic replicon (Figure 2A-C). Other types of IFNs, including IFN-λ, did not shown any notable antiviral activity against HEV (Figure 3).

Previous studies have provided evidence of counteracting IFN response by HEV [33]. In our study, we also observed that HEV inoculation could indeed inhibit IFN-α induced phosphorylation of STAT1 and attenuate the induction of ISGs in Huh7 cells (Supplementary Figure 4C and 4D). Nevertheless, this inhibitory effect was rather minor, which may only partially contribute to the resistance of HEV to interferon treatment. Thus, the insensitivity and resistance of HEV to IFN treatments may be because of the intrinsic characteristics and pathogenesis of HEV itself. Therefore, the scenario of developing IFN-based treatment against HEV shall be carefully re-considered. Interestingly, a recent large retrospective, multicenter study showed that ribavirin as monotherapy could be very effective for treating chronic HEV infection that viral clearance was observed in the majority of patients [34]. In contrast, ribavirin monotherapy hardly has detectable effect on HCV viral load reduction[35, 36]. Only when combined with IFN-α, it doubles the response rate, compared with IFN-α alone [37].

Despite the inferiority of HEV in responding to exogenous IFN treatment, we in fact demonstrated a superior function of the basal interferon signaling, which mediates IFN-α, γ and λ signaling transduction, in protecting against HEV infection. Pharmacological inhibition of JAK1, the key upstream kinase controlling JAK-STAT cascades of the IFN pathway, has resulted in drastic facilitation of HEV but not HCV infection in cell culture models (Figure 4A-C). Consistently, by gene silencing of JAK1, STAT1 and IRF9, key factors of JAK-STAT cascades, HEV replication was efficiently potentiated (Figure 5B-D). These results highlighted the importance and mechanisms of basal IFN signaling in protecting HEV infection.

This probably at least partially explains the distinct incidence of chronic development upon exposure to HEV or HCV. In general population, HEV is mostly acute and self-limiting, except in very young children, pregnant women and immunocompromised patients that could cause severe diseases [1]. Chronic hepatitis E has so far only been reported in immunocompromised patients who are lacking of adequate immune defense power[20, 38]. However, 55% to 85% individuals infected with HCV are not able to clear the virus, but develop chronic hepatitis C [39]. Even an activated endogenous IFN response is ineffective in eradicating HCV, once chronic infection is established [40]. The only option to cure chronic HCV is antiviral treatment, including IFN-based therapies. The fact that one-third of organ transplantation patients with chronic HEV could achieve virus clearance even without any treatment, but with dose reduction of immunosuppressant [38], suggests the indispensable

role of endogenous innate immunity in HEV recovery. In addition, during the early stage of HEV infection, patients always remain subclinical and represent no apparent symptom at all. This rapidly turn to a self-limiting illness with spontaneously cleaning of HEV and need no specific treatment [41]. The phenomenon of quick clearance of HEV infection by body itself without any treatment may be associated to the critical role of defense mechanism of basal IFN signaling in combating HEV infection. Therefore, the data in current study delineate that endogenous JAK-STAT signaling exerts much potency in protecting against HEV than HCV infection. The different sensitivities between HCV and HEV to endogenous IFN signaling may also determine the distinct clinical course and outcome between hepatitis C and hepatitis E patients.

In conclusion, we revealed that HEV is in general insensitive to the regulation of cytokines and chemokines. IFN-α treatment exerts moderate but delayed antiviral activity against HEV infection in experimental models and in patients, which suggested the ineffectiveness of interferon-based monotherapy in treating chronic hepatitis E. Interestingly, blocking the basal IFN pathway resulted in drastic facilitation of HEV infection, suggesting that basal IFN pathway can effectively protect against HEV infection. Thus, this study has shed new light on the molecular insight of HEV-host interaction, in particular the role of therapeutically activated and the basal IFN signaling. This bears significant implications in management of HEV patients and future therapeutic development.

Supplementary Figures

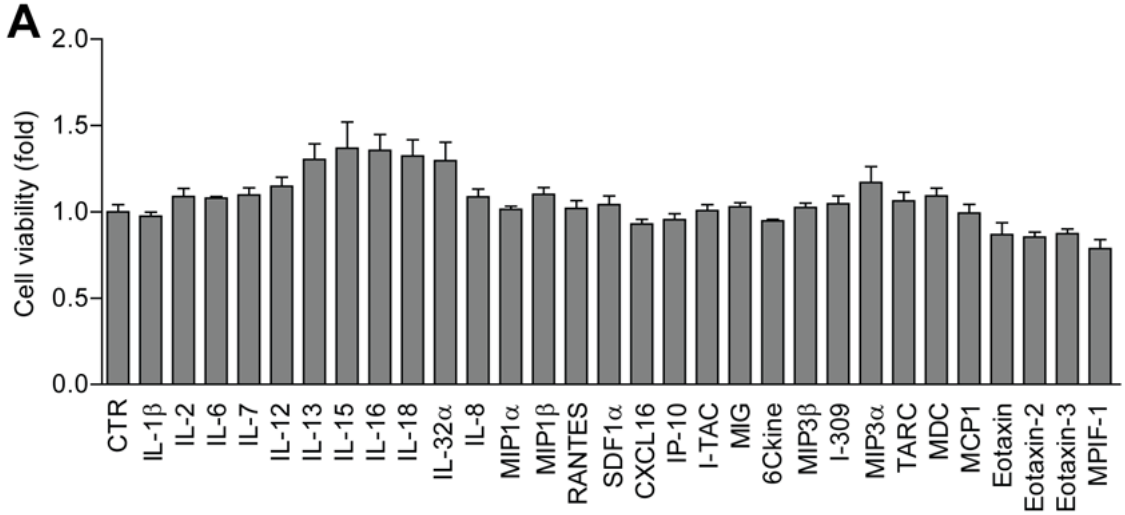

Supplementary Figure 1.

Cytokines/chemokines did not affect cell proliferation at 72 hrs determined by MTT assay (OD_{490} value) (Mean ± SD, n = 4).

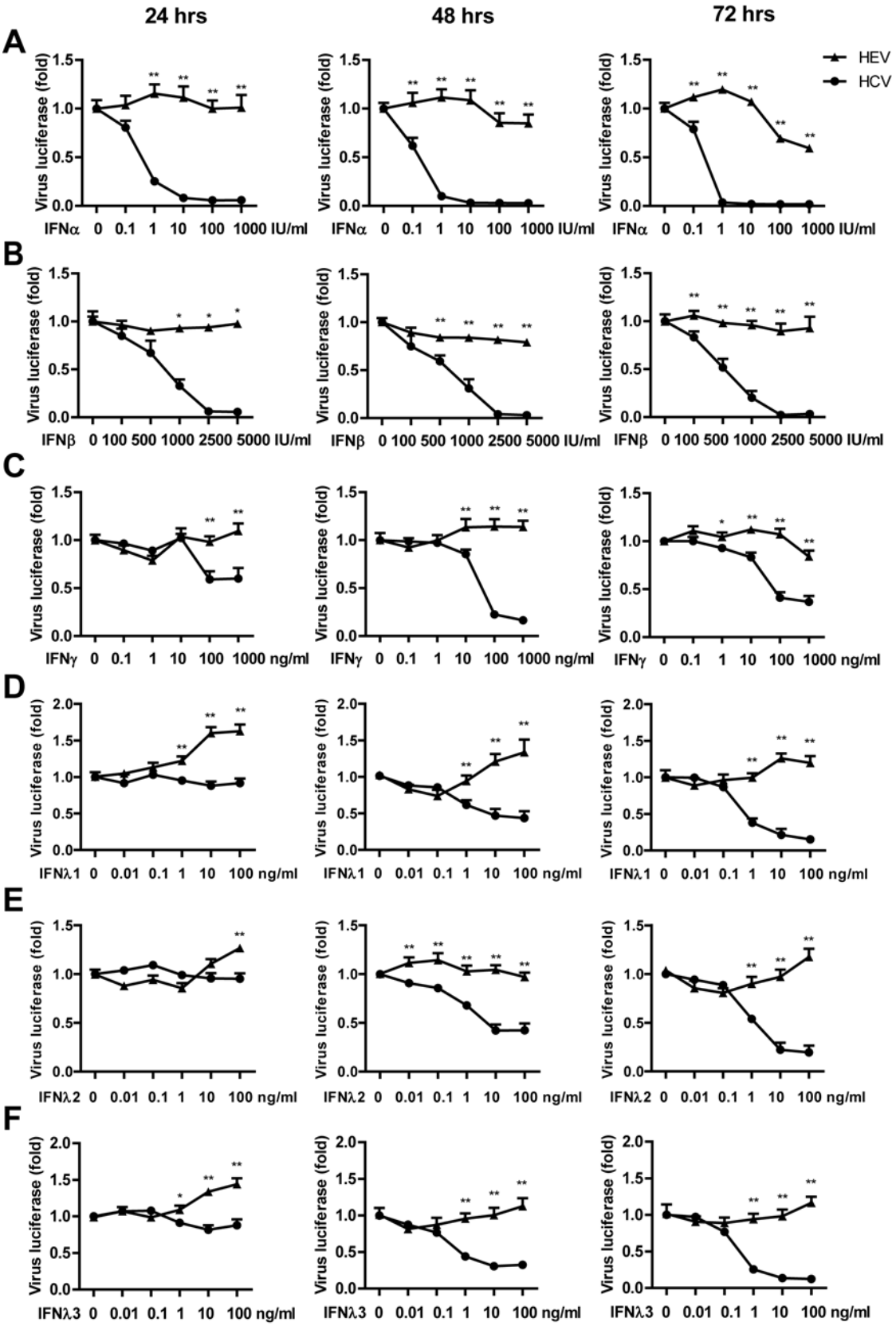

Supplementary Figure 2.

(A) IFN-α, (B) IFN-β, (C) IFN-γ, (D) IFN-λ1, (E) IFN-λ2 and (F) IFN-λ3 had significantly more potent antiviral effects against HCV than HEV in the subgenomic replication models. Treatment time was indicated as 24, 48 or 72 hrs. * $P < 0.05$; ** $P < 0.01$.

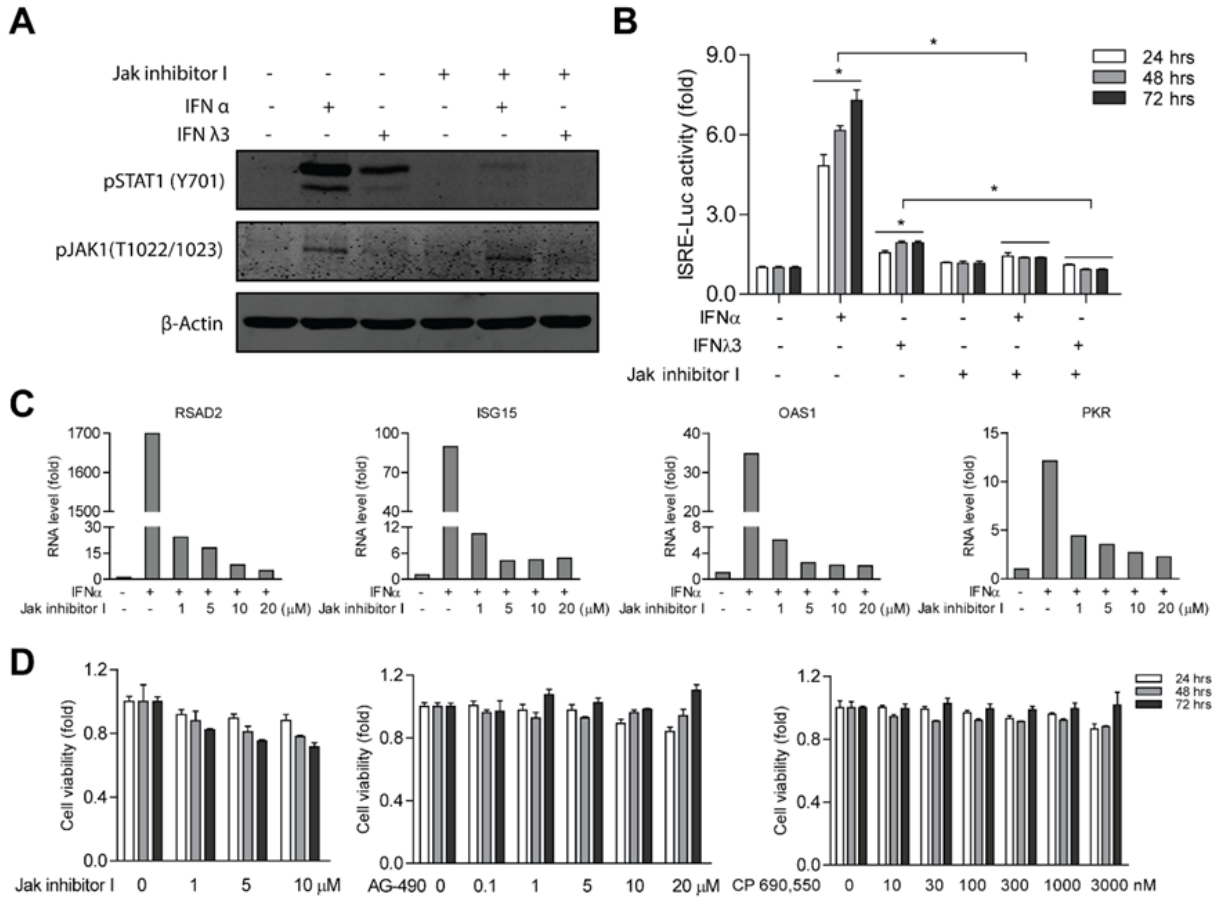

Supplementary Figure 3.

(A) Western blot showed treatment of Jak inhibitor I for 48 hrs effectively inhibited downstream target of JAK1, the phosphorylation of STAT1, induced by treatment of IFN-α or IFN-λ for 30 min. β-actin served as an internal reference. (B) Jak inhibitor I significantly inhibited the stimulation of the IFN response reporter, the ISRE-luciferase transcription reporter by IFN-α or IFN-λ for 30 min. (Mean ± SD, n = 4). (C) Jak inhibitor I blocked the induction ISGs of RSAD2, ISG15, OAS1 and PKR triggered by IFN-α. (D) Jak inhibitor I, AG-490 and CP 690550 did not affect cell proliferation determined by MTT assay (OD_{490} value) (Mean ± SD, n = 3). Treatment time was indicated as 24, 48 or 72 hrs. * $P < 0.05$; ** $P < 0.01$.

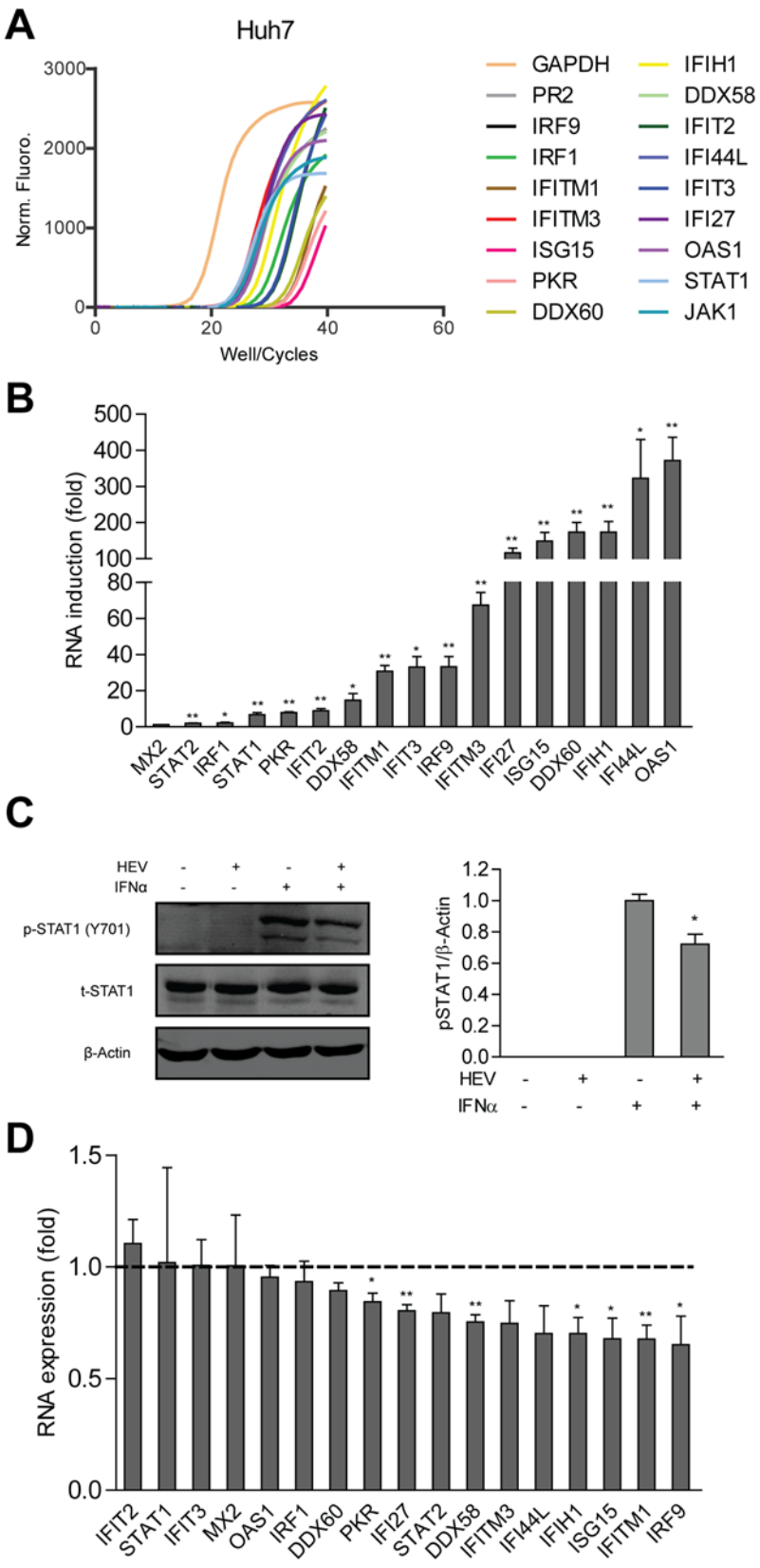

Supplementary Figure 4.

(A) The basal expression of 16 ISGs was determined in naïve Huh7 cells by qRT-PCR. (B) The expression of 16 ISGs were significantly stimulated by treatment of 1000 IU/mL IFN-α for 24 hrs (Mean ± SD, n = 4). (C) Western blot assay showed that the elevation of p-STAT1 level was significantly attenuated upon 1000 IU/mL IFN-α in HEV infected compared to naïve Huh7 cells for 48 hrs. β-actin served as an internal reference. (Mean ± SD, n = 3). (D) Inoculation of HEV moderately inhibited the stimulation of most of 16 tested IGSs upon treatment with 1000 IU/mL IFN-α for 24 hrs (Mean ± SD, n = 4-6). * P < 0.05; ** P < 0.01.

References

1. Kamar, N., et al., Hepatitis E virus infection. *Clin Microbiol Rev*, 2014. **27**(1): p. 116-38.
2. Kamar, N., et al., Hepatitis E. *Lancet*, 2012. **379**(9835): p. 2477-88.
3. Zhou, X., et al., Epidemiology and management of chronic hepatitis E infection in solid organ transplantation: a comprehensive literature review. *Rev Med Virol*, 2013. **23**(5): p. 295-304.
4. Kumar, A., et al., Association of cytokines in hepatitis E with pregnancy outcome. *Cytokine*, 2014. **65**(1): p. 95-104.
5. Tripathy, A.S., et al., Cytokine profiles, CTL response and T cell frequencies in the peripheral blood of acute patients and individuals recovered from hepatitis E infection. *PLoS One*, 2012. **7**(2): p. e31822.
6. Tripathy, A.S., et al., Peripheral T regulatory cells and cytokines in hepatitis E infection. *Eur J Clin Microbiol Infect Dis*, 2012. **31**(2): p. 179-84.
7. Devhare, P.B., et al., Analysis of antiviral response in human epithelial cells infected with hepatitis E virus. *PLoS One*, 2013. **8**(5): p. e63793.
8. Heim, M.H., Interferons and hepatitis C virus. *Swiss Med Wkly*, 2012. **142**: p. w13586.
9. Randall, R.E. and S. Goodbourn, Interferons and viruses: an interplay between induction, signalling, antiviral responses and virus countermeasures. *J Gen Virol*, 2008. **89**(Pt 1): p. 1-47.
10. Ramos, E.L., Preclinical and clinical development of pegylated interferon-lambda 1 in chronic hepatitis C. *J Interferon Cytokine Res*, 2010. **30**(8): p. 591-5.
11. Shindo, H., et al., IL-28B (IFN-lambda3) and IFN-alpha synergistically inhibit HCV replication. *J Viral Hepat*, 2013. **20**(4): p. 281-9.
12. Muir, A.J., et al., A randomized phase 2b study of peginterferon lambda-1a for the treatment of chronic HCV infection. *J Hepatol*, 2014. **61**(6): p. 1238-46.
13. Brown, L.A., et al., Acute and chronic alcohol abuse modulate immunity. *Alcohol Clin Exp Res*, 2006. **30**(9): p. 1624-31.
14. Haagsma, E.B., et al., Treatment of chronic hepatitis E in liver transplant recipients with pegylated interferon alpha-2b. *Liver Transpl*, 2010. **16**(4): p. 474-7.
15. Kamar, N., et al., Pegylated interferon-alpha for treating chronic hepatitis E virus infection after liver transplantation. *Clin Infect Dis*, 2010. **50**(5): p. e30-3.
16. Sarasin-Filipowicz, M., et al., Interferon signaling and treatment outcome in chronic hepatitis C. *Proc Natl Acad Sci U S A*, 2008. **105**(19): p. 7034-9.
17. Shukla, P., et al., Adaptation of a genotype 3 hepatitis E virus to efficient growth in cell culture depends on an inserted human gene segment acquired by recombination. *J Virol*, 2012. **86**(10): p. 5697-707.
18. Zhou, X., et al., Rapamycin and everolimus facilitate hepatitis E virus replication: revealing a basal defense mechanism of PI3K-PKB-mTOR pathway. *J Hepatol*, 2014. **61**(4): p. 746-54.
19. Debing, Y., et al., Ribavirin inhibits in vitro hepatitis E virus replication through depletion of cellular GTP pools and is moderately synergistic with alpha interferon. *Antimicrob Agents Chemother*, 2014. **58**(1): p. 267-73.
20. Wang, Y., et al., Calcineurin inhibitors stimulate and mycophenolic acid inhibits replication of hepatitis E virus. *Gastroenterology*, 2014. **146**(7): p. 1775-83.
21. Shukla, P., et al., Cross-species infections of cultured cells by hepatitis E virus and discovery of an infectious virus-host recombinant. *Proc Natl Acad Sci U S A*, 2011. **108**(6): p. 2438-43.
22. Pan, Q., et al., Mycophenolic acid augments interferon-stimulated gene expression and inhibits hepatitis C Virus infection in vitro and in vivo. *Hepatology*, 2012. **55**(6): p. 1673-83.
23. Pan, Q., et al., Combined antiviral activity of interferon-alpha and RNA interference directed against hepatitis C without affecting vector delivery and gene silencing. *J Mol Med (Berl)*, 2009. **87**(7): p. 713-22.

24. Nishitsuji, H., et al., Hepatitis C virus infection induces inflammatory cytokines and chemokines mediated by the cross talk between hepatocytes and stellate cells. *J Virol*, 2013. **87**(14): p. 8169-78.
25. Kohli, A., et al., Treatment of hepatitis C: a systematic review. *JAMA*, 2014. **312**(6): p. 631-40.
26. Padmanabhan, P., U. Garaigorta, and N.M. Dixit, Emergent properties of the interferon-signalling network may underlie the success of hepatitis C treatment. *Nat Commun*, 2014. **5**: p. 3872.
27. Berenguer, M., et al., Hepatitis C virus viral kinetics during alpha-2a or alpha-2b pegylated interferon plus ribavirin therapy in liver transplant recipients with different immunosuppression regimes. *J Clin Virol*, 2012. **53**(3): p. 231-8.
28. Pan, Q., et al., Ribavirin enhances interferon-stimulated gene transcription by activation of the interferon-stimulated response element. *Hepatology*, 2011. **53**(4): p. 1400-1; author reply 1402.
29. Zhou, X., et al., Modulating innate immunity improves hepatitis C virus infection and replication in stem cell-derived hepatocytes. *Stem Cell Reports*, 2014. **3**(1): p. 204-14.
30. Zeytun, A., et al., Induction of cytokines and chemokines by Toll-like receptor signaling: strategies for control of inflammation. *Crit Rev Immunol*, 2010. **30**(1): p. 53-67.
31. Lin, F.C. and H.A. Young, Interferons: Success in anti-viral immunotherapy. *Cytokine Growth Factor Rev*, 2014. **25**(4): p. 369-76.
32. Melchjorsen, J., Learning from the messengers: innate sensing of viruses and cytokine regulation of immunity - clues for treatments and vaccines. *Viruses*, 2013. **5**(2): p. 470-527.
33. Dong, C., et al., Suppression of interferon-alpha signaling by hepatitis E virus. *Hepatology*, 2012. **55**(5): p. 1324-32.
34. Kamar, N., et al., Ribavirin for chronic hepatitis E virus infection in transplant recipients. *N Engl J Med*, 2014. **370**(12): p. 1111-20.
35. Pawlotsky, J.M., et al., Antiviral action of ribavirin in chronic hepatitis C. *Gastroenterology*, 2004. **126**(3): p. 703-14.
36. Rotman, Y., et al., Effect of ribavirin on viral kinetics and liver gene expression in chronic hepatitis C. *Gut*, 2014. **63**(1): p. 161-9.
37. Poynard, T., et al., Randomised trial of interferon alpha2b plus ribavirin for 48 weeks or for 24 weeks versus interferon alpha2b plus placebo for 48 weeks for treatment of chronic infection with hepatitis C virus. International Hepatitis Interventional Therapy Group (IHIT). *Lancet*, 1998. **352**(9138): p. 1426-32.
38. Wang, Y., et al., Chronic hepatitis E in solid-organ transplantation: the key implications of immunosuppressants. *Curr Opin Infect Dis*, 2014. **27**(4): p. 303-8.
39. Hoofnagle, J.H., Course and outcome of hepatitis C. *Hepatology*, 2002. **36**(5 Suppl 1): p. S21-9.
40. Meissner, E.G., et al., Endogenous intrahepatic IFNs and association with IFN-free HCV treatment outcome. *J Clin Invest*, 2014. **124**(8): p. 3352-63.
41. Aggarwal, R. and S. Jameel, Hepatitis E. *Hepatology*, 2011. **54**(6): p. 2218-26.

Chapter 5

RIG-I Is a Key Antiviral Interferon-Stimulated Gene Against Hepatitis E Virus Dispensable of Interferon Production

Lei Xu[1], Wenshi Wang[1], Yunlong Li[2], Xinying Zhou[1], Yuebang Yin[1], Yijin Wang[1], Robert A. de Man[1], Luc J. W. van der Laan[3], Fen Huang[2], Nassim Kamar[4,5,6], Maikel P. Peppelenbosch[1] and Qiuwei Pan[1]

[1]Department of Gastroenterology and Hepatology, Postgraduate School Molecular Medicine, Erasmus MC-University Medical Center, Rotterdam, the Netherlands

[2]Medical Faculty, Kunming University of Science and Technology, Kunming, China

[3]Department of Surgery, Postgraduate School Molecular Medicine, Erasmus MC-University Medical Center, Rotterdam, the Netherlands

[4]Department of Nephrology and Organ Transplantation, CHU Rangueil, Toulouse, France.

[5]INSERM U1043, IFR-BMT, CHU Purpan, Toulouse, France

[6]University Toulouse III-Paul Sabatier, Toulouse, France

Hepatology. 2017. In Press

Abstract

Interferons (IFNs) are broad antiviral cytokines that exert their function by inducing the transcription of hundreds of IFN-stimulated genes (ISGs). However, little is known about the antiviral potential of these cellular effectors on hepatitis E virus (HEV) infection, the leading cause of acute hepatitis globally. In this study, we profiled the antiviral potential of a panel of important human ISGs on HEV replication in cell culture models by overexpression of an individual ISG. The mechanism of action of the key anti-HEV ISG was further studied. We identified retinoic acid–inducible gene I (RIG-I), melanoma differentiation–associated protein 5, and IFN regulatory factor 1 (IRF1) as the key anti-HEV ISGs. We found that basal expression of RIG-I restricts HEV infection. Pharmacological activation of the RIG-I pathway by its natural ligand 5'-triphosphate RNA potently inhibits HEV replication. Overexpression of RIG-I activates the transcription of a wide range of ISGs. RIG-I also mediates but does not overlap with IFN-a-initiated ISG transcription. Although it is classically recognized that RIG-I exerts antiviral activity through the induction of IFN production by IRF3 and IRF7, we reveal an IFNindependent antiviral mechanism of RIG-I in combating HEV infection. We found that activation of RIG-I stimulates an antiviral response independent of IRF3 and IRF7 and regardless of IFN production. However, it is partially through activation of the Janus kinase (JAK)–signal transducer and activator of transcription (STAT) cascade of IFN signaling. RIG-I activated two distinct categories of ISGs, one class of JAK-STAT-dependent and the other of JAK-STAT-independent, which coordinately contribute to the anti-HEV activity. Conclusion: We identified RIG-I as an important anti-HEV ISG that can be pharmacologically activated; activation of RIG-I stimulates the cellular innate immunity against HEV regardless of IFN production but partially through the JAK-STAT cascade of IFN signaling.

Keyword: HEV; ISG; Retinoic acid-inducible gene I; JAK-STAT pathway

Introduction

Hepatitis E virus (HEV) infection is the most common cause of acute viral hepatitis worldwide [1]. As a single-strand RNA virus, HEV has been divided into 4 genotypes (gt) [1]. Although acute HEV infections are mostly self-limiting, gt1 HEV infection during pregnancy may lead to high mortality up to 30% [2]. In immunosuppressed patients, such as organ transplant recipients, gt3 HEV infection can cause chronic hepatitis [2]. For those chronic patients, monotherapy or the combination of ribavirin or/and pegylated Interferon-α (PegIFN-α) have been used as off-label treatment [1]. The observation that different populations with different status of their immune system have distinct outcomes of HEV infection highlights the importance of studying HEV-host interactions.

The innate immune response plays an essential role in defending viral infections. Patients with genetic deficiencies in the innate immune system are often pro to viral infection and develop more severe symptoms [3, 4]. In response to viral infection, host cells produce virus-induced cytokines including interferons (IFNs), particularly type I IFN (IFN-α and -β), which have potent antiviral activity against a broad spectrum of viruses [5]. Type I IFNs promote an antiviral state in an autocrine or paracrine manner by transcriptional induction of hundreds of interferon-stimulated genes (ISGs) [6]. However, excessive accumulation of type I IFNs may evoke pathological effects to the organism [7]. Recently, emerging studies have described the type I IFNs independent innate antiviral defense [8, 9]. These IFN-independent antiviral mechanisms including the production of alternative antiviral cytokines (*e.g.* IFN-λ or interleukin 22) and the basal expression of direct antiviral ISGs [9]. The basal expression of these ISGs may be attributed to tonic IFN signaling and this establishes a cell-autonomous antiviral status of the host, but independent of virus-triggered IFN production. Therefore, ISGs play important roles in both IFN-dependent and -independent antiviral mechanisms.

As the ultimate antiviral effectors, ISGs are transcriptionally induced through the Janus kinase/signal transducers and activators of transcription (JAK-STAT) pathway by tonic or exogenous IFNs. In previous studies, more than 380 individual human ISGs have been tested for their antiviral effects on a wide species of viruses including many important human and animal viruses [10, 11]. Surprisingly, only small subsets of ISGs exert antiviral activities against either a specific or broad spectrum of viruses. Unexpectedly, a few ISGs

even promote the replication of certain viruses [10, 11]. Given the fact that IFN-α has anti-HEV activity *in vitro* and is probably also effective in chronic patients [12-14], this strongly suggests that ISGs may play a vital role in IFN-mediated HEV clearance. Furthermore, a genome-wide transcriptome profiling has identified the up-regulation of 30 genes in blood cells of chronic HEV patients, of which 25 are ISGs [15].

Because the function of ISGs during HEV infection remains largely elusive, we have profiled the effects of a panel of ISGs that are known to have anti- or pro-viral effects on certain viruses [10, 11]. We found most of these ISGs only have minor but some have potent anti-HEV effects. Among those ISGs, RIG-I is a key member that effectively restricts HEV replication. Furthermore, biological or pharmacological activation of RIG-I exerts potent anti-HEV effects. Mechanistically, it robustly activates the innate cellular antiviral response, unexpectedly dispensable of IFN production, but requiring the key elements of the JAK-STAT signaling.

Materials and Methods

HEV cell culture models

Multiple cell lines were used for supporting HEV replication, including Huh7.5 cells: a RIG-I defective hepatoma cell line that derived from Huh7 cells; A549 cells: a human lung epithelial carcinoma cell line that widely used for supporting HEV replication [16]. HepaRG cells: a hepatic cell line which retains many characteristics of primary human hepatocytes that also permissive for HEV replication. For the full-length HEV model, a plasmid construct containing the full-length HEV genome (Kernow-C1 p6 clone, GenBank Accession Number: JQ679013) was linearized at a 3' terminal MluI. Capped HEV viral RNA transcripts were generated by the Ambion *mMESSAGE* mMACHINE® *in vitro* RNA transcription Kit (Thermo Fisher Scientific Life Sciences) [16]. Huh7.5 cells, A549 cells and HepaRG cells were electroporated using the Bio-Rad's electroporation systems (240 V, pulse length 0.5, number 1 and cuvette 4 mm) with full-length HEV viral RNA to generate consecutive HEV-infected cell models, Huh7.5-p6, A549-p6 and HepaRG-p6. Briefly, cells were collected and washed with 5 mL Opti-MEM (Thermo Fisher Scientific Life Sciences) for three times. The cell pellet was resuspended with 100 µL Opti-MEM and mixed with 10 µg p6 full-length HEV RNA and then subjected to electroporation. To generate the subgenomic (p6-Luc) HEV model, a construct containing subgenomic HEV was also used. This plasmid has an HEV sequence in

which the 5' portion of HEV ORF2 was replaced with the in-frame *Gaussia princeps* luciferase reporter gene to generate subgenomic (p6-Luc) [16]. The luciferase has a signal sequence that let it secreted into medium, and therefore, measurement of secreted luciferase activity represents HEV replication levels. Huh7.5 cells were electroporated as described above with HEV subgenomic RNA to generate subgenomic HEV replication model, Huh7.5-p6-Luc.

HEV reinfection assays

Supernatant that contains HEV viral particles were collected from the full-length HEV infectious cells (Huh7.5-p6) that cultured for 96 h. The supernatant was filtered by 0.45 µm filter to get rid of dead cell and then was centrifuged for 30 min (10 000 rpm) to remove cell debris. Next, 2 h ultracentrifugation (22 000 rpm) was used to purify and concentrate HEV virus particles (SW28 rotor; Beckman Coulter, Brea CA, USA). Subsequently, the collected pellet was resuspended and was diluted to 1×10^7 HEV viral RNA copies/mL and then stored at -80 °C as described previously [17]. For HEV infection assay, Huh7.5 and A549 cells were seeded into 12-well plates at a density of 7×10^4 cells per well. The next day, for each well, 400 µL HEV stock that contains 1×10^7 viral RNA copies/mL HEV was incubated with target cells at 37 °C for 6 h. Next, the HEV inoculum was removed and cell layers were washed 3 times with 1 mL PBS followed by adding 1 mL fresh medium to each well. For 6-well plates, cells were seeded at a density of 1.4×10^5 per well. The next day, for each well, target cells were incubated with 800 µL HEV stock at 37 °C for 6 h. Then, the HEV inoculum was removed and washed as usual and then added 2 mL fresh medium.

Lentivirus production and transduction assays

pTRIP.CMV.IVSb.ISG.ires.TagRFP based ISG overexpression vectors were kind gifts from Prof. Charles M. Rice (the Rockefeller University) [10]. Two vectors expressing *Photinus pyralis* luciferase (Fluc) or GFP as reporter genes were used as a control. Lentiviral pseudoparticles were generated in 293T cells by co-transfection of ISG expression plasmid (pTRIP.CMV.IVSb.ISG.ires.TagRFP), HIV gag-pol and VSV-G in a ratio of 1: 0.8: 0.2 as described and lentiviral stocks were stored at -80 °C [10]. For transduction assays, cells were seeded into 24-well plates at a density of 5×10^4 cells per well and transduced with lentiviral pseudoparticles at 37 °C. pLKO.1 based shRNA lentiviral vectors (Biomics Center in Erasmus Medical Center) targeting RIG-I was used to knockdown RIG-I gene expression and scrambled control vector (shSCR) was used as a control. Lentiviral pseudoparticles were

generated as described previously [17]. To obtain stable gene knockdown cell line, cells were transduced with shRNA lentiviral particles for 3 days and selected by puromycin (Sigma-Aldrich, Zwijndrecht, the Netherlands) at a concentration of 2.5 μg/mL. After selection, optimal knockdown cell lines were chosen. The shRNA sequences are listed in Table S1 in Supporting Information.

Statistical analysis

GraphPad Prism 5 software was used for data analysis using a Mann-Whitney test. All results were presented as mean ± standard errors of the means (SEM). P values of less than 0.05 (single asterisks in figures) were considered statistically significant; whereas P values less than 0.01 (double asterisks) and 0.001 (triple asterisks) were considered highly significant. Further details are provided in the Supporting Information.

Results

Identification of antiviral ISGs against HEV replication

To identify key ISGs that regulate HEV replication, 25 important human ISGs which are known to have anti- or pro-viral effects on certain viruses [10] were tested in two Huh7.5 cells based HEV models (Huh7.5-p6-Luc and Huh7.5-p6). Huh7.5 is an RIG-I defective hepatoma cell line derived from Huh7 cells, which was widely used for supporting viral infections (Supporting Fig. S1A) [18]. These ISGs include MAP3K14, IFI44L, RIG-I (also known as DDX58), HPSE, RTP4, NAMPT (also known as PBEF1), IRF1, IFITM1, IFITM2, IFITM3, C6orf150 (also known as cGAS), UNC84B (also known as SUN2), IRF2, IRF7, IRF9, IFI6, OASL, DDX60, MOV10, TREX1, MDA5 (also known as IFIH1), ADAR, FAM46C, LY6E and MCOLN2 [10].

Ectopic overexpression of each ISG was delivered by a bicistronic lentiviral vector co-expressing the ISG and a red fluorescent protein (TagRFP). Two vectors that express a *Photinus pyralis* luciferase (Fluc) gene or a green fluorescent protein (GFP) gene were used as controls [10]. The successful overexpression of each ISG was confirmed by flow cytometry analysis to measure the expression of TagRFP (Supporting Fig. S1B-S1F). Transient transfection was used to overexpression ISG when lentiviral stocks failed to achieve high-level transduction [10]. Before profiling on HEV, each ISG was first tested for the ability to inhibit HCV replication in Huh7.5 cell-based HCV luciferase replicon model [10]. Similar to the previous study, most ISGs inhibit HCV replication to some extent; whereas several genes

(IRF1, IRF2 and RIG-I) have strong anti-HCV effects (Supporting Fig. S1G). Next, all ISGs were tested for their anti-HEV ability in a subgenomic HEV model (Huh7.5-p6-Luc). At 24 h after lentivirus transduction, most genes inhibited HEV-related luciferase activity to some extent (Fig. 1A). One gene named RIG-I was found to have strong anti-HEV activity at 48 h post transduction (Fig. 1B). More anti-HEV ISGs were identified 72 h after transduction, including IRF1, MDA5 and RIG-I (Fig. 1C). These genes could inhibit HEV-related luciferase activity by almost 50% compared to control. To further validate the antiviral ability, those ISGs were also tested in the full-length infectious HEV model (Huh7.5-p6). A similar inhibition pattern was obtained in this model (Fig. 1D). At 48 h after transduction, IRF1, MDA5 and RIG-I potently decreased HEV viral RNA level; whereas most of the other genes showed minor effects.

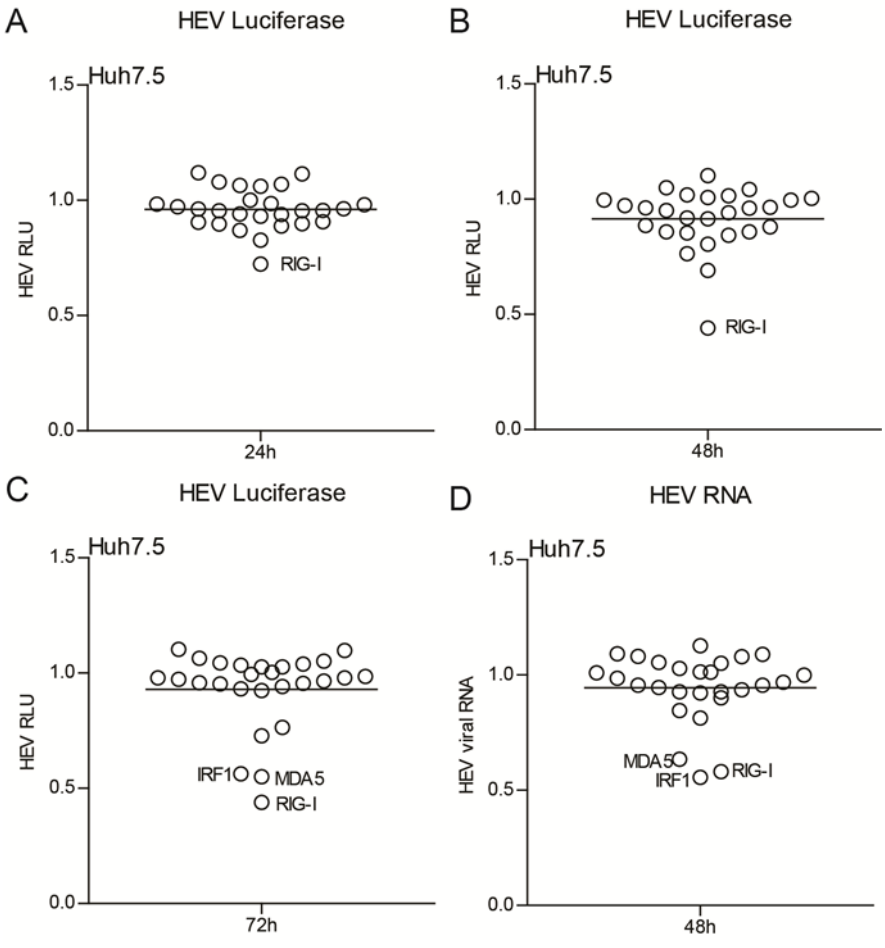

FIG. 1. Identification of ISGs that inhibit HEV replication.

Luciferase activity analysis of HEV-related *Gaussia* luciferase activity in Huh7.5-p6-Luc cells transduced with ISG overexpression or Fluc vector for 24 h (A), 48 h (C) or 72 h (C) (n = 4 independent experiments with each of 2 replicates). RLU: relative luciferase unit. (D) qRT-PCR analysis of HEV viral RNA level in Huh7.5-p6 cells transduced with ISG overexpression or Fluc vector for 48 h (n = 4). Data were normalized to the Fluc control (set as 1) and presented in dot plots.

RIG-I is a key anti-HEV ISG

Among these three potent anti-HEV ISGs, we have previously demonstrated that IRF1 inhibits HEV replication by stimulating antiviral ISG expressions [17]. Both RIG-I and MDA5 are pattern recognition receptors (PRRs) that sense viral RNA in the cytoplasm [19]. In this study, we mainly focused on the antiviral potential of RIG-I. To validate the anti-HEV activity of RIG-I, we performed additional independent experiments in two Huh7.5-based HEV models (Huh7.5-p6 and Huh7.5-p6-Luc). Lentiviral transduced RIG-I overexpression was confirmed in Huh7.5-p6 cells by qRT-PCR and immunoblotting (Fig. 2A). In both models, RIG-I overexpression inhibited HEV replication to an extent similar to a high dose of IFN-α treatment (Fig. 2B). Next, we confirmed the anti-HEV ability of RIG-I in different cell models: a human lung epithelial cell line A549 that is widely used for HEV propagation and a human hepatic progenitor cell-derived cell line HepaRG. Both of them are capable of supporting long-term HEV replication (A549-p6 and HepaRG-p6) [17]. As shown in Fig. 2C and 2D, RIG-I overexpression also significantly inhibited HEV replication in both HepaRG and A549 based HEV models.

To further explore the role of basal RIG-I in constraining HEV infection, RNAi approach was used to silence RIG-I gene expression. HEV RNA level was significantly increased in RIG-I silenced A549 cells (Fig. 2E and 2F). As expected, in RIG-I defective Huh7.5 cells, RIG-I knockdown did not affect HEV infection (Supporting Fig. S2A and S2B) and we indeed observed that RIG-I defected Huh7.5 cell are more permissive for supporting HEV infection (Supporting Fig. S2C). These results have demonstrated that RIG-I has potent anti-HEV ability and the basal expression of RIG-I plays important role in defending HEV infection.

Pharmacological activation of RIG-I stimulates an antiviral response that inhibits HEV replication

To explore the antiviral response induced by RIG-I pathway, the natural ligand of RIG-I 5'pppRNA was used to activate the RIG-I signaling [20]. Different concentrations of RIG-I agonist were used to induce an antiviral response in A549 cells, a model with functional RIG-I expression (Supporting Fig. S1A). As shown in Fig. 3A, gene expression of type I IFN (IFN-β) and type III IFN (IFN-λ) was significantly induced by RIG-I agonist 48 h or 72 h after treatment. Concurrently, the expression of many ISGs including STAT1, IFIH1, PKR, TRAIL, RANTES and RIG-I were also significantly induced by 5'pppRNA treatment (Fig. 3A).

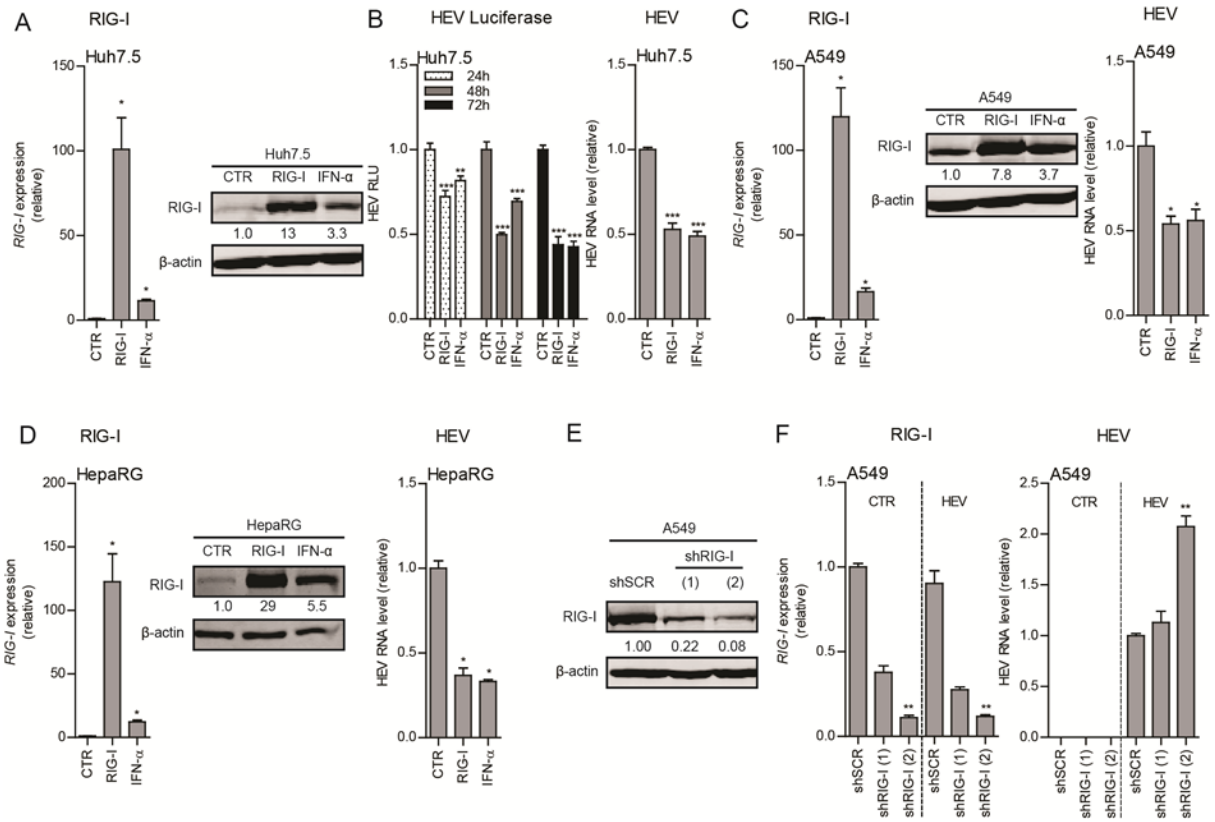

FIG. 2. RIG-I inhibits HEV replication in multiple cell models.

qRT-PCR analysis and immunoblot analysis of RIG-I expression in Huh7.5-p6 cells **(A)**, A549-p6 cells **(C)** and HepaRG-p6 cells **(D)** transduced with RIG-I, Fluc vector or treated with IFN-α (1000 IU/mL) for 48 h (qRT-PCR: n = 4). **(B)** Analysis of HEV-related *Gaussia* luciferase activity in Huh7.5-p6-Luc cells transduced with RIG-I, Fluc vector or treated with IFN-α (1000 IU/mL) for 24 h, 48 h or 72 h (n = 4 independent experiments with each of 3 - 4 replicates) and qRT-PCR analysis of HEV viral RNA level in Huh7.5-p6 cells transduced with RIG-I vector or treated with IFN-α (1000 IU/mL) for 48 h (qRT-PCR: n = 8). RLU: relative luciferase unit. qRT-PCR analysis of HEV viral RNA level in A549-p6 cells **(C)** and HepaRG-p6 cells **(D)** transduced with RIG-I, Fluc vector or treated with IFN-α (1000 IU/mL) for 48 h (n = 4). **(E)** Immunoblot analysis of RIG-I expression in A549 cells transduced with lentiviral shRNA vector targeting RIG-I (shRIG-I(1) and shRIG-I(2)) or scrambled control (shSCR). Stable RIG-I knockdown or shSCR control A549 cells were infected with HEV. RIG-I expression level and HEV viral RNA level **(F)** were analyzed by qRT-PCR 72 h after HEV infection. Data were normalized to the Fluc control (CTR, set as 1, A-D) or to the scrambled control (shSCR, set as 1, F). Data are means ± SEM. *P < 0.05; **P < 0.01; ***P < 0.001; NS, not significant. For immunoblot results (A, C, D and E), band intensity of each lane was quantified by Odyssey Software. Immunoblot quantification results were normalized to β-actin expression and control was set as 1.

Correspondingly, treatment with RIG-I agonist has resulted in a significant reduction of HEV replication in A549-p6 cells. With 1000 ng/mL 5'pppRNA treatment, the HEV viral RNA were inhibited by 67.8% ± 8.1% (mean ± SEM) (n = 7; P < .01), 90.0% ± 8.6% (n = 6; P < .01) at 48 h and 72 h after treatment, respectively (Fig. 3B). Since Huh7.5 cells are RIG-I defected cells (Supporting Fig. S1A), RIG-I agonist was unable to induce any antiviral response as expected (Supporting Fig. S2D).

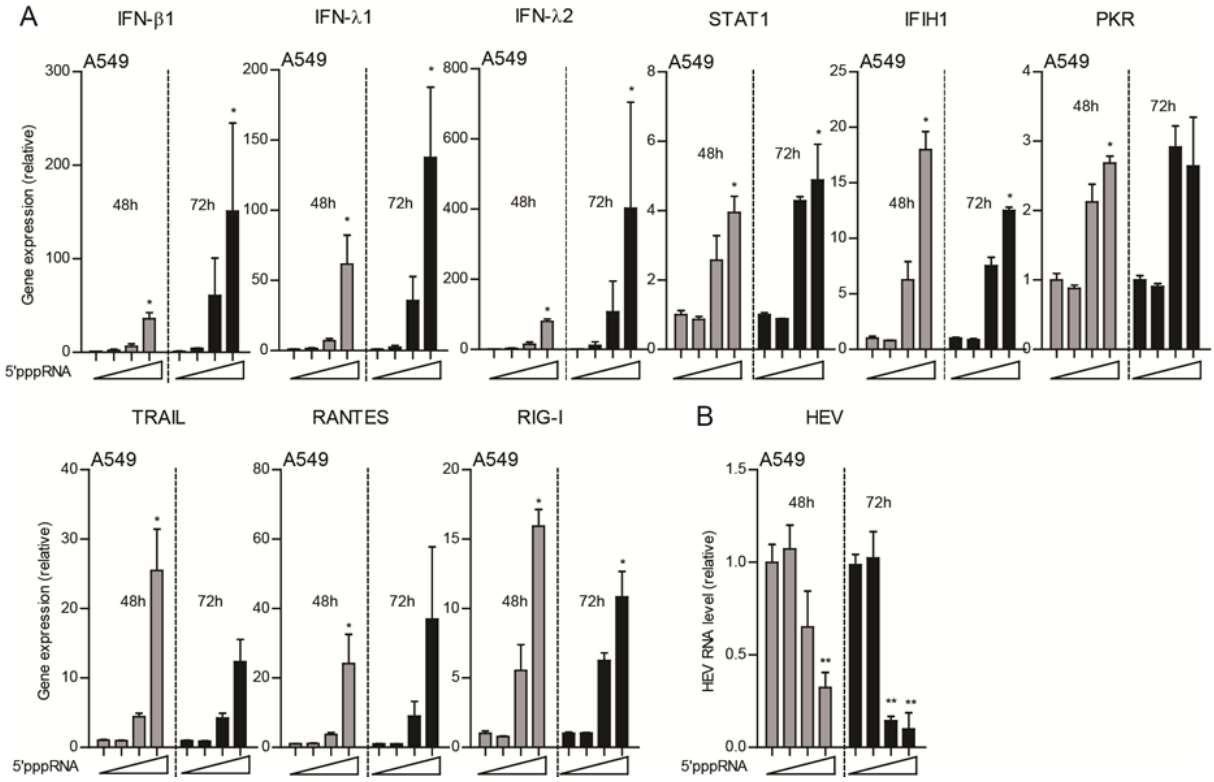

FIG. 3. 5'pppRNA stimulates an antiviral response that inhibits HEV.

A549-p6 cells were transfected with various concentrations of 5'pppRNA (10 ng/mL, 100 ng/mL and 1000 ng/mL), IFN gene mRNA levels, ISG mRNA levels **(A)** and HEV viral RNA level **(B)** were analyzed by real-time qRT-PCR 48 h or 72 h after transfection (A: n = 3-5; B: n = 6-8). Data were normalized to a control that was transfected with PEI-Mix but without 5'pppRNA at each time point (48 h and 72 h, both set as 1), respectively. Data are means ± SEM. *P < 0.05; **P < 0.01; ***P < 0.001; NS, not significant.

To clarify whether the antiviral activity of 5'pppRNA exclusively relies on RIG-I pathway, we employed wild-type mouse embryonic fibroblasts (MEF) cells (WT, RIG-I$^{+/+}$) and RIG-I deficient MEF cells (RIG-I$^{-/-}$). These two MEF cell lines were transfected with different concentrations of 5'pppRNA. 1000 ng/mL 5'pppRNA treatment induced mouse IFN genes (mouse IFN-β, mIFN-β; mouse IFN-λ, mIFN-λ) more than 1000-fold at 24 h after stimulation (Supporting Fig. S3A). In contrast, no IFN gene was induced in RIG-I$^{-/-}$ MEF, indicating that this is exclusively dependent on the RIG-I signaling (Supporting Fig. S3A). Meanwhile, 5'pppRNA activated the expression of many mouse ISGs, including mMX1, mIRF9, mIFIH1, mSTAT1, mIRF1, mPML, mXAF, mIRF7, mISG15 and mRIG-I in RIG-I$^{+/+}$ MEF cells (Supporting Fig. S3A). After 48 h treatment, IFN gene and ISG expression was significantly induced by 5'pppRNA, although, to a less extent compared to 24 h after treatment (Supporting Fig. S3B). Hence, the anti-HEV activity of 5'pppRNA was specifically via RIG-I. We now demonstrated

that pharmacological activation of RIG-I stimulates an antiviral response that inhibits HEV replication specifically via RIG-I.

RIG-I activates the transcription of a wide range of ISGs

RIG-I has been shown to trigger STAT1 activation and ISG expression [21]. In general, the activation of STAT1 leads to the formation and nuclear translocation of IFN-stimulated gene factor 3 (ISGF3). This complex further binds to the IFN-stimulated response element (ISRE) motifs in the genome DNA and drives the transcription of ISGs. A recent study has reported that RIG-I overexpression stimulates ISRE promoter activity [22]. Thus, we employed a transcriptional reporter system that mimics IFN response with a reporter luciferase gene that was driven by multiple ISREs (ISRE-Luc). As shown in Fig. 4A, RIG-I significantly increased the ISRE-related luciferase activity. The activation of ISRE element usually leads to the transcription of ISGs that contain this element in their promoter regions. Therefore, we measured gene expression of a wide range of important antiviral ISGs. As shown in Fig. 4B-4D, RIG-I overexpression stimulated the expression of a large number of ISGs in Huh7.5, A549 and HepaRG cells. Interestingly, the ISG expression pattern induced by RIG-I was different from IFN-α treatment (Supporting Fig. S4A-S4C). The induction of some important ISGs was further confirmed by immunoblotting at protein levels (Fig. 4E and 4F).

RIG-I mediates IFN-α-induced antiviral ISG transcription

Gene expression profile analysis in the previous study revealed that 5'pppRNA treatment induced a distinct transcriptome compared to IFN-α treatment [20]. Besides, as a nucleic acid sensor, RIG-I is also an ISG that can be induced by IFN-α treatment and we already demonstrated that RIG-I activates the expression of many ISGs (Fig. 4). Therefore, we hypothesized that RIG-I may reinforce the IFN-α initiated ISG induction. We thus investigated the association of RIG-I expression with the response to IFN-α treatment. Indeed, in RIG-I overexpressed Huh7.5 cells, IFN-α induced ISG expression was significantly enhanced (Fig. 5A). Similarly, IFN-α induced ISG expression was also enhanced in RIG-I transduced A549 cells (Fig. 5B).

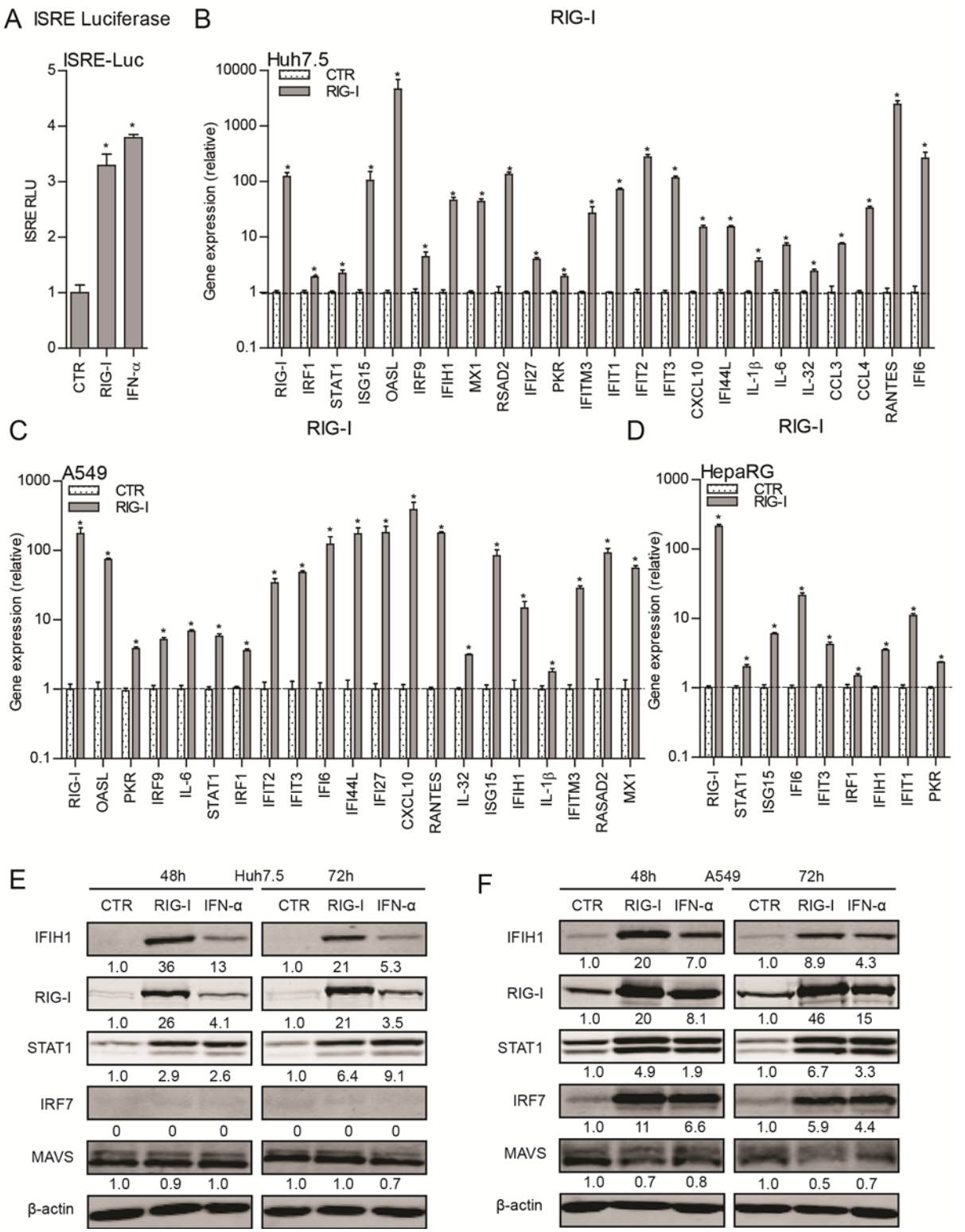

FIG. 4. RIG-I activates the transcription of a wide range of ISGs.

(A) Analysis of ISRE related *firefly* luciferase activity in Huh7-ISRE-Luc cells transduced with RIG-I vector or treated with IFN-α (1000 IU/mL) for 48 h (n = 3 independent experiments with each of 1-2 replicates). qRT-PCR analysis of ISG mRNA levels in Huh7.5-p6 cells **(B)**, A549-p6 cells **(C)** and HepaRG-p6 cells **(D)** transduced with RIG-I or Fluc vector for 48 h (n = 6). Immunoblot analysis of ISG protein levels in Huh7.5-p6 cells **(E)** and A549-p6 cells **(F)** transduced with RIG-I or Fluc vector for 48 h or 72 h. Date in (A) were normalized to the untreated Fluc control (CTR, set as 1). Data in (B-D)

were normalized to the Fluc control (CTR, set as 1). Data are means ± SEM. *P < 0.05; **P < 0.01; ***P < 0.001; NS, not significant. For immunoblot results (E and F), band intensity of each lane was quantified by Odyssey Software. Immunoblot quantification results were normalized to β-actin expression and control was set as 1.

To further determine the role of RIG-I in IFN-α-activated cell signaling, the RIG-I knockdown A549 cell line and RIG-I deficient MEF cell line (RIG-I$^{-/-}$) were employed. In A549 cells, RIG-I deficiency significantly attenuated the ISG induction ability of IFN-α (Fig. 5C). Consistently, in RIG-I deficient MEF cells (RIG-I$^{-/-}$), the ISG induction ability of mIFN-α (mouse IFN-α) was also significantly reduced (Fig. 5D). In contrast, the ISG induction ability of mIFN-α was not affected in IRF3/7$^{-/-}$ or NFκB$^{-/-}$ MEF cells (Supporting Fig. S5A and S5B). Taken together, these results demonstrated that RIG-I functionally contributes to the antiviral ISG induction ability of IFN-α.

RIG-I activates the innate anti-HEV immune response dispensable of interferon production

RIG-I is a cytosolic nucleic acid sensor and the binding of viral RNA to RIG-I leads to the activation of downstream pathways that eventually triggers IFN gene expression via IRF3 and IRF7 [19]. In turn, the secreted IFNs establish antiviral response in infected and surrounding cells by stimulating the expression of ISGs. To further study the ISG induction ability of RIG-I pathways, the activator of RIG-I 5'pppRNA were transfected in IRF3/7 double knockout MEF cells (IRF3/7$^{-/-}$). Indeed, 5'pppRNA failed to induce IFN-β expression in the IRF3/7$^{-/-}$ cells (Fig. 6A). Strikingly, 5'pppRNA is still capable of inducing ISGs in the absent of IRF3/7 and IFN-β expression (Fig. 6B). These results indicate RIG-I could also stimulate ISG transcription in IFN-independent manners. Next, we determined the mRNA expression levels of IFN genes in RIG-I overexpressed Huh7.5 cell line, a cell line that unable to produce any IFNs [23]. We found that the mRNA expression level of IFN genes was very low and no IFN gene (IFN-α, -β and -λ) was induced by RIG-I overexpression in Huh7.5-p6 cells (Fig. 6C, Supporting Fig. S6A). Furthermore, no IFN gene was up-regulated in HepaRG-p6 cells by RIG-I overexpression (Supporting Fig. S6B-S6C). To confirm the lack of IFN production in these RIG-I overexpressed cells, conditioned medium (supernatant) from the RIG-I transduced Huh7.5-p6 cells was collected (Fig. 6D). Two IFN sensitive assays were performed: an IFN functional assay and an HCV replicon-based bioassay. The IFN functional assay was based on a transcriptional reporter system that mimics IFN response as used above (Fig. 4A). As shown in Fig. 6E,

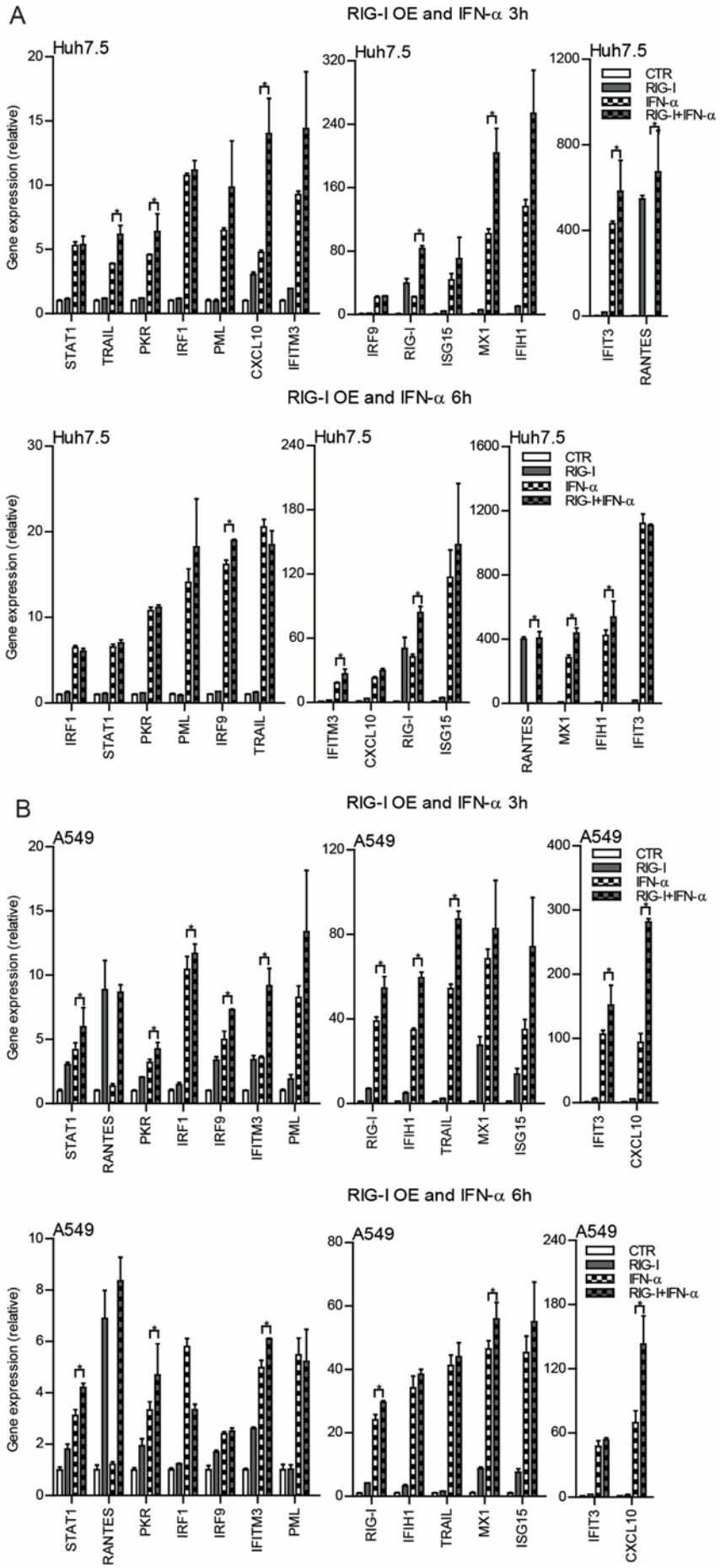

FIG. 5. RIG-I mediates IFN-α-induced antiviral ISG transcription.

qRT-PCR analysis of ISG mRNA expression levels. Huh7.5 cells were transduced with RIG-I or Fluc vector, at 48 h post-transduction cells were treated with IFN-α (1000 IU/mL) for 3 h or 6 h **(A)** (n = 4). A549 cells were transduced with RIG-I or Fluc vector, at 48 h post-transduction cells were treated with IFN-α (1000 IU/mL) for 3 h or 6 h **(B)** (n = 4). Data in (A and B) were normalized to untreated the Fluc control (CTR, set as 1). A549 cells were transduced with lentiviral shRNA vectors targeting RIG-I or scrambled control (shSCR). The stable RIG-I knockdown and control A549 cells were treated with IFN-α (1000 IU/mL) for 3 h or 6 h **(C).** ISG mRNA levels were analyzed by qRT-PCR (n = 6). qRT-PCR analysis of mouse ISG mRNA levels in WT and RIG-I$^{-/-}$ MEF cells treated with mouse IFN-α (mIFN-α, 1000 IU/mL) for 3 h or 6 h **(D)** (n = 6). Data in (C) were normalized to the untreated scrambled control (shSCR CTR, set as 1). Data in (D) were normalized to untreated WT MEF cells (WT CTR, set as 1). Data are means ± SEM. *P < 0.05; **P < 0.01; ***P < 0.001; NS, not significant.

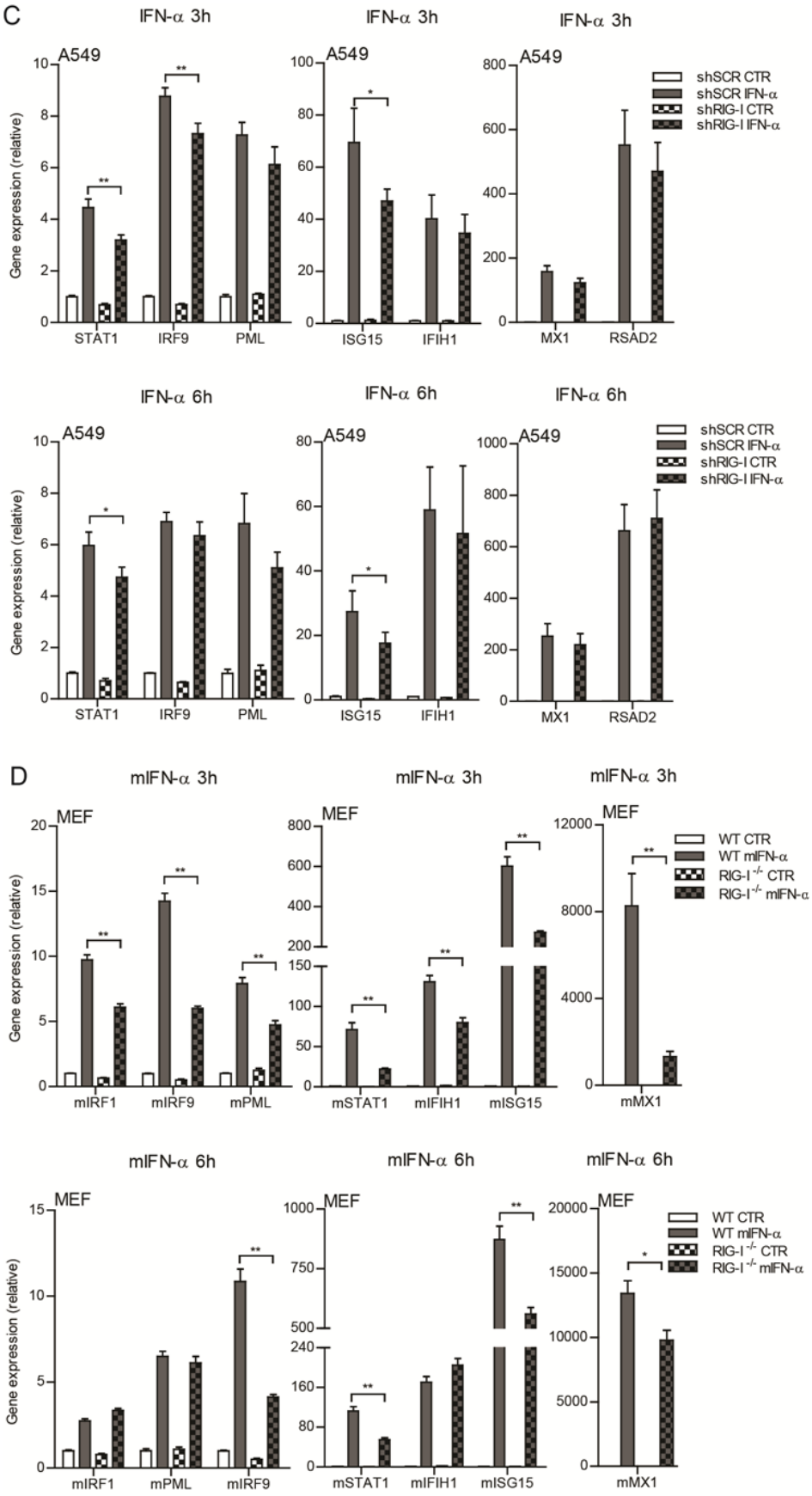

conditioned medium collected from RIG-I overexpressed Huh7.5-p6 cells was not able to induce ISRE activation. Furthermore, this conditioned medium did not affect HCV-related luciferase activity (Fig. 6F). Similarly, conditioned medium collected from HepaRG cells also failed to activate ISRE-related luciferase activity (Supporting Fig. S6D). These results suggest that ectopic overexpression of RIG-I did not trigger IFN expression and production. Thus, we demonstrated that RIG-I could activate innate immune response dispensable of IFN production.

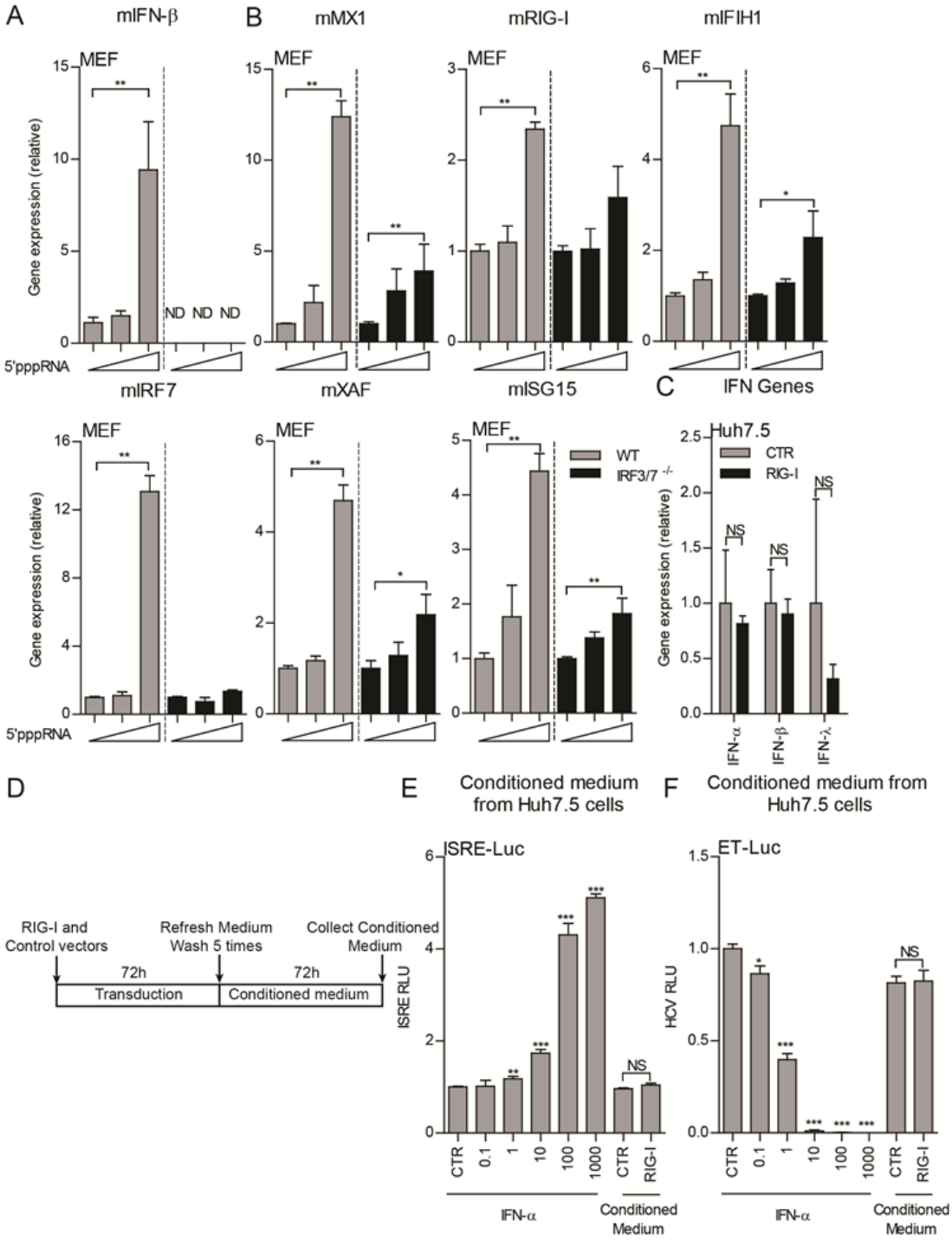

FIG. 6. RIG-I activates an immune response dispensable of interferon production.

WT and IRF3 and IRF7 double deficient (IRF3/7$^{-/-}$) mouse embryonic fibroblasts (MEF) cells were transfected with various concentrations of 5'pppRNA (100 ng/mL and 1000 ng/mL), mouse IFN-β (mIFN-β) **(A)** and mouse ISG **(B)** mRNA levels were analyzed by qRT-PCR 24 h after transfection (n = 6). **(C)** qRT-PCR analysis of IFN gene mRNA levels in Huh7.5-p6 cells transduced with RIG-I or Fluc vector for 48 h (n = 4). **(D)** Production of conditioned medium (supernatant). Cells were transduced with RIG-I or GFP (CTR) vector for 72 h and then the cells were washed 5 times and medium was refreshed. Cells were cultured for another 72 h and supernatant was collected as conditioned medium. Analysis of ISRE-related *firefly* luciferase activity in Huh7-ISRE-Luc cells **(E)** or HCV-related *firefly* luciferase activity in Huh7.5-ET-Luc cells **(F)** that treated with conditioned medium from Huh7.5 cells or various concentrations of IFN-α for 48 h (n = 3 independent experiments with each of

3 - 4 replicates). Data in (A) and (B) were normalized to a control that transfected with PEI-Mix but without 5'pppRNA in each cell line (WT and IRF3/7$^{-/-}$, both set as 1), respectively. Data in (C) was normalized to the Fluc control (CTR, set as 1). Data in (E) and (F) were normalized to the untreated GFP control (CTR, set as 1). Data are means ± SEM. *P < 0.05; **P < 0.01; ***P < 0.001; NS, not significant.

RIG-I mediated ISG transcription and anti-HEV activity partially through activation of JAK-STAT pathway.

The previous study has demonstrated that RIG-I can augment STAT1 activation, which is a key element of JAK-STAT cascade within the IFN pathway [21]. Consistent with these results, we also observed that RIG-I overexpression induced the phosphorylation of STAT1 at 701 site in Huh7.5-p6 cells, which is an indispensable marker of JAK-STAT pathway activation (Fig. 7A).

To elucidate whether the ISG induction and anti-HEV abilities of RIG-I are through the activation of STAT1, we used a JAK inhibitor named CP-690550 (Tofacitinib) to pharmacologically block the JAK-STAT pathway. In Huh7.5-p6 cells, RIG-I and IFN-α induced STAT1 phosphorylation were totally blocked by CP-690550 (Fig. 7B). Meanwhile, lentiviral-delivered RIG-I overexpression was not affected by this inhibitor (Fig. 7B and 7C). Surprisingly, we found that RIG-I-induced ISRE activation was not totally diminished by this inhibitor; whereas IFN-α triggered ISRE activation was totally blocked (Fig. 7C). These results suggest that RIG-I-induced ISRE activation partially independent of its STAT1 phosphorylation ability. Next, we tested the mRNA expression level of 23 RIG-I inducible ISGs in RIG-I overexpressed Huh7.5-p6 cells treated with JAK inhibitor CP-690550. Surprisingly, among these 23 tested RIG-I inducible ISGs, only 10 genes were affected by CP-690550 treatment, but the others were not affected at all (Fig. 7D and 7E). As a positive control, the expression level of all these 23 genes that induced by IFN-α was totally diminished by this inhibitor (Supporting Fig. S7A and S7B). Consequently, the anti-HEV ability of RIG-I was only partially blocked by CP-690550; whereas the anti-HEV effects of IFN-α were totally abolished (Fig. 7F). To further confirm these results, another JAK inhibitor named JAK inhibitor 1 was used to treat RIG-I transduced Huh7.5-p6 cells. As expected, similar results were obtained (Supporting Fig. S8). To explore whether this is a common mechanism in different cell lines, we also used this JAK inhibitors 1 to treat RIG-I overexpressed HepaRG-p6 cells and similar results were obtained (Supporting Fig. S9).

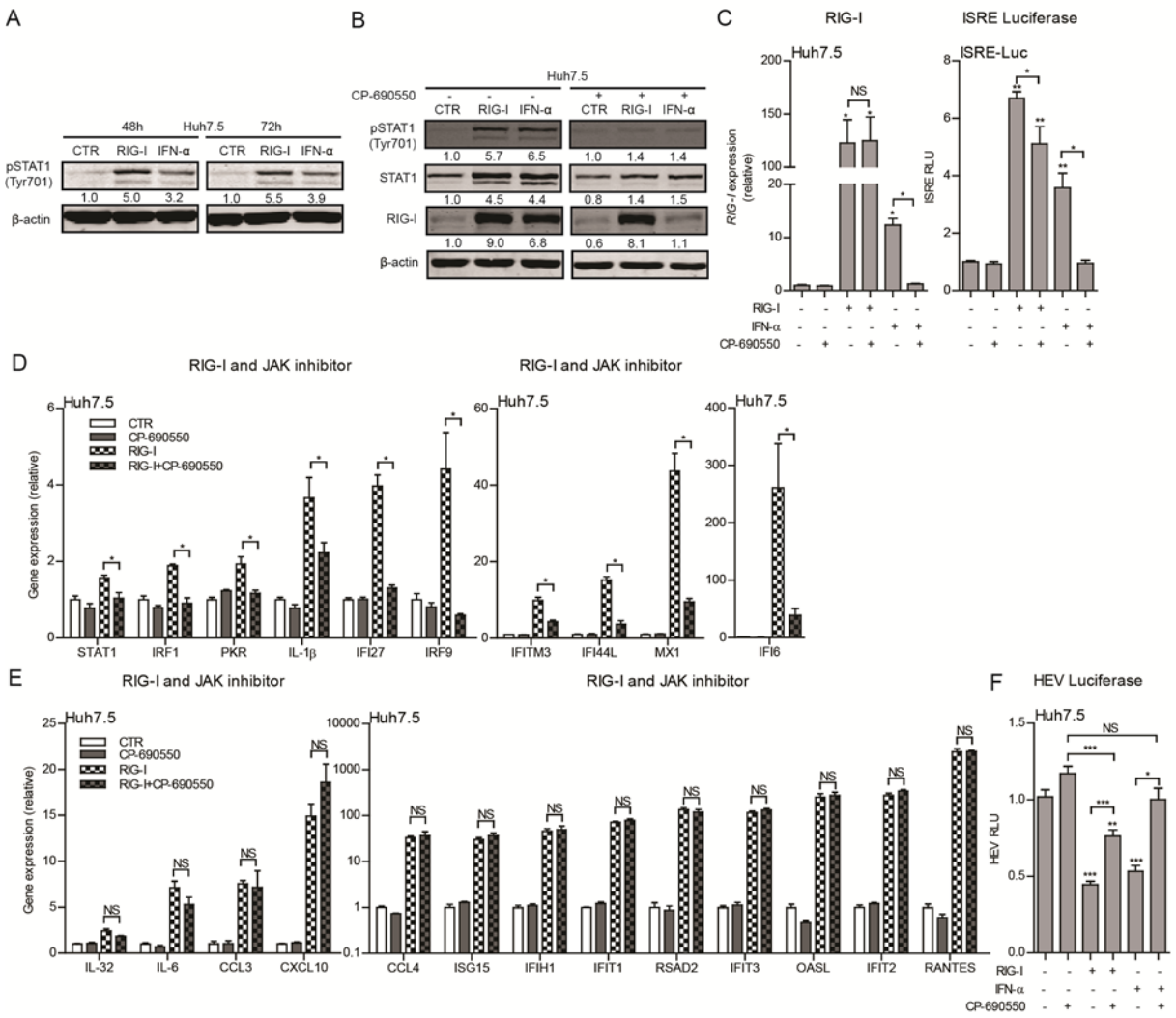

FIG. 7. JAK inhibitor CP-690550 partially diminishes RIG-I-induced ISG transcription and anti-HEV activity.

(A) Immunoblot analysis of p-STAT1 (Tyr^{701}) expression in Huh7.5 cells transduced with RIG-I vector or treated with IFN-α (1000 IU/mL) for 48 h or 72 h. **(B)** Immunoblot analysis of ISG protein levels in Huh7.5 cells transduced with RIG-I vector or treated with IFN-α (1000 IU/mL) or CP-690550 (1000 ng/mL) for 48 h. qRT-PCR analysis of RIG-I mRNA level in Huh7.5-p6 cells and analysis of ISRE-related *firefly* luciferase activity in Huh7-ISRE-Luc cells **(C)** transduced with RIG-I vector or treated with IFN-α (1000 IU/mL) or CP-690550 (1000 ng/mL) for 48 h (qRT-PCR: n = 4; ISRE: n = 3 independent experiments with each of 2 replicates). **(D and E)** qRT-PCR analysis of ISG mRNA levels in Huh7.5 cells transduced with RIG-I vector or treated with CP-690550 (1000 ng/mL) for 48 h (n =5-6). **(F)** Analysis of HEV related *Gaussia* luciferase activity in Huh7-p6-Luc cells transduced with RIG-I vector or treated with IFN-α (1000 IU/mL) or CP-690550 (1000 ng/mL) for 72 h. (n = 4 independent experiments with each of 3 - 4 replicates). For immunoblot results (A and B), band intensity of each lane was quantified by Odyssey Software. Immunoblot quantification results were normalized to β-actin expression and control was set as 1. Data in (C left panel, D and E) were normalized to the untreated Fluc control (CTR, set as 1). Date in (C right panel and F) were normalized to the untreated GFP control (CTR, set as 1). Data are means ± SEM. *P < 0.05; **P < 0.01; ***P < 0.001; NS, not significant.

To further confirm the ISG induction ability of RIG-I is not totally dependent on the JAK-STAT pathway, we overexpressed RIG-I in STAT1 deficient human (STAT1$^{-/-}$) fibrosarcoma

cells [24]. In STAT1$^{-/-}$ cell, RIG-I failed to induce STAT1 phosphorylation (Fig. 8A). A similar ISG induction pattern was also observed in RIG-I overexpressed STAT1$^{-/-}$ cells. Some genes such as STAT1, IRF9 and IFI6 can only be induced in WT cell but not in STAT1$^{-/-}$ cells by RIG-I, although RIG-I overexpression level was similar in both cell lines (Fig. 8B and 8C). Meanwhile, another group includes genes that can be activated in both WT and STAT1$^{-/-}$ cells such as IFIT1, RANTES and CXCL10 (Fig. 8D). As a control, IFN-α induced ISG transcription was totally abolished in STAT1$^{-/-}$ cells (Supporting Fig. S10A). Together, these results demonstrated that RIG-I activates ISG transcription and exerts its anti-HEV activity partially through the activation of the JAK-STAT pathway.

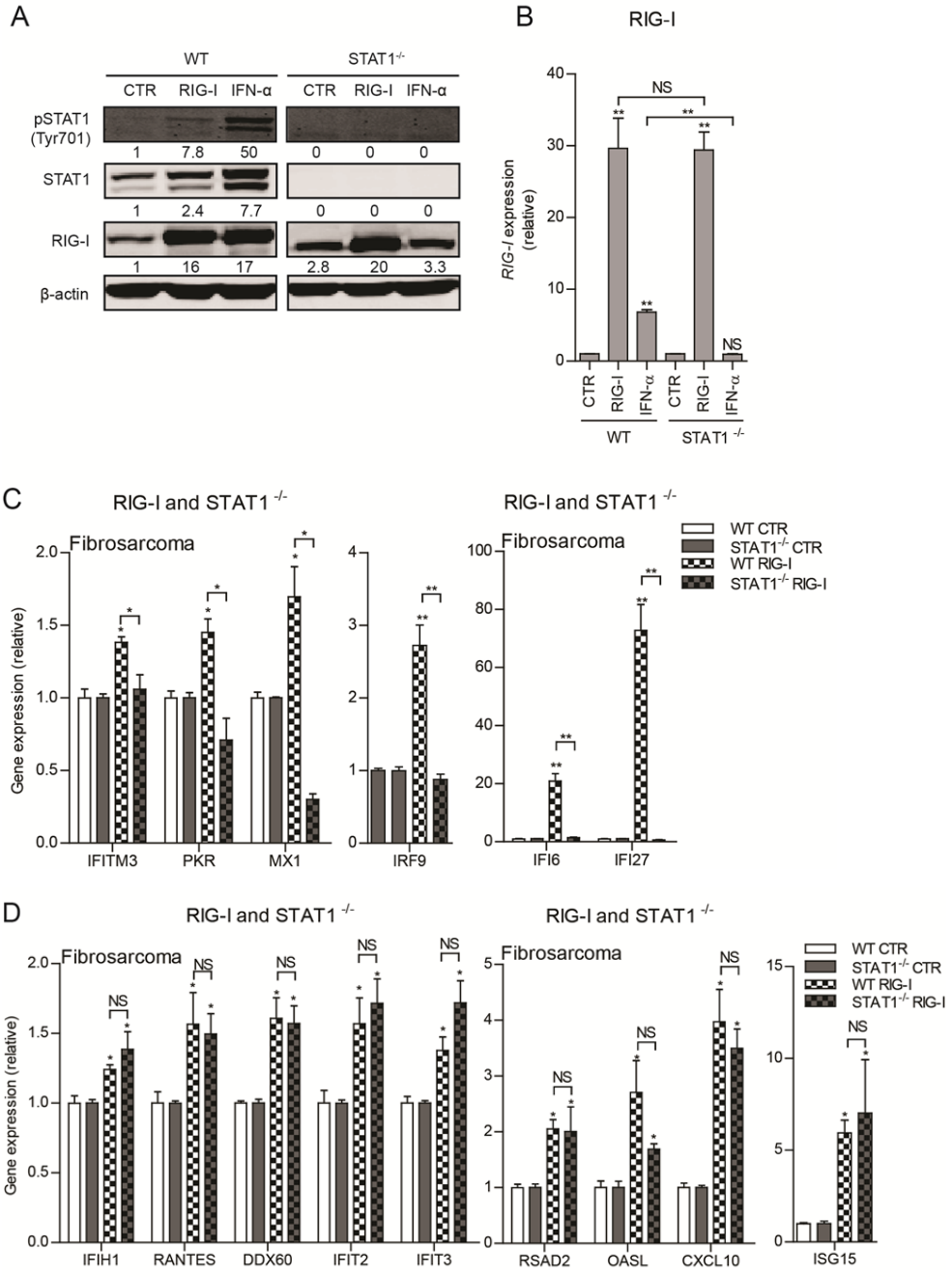

FIG. 8. The ISG induction ability of RIG-I is partially diminished in STAT1 deficient cells.

(A) Immunoblot analysis of ISG protein levels in WT and STAT1 deficient ($STAT1^{-/-}$) fibrosarcoma cells transduced with RIG-I vector or treated with IFN-α (1000 IU/mL) for 48 h. **(B)** qRT-PCR analysis of RIG-I mRNA level in WT and $STAT1^{-/-}$ cells transduced with RIG-I vector or treated with IFN-α (1000 IU/mL) for 48 h (n =4-5). **(C and D)** qRT-PCR analysis of ISG mRNA levels in WT and $STAT1^{-/-}$ cells transduced with RIG-I or Fluc vector for 48 h (n = 4-5). For immunoblot results (A), band intensity of each lane was quantified by Odyssey Software. Immunoblot quantification results were normalized to β-actin expression and control was set as 1. Data in (C) were normalized to the untreated Fluc control (CTR, set as 1). Date in (D) and (E) were normalized to untreated WT and $STAT1^{-/-}$ cells, respectively (both set as 1). Data are means ± SEM. *P < 0.05; **P < 0.01; ***P < 0.001; NS, not significant.

Discussion

Currently, IFNs in particular IFN-α have been approved for treating viral infections including chronic hepatitis B (HBV) and C virus (HCV) infections [6]. In some cases, IFN-α has been used as an off-label drug to treat chronic HEV infection [12, 25]. *In vitro* study also showed the inhibition of HEV replication by IFN-α treatment [13, 14, 26]. IFN-α exerts its antiviral ability through the induction of ISGs, but how these ISGs affect HEV replication are still largely unknown. This study comprehensively profiled the antiviral ability of many important human ISGs described previously [10]. We found that most of these ISGs showed minor anti-HEV effect. In contrast, several previously reported broad antiviral ISGs including MDA5, IRF1 and RIG-I were identified as strong anti-HEV ISGs. Previously, we have demonstrated that IRF1 inhibits HEV replication by activating antiviral ISGs [17]. RIG-I is a pattern recognition receptor (PRR) and numerous studies have demonstrated that it plays important roles in defending a wide spectrum of virus infections such as HCV [10, 20], HBV [27] and influenza virus [28]. Here, in this study we comprehensively investigated the antiviral potential of RIG-I and its mechanism-of-action.

RIG-I, as a PPR, senses the viral RNA in the cytoplasm during infection. Binding of RIG-I with its ligand such as 5'-triphosphorylated RNA activates the downstream signaling pathway through the adaptor proteins mitochondrial antiviral signaling protein (MAVS). Classically, the aggregation of MAVS in mitochondrial subsequently leads to the production of type I and III IFNs through the phosphorylation of IRF3 and IRF7. The produced IFN proteins subsequently activate ISG expression in infected and bystander cells to eradicate the virus and prevent further infections. In this study, we observed overexpression of RIG-I activated transcription and expression of a wide range of ISGs, and many of them are known to have strong antiviral activities [10, 11, 17, 20, 29-32].

Although working as a cytosolic nucleic acid sensor that triggers IFN production, RIG-I itself is also an ISG regulated by IFN-initiated JAK-STAT cascade. This feedback amplification loop is able to enhance the responsiveness of host cells to infection. It has been shown that 5'pppRNA treatment induced a broader transcriptome compared to IFN-α treatment. Consistently, we found that a combinatorial action of IFN-α treatment and RIG-I overexpression in ISG induction and anti-HEV activity. Conversely, IFN-α induced ISG transcription was attenuated when RIG-I was deleted (Fig. 5). These results suggest that RIG-I partially mediates the ISG transcription activity of IFN-α.

Classically, the main antiviral function of RIG-I is believed via the induction of IFN production upon sensing cytosolic viral nucleic acid. However, we found that RIG-I overexpression in our models doesn't induce the production of IFNs, but triggers the transcription of a wide range of genes including ISGs, chemokines and cytokines, without the activation of downstream MAVS pathway (Fig. 4E). In fact, emerging recent studies have proposed additional antiviral mechanisms of RIG-I that are partially dependent or independent of IFNs [27, 28, 33].

It has been demonstrated that induction of ISGs and antiviral ability by RIG-I activation were only partially reduced in the absence of IFN-α/β receptors [20]. Additionally, RIG-I can exert broad antiviral activity in the models that have defected IFN signaling [10]. We now observed that in cells that lacking of the key downstream components of RIG-I pathway (IRF3 and IRF7), the RIG-I activator 5'pppRNA is still able to induce ISG expression (Fig. 6A) without activating IFN genes. In line with this, we also observed that in Huh7.5 cells (a cell line which could not produce any IFN protein), RIG-I overexpression induces ISG transcription and exerts potent anti-HEV activity (Fig. 2). Together with recent reports, our observations strongly support that RIG-I can also execute its antiviral action via IFN-independent mechanisms. However, these IFN-dispensable actions are diverse and their exact mechanisms remain largely elusive.

Typically, the activation of RIG-I will trigger the activation of IRF3/7 and NF-κB through the MAVS antiviral singling.[20, 34] Activation of NF-κB pathway leads to the transcription of many pro-inflammatory genes including IFN genes. Our previous study also revealed that the NF-κB complex can directly bind to ISRE and drives its transcription of some ISGs.[35] Interestingly, many of the pro-inflammatory genes are regulated by both the NF-κB and JAK-STAT pathways. For instance, the transcription of CXCL10 is positively

regulated by ISRE and NF-κB during viral infection.[36] It has been reported that MEF cells with a defected NF-κB pathway were more sensitive to the antiviral action of type I IFN.[37] We also observed that the IFN induced expression of some ISGs was enhanced in NF-κB KO MEF cells; whereas the expression of other genes was lower or unaffected (Supporting Fig. S5). Furthermore, a subset of RIG-I induced ISGs were unaffected when JAK-STAT pathway was blocked (Fig 7E), indicating the involvement of additional regulatory mechanisms. Thus, RIG-I and its down downstream pathways form a large complex web. Besides JAK-STAT cascade, other pathways such as NF-κB may also involve the regulation of RIG-I mediated ISG induction and antiviral activity.

A previous study demonstrated that RIG-I overexpression triggers STAT1 activation and ISG expression independent of its canonical MAVS pathway [21]. We now confirmed that overexpression of RIG-I activated STAT1 phosphorylation at 701 site (Fig. 7A) without the involvement of IFNs. We further addressed the contribution of STAT1 phosphorylation to the anti-HEV action of RIG-I. By using pharmacological inhibitors to block the JAK-STAT pathway, we demonstrated that RIG-I induced ISG transcription and anti-HEV activity is only partially but IFN-α mediated effect are totally dependent on this cascade. Furthermore, in a JAK-STAT deficient cell model, only a small proportion of RIG-I inducible ISGs were affected upon RIG-I overexpression. We thus classified these RIG-I inducible ISGs into two categories. One group, including STAT1, IRF1 and IRF9, is completely dependent on RIG-I-induced STAT1 phosphorylation. The other group, including IFIT1, IFIH1 and RANTES, is induced independently of JAK-STAT pathway. Of note, both subsets may contribute to the anti-HEV ability of RIG-I, since the anti-HEV action of RIG-I was only partially attenuated by blocking JAK-STAT pathway (Fig. 7E). Recently, accumulating evidence unrevealed direct antiviral action of RIG-I independent of its downstream IFN production effect [27, 28, 33]. However, whether RIG-I has the direct anti-HEV effect is still unknown and need further investigation.

IFN-α and ribavirin have been used as monotherapy or combination for treating chronic HEV patients. Ribavirin monotherapy appears effective in many patients but failed in a substantial proportion of cases probably due to the development of drug resistance mutations in the viral genome [38-40]. IFN-α seems also effective but is associated with organ rejection, since most of the chronic HEV patients are immunocompromised organ recipients [41]. It is also well-known that excessive exposure to IFNs can result in pathogenesis to the host, and treatment of IFN-α is associated with various severe side effects in patients [42].

Therefore, dissecting the antiviral and the pathogenic mechanisms is necessary for developing specific antiviral strategies while avoiding unnecessary side effects. Our identification of RIG-I as a key anti-HEV ISG and its activation by the natural ligand 5'pppRNA exerting potent anti-HEV activity have provided proof-of-concept for designing such specific anti-HEV approach. Several RIG-I agonists (ImOl-100, Rigontec; MCT-465, Multicell Technologies; SB-9200, Spring Bank Pharmaceuticals) are at various stages of pre-clinical or clinical development for treating viral infections [43]. Thus, the possibility of using these RIG-I agonists in treating HEV infection deserves further evaluations.

In conclusion, we have identified RIG-I as a key anti-HEV ISG that inhibit HEV replication. Biological or pharmacological activation of the RIG-I pathway potently inhibit HEV replication. We further observed ectopic overexpression of RIG-I activated the transcription of many antiviral ISGs to establish an anti-HEV status. This is dispensable of IFN production but partially through the activation of JAK-STAT cascade. Thus, this study revealed new insights of HEV-host interactions, and provided novel avenues for antiviral drug development.

Funding Information

This research is supported by the European Association for the Study of the Liver (EASL) for a Sheila Sherlock Fellowship (to Q. Pan), the Netherlands Organization for Scientific Research (NWO/ZonMw) for a VENI grant (No. 916-13-032) (to Q. Pan), the Dutch Digestive Foundation (MLDS) for a career development grant (No. CDG 1304) (to Q. Pan), the Daniel den Hoed Foundation for a Centennial Award fellowship (to Q. Pan), the Erasmus MC Mrace grant (to Q. Pan) and the China Scholarship Council for funding PhD fellowships to L. Xu (201306300027), W. Wang (201303250056), X. Zhou (No. 201206150075), Y. Yin (201307720045) and Y. Wang (201207720007).

Acknowledgements

The authors gratefully thank Dr. Charles M. Rice (the Rockefeller University) for generously providing the overexpression lentiviral vector, Dr. Suzanne U. Emerson (National Institute of Allergy and Infectious Diseases, NIH, USA) for generously providing the plasmids to generate subgenomic and full-length HEV genomic RNA, Dr. Ralf Bartenschlager and Dr. Volker Lohmann (University of Heidelberg, Germany) for providing the HCV replicon cells., Dr. Sanna M. Mäkelä (National Institute for Health and Welfare Viral Infections Unit, Helsinki,

Finland) for providing WT and RIG-I$^{-/-}$ MEF cells generated by Dr. Michael J. Gale (Department of Immunology University of Washington) and WT, IRF3/7$^{-/-}$ and NFκB$^{-/-}$ MEF cells generated by Dr. A. Hoffmann (Signaling Systems Lab, Los Angeles, CA). We also thank Dr. George R. Stark (Lerner Research Institute) for providing WT and STAT1$^{-/-}$ human fibrosarcoma cells.

Abbreviations

HEV, hepatitis E virus; ISGs, interferon stimulated genes; IFN, interferon; IFN-α, interferon-α; mIFN-α, mouse interferon-α; RIG-I, retinoic acid-inducible gene I; MDA5, melanoma differentiation-Associated protein 5; JAK1, janus kinase 1; STAT1, signal transducers and activators of transcription 1; Fluc, *Photinus pyralis* luciferase; IRF1/2/7/9, interferon regulatory factor 1/2/7/9; PRRs, pattern recognition receptors; ISRE, IFN-stimulated response element; ISGF3, IFN-stimulated gene factor 3; MEF, mouse embryonic fibroblasts; TagRFP, red fluorescent protein; FCS, fetal calf serum; qRT-PCR, quantitative RT-PCR; GFP, green fluorescent protein; shRNA, short hairpin RNA; MTT, 3-(4,5-dimethylthiazol-2-yl)-2,5-diphenyltetrazolium bromide; RP2, human retinitis pigmentosa 2; GAPDH, glyceraldehyde 3-phosphate dehydrogenase.

Supplemental Materials and Methods

Reagents

Human IFN-α (Thermo Fisher Scientific, Life Sciences, the Netherlands) was dissolved in PBS. Mouse IFN-α (mIFN-α) was obtained from Thermo Fisher Scientific (#121001, Life Sciences). CP-690550 (Tofacitinib) was obtained from Santa Cruz Biotechnology and dissolved in DMSO. JAK inhibitor 1 (CAS 457081-03-7) was also obtained from Santa Cruz Biotechnology and dissolved in DMSO at a final concentration of 5 mg/mL. Dimethyl sulfoxide (DMSO, Sigma, Zwijndrecht, the Netherlands) was used as vehicle control at different concentrations. 5'ppp-dsRNA was purchased from InvivoGen (#tlrl-3prna, InvivoGen, CA, USA). Phospho-STAT1 (Tyr^{701}) (58D6, Rabbit mAb, #9167), STAT1 (Rabbit mAb, #9172), MDA5 (IFIH1) (D74E4, Rabbit mAb, #5321) and IRF7 (D2A1J, Rabbit mAb, #13014) antibodies were obtained from Cell Signaling Technology (Danvers, MA, USA). MAVS antibody (E-3, Mouse mAb, #sc-166583), RIG-I antibody (H-300, Rabbit polyclonal, #sc-98911) and β-actin antibody (C-4, Mouse mAb, #sc-47778) were obtained from Santa Cruz Biotechnology (Santa Cruz, CA, USA).

800CW Goat anti-Rabbit IgG (H + L) or 680RD Goat anti-Mouse IgG (H + L) IRDye®-conjugated secondary antibodies were obtained from Li-COR Biosciences (Lincoln, NE, USA).

Cell culture

Huh7.5 cells, 293T cells and A549 cells were grown in Dulbecco's modified Eagle medium (DMEM) (Lonza Biowhittaker, Verviers, Belgium) supplemented with 10% (v/v) fetal calf serum (FCS) (Hyclone, Lonan, Utah) and antibiotics. HepaRG cell line was maintained in William's medium (Thermo Fisher Scientific Life Sciences) as described previously [17]. Hepatitis C virus (HCV) luciferase replication models (ET-Luc) was based Huh7.5 cells coupled with a subgenomic HCV bicistronic replicon (I389/NS3-3V/LucUbiNeo-ET). Huh7.5-ET-Luc cells were grown in DMEM with 250 µg/mL G418 (Sigma Aldrich, Zwijndrecht, the Netherlands). ISRE (IFN-stimulated response element) activation reporter model (Huh7-ISRE-Luc) was based on Huh7 cells that expressing the *firefly* luciferase reporter gene driven by a promoter containing multiple ISRE elements (SBI Systems Biosciences, Mountain View, CA). Luciferase activity represents ISRE promoter activation level and this cell line was maintained in DMEM with 10% FCS and antibiotics.

Mouse embryonic fibroblast cells (MEFs) were grown in DMEM with 10% FCS, 0.6 µg/mL penicillin, 60 µg/mL streptomycin, 2 mM L-glutamine and 20 mM HEPES as described previously [29]. WT and RIG-I$^{-/-}$ MEF cells were generated by Dr. Michael J. Gale (Department of Immunology University of Washington). WT, IRF3/7$^{-/-}$ and NFκB$^{-/-}$ MEF cells were generated by Dr. A. Hoffmann (Signaling Systems Lab, Los Angeles, CA). All these MEF cells were kindly provided by Dr. Sanna M. Mäkelä (National Institute for Health and Welfare Viral Infections Unit, Helsinki, Finland) with the permission of Dr. Michael J. Gale and Dr. A. Hoffmann [29]. WT (fTGH) and STAT1 deficient (U3A, STAT1$^{-/-}$) human fibrosarcoma cells were grown in DMEM with 10% FCS and antibiotics. WT and STAT1$^{-/-}$ fibrosarcoma cells were kind gifts of Prof. George R. Stark (Lerner Research Institute) [44].

RNA and DNA transfection

Polyethylenimine (PEI, Sigma-Aldrich, Zwijndrecht, the Netherlands) was used for transfection of 5'pppRNA in A549 and MEF cells. Cells were seeded in 96-well plates at a density of 1 × 10^4 cells per well. The next day, the medium was removed and cell layer was washed by Opti-MEM. Different concentrations of 5'pppRNA were transfected with PEI in a total volume of 100 µL Opti-MEM. After 5 h, the medium was changed to normal medium.

For lentiviral stocks failed to reach high-level transduction efficacy, DNA-transfection-based overexpression approach was used. Briefly, 7×10^4 Huh7.5 cells were seeded into 24-well plates per well. After cells adhered to the plate, 400 ng lentiviral ISG plasmids were transfected with PEI (Sigma-Aldrich, Zwijndrecht, the Netherlands) in a total volume of 1 mL Opti-MEM per well. After 5 h, the medium was changed to normal DMEM medium that contains 10% FBS.

Measurement of luciferase activity

Measurement of secreted *Gaussia* luciferase activity was conducted by using *BioLux*® *Gaussia* Luciferase Flex Assay Kit (New England Biolabs, Ipswich, MA, USA) according to the manufacturer's instructions. Luminescence signal was monitored by using a LumiStar Optima luminescence counter (BMG Lab Tech, Offenburg, Germany). Measurement of *firefly* luciferase activity was conducted by adding luciferin potassium salt (Sigma-Aldrich, Zwijndrecht, the Netherlands) to cells at a final concentration of 0.1 mM. 10 min after incubation, luciferase activity was measured.

Interferon production bioassay

10×10^4 cells per well were seeded into 6-well plates. Cells were transduced with control or RIG-I lentiviral pseudoparticles at 37 °C as described above. 72 h later, lentiviral particles were removed and cell layer was washed 3 times with PBS. Next, the medium wad refreshed and cultured for another 72 h to let the produced cytokines secreted into the medium. Subsequently, the supernatant (conditioned medium) was collected and then filtered by a 0.45 μm filter. To detect the secreted IFN proteins in conditioned medium, two luciferase reporter models which are extremely sensitive to interferon treatments were used. Huh7.5-ET-Luc luciferase model is an HCV replicon which the HCV-related *firefly* luciferase activity can be potently inhibited by low concentration of IFN-α treatments. Huh7-ISRE-Luc is a luciferase reporter model in which the *firefly* luciferase gene was driven by a promoter containing multiple ISRE elements. In this model, the *firefly* luciferase activity can be potently induced by low concentration of IFN-α treatment. Therefore, these two luciferase models can be used to sensitively assess the presence of IFN proteins in the conditioned medium.

Real-time Quantitative RT-PCR (Real-time qRT-PCR)

RNA was isolated from cells using the Machery-NucleoSpin RNA II kit (Bioke, Leiden, Netherlands). RNA concentration was quantified by a Nanodrop ND-1000 Spectrophotometer (Thermo, DE, USA). 500 ng RNA was reverse transcribed to cDNA by using Takara cDNA Synthesis Kit with random hexamer primers according to manufacturer's instructions (Takara Bio, Inc., Shiga, Japan). Host gene expression and intracellular HEV level were quantified by SYBR-Green-based (Applied Biosystems® SYBR® Green PCR Master Mix, Thermo Fisher Scientific Life Sciences) real-time PCR on the StepOnePlus™ System (Thermo Fisher Scientific Life Sciences). For all human cell lines, two genes GAPDH and RP2 (Human retinitis pigmentosa 2) were used as housekeeping genes and expression level of target genes was normalized to GAPDH and RP2 by the $2^{-\Delta\Delta CT}$ method. For all mouse cell lines, one gene mGAPDH was used as housekeeping genes and expression level of target genes was normalized to mGAPDH by the $2^{-\Delta\Delta CT}$ method. Primers sets used for this study were listed in Table S2 and Table S3 in Supporting Information.

Quantification of HEV replication

Huh7.5-p6 and Huh7.5-p6-Luc are two well-established HEV models that could stably support HEV replication for a long term. In these two cell models, HEV-related *Gaussia* luciferase activity and HEV viral RNA level were measured over 3 months after electroporation when the HEV replication level was stable as described above. Lentivirus transduction and HEV RNA quantification were performed 2 weeks and 4 weeks after HEV RNA electroporation in A549-p6 and HepaRG-p6 models, respectively. WT and RIG-I$^{-/-}$ cells were infected with HEV virus stock as described in reinfection assays for 24 h. 3 days after HEV infection, cells were transfected with 5'pppRNA and HEV viral RNA was quantified 48 h after transfection. Intracellular HEV viral RNA was isolated from cellular lysates. The cells were lysed by using 350 mL RA1 buffer (Bioke, Leiden, The Netherlands) followed by RNA isolation as described above. Primer sequences for detecting HEV viral RNA were 5'-ATCGGCCAGAAGTTGGTTTTTAC-3' (sense) and 5'-CCGTGGCTATAACTGTGGTCT-3' (antisense). qRT-PCR was performed as follows: 10 min at 95 °C, 40 cycles of 15 s at 95 °C, 30 s at 58 °C, and 30 s at 72 °C.

Immunoblot analyses

Whole cell lysates were suspended in SDS sample buffer and heated at 95 °C for 5 min. Proteins were separated in 10% sodium dodecyl sulphate-polyacrylamide (SDS-PAGE) gel

and were transferred onto a PVDF membrane (InvitroGen). Membranes were blocked for 1h at room temperature and then were probed with primary antibodies overnight at 4 °C. Rabbit anti-p-STAT1 (1: 1000), anti-STAT1 (1: 1000), anti-IRF7 (1: 1000), anti-MDA5 (1: 1000), anti-RIG-I (1: 1000) antibodies or mouse anti-MAVS (1: 1000) and anti-β-actin (1: 1000) were used. Membranes were incubated at room temperature with goat anti-rabbit or goat anti-mouse IRDye®-conjugated secondary antibodies (Li-COR Biosciences, Lincoln, USA) (1: 5000). β-actin was served as loading control. Antibody signals were detected by Odyssey Infrared Imaging System and were visualized by Odyssey 3.0 software. Band intensity was quantified by Odyssey Software and normalized to the β-actin signal. The quantification result was showed below each band.

MTT assay

Cells were seeded in 96-well plates and cell viability was determined by adding 10 mM 3-(4,5-Dimethylthiazol-2-yl)-2,5-Diphenyltetrazolium Bromide (MTT) (Sigma, Zwijndrecht, the Netherlands). After 3 h, the medium was replaced with 100 μL of DMSO and was incubated for another 50 min. Absorbance was measured by absorbance reader (Bio-Rad, CA, USA) at a wavelength of 490 nm.

Flow cytometry analysis

The positive percentage of cells transduced with lentivirus was determined by directly detect TagRFP protein expression level. Cells were analyzed on a FACSAria™ flow cytometer (BD Biosciences) equipped with a 561-nm laser.

Supplementary Table 1. Lentiviral shRNA sequences.

No.	Gene	ACCESSION	Sequences	Target Sequence
shRIG-I(1)	DEAD (Asp-Glu-Ala-Asp) box polypeptide 58	NM_014314.3	CCGGCCAGAGAAACTTGCCAGTTATCTCGAGATAACTGGCAAGTTTCTCTGGTTTTTTG	CCAGAGAAACTTGCCAGTTAT
shRIG-I(2)	DEAD (Asp-Glu-Ala-Asp) box polypeptide 58	NM_014314.3	CCGGCCAGAATTATCCCAACCGATACTCGAGTATCGGTTGGGATAATTCTGGTTTTTTG	CCAGAATTATCCCAACCGATA

Supplementary Table 2. Primer sequences for human cells.

Gene	F-Sequences (5’ to 3’)	R-Sequences (5’ to 3’)
ADAR	TCCGTCTCCTGTCCAAAGAAGG	TTCTTGCTGGGAGCACTCACAC
CCL3	ACTTTGAGACGAGCAGCCAGTG	TTTCTGGACCCACTCCTCACTG
CCL4	GCTTCCTCGCAACTTTGTGGTAG	GGTCATACACGTACTCCTGGAC

CXCL10	GGTGAGAAGAGATGTCTGAATCC	GTCCATCCTTGGAAGCACTGCA
DDX60	GGTGTTTTCACCAGGGAGTATCG	CCAGTTTTGGCGATGAGGAGCA
GAPDH	TGTCCCCACCCCCAATGTATC	CTCCGATGCCTGCTTCACTACCTT
IFI27	CGTCCTCCATAGCAGCCAAGAT	ACCCAATGGAGCCCAGGATGAA
IFI44L	TGCACTGAGGCAGATGCTGCG	TCATTGCGGCACACCAGTACAG
IFI6	TGATGAGCTGGTCTGCGATCCT	GTAGCCCATCAGGGCACCAATA
IFIH1(MDA5)	GCTGAAGTAGGAGTCAAAGCCC	CCACTGTGGTAGCGATAAGCAG
IFIT1	GCCTTGCTGAAGTGTGGAGGAA	ATCCAGGCGATAGGCAGAGATC
IFIT2	GGAGCAGATTCTGAGGCTTTGC	GGATGAGGCTTCCAGACTCCAA
IFIT3	CCTGGAATGCTTACGGCAAGCT	GAGCATCTGAGAGTCTGCCCAA
IFITM3	CTGGGCTTCATAGCATTCGCCT	AGATGTTCAGGCACTTGGCGGT
IFN-α	TGGGCTGTGATCTGCCTCAAAC	CAGCCTTTTGGAACTGGTTGCC
IFN-β1	CTTGGATTCCTACAAAGAAGCAGC	TCCTCCTTCTGGAACTGCTGCA
IFN-λ1	GGAAGACAGGAGAGCTGCAACT	AACTGGGAAGGGCTGCCACATT
IFN-λ2	TCGCTTCTGCTGAAGGACTGCA	CCTCCAGAACCTTCAGCGTCAG
IL-1β	CCACAGACCTTCCAGGAGAATG	GTGCAGTTCAGTGATCGTACAGG
IL-32	TCAAAGAGGGCTACCTGGAGAC	TCTGTTGCCTCGGCACCGTAAT
IL-6	AGACAGCCACTCACCTCTTCAG	TTCTGCCAGTGCCTCTTTGCTG
IRF1	GAGGAGGTGAAAGACCAGAGCA	TAGCATCTCGGCTGGACTTCGA
IRF2	TAGAGGTGACCACTGAGAGCGA	CTCTTCATCGCTGGGCACACTA
IRF9	CCACCGAAGTTCCAGGTAACAC	AGTCTGCTCCAGCAAGTATCGG
ISG15	CTCTGAGCATCCTGGTGAGGAA	AAGGTCAGCCAGAACAGGTCGT
JAK1	GAGACAGGTCTCCCACAAACAC	GTGGTAAGGACATCGCTTTTCCG
MX1	GGCTGTTTACCAGACTCCGACA	CACAAAGCCTGGCAGCTCTCTA
NAMPT	CTCCACCAGAACCGAAGGCAAT	AGGGTTACAAGTTGCTGCCACC
OASL	GTGCCTGAAACAGGACTGTTGC	CCTCTGCTCCACTGTCAAGTGG
PKR	GAAGTGGACCTCTACGCTTTGG	TGATGCCATCCCGTAGGTCTGT
PML	CCGTCATAGGAAGTGAGGTCTTC	GTTTTCGGCATCTGAGTCTTCCG
RANTES	CCTGCTGCTTTGCCTACATTGC	ACACACTTGGCGGTTCTTTCGG
RIG-I	CACCTCAGTTGCTGATGAAGGC	GTCAGAAGGAAGCACTTGCTACC
RP2	CCCATTAAACTCCAAGGCAA	AAGCTGAGGATGCTCAAAGG
RSAD2	CCAGTGCAACTACAAATGCGGC	CGGTCTTGAAGAAATGGCTCTCC
STAT1	ATGGCAGTCTGGCGGCTGAATT	CCAAACCAGGCTGGCACAATTG
STAT2	CAGGTCACAGAGTTGCTACAGC	CGGTGAACTTGCTGCCAGTCTT
TRAIL	TGGCAACTCCGTCAGCTCGTTA	AGCTGCTACTCTCTGAGGACCT

Supplementary Table 3. Primer sequences for mouse cells.

Gene	F-Sequences (5’ to 3’)	R-Sequences (5’ to 3’)
mIFIH1	TGCGGAAGTTGGAGTCAAAGCG	TGCGGAAGTTGGAGTCAAAGCG
mIFN-β	AAGAGTTACACTGCCTTTGCCATC	CACTGTCTGCTGGTGGAGTTCATC
mIFN-λ	CCAGTGGAAGCAAAGGATTGCC	GCACCTCATGTCCTTCTCAAGC
mIRF1	TCCAAGTCCAGCCGAGACACTA	ACTGCTGTGGTCATCAGGTAGG
mIRF7	CCTCTGCTTTCTAGTGATGCCG	CGTAAACACGGTCTTGCTCCTG
mIRF9	CAACATAGGCGGTGGTGGCAAT	GTTGATGCTCCAGGAACACTGG
mISG15	CATCCTGGTGAGGAACGAAAGG	CTCAGCCAGAACTGGTCTTCGT
mMX1	TGGACATTGCTACCACAGAGGC	TGGACATTGCTACCACAGAGGC
mPML	GTCTAAGACCCAACCTGTGGCT	CTTCATGGAGCCGACTGTCTGA
mRIG-I	AGCCAAGGATGTCTCCGAGGAA	ACACTGAGCACGCTTTGTGGAC
mSTAT1	GCCTCTCATTGTCACCGAAGAAC	TGGCTGACGTTGGAGATCACCA
mXAF	CTGCGCTTCATAGTCCTTTGCC	AGGGTGCTGTTGGCTTTCCTTG

Supplementary Figures

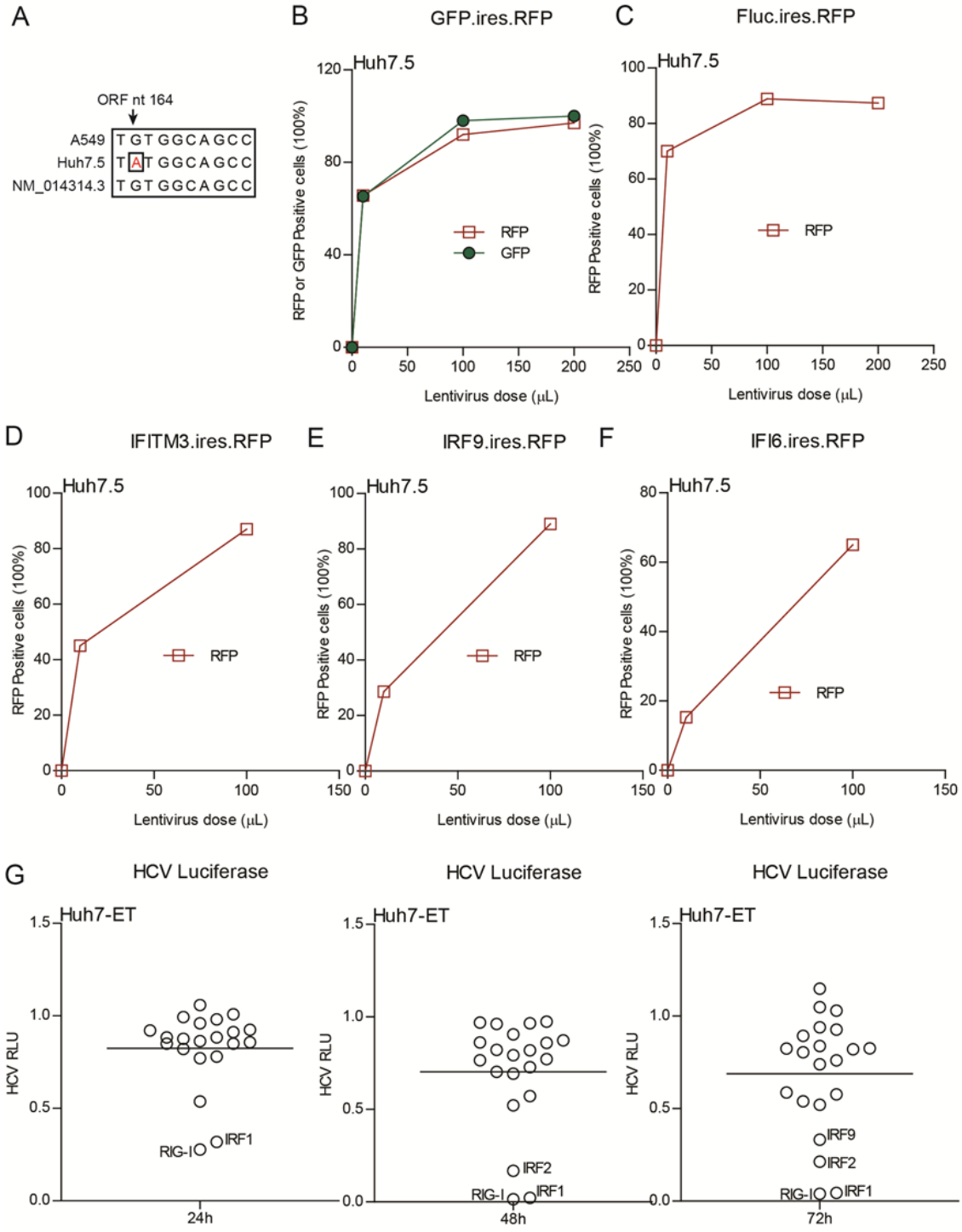

Figure S1. ISG-coupled TagRFP overexpression and the validation of their anti-HCV activities.

(A) Sequencing analysis of RIG-I mutation in Huh7.5 and A549 cells. The mutation of RIG-I in ORF nt 164 in Huh7.5 cells was indicated as red. **(B)** Flow cytometry analysis of GFP or RFP positive cells in Huh7.5 cells transduced with GFP vector at the indicated doses for 48 h. **(C-F)** Flow cytometry analysis of RFP positive cells in Huh7.5 cells transduced with ISG.ires.RFP and Fluc vector at the indicated doses for 48 h. **(G)** Analysis of HCV related *firefly* luciferase activity in Huh7.5-ET-Luc cells transduced with ISG or GFP vector for 24 h, 48 h or 72 h (n = 4 independent experiments with each of

2 replicates). RLU: relative luciferase unit. Data in (G) were normalized to the GFP control (set as 1) and presented in dot plots.

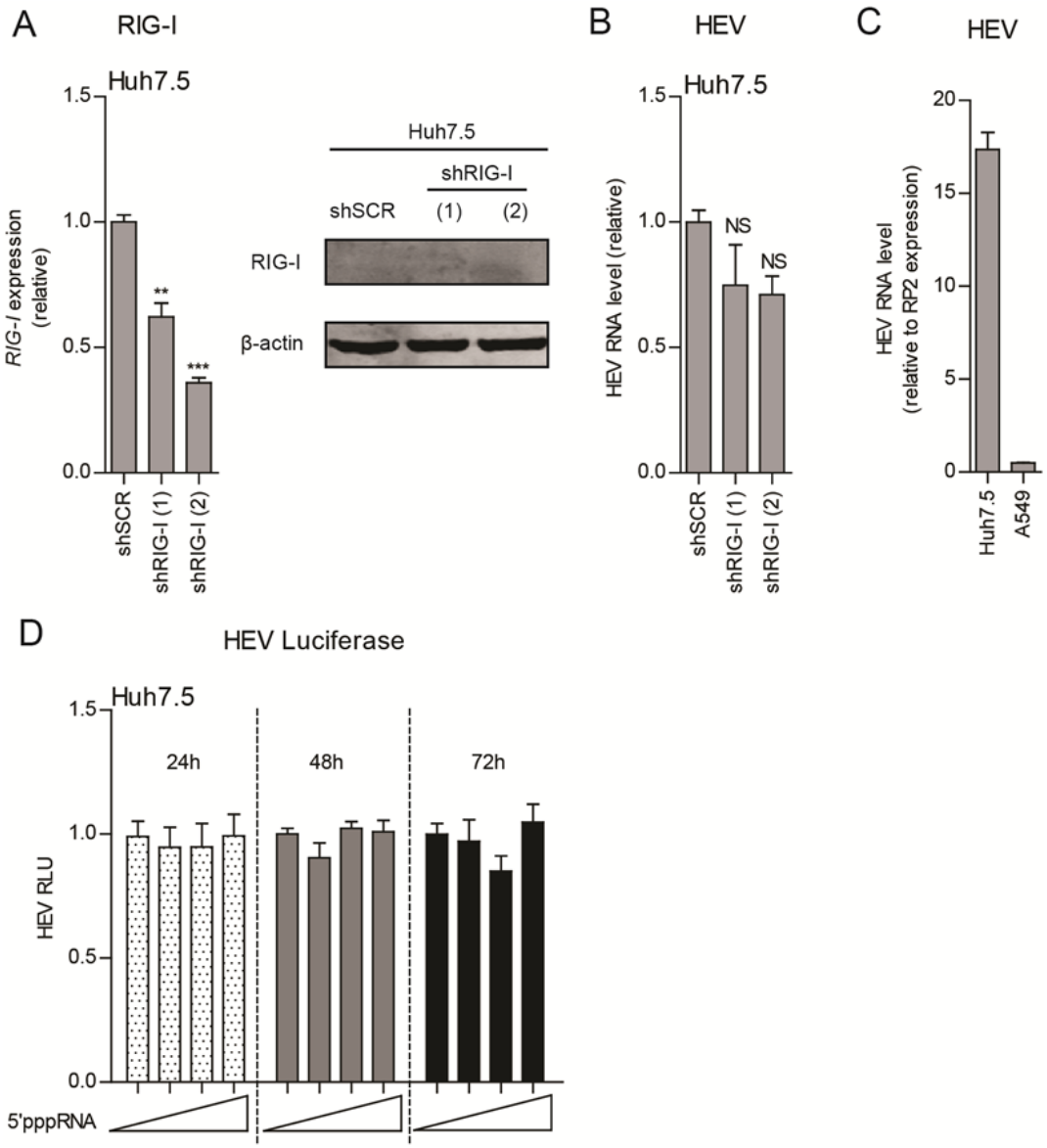

Figure S2. Gene knockdown of RIG-I in Huh7.5 cells does not affect HEV infection and 5'pppRNA does not stimulate an antiviral response in this cells.

qRT-PCR analysis and immunoblot analysis of RIG-I expression in Huh7.5 cells transduced with lentiviral shRNA vectors targeting RIG-I (shRIG-I(1) and shRIG-I(2)) or scrambled control (shSCR). **(B)** Stable RIG-I knockdown or scrambled control (shSCR) Huh7.5 cells were infected with HEV and HEV viral RNA level was analyzed by qRT-PCR 72 h after infection. **(C)** Huh7.5 cells and A549 cells were infected with HEV and HEV viral RNA level was analyzed by qRT-PCR 72 h after infection. Date in (A) and (B) were normalized to the scrambled control (shSCR, set as 1). Date in (C) were normalized with one housekeeping gene RP2 and presented relative to RP2 expression. **(D)** Huh7.5-p6-Luc cells were transfected with various concentrations of 5'pppRNA (10 ng/mL, 100 ng/mL and 1000 ng/mL). HEV related *Gaussia* luciferase activity was analyzed at 24 h, 48 h or 72 h after transfection (n = 2 independent experiments with each of 2 - 3 replicates). RLU: relative luciferase unit. Data were normalized to a control that transfected with PEI-Mix but without 5'pppRNA at each time point (24 h, 48 h and 72 h, all set as 1), respectively.

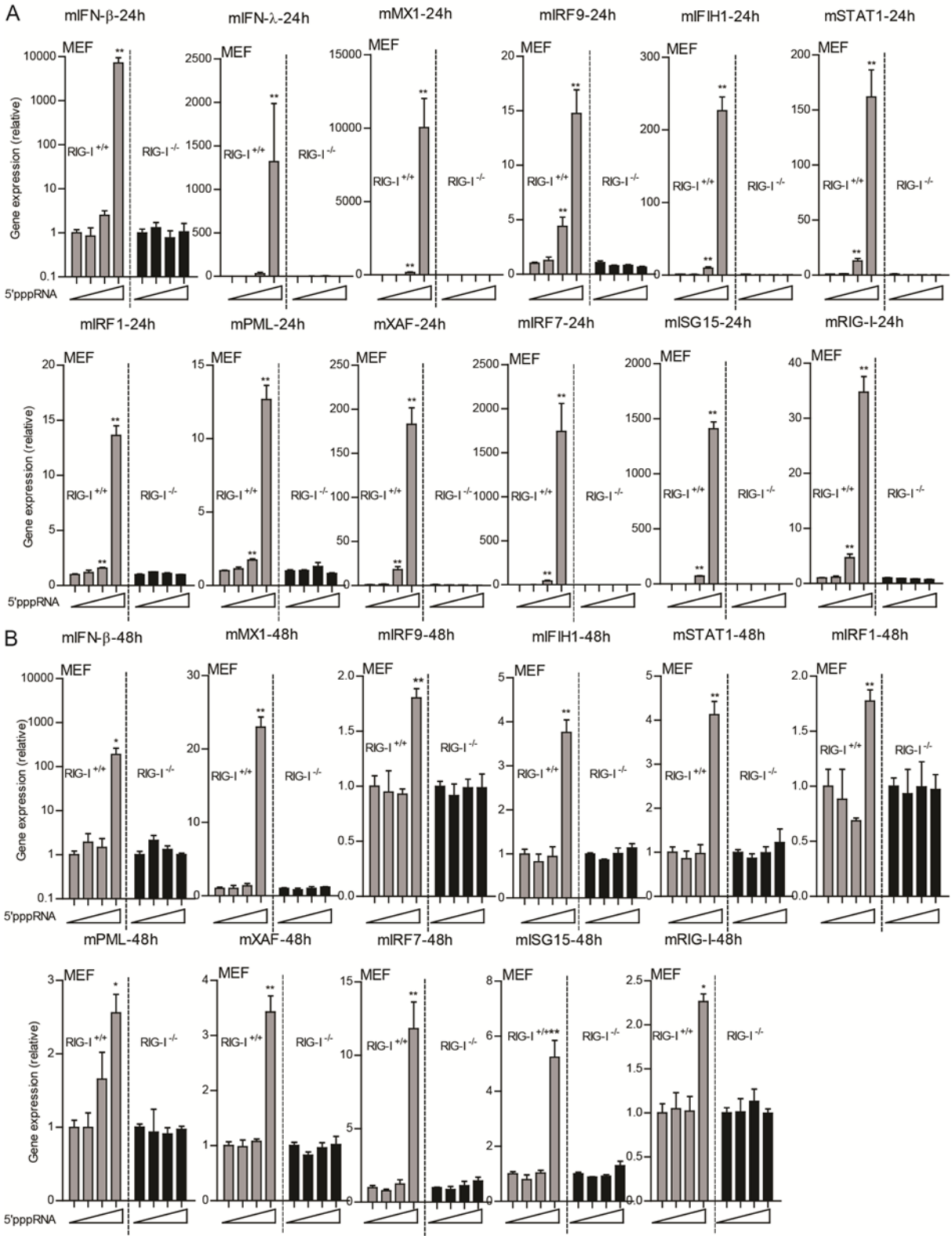

Figure S3. The antiviral ability of 5'pppRNA is dependent on functional RIG-I signaling.

WT (RIG-I$^{+/+}$) and RIG-I deficient (RIG-I$^{-/-}$) mouse embryonic fibroblasts (MEF) cells were transfected with various concentrations of 5'pppRNA (10 ng/mL, 100 ng/mL and 1000 ng/mL), mouse IFN genes (mIFN-β and mIFN-λ) and mouse ISGs including mMX1, mIRF9, mIFIH1, mSTAT1, mIRF1, mPML, mXAF, mIRF7, mISG15 and mRIG-I mRNA level was analyzed by qRT-PCR 24 h **(A)** or 48 h **(B)** after transfection (n = 6). Data were normalized to a control that transfected with PEI-Mix but without

5'pppRNA at each cell line (RIG-I$^{+/+}$ and RIG-I$^{-/-}$, both set as 1), respectively. Data are means ± SEM. *P < 0.05; **P < 0.01; ***P < 0.001; NS, not significant.

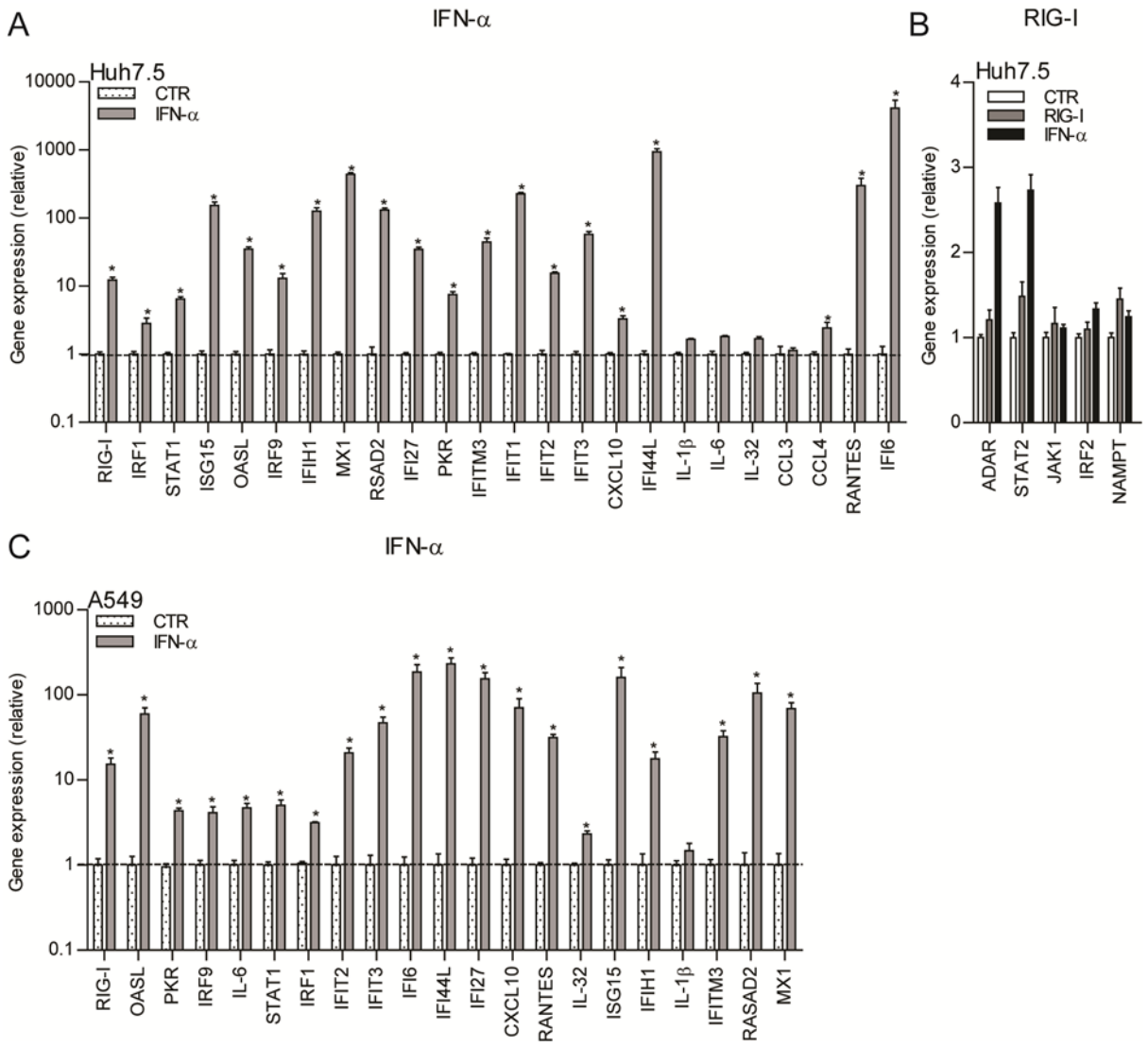

Figure S4. IFN-α activates ISG transcription in different cell lines.

qRT-PCR analysis of ISG mRNA levels in Huh7.5-p6 cells **(A)** and A549-p6 cells **(C)** treated with IFN-α (1000 IU/mL) for 48 h (n = 4). **(B)** qRT-PCR analysis of ISG mRNA levels in Huh7.5-p6 cells transduced with RIG-I or Fluc vector or treated with IFN-α (1000 IU/mL) for 48 h (n = 2 - 3). Data were normalized to the untreated Fluc control (CTR, set as 1). Data are means ± SEM. *P < 0.05; **P < 0.01; ***P < 0.001; NS, not significant.

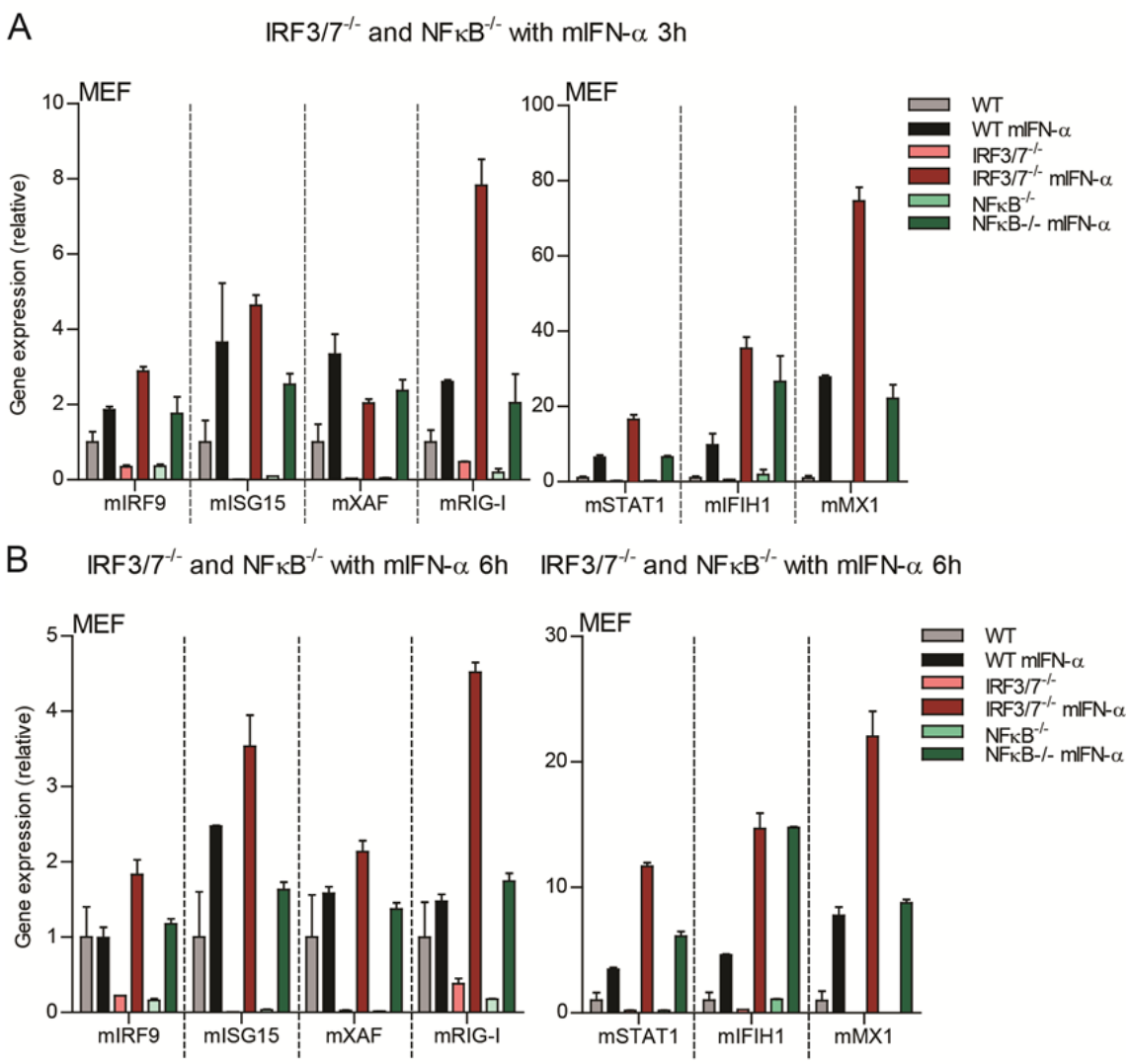

Figure S5. The ISG induction ability of mIFN-α is not attenuated in IRF3/7$^{-/-}$ and NFκB$^{-/-}$ cells.

qRT-PCR analysis of mouse ISG mRNA levels in WT, IRF3/IRF7 double deficient (IRF3/7$^{-/-}$) or NFκB deficient (NFκB$^{-/-}$) mouse embryonic fibroblasts (MEF) cells treated with mouse IFN-α (mIFN-α, 1000 IU/mL) for 3 h **(A)** or 6 h **(B)** (n = 3). Data in (A) were normalized to the untreated Fluc control (CTR, set as 1). Data in (B) and (C) were normalized to untreated WT MEF cells (WT CTR, set as 1). Data are means ± SEM. *P < 0.05; **P < 0.01; ***P < 0.001; NS, not significant.

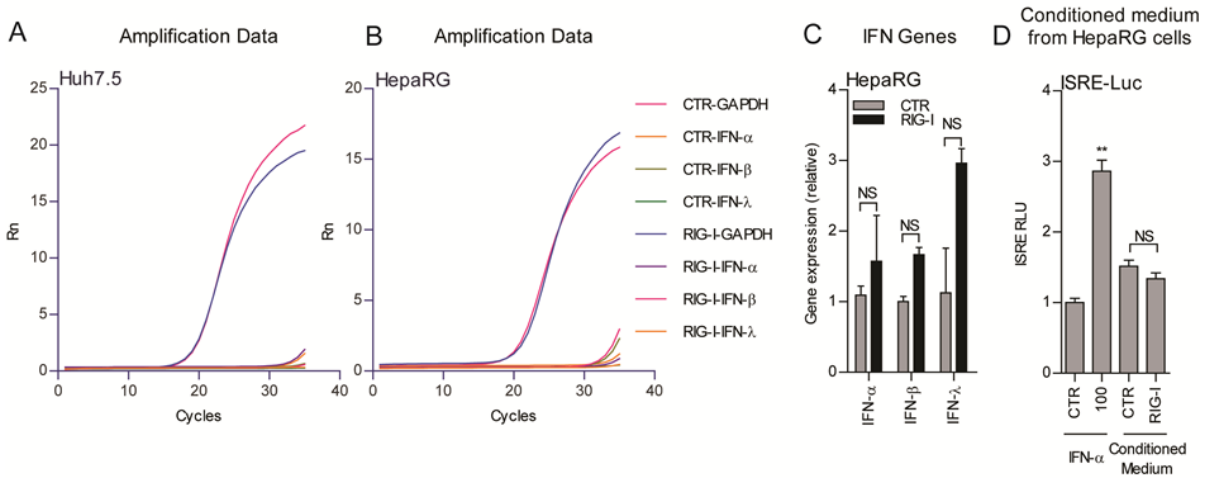

Figure S6. RIG-I overexpression does not trigger ISG production in HepaRG cells.

Plot of qRT-PCR analysis of IFN gene expression in Huh7.5-p6 **(A)** and HepaRG-p6 cells **(B)** transduced with RIG-I or Fluc (CTR) vector for 48 h. Rn: Fluorescence signal from the reporter dye normalized to that from the negative control. **(C)** qRT-PCR analysis of IFN gene mRNA levels in HepaRG-p6 cells transduced with RIG-I or Fluc vector for 48 h (n = 4). **(D)** Analysis of ISRE-related firefly luciferase activity in Huh7-ISRE-Luc cells treated with conditioned medium from HepaRG cells or IFN-α (100 IU/mL) for 48 h (n = 2 independent experiments with each of 2 - 3 replicates). Data in (C) were normalized to the Fluc control (CTR, set as 1). Data in (D) were normalized to the untreated GFP control (CTR, set as 1). Data are means ± SEM. *P < 0.05; **P < 0.01; ***P < 0.001; NS, not significant.

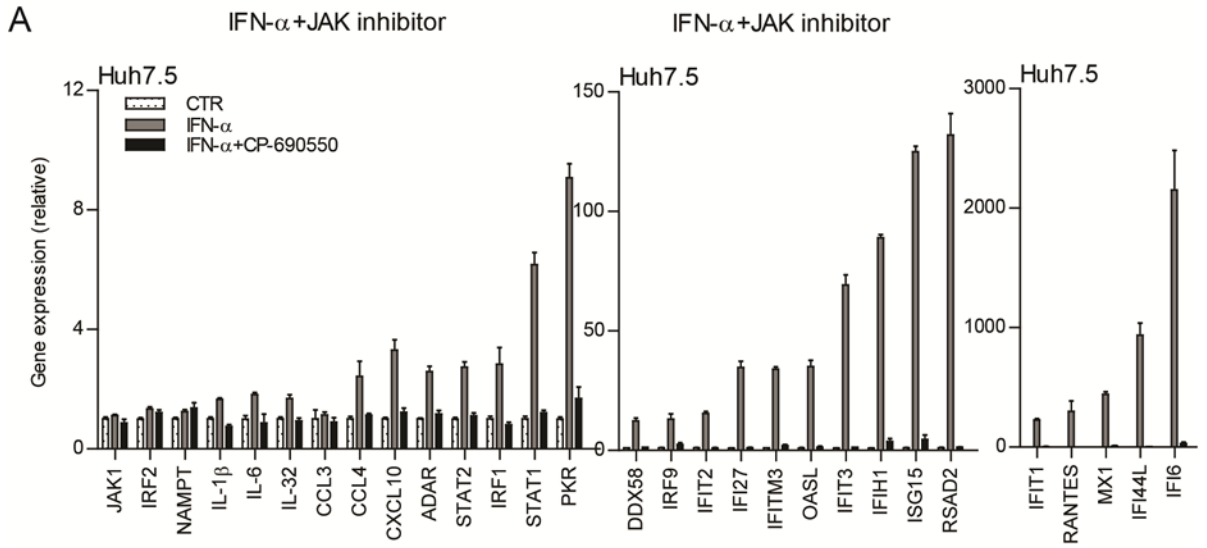

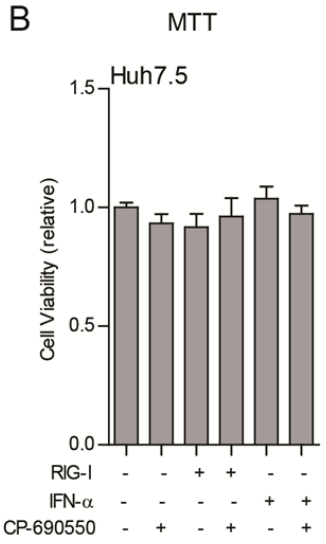

Figure S7. JAK inhibitor CP-690550 totally abolishes IFN-α induced ISG transcription.

(A) qRT-PCR analysis of ISG mRNA levels in Huh7.5-p6 cells treated with IFN-α (1000 IU/mL) or CP-690550 (1000 ng/mL) for 48 h (n =5-6). **(B)** MTT assay analysis of cell viability in Huh7.5-p6 cells transduced with RIG-I vector or treated with IFN-α (1000 IU/mL) or CP-690550 (1000 ng/mL) for 48 h (n = 2 independent experiments with each of 2 replicates). Data were normalized to the untreated control (CTR, set as 1). Data are means ± SEM.

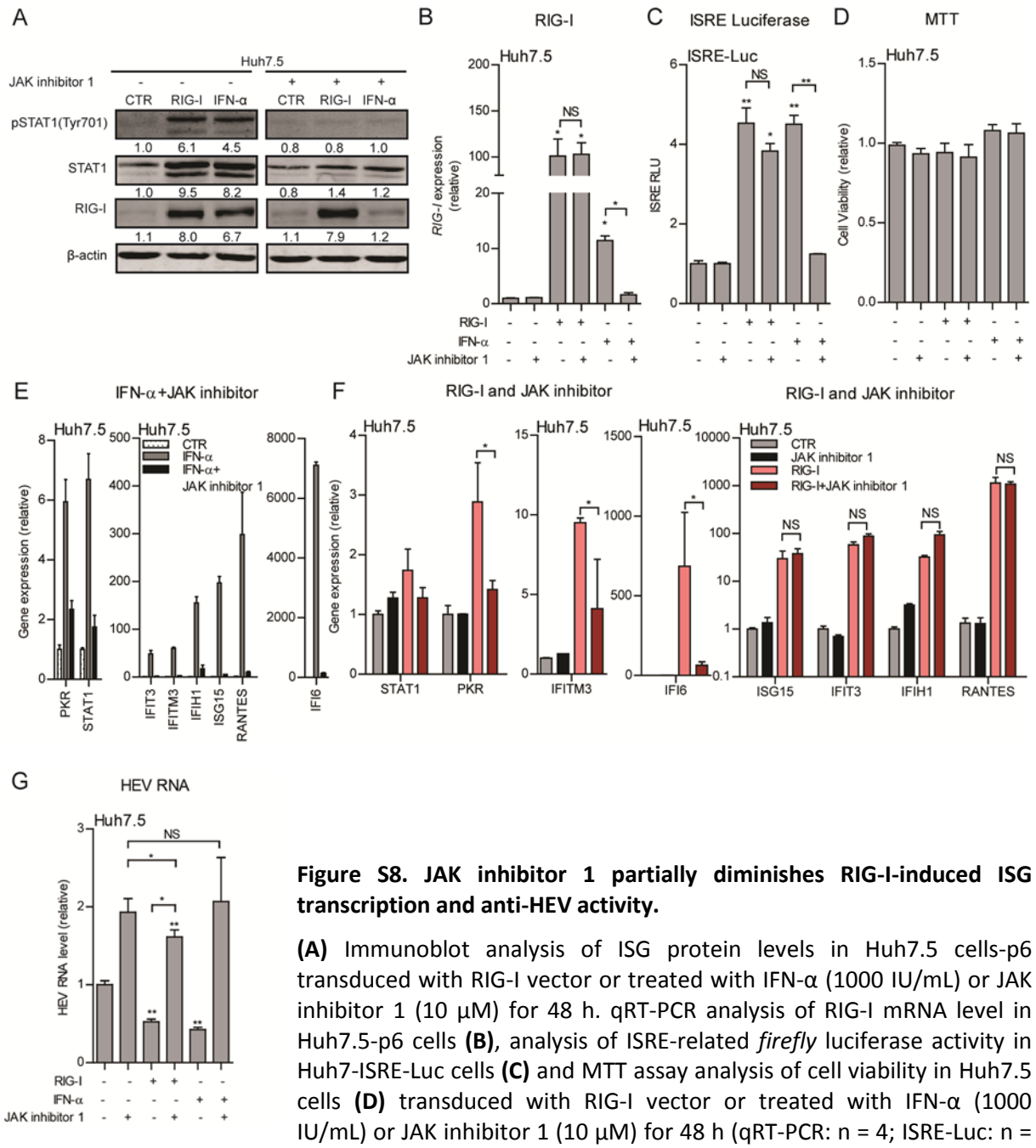

Figure S8. JAK inhibitor 1 partially diminishes RIG-I-induced ISG transcription and anti-HEV activity.

(A) Immunoblot analysis of ISG protein levels in Huh7.5 cells-p6 transduced with RIG-I vector or treated with IFN-α (1000 IU/mL) or JAK inhibitor 1 (10 μM) for 48 h. qRT-PCR analysis of RIG-I mRNA level in Huh7.5-p6 cells **(B)**, analysis of ISRE-related *firefly* luciferase activity in Huh7-ISRE-Luc cells **(C)** and MTT assay analysis of cell viability in Huh7.5 cells **(D)** transduced with RIG-I vector or treated with IFN-α (1000 IU/mL) or JAK inhibitor 1 (10 μM) for 48 h (qRT-PCR: n = 4; ISRE-Luc: n = 3 independent experiments with each of 2 replicates; MTT: 2 independent experiments with each of 2 replicates). **(E)** qRT-PCR analysis of ISG mRNA levels in Huh7.5-p6 cells treated with IFN-α (1000 IU/mL) or JAK inhibitor 1 (10 μM) for 48 h (n =3). **(F)** qRT-PCR analysis of ISG mRNA levels in Huh7.5-p6 cells transduced with RIG-I vector or treated with JAK inhibitor 1 (10 μM) for 48 h (n = 4). **(G)** qRT-PCR analysis of HEV viral RNA level in Huh7.5-p6 cells transduced with RIG-I vector or treated with IFN-α (1000 IU/mL) or JAK inhibitor 1 (10 μM) for 48 h (n = 6). For immunoblot results (A), band intensity of each lane was quantified by Odyssey Software. Immunoblot quantification results were normalized to β-actin expression and control was set as 1. Data in (B, E, F and G) were normalized to the untreated Fluc control (CTR, set as 1). Date in (C and D) were normalized to the untreated GFP control (CTR, set as 1). Data are means ± SEM. *P < 0.05; **P < 0.01; ***P < 0.001; NS, not significant.

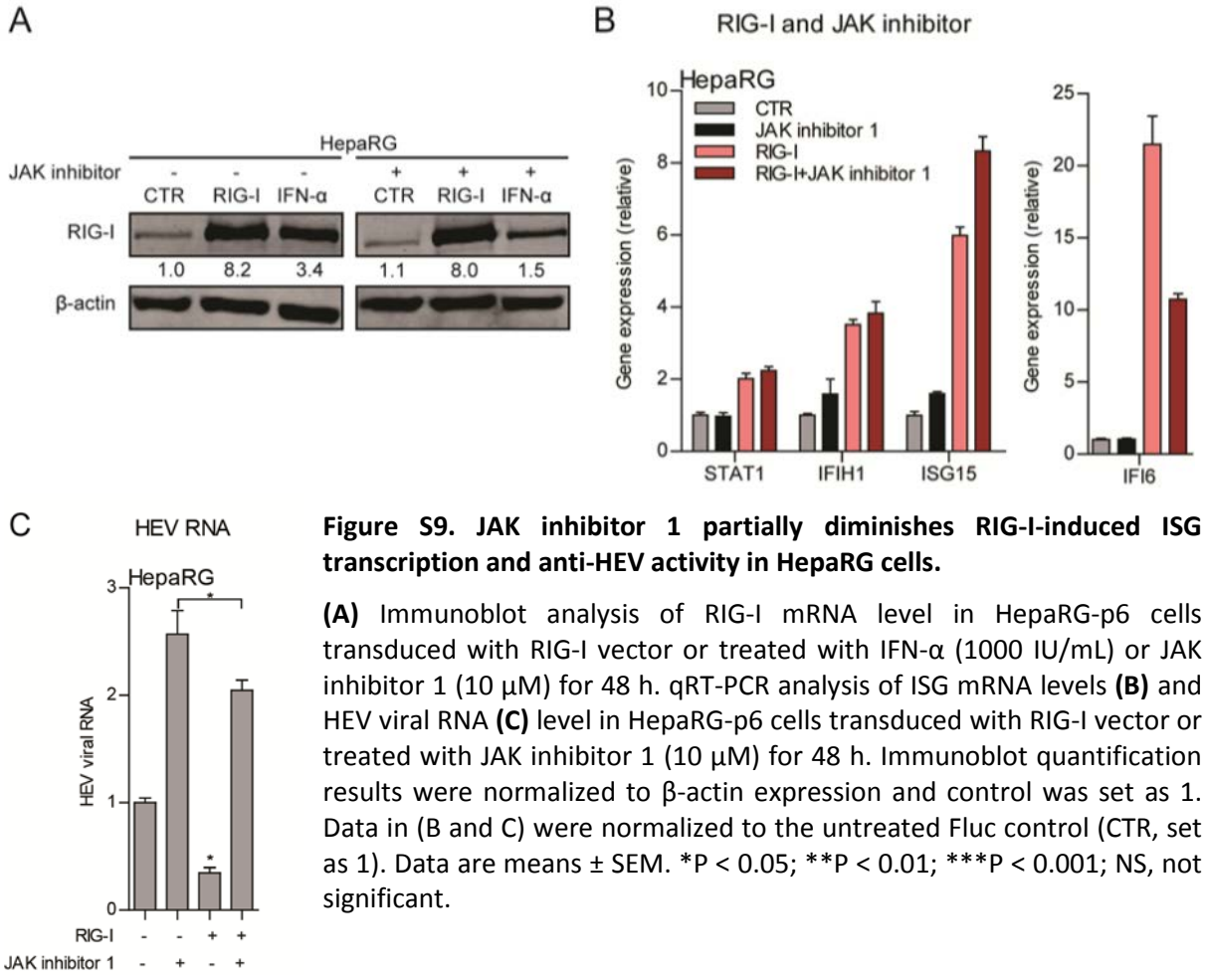

Figure S9. JAK inhibitor 1 partially diminishes RIG-I-induced ISG transcription and anti-HEV activity in HepaRG cells.

(A) Immunoblot analysis of RIG-I mRNA level in HepaRG-p6 cells transduced with RIG-I vector or treated with IFN-α (1000 IU/mL) or JAK inhibitor 1 (10 μM) for 48 h. qRT-PCR analysis of ISG mRNA levels **(B)** and HEV viral RNA **(C)** level in HepaRG-p6 cells transduced with RIG-I vector or treated with JAK inhibitor 1 (10 μM) for 48 h. Immunoblot quantification results were normalized to β-actin expression and control was set as 1. Data in (B and C) were normalized to the untreated Fluc control (CTR, set as 1). Data are means ± SEM. *P < 0.05; **P < 0.01; ***P < 0.001; NS, not significant.

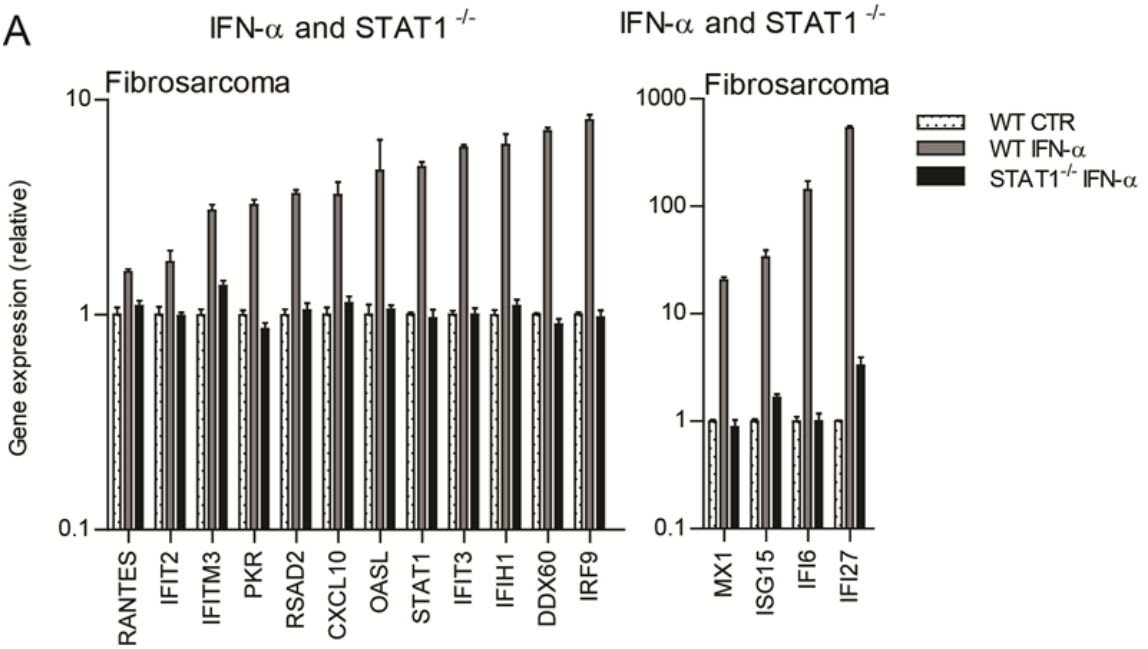

Figure S10. IFN-α does not induce ISG expression in STAT1 deficient cells.

(A) qRT-PCR analysis of ISG mRNA levels in WT and STAT1 deficient ($STAT1^{-/-}$) fibrosarcoma cells treated with IFN-α (1000 IU/mL) for 48 h (n = 4). Date were normalized to untreated WT and $STAT1^{-/-}$ cells, respectively (both set as 1). Data are means ± SEM.

References

1. Debing, Y., et al., Update on Hepatitis E Virology:Implications for Clinical Practice. *J Hepatol*, 2016. **65**(1): p. 200-12.
2. Kamar, N., et al., Hepatitis E. *Lancet*, 2012. **379**(9835): p. 2477-88.
3. Andersen, L.L., et al., Functional IRF3 deficiency in a patient with herpes simplex encephalitis. *J Exp Med*, 2015. **212**(9): p. 1371-9.
4. Ciancanelli, M.J., et al., Infectious disease. Life-threatening influenza and impaired interferon amplification in human IRF7 deficiency. *Science*, 2015. **348**(6233): p. 448-53.
5. Borden, E.C., et al., Interferons at age 50: past, current and future impact on biomedicine. *Nat Rev Drug Discov*, 2007. **6**(12): p. 975-90.
6. Schneider, W.M., M.D. Chevillotte, and C.M. Rice, Interferon-stimulated genes: a complex web of host defenses. *Annu Rev Immunol*, 2014. **32**: p. 513-45.
7. Santiago-Raber, M.L., et al., Type-I interferon receptor deficiency reduces lupus-like disease in NZB mice. *J Exp Med*, 2003. **197**(6): p. 777-88.
8. Iversen, M.B., et al., An innate antiviral pathway acting before interferons at epithelial surfaces. *Nat Immunol*, 2016. **17**(2): p. 150-8.
9. Paludan, S.R., Innate Antiviral Defenses Independent of Inducible IFNalpha/beta Production. *Trends Immunol*, 2016. **37**(9): p. 588-96.
10. Schoggins, J.W., et al., A diverse range of gene products are effectors of the type I interferon antiviral response. *Nature*, 2011. **472**(7344): p. 481-5.
11. Schoggins, J.W., et al., Pan-viral specificity of IFN-induced genes reveals new roles for cGAS in innate immunity. *Nature*, 2014. **505**(7485): p. 691-5.
12. Kamar, N., et al., Pegylated interferon-alpha for treating chronic hepatitis E virus infection after liver transplantation. *Clin Infect Dis*, 2010. **50**(5): p. e30-3.
13. Zhou, X., et al., Disparity of basal and therapeutically activated interferon signalling in constraining hepatitis E virus infection. *J Viral Hepat*, 2016. **23**(4): p. 294-304.
14. Todt, D., et al., Antiviral activity of different interferon (sub-) types against hepatitis E virus replication. *Antimicrob Agents Chemother*, 2016.
15. Moal, V., et al., Chronic hepatitis E virus infection is specifically associated with an interferon-related transcriptional program. *J Infect Dis*, 2013. **207**(1): p. 125-32.
16. Shukla, P., et al., Adaptation of a genotype 3 hepatitis E virus to efficient growth in cell culture depends on an inserted human gene segment acquired by recombination. *J Virol*, 2012. **86**(10): p. 5697-707.
17. Xu, L., et al., IFN regulatory factor 1 restricts hepatitis E virus replication by activating STAT1 to induce antiviral IFN-stimulated genes. *FASEB J*, 2016. **30**(10): p. 3352-3367.
18. Sumpter, R., Jr., et al., Regulating intracellular antiviral defense and permissiveness to hepatitis C virus RNA replication through a cellular RNA helicase, RIG-I. *J Virol*, 2005. **79**(5): p. 2689-99.
19. Cao, X., Self-regulation and cross-regulation of pattern-recognition receptor signalling in health and disease. *Nat Rev Immunol*, 2015. **16**(1): p. 35-50.
20. Goulet, M.L., et al., Systems analysis of a RIG-I agonist inducing broad spectrum inhibition of virus infectivity. *PLoS Pathog*, 2013. **9**(4): p. e1003298.
21. Jiang, L.J., et al., RA-inducible gene-I induction augments STAT1 activation to inhibit leukemia cell proliferation. *Proc Natl Acad Sci U S A*, 2011. **108**(5): p. 1897-902.
22. Kane, M., et al., Identification of Interferon-Stimulated Genes with Antiretroviral Activity. *Cell Host Microbe*, 2016. **20**(3): p. 392-405.
23. Keskinen, P., et al., Impaired antiviral response in human hepatoma cells. *Virology*, 1999. **263**(2): p. 364-75.
24. Rabbani, M.A., et al., Identification of IFN-stimulated gene (ISG) proteins that inhibit human parainfluenza virus type 3. *J Virol*, 2016.

25. Haagsma, E.B., et al., Treatment of chronic hepatitis E in liver transplant recipients with pegylated interferon alpha-2b. *Liver Transpl*, 2010. **16**(4): p. 474-7.
26. Debing, Y., et al., Ribavirin inhibits in vitro hepatitis E virus replication through depletion of cellular GTP pools and is moderately synergistic with alpha interferon. *Antimicrob Agents Chemother*, 2014. **58**(1): p. 267-73.
27. Sato, S., et al., The RNA sensor RIG-I dually functions as an innate sensor and direct antiviral factor for hepatitis B virus. *Immunity*, 2015. **42**(1): p. 123-32.
28. Weber, M., et al., Influenza virus adaptation PB2-627K modulates nucleocapsid inhibition by the pathogen sensor RIG-I. *Cell Host Microbe*, 2015. **17**(3): p. 309-19.
29. Makela, S.M., et al., RIG-I Signaling Is Essential for Influenza B Virus-Induced Rapid Interferon Gene Expression. *J Virol*, 2015. **89**(23): p. 12014-25.
30. Lucas, T.M., J.M. Richner, and M.S. Diamond, The Interferon-Stimulated Gene Ifi27l2a Restricts West Nile Virus Infection and Pathogenesis in a Cell-Type- and Region-Specific Manner. *J Virol*, 2016. **90**(5): p. 2600-15.
31. Mboko, W.P., et al., Interferon regulatory factor 1 restricts gammaherpesvirus replication in primary immune cells. *J Virol*, 2014. **88**(12): p. 6993-7004.
32. Reynaud, J.M., et al., IFIT1 Differentially Interferes with Translation and Replication of Alphavirus Genomes and Promotes Induction of Type I Interferon. *PLoS Pathog*, 2015. **11**(4): p. e1004863.
33. Yao, H., et al., ATP-Dependent Effector-like Functions of RIG-I-like Receptors. *Mol Cell*, 2015. **58**(3): p. 541-8.
34. Ramos, H.J. and M. Gale, Jr., RIG-I like receptors and their signaling crosstalk in the regulation of antiviral immunity. *Curr Opin Virol*, 2011. **1**(3): p. 167-76.
35. Wang, W., et al., Convergent Transcription of Interferon-stimulated Genes by TNF-alpha and IFN-alpha Augments Antiviral Activity against HCV and HEV. *Sci Rep*, 2016. **6**: p. 25482.
36. Brownell, J., et al., Direct, interferon-independent activation of the CXCL10 promoter by NF-kappaB and interferon regulatory factor 3 during hepatitis C virus infection. *J Virol*, 2014. **88**(3): p. 1582-90.
37. Pfeffer, L.M., et al., Role of nuclear factor-kappaB in the antiviral action of interferon and interferon-regulated gene expression. *J Biol Chem*, 2004. **279**(30): p. 31304-11.
38. Debing, Y., et al., Hepatitis E virus mutations associated with ribavirin treatment failure result in altered viral fitness and ribavirin sensitivity. *J Hepatol*, 2016. **65**(3): p. 499-508.
39. Todt, D., et al., In vivo evidence for ribavirin-induced mutagenesis of the hepatitis E virus genome. *Gut*, 2016. **65**(10): p. 1733-43.
40. Debing, Y., et al., A mutation in the hepatitis E virus RNA polymerase promotes its replication and associates with ribavirin treatment failure in organ transplant recipients. *Gastroenterology*, 2014. **147**(5): p. 1008-11 e7; quiz e15-6.
41. Peters van Ton, A.M., T.J. Gevers, and J.P. Drenth, Antiviral therapy in chronic hepatitis E: a systematic review. *J Viral Hepat*, 2015. **22**(12): p. 965-73.
42. Manns, M.P., H. Wedemeyer, and M. Cornberg, Treating viral hepatitis C: efficacy, side effects, and complications. *Gut*, 2006. **55**(9): p. 1350-9.
43. Junt, T. and W. Barchet, Translating nucleic acid-sensing pathways into therapies. *Nat Rev Immunol*, 2015. **15**(9): p. 529-44.
44. Cheon, H. and G.R. Stark, Unphosphorylated STAT1 prolongs the expression of interferon-induced immune regulatory genes. *Proc Natl Acad Sci U S A*, 2009. **106**(23): p. 9373-8.

Chapter 6

Interferon Regulatory Factor 1 Restricts Hepatitis E Virus Replication by Activating STAT1 to Induce Antiviral Interferon-stimulated Genes

Lei Xu[1], Xinying Zhou[1], Wenshi Wang[1], Yijin Wang[1], Yuebang Yin[1], Luc J. W. van der Laan[2], Dave Sprengers[1], Herold J. Metselaar[1], Maikel P. Peppelenbosch[1] and Qiuwei Pan[1]

[1]Department of Gastroenterology and Hepatology, Postgraduate School Molecular Medicine, Erasmus MC-University Medical Center, Rotterdam, the Netherlands

[2]Department of Surgery, Postgraduate School Molecular Medicine, Erasmus MC-University Medical Center, Rotterdam, the Netherlands

The FASEB Journal. 2016. 30(10): 3352-3367

Abstract

IFN regulatory factor 1 (IRF1) is one of the most important IFN-stimulated genes (ISGs) in cellular antiviral immunity. Although hepatitis E virus (HEV) is a leading cause of acute hepatitis worldwide, how ISGs counteract HEV infection is largely unknown. This study was conducted to investigate the effect of IRF1 on HEV replication. Multiple cell lines were used in 2 models that harbor HEV. In different HEV cell culture systems, IRF1 effectively inhibited HEV replication. IRF1 did not trigger IFN production, and chromatin immunoprecipitation sequencing data analysis revealed that IRF1 bound to the promoter region of signal transducers and activators of transcription 1 (STAT1). Functional assay confirmed that IRF1 could drive the transcription of STAT1, resulting in elevation of total and phosphorylated STAT1 proteins and further activating the transcription of a panel of downstream antiviral ISGs. By pharmacological inhibitors and RNAi-mediated gene-silencing approaches, we revealed that antiviral function of IRF1 is dependent on the JAK-STAT cascade. Furthermore, induction of ISGs and the anti-HEV effect of IRF1 overlapped that of IFNα, but was potentiated by ribavirin. We demonstrated that IRF1 effectively inhibits HEV replication through the activation of the JAK-STAT pathway, and the subsequent transcription of antiviral ISGs, but independent of IFN production.

Keywords: innate immunity; ribavirin; transcription

Introduction

Hepatitis E virus (HEV) infection is one of the most common causes of acute hepatitis, particularly in developing countries [1]. Although it is often a self-limiting disease, fulminant hepatitis and high mortality have been reported in pregnant women [2]. In Western countries, chronic HEV has frequently been reported in immunocompromised patients and is the potential cause of graft loss and even mortality [3, 4]. However, the underlying mechanisms of how the host combats HEV infection remain largely elusive.

Upon viral infection, the host rapidly reacts by producing panel of inflammatory cytokines and chemokines to orchestrate the immunologic reaction to the pathogenic invasion [5]. Within this group of anti-viral mediators, IFNs are vital cytokines for innate defense against viral infection [6]. Because of its potent antiviral activity, pegylated IFNα (PEG-IFNα) has been used for decades to treat chronic hepatitis B virus (HBV) and hepatitis C virus (HCV)infections [7, 8]. Because no registered medication is available for HEV infection, PEG-IFNα, ribavirin, or a combination of both has been used as off-label treatments for some cases of HEV infection, although the efficacy is still inconclusive [9]. Mechanistically, type I IFN molecules bind to cell surface receptors and subsequently initiate a signaling cascade. This binding triggers the phosphorylation of preassociated Janus kinase 1 (JAK1). Subsequently, the JAK1 phosphorylation leads to the recruitment and phosphorylation of signal transducers and activators of transcription 1 and 2 (STAT1 and -2), which further bind to IFN regulatory factor 9 (IRF9) to form the IFN-stimulated gene factor 3 (ISGF3) complex. ISGF3 translocates to the nucleus to activate transcription of IFN-stimulated genes (ISGs), which are in turn regulated by the IFN-stimulated response element (ISRE). The products of ISGs are thought to be the ultimate antiviral effectors [10].

Although there are hundreds of ISGs, in fact, only a few have specific or broad antiviral effects [10]. IRF1 is one of the most important ISGs that has been shown to effectively inhibit HCV, yellow fever virus, chikungunya virus, and Venezuelan equine encephalitis virus infections among the 380 tested ISGs [11]. A further follow-up study demonstrated that IRF1 potently inhibits the replication of 14 different viruses, representing 7 families, including different DNA and RNA viruses [10]. However, the exact antiviral mechanism of IRF1 remains unclear.

Given the importance of IRF1 in innate defense against viral infection but insufficient knowledge of HEV, we investigated the role of IRF1 in HEV infection and the interactions with antiviral treatments by using cell culture models. We found that, independent of IFN production, IRF1 effectively restricts HEV replication through the activation of JAK-STAT cascade and the subsequent induction of a wide range of ISGs. We further demonstrated that the anti-HEV effect of IRF1 overlaps IFNα, but is augmented by ribavirin.

Materials and Methods

Reagents

Human IFNα (Thermo Fisher Scientific Life Sciences, Waltham, MA, USA) was dissolved in PBS. Stocks of JAK inhibitor 1 (CAS 457081-03-7, Santa Cruz Biotechnology, Santa Cruz, CA, USA) were dissolved in DMSO with a final concentration of 5 mg/mL. Stocks of CP-690550 (tofacitinib) (Santa Cruz Biotechnology) were dissolved in DMSO with a final concentration of 10 mg/mL. Stock of ribavirin was dissolved in PBS with a final concentration of 10 mg/mL. Matched concentrations of DMSO were used as vehicle control. Phospho-STAT1 (Tyr^{701}) (58D6, Rabbit mAb, 9167), STAT1 (Rabbit mAb, 9172), and IRF1 (D5E4, Rabbit mAb, 8478) antibodies were obtained from Cell Signaling Technology (Danvers, MA, USA). IRF9 antibody was obtained from LSBio (rabbit polyclonal, LS-C155416; Life Span BioSciences, Inc., Seattle, WA, USA). β-Actin antibodies (mouse monoclonal, sc-47778) were obtained from Santa Cruz Biotechnology (Santa Cruz, CA, USA). Anti-rabbit and -mouse IRDye-conjugated secondary antibodies (Li-Cor Biosciences, Lincoln, NE, USA) were also used.

Cell culture

Naive or vector-transduced Huh7 human hepatoma cells, HEK293T cells, A549 human lung epithelial carcinoma cells, and MRC5 human fetal lung fibroblasts [12] were cultured in DMEM (Lonza Biowhittaker, Verviers, Belgium) complemented with 10% (v/v) fetal calf serum (FCS) (Hyclone, Logan, UT, USA), 100 IU/mL penicillin, and 100 mg/mL streptomycin. The HepaRG cell line was maintained in William's medium (Thermo Fisher Scientific Life Sciences) supplemented with 10% FCS, 100 IU/mL penicillin, 100 mg/mL streptomycin, 5 mg/mL insulin, and 5×10^{-7} M hydrocortisone hemisuccinate (Sigma-Aldrich, Zwijndrecht, The Netherlands) [13]. Huh7 cells containing a subgenomic HCV bicistronic replicon (I389/NS3-3V/LucUbiNeo-ET, Huh7-ET-Luc) were maintained with 250 mg/mL G418 (Sigma-

Aldrich), and viral replication was monitored by measuring *firefly* luciferase activity [14]. For the ISRE reporter model (Huh7-ISRE-Luc), Huh7 cells were transduced with a lentiviral transcriptional reporter system expressing the *firefly* luciferase gene driven by a promoter containing multiple ISRE promoter elements (SBI Systems Biosciences, Mountain View, CA, USA); luciferase activity represents ISRE promoter activation [15].

HEV cell culture models

In this study, multiple cell lines were used for HEV replication, including a human hepatoma cell line, Huh7 [16, 17]; a human lung epithelial carcinoma cell line, A549 [18]; a human fetal lung fibroblast cell line, MRC5; and a hepatic cell line, HepaRG, that retains many characteristics of primary human hepatocytes. For the full-length HEV model, a plasmid construct containing the full-length HEV genome (Kernow-C1 p6 clone; GenBank Accession Number JQ679013) was used to generate HEV genomic RNA with the *Ambion* mMessage mMachine *in vitro* RNA transcription Kit (Thermo Fisher Scientific Life Sciences) [16]. Huh7 and HepaRG cells were electroporated with full-length HEV genome RNA, to generate consecutive HEV-infected cell models, Huh7-p6 and HepaRG-p6. For the subgenomic HEV model, a construct containing subgenomic HEV in which the 5' portion of HEV ORF2 was replaced with the in-frame *Gaussia princeps* luciferase reporter gene to yield p6-Luc [16]. Huh7 and A549 cells were electroporated with HEV subgenomic RNA to generate an HEV subgenomic model, Huh7-p6-Luc and A549-p6-Luc, in which the accumulation of secreted luciferase serves as a reporter for HEV replication. For the HEV genotype 1 replicon model, viral RNA was generated from a Sar55/S17/luc-encoding plasmid. Huh7 cells were electroporated with Sar55/S17/luc HEV RNA to generate a genotype 1 replicon model [16, 19].

Reinfection assays

Supernatant from a full-length Huh7-p6 HEV model was collected and purified by ultracentrifugation. The supernatant was first filtered through 0.45 mm filter followed by centrifugation at 10 000 rpm for 30 min to remove cell debris and then 22 000 rpm for 2 h to pellet HEV virus (SW28 rotor; Beckman Coulter, Brea CA, USA). The pellet was suspended and diluted to 1×10^7 HEV viral RNA copies/mL. The diluted HEV virus stock was stored at -80 °C. For HEV infection, Huh7, HepaRG, A549, and MRC5 cells were seeded into 12-well plates at a density of 7×10^4 cells per well and incubated for 24 h. Next, different cells were incubated with 400 mL HEV stock diluted to 1×10^7 viral RNA copies/mL per well at 37 °C for

6 h. Then, the inoculum was removed, and cell layers were washed 3 times with 1 mL PBS, and 1 mL fresh medium was added to each well. For 6-well plates, different cells were seeded at a density of 1.4×10^5 cells per well and incubated for 24 h. Next, different cells were incubated with 800 mL HEV stock diluted to 1×10^7 viral RNA copies/mL per well at 37 °C for 6 h. Then, the inoculum was removed, and cell layers were washed 3 times with 3 mL PBS, and 2 mL fresh medium was added to each well.

To investigate the anti-viral effect of IRF1 in HEV refection models, Huh7 cells were transduced with IRF1 or infected by HEV at the following time points: 1) HEV infection and IRF1 transduction were started at the same time. After 6 h, the inoculum was removed, and 1 mL of medium with IRF1 lentivirus was added to each well. Intracellular HEV viral RNA was measured after 48 h. 2) Huh7 cells were first transduced with IRF1 for 48 h and then were infected with HEV for 6 h. Next, the inoculum was removed, and 1 mL of fresh medium was added to each well. HEV viral RNA was quantified 48 h after HEV infection. 3) Huh7 cells were first infected with HEV for 6 h. At 24 h after HEV infection, IRF1 was transduced, and HEV RNA was quantified at 48 h after transduction.

Gene knockdown and overexpression by lentiviral vectors

For gene knockdown, pLKO.1-based lentiviral vectors (Sigma-Aldrich) targeting IRF1, STAT1, IRF9, and nontargeted control vector (shCTR) were obtained from the Biomics Center in Erasmus Medical Center. Lentiviral pseudoparticles were generated in HEK293T cells according to a published method [20]. To generate a stable gene-knockdown cell line, Huh7 cells were transduced with lentiviral particles for 3 d. Because the vectors also express a puromycin resistance gene, transduced cells were subsequently selected by adding 2.5 μg/mL puromycin (Sigma-Aldrich) to the cell culture medium. After selection, cell lines showing optimal gene knockdown were chosen. pTRIP.CMV.IVSb.ISG.ires.TagRFP-based IRF1 overexpression vector was a kind gift from Prof. Charles M. Rice (Rockefeller University, New York, NY, USA) [11]. Meanwhile, 2 vectors expressing reporter genes *Photinus pyralis* luciferase (Fluc) or green fluorescent protein (GFP) were used as the control (also kind gifts from Prof. Charles M. Rice). Lentiviral pseudoparticles were generated as described and stored at -80 °C. A spinoculation method was used, as described for the IRF1 transduction assay. Target cell lines were seeded into 12-well plates at a density of 7×10^4 cells per well and transduced with lentiviral pseudoparticles at 37 °C for 24, 48, or 72 h. The transduction

time of each experiment is described in the legend of each figure, along with the control vector used.

Quantification of HEV replication

Two Huh7-based HEV models, Huh7-p6 and Huh7-p6-Luc, were well-established models that could stably harbor HEV replication for the long term. In this study, HEV viral RNA and HEV-related luciferase activity were measured; ~2 mo after HEV RNA electroporation when the HEV viral RNA level and luciferase activity were at a stable level. For the HepaRG-p6 and A549-p6-Luc models, lentivirus transduction and HEV RNA quantification were performed 4 and 2 wk, respectively, after HEV RNA electroporation. MRC5 cells were infected by stock HEV virus medium as described in reinfection assays for 24 h. One week after HEV infection, IRF1 was transduced in MRC5 cells, and HEV RNA was quantified 48 h after transduction. For HEV-related *Gaussia* luciferase analysis (HEV-p6-Luc), the activity of secreted luciferase in the cell culture medium was measured by BioLux *Gaussia* Luciferase Flex Assay Kit (New England Biolabs, Ipswich, MA, USA), according to the manufacturer's instructions. Luciferase activity was quantified with a LumiStar Optima luminescence counter (BMG Lab Tech, Offenburg, Germany). For the *firefly* and *Photinus pyralis* luciferases, luciferin potassium salt (100 mM; Sigma-Aldrich) was added to the cells and incubated for 10 min at 37 °C, and luciferase activity was measured. For the HEV-p6 model, intracellular RNA was isolated from cellular lysates. The cells were lysed with 350 mL RA1 buffer (Bioke, Leiden, the Netherlands). RNA was isolated by using the Machery-Nucleo Spin RNAII kit (Bioke) and quantified by a Nanodrop ND-1000 Spectrophotometer (Thermo Fisher Scientific Life Sciences). cDNA was prepared from total RNA with a cDNA Synthesis Kit (Takara Bio, Inc., Shiga, Japan) with random hexamer primers. Intracellular HEV level and host gene expression were quantified by SYBR-Green-based (Applied Biosystems SYBR Green PCR Master Mix; Thermo Fisher Scientific Life Sciences) real-time PCR with the StepOnePlus System (Thermo Fisher Scientific Life Sciences). PCR steps consisted of a 10 min holding stage (95 °C) followed by 40 cycles of 15 s at 95 °C, 30 s at 58 °C, and 30 s at 72 °C. GAPDH and RP2 (human retinitis pigmentosa 2) were used as housekeeping genes, and all gene expression levels (relative) were normalized to GAPDH and RP2 using the $2^{-\Delta\Delta CT}$ method. The HEV primer sequences were 5'-ATCGGCCAGAAGTTGGTTTTTAC-3' (sense) and 5'-CCGTGGCTATAACTGTGGTCT-3' (antisense); the primer sequences of housekeeping gene GAPDH were 5'-TGTCCCCACCCCCAATGTATC-3'

(sense) and 5'-CTCCGATGCCTGCTTCACTACCTT-3' (antisense); and the primers of housekeeping gene RP2 were 5'-CCCATTAAACTCCAAGGCAA-3' (sense) and 5'-AAGCTGAGGATGCTCAAAGG-3' (antisense).

IFN production bioassay

Cells were seeded into 6-well plates at a density of 10×10^4 cells per well and transduced with IRF1 or control lentiviral particles at 37 °C. After 72 h, lentiviral particles were removed, and cells were washed 3 times with PBS and cultured for another 72 h. The cultured supernatant was subsequently collected and filtered through a 0.45 mm pore size membrane and added to 2 luciferase reporter cell lines, Huh7-HCV-Luc and Huh7-ISRE-Luc, that are sensitive to IFNs.

Immunoblot analysis

Whole-cell extracts were obtained and heated at 95 °C for 5 min. Proteins were subjected to a 10 - 15% sodium dodecyl sulfatepolyacrylamide gel (SDS-PAGE), separated at 120 V for 100 min, and electrophoretically transferred onto a PVDF membrane (pore size: 0.45 mm; Thermo Fisher Scientific Life Sciences) for 1.5 h with an electric current of 250 mA. Subsequently, the membrane was blocked with blocking buffer (Li-Cor Biosciences) in 1 × PBS containing 0.1% Tween-20. Membranes were incubated with primary antibodies overnight at 4 °C. Rabbit anti-IRF1, p-STAT1, STAT1, IRF9 (1: 1 000) antibodies or mouse anti-b-actin (1: 2 000) were diluted in 5% (mass/vol) bovine serum albumin in 1 × PBS containing 0.1% Tween-20. The membrane was washed 3 times, followed by incubation for 1 h with anti-rabbit or anti-mouse IRDye-conjugated secondary antibodies (1: 5 000; Li-Cor Biosciences) at room temperature. β-Actin served as the loading standard. The membrane was scanned by Odyssey Infrared Imaging System (Li-Cor Biosciences). Results were visualized with Odyssey 3.0 software. Band intensity data of each immunoblot was also quantified by Odyssey Software.

MTT assay

Cells were seeded in 96-well plates, and 10 mM 3-(4,5-dimethylthiazol-2-yl)-2,5-diphenyltetrazolium bromide (MTT) (Sigma-Aldrich) was added. The plate was incubated at 37 °C with 5% CO_2 for 3 h, then the medium was removed, 100 mL of DMSO was added to each well, and the microplate was incubated at 37 °C for 50 min. The absorbance of each

well was read on the microplate absorbance reader (Bio-Rad, Hercules, CA, USA) at a wavelength of 490 nm.

Confocal microscopy analysis

Huh7 cells (1×10^4) were seeded on glass slides in a 6-well plate. The cells were transduced with overexpressed IRF1, Fluc, or GFP control lentiviruses for 48 h. For IRF1 protein immunofluorescence staining, IRF1 antibody (1: 200, D5E4, rabbit mAb, 8478; Cell Signaling Technology) was used as the primary antibody. Anti-rabbit-Alexa Fluor 488-conjugated antibody (1: 1 000; Cell Signaling Technology) was used as the secondary antibody. The cells were visualized in an inverted LSM 510 confocal microscope (Zeiss LSM 510, Jena, Germany) using a 40 × oil immersion objective with 1.7 × zoom in. All images were analyzed with a Zeiss LSM Image Browser (version 4.2).

Chromatin immunoprecipitation-sequencing data analysis

Chromatin immunoprecipitation-sequencing (ChIP-seq) datasets for IRF1 in K562 cells were retrieved from the ENCODE database (http://www.genome.ucsc.edu/ENCODE/dataMatrix/-encodeData-MatrixHuman.htmL/; University of Santa Cruz, CA, USA). ChIP-seq datasets were processed and mapped to the hg19 reference genome [21]. ChIP-seq datasets with multiple replicates were merged. Model-based analysis for ChIP-seq (MACS 1.4.2) was used for peak calling and for the generation of binding profiles [22]. The sequencing profiles of IRF1 were created in the IGV browser [23].

Statistical analysis

All results are presented as means ± SEM. Comparisons between groups were determined with the Mann-Whitney U test. Differences were significant at $P < 0.05$.

Results

IRF1 effectively inhibits HEV replication

Although IRF1 exerts cell-autonomous antiviral activity toward a broad range of viruses [10, 11], its capacity to combat HEV infection remains unexplored. To determine the role of IRF1 in HEV infection, we first tested the effect of forced IRF1 expression in 2 Huh7 cell line-based HEV models. Successful overexpression of IRF1 was visualized by red fluorescent protein (TagRFP) expression under the confocal electron microscope, because the bicistronic lentiviral vector coexpresses IRF1 and a TagRFP reporter (Supplemental Fig. S1A).

Consistently, IRF1 mRNA expression (Fig. 1A) and protein level (Fig. 1B, C) were increased in overexpressing cells compared with those induced by high-dose IFNα (1000 IU/mL). Of note, immunofluorescence staining of IRF1 showed that it was predominantly located in the nucleus (Fig. 1C). To exclude the nonspecific effect of lentivirus transduction, we used 2 control vectors that were used in previous study that expressed reporter genes Fluc or GFP [11]. Transduction efficiency was confirmed by different methods, including visualization of TagRFP expression (data not shown), measurement of Photinus pyralis luciferase activity (Supplemental Fig. S1B), and quantitation of TagRFP mRNA expression level in transduced cells. As expected, Fluc and GFP control did not affect HEV replication in 2 Huh7-based models (Supplemental Fig. S1C, D).

Next, we showed that overexpression of IRF1 could profoundly inhibit HCV replication in an Huh7-based HCV luciferase replicon model, Huh7-ET Luc (Supplemental Fig. S1E), without affecting cell viability (Supplemental Fig. S1F), which was consistent with results reported earlier [11]. After 48 or 72 h of IRF1 transduction, HEV was significantly inhibited in both the HEV Huh7-p6-Luc replicon and full-length infectious models (Fig. 1D). The antiviral activity of IRF1 in both models was equivalent to high-dose IFNα (1000 IU/mL) treatment. Moreover, IRF1 could also effectively inhibit genotype 1 HEV-related luciferase activity in the Huh7-based genotype 1 HEV replicon model, Sar55/S17/luc (Fig. 1E). To further validate the antiviral ability of IRF1, we used 3 additional human cell lines. A human hepatic progenitor cell–derived cell line, HepaRG, which exhibits many characteristics of primary human hepatocytes [13]; a lung epithelial carcinoma cell line, A549, which is widely used for HEV propagation [18]; and a human fetal lung fibroblast cell line, MRC5 [12], were used to further confirm the anti-HEV effects of IRF1. The overexpression of IRF1 in these cell lines was confirmed by measuring IRF1 mRNA and protein expression (Supplemental Fig. S1G, H). Consistently, overexpression of IRF1 significantly inhibited the intracellular HEV RNA level, as well as HEV-related luciferase activity (Fig. 1F) in these cell lines. To validate the antiviral ability of IRF1 in the reinfection HEV model, Huh7 cells were infected by HEV or transduced with IRF1 at different time points (described previously). The result showed that overexpression of IRF1 significantly inhibited HEV infection when IRF1 was transduced with (same time, Supplemental Fig. S1I), before (pre, Supplemental Fig. S1J), or after (post, Supplemental Fig. S1K) HEV infection. Taken together, these results demonstrate that IRF1 overexpression effectively inhibits HEV replication and infection in different cell culture

models. Furthermore, we investigated whether HEV infection would trigger IRF1 expression in different cell lines, including Huh7, HepaRG, A549, and MRC5. Each cell line was infected by HEV. We found that IRF1 expression can be induced at an early stage of HEV infection (2 h after infection) in HepaRG and A549 cells (Supplemental Fig. S2A, B). In MRC5 and Huh7 cells, IRF1 was just slightly induced 2 or 6 h after infection, respectively.

Subsequently, we determined whether basal IRF1 is necessary for anti-HEV immunity. This investigation was pursued by a loss-of-function approach involving knockdown of IRF1 by lentiviral-based short hairpin RNA (shRNA) constructs. A non-targeted vector was used as a control (shCTR). Gene silencing of IRF1 was confirmed by immunoblot analysis and real-time quantitative RT-PCR (qRT-PCR) (Fig. 1G, H). Consistently, knockdown of IRF1 significantly promoted HEV replication (Fig. 1H). Thus, both gain- and loss-of-function assays demonstrated that IRF1 plays an important role in restricting HEV replication.

IRF1 overexpression does not trigger IFN production

Because of the comparable anti-HEV effect of IRF1 and IFNα, we investigated whether IRF1 triggers IFN production in our cell culture systems, since IRF1 has been reported to induce IFNβ expression in particular cell types [24].We first investigated the effect of IRF1 on the gene expression level of different IFNs, including IFNα, -β, and -λ in different cell lines. We found that the basal mRNA expression levels of several IFN genes including IFNα, -β, and -λ were very low in Huh7 and HepaRG cells (Supplemental Fig. S2C) and were not significantly affected, even by IRF1 overexpression (Fig. 2A). These results are consistent with those in another study that no IFN genes are affected in IRF1-overexpressing Huh7 cells. In addition, the expression of all 3 IFN genes was not affected by IRF1 overexpression in A549 and MRC5 cells (Fig. 2B). As a positive control, the IFN β and-λ genes were effectively induced by the RIG-I activator 5'pppRNA [25] in A549 cells. To further confirm the lack of IFN production in IRF1-overexpressing cells, we collected the conditioned medium from the transduced cells (supernatant) and performed an IFN functional assay, as well as a highly sensitive HCV-based bioassay (Fig. 2C) [26]. To this end, we used a lentiviral transcriptional reporter system to mimic IFN response by expressing the *firefly* luciferase driven by a promoter containing multiple ISREs [15].

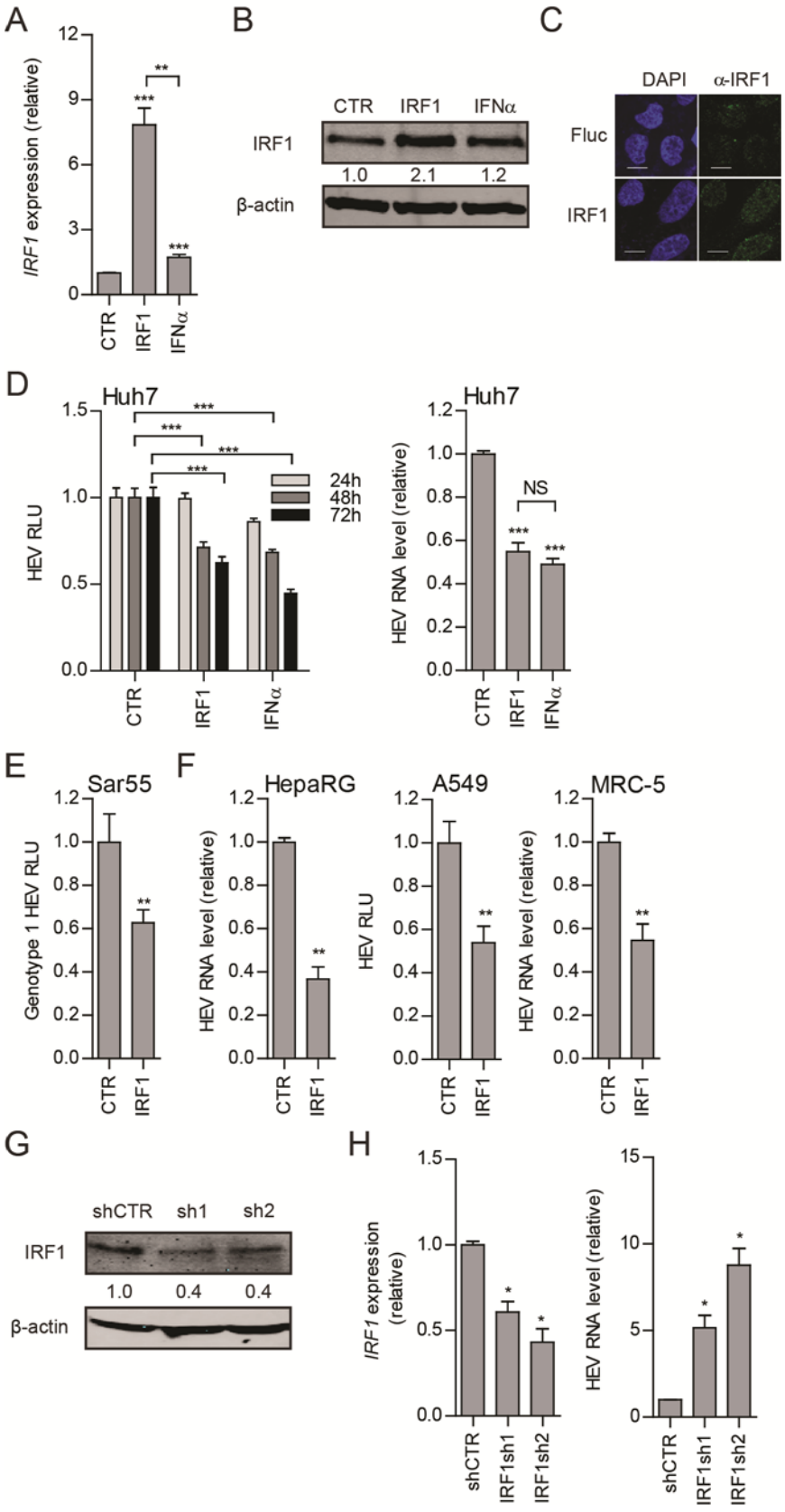

Figure 1. IRF1 effectively inhibits HEV replication.

A) Real-time qRT-PCR analysis of IRF1 mRNA expression in Huh7 cells transduced with IRF1 or Fluc (control) vectors or treated with IFNα (1000 IU/mL) for 48 h (n = 7). Data were normalized to 2 housekeeping genes, GAPDH and RP2. B, C) Immunoblot (B) and immunofluorescence (C) analyses of Huh7 cells transduced with IRF1, Fluc (CTR) vector or treated with IFNα (1000 IU/mL) for 48 h. Band intensity data of each immunoblot was quantified by Odyssey Software. All data were normalized to actin expression, and control was set as 1. Green: IRF1 protein; blue: DAPI. Scale bar, 10 mm. D) HEV viral replication related *Gaussia* luciferase activity in Huh7-p6-Luc model transduced with IRF1 or Fluc vector or treated with IFNα (1000 IU/mL) for 24 h, 48 h or 72 h (n = 4 independent experiments with each of 3 - 4 replicates) and real-time qRT-PCR analysis of HEV viral RNA in Huh7-p6 full-length HEV model transduced with IRF1 or Fluc vector or treated with IFNα (1000 IU/mL) for 48 h (n = 7). RLU: relative luciferase unit. E) Genotype 1 HEV (Sar55/S17/luc) viral replication-related *Gaussia* luciferase activity in Huh7-Sar55/S17/luc model transduced with IRF1 or Fluc vector for 48 h (n = 4 independent experiments with each of 3 - 4 replicates). F) HEV viral replication-related *Gaussia* luciferase activity in a A549-p6-Luc model (n = 4 independent experiments with each of 3 - 4 replicates) or qRT-PCR analysis of HEV viral RNA in HepaRG-p6-HEV

and MRC-5-p6 HEV models transduced with IRF1 or Fluc vector for 48 h (HepaRG: n = 4; MRC-5: n = 5). G) Immunoblot analysis of Huh7 cells transduced with lentiviral shRNA vectors targeting IRF1 or nontargeted control (shCTR). H) Real-time qRT-PCR analysis of IRF1 and HEV viral RNA level relative to shCTR (n = 3-5). Data were normalized to Fluc control (CTR, set as 1) (D-F) and are means ± SEM. *P < 0.05; **P < 0.01; ***P < 0.001; NS, not significant.

As shown in Fig. 2D, the supernatant from IRF1-overexpressing Huh7 cells was unable to stimulate an IFN response in the ISRE reporter assay. Meanwhile, supernatants from HepaRG, A549, and MRC5 cells did not stimulate IFN response (Fig. 2F) in the ISRE reporter assay. Although the HCV replicon is very sensitive to IFN, the supernatant collected from IRF1 transduced cells did not affect HCV replication (Fig. 2E). These data indicate that IRF1 overexpression does not trigger IFN production in Huh7, HepaRG, A549, and MRC5 cells.

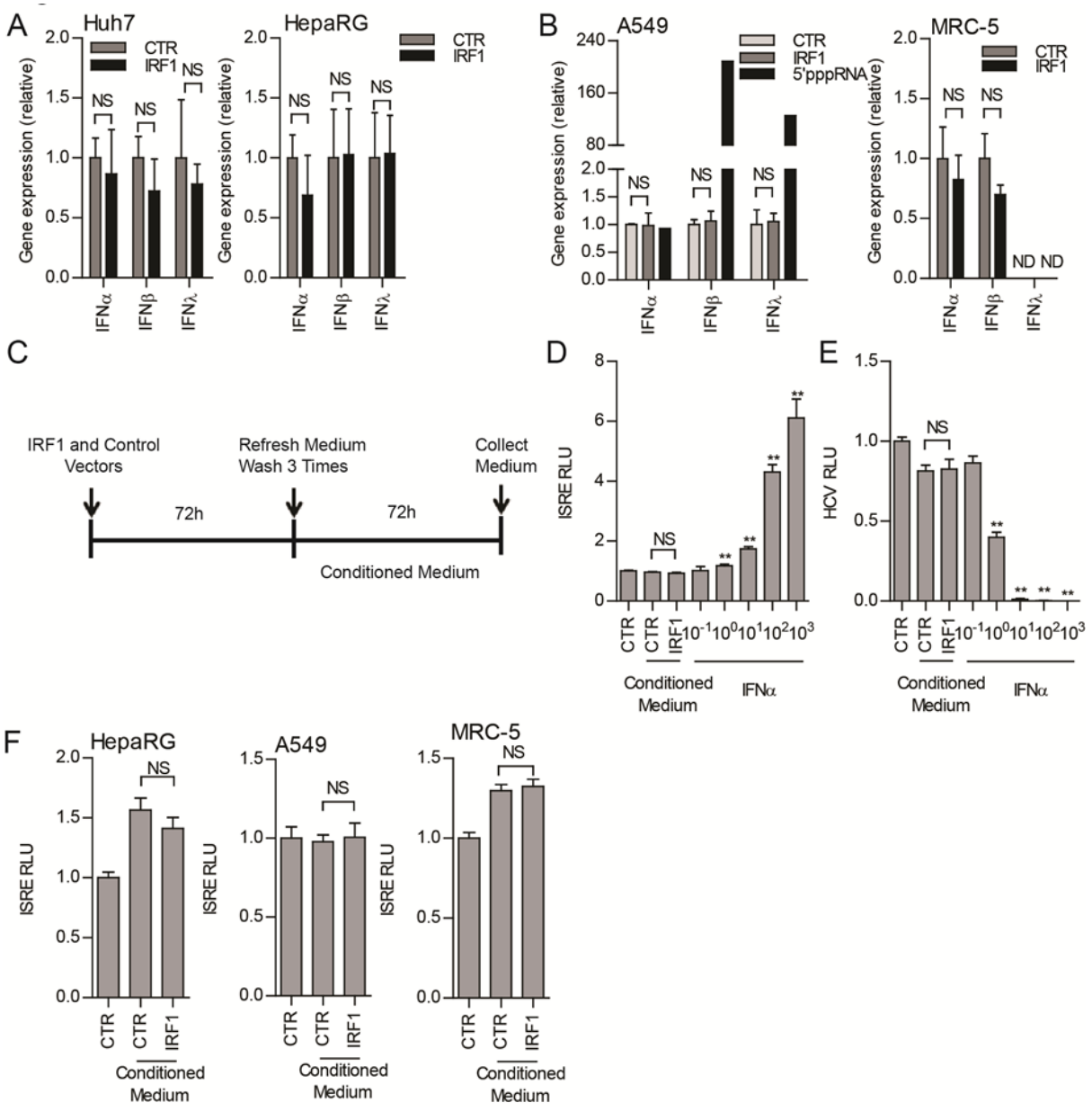

Figure 2. IRF1 overexpression does not trigger IFN production.

A, B) Real-time qRT-PCR analysis of IFN gene expression in Huh7 (A), HepaRG (A), A549 (B) and MRC5 (B) cells transduced with IRF1 or Fluc vector for 48 h (n = 3). For A549 cells, 5'pppRNA (0.1 mg/mL) was transfected as a positive control (IRF1, n = 3; 5'pppRNA, n = 1). Data were normalized to Fluc control (CTR, set as 1). C) Production of conditioned medium (supernatant). D, E) ISRE *firefly* luciferase activity in Huh7-ISRE-Luc model (D) and HCV luciferase activity in Huh7-ET-Luc model (E) treated with conditioned medium from Huh7 cells or IFNα for 48 h (n = 3 independent experiments with each of 3–4 replicates). F) ISRE *firefly* luciferase activity in Huh7-ISRE-Luc treated with conditioned medium from HepaRG, A549, or MRC5 cells for 48 h (n = 3 independent experiments with each of 2 - 3 replicates). Data were normalized to GFP control (D-F) (CTR, set as 1). Data are means ± SEM. **P < 0.01. NS, not significant.

IRF1 activates STAT1 gene transcription leading to enhanced protein expression and phosphorylation

IRF1 was first described as a transcription factor [24] and has more than 200 binding sites in the human genome [27]. By retrieving genome-wide IRF1 ChIP-seq data from the ENCODE ChIP-seq Experiment Matrix database, we unexpectedly found that IRF1 bound directly to the promoter region of the STAT1 gene (Fig. 3A), a key component of IFN signaling.

To validate whether IRF1 induces transcription of STAT1 in our system, we first tested mRNA expression of STAT1 in IRF1-overexpressing Huh7 cells. Indeed, we observed that overexpression of IRF1 potently induced mRNA expression of STAT1 (Fig. 3B), but not JAK or STAT2 (Fig. 3C). In addition, IRF1 also potently induced STAT1 mRNA expression in HepaRG, A549, and MRC5 cells (Fig. 3D). Induction led to enhanced expression of STAT1 protein and activation of STAT1 phosphorylation at the Tyr^{701} site, which is an indispensable marker of STAT1 activation (Fig. 3E). In addition, IRF1 led to enhanced expression of STAT1 protein and activation of STAT1 phosphorylation in HepaRG, A549, and MRC5 cells (Fig. 3F). The results demonstrated that IRF1 effectively activates STAT1 gene transcription, resulting in enhanced protein expression and phosphorylation.

IRF1 activates the transcription of antiviral ISGs

In general, binding of IFNs to their receptors activates JAK1, resulting in tyrosine phosphorylation of STAT1 and -2, followed by the formation and nuclear translocation of the STAT1-STAT2-IRF9 complex, a transcription factor complex known as ISGF3, which in turn binds to the ISRE motifs in the genome DNA and subsequently drives the global transcription of ISGs to establish an antiviral status [28]. Since IRF1 activates STAT1, we further investigated whether it can also trigger functional effects of STAT1 activation including ISG transcription. Indeed, IRF1 could significantly increase ISRE-regulated luciferase activity (Fig. 4A)

comparable to high-dose IFNα treatment in the Huh7-ISRE-Luc model. Furthermore, IRF1 stimulated the expression of 17 tested ISGs at various levels (Fig. 4B and Supplemental Fig. S2D), whereas the control GFP or Fluc vectors did not affect their expression (Supplemental Fig. S2E). The stimulation of ISGs by IRF1 was further confirmed in HepaRG, A549, and MRC5 cells (Fig. 4C-E). These results triggered us to further investigate whether these actions of IRF1 occur totally via the JAK-STAT pathway.

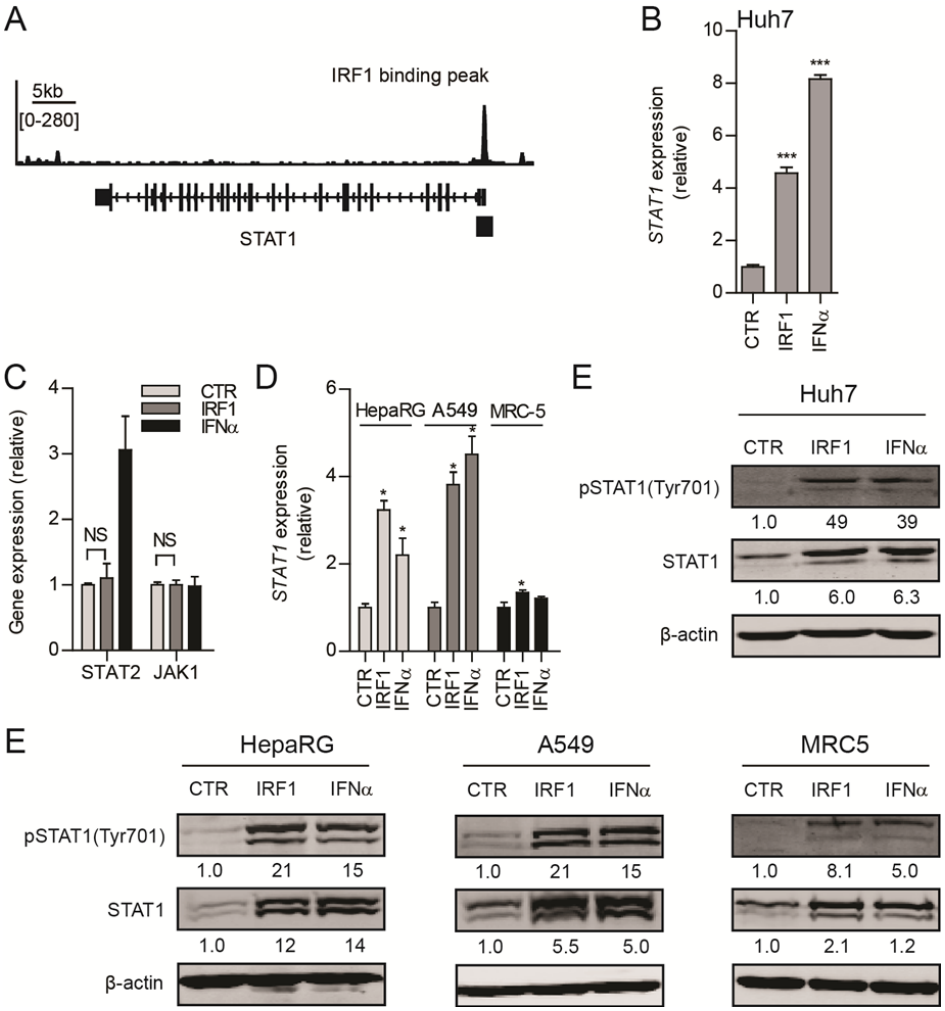

Figure 3. IRF1 activates STAT1 gene transcription leading to enhanced protein expression and phosphorylation.

A) STAT1 genes with IRF1 binding to their promoter regions. The normalized binding signals were used as the input data. Binding peak detection was performed with PeakSeq v1.01 for identifying and ranking peak regions in ChIP-Seq data analysis. The y-axis value represents the binding signaling value; the black bar in the left corner represents the scale (5000 bp). B, C) Real-time qRT-PCR analysis of STAT1 expression (B, n = 8) and STAT2 and JAK1 expression (C, n = 3) in Huh7 cells transduced with IRF1 vector or treated with IFNα (1000 IU/mL) for 48 h. D) Real-time qRT-PCR analysis of STAT1 expression in HepaRG, A549, and MRC5 cells transduced with IRF1 vector or treated with IFNα (1000 IU/mL) for 48 h (n = 5-6). E, F) Immunoblot of Huh7 (E), HepaRG (F), A549 (F) and MRC5 (F) cells overexpressing IRF1 or treated with IFNα (1000 IU/mL) for 48 h. pSTAT1 (Tyr^{701}), STAT1 phosphorylated at the Tyr^{701} site. Data were normalized to Fluc control (CTR, set as 1) (B-D) and are means ± SEM. *P < 0.05; ***P < 0.001; NS, not significant.

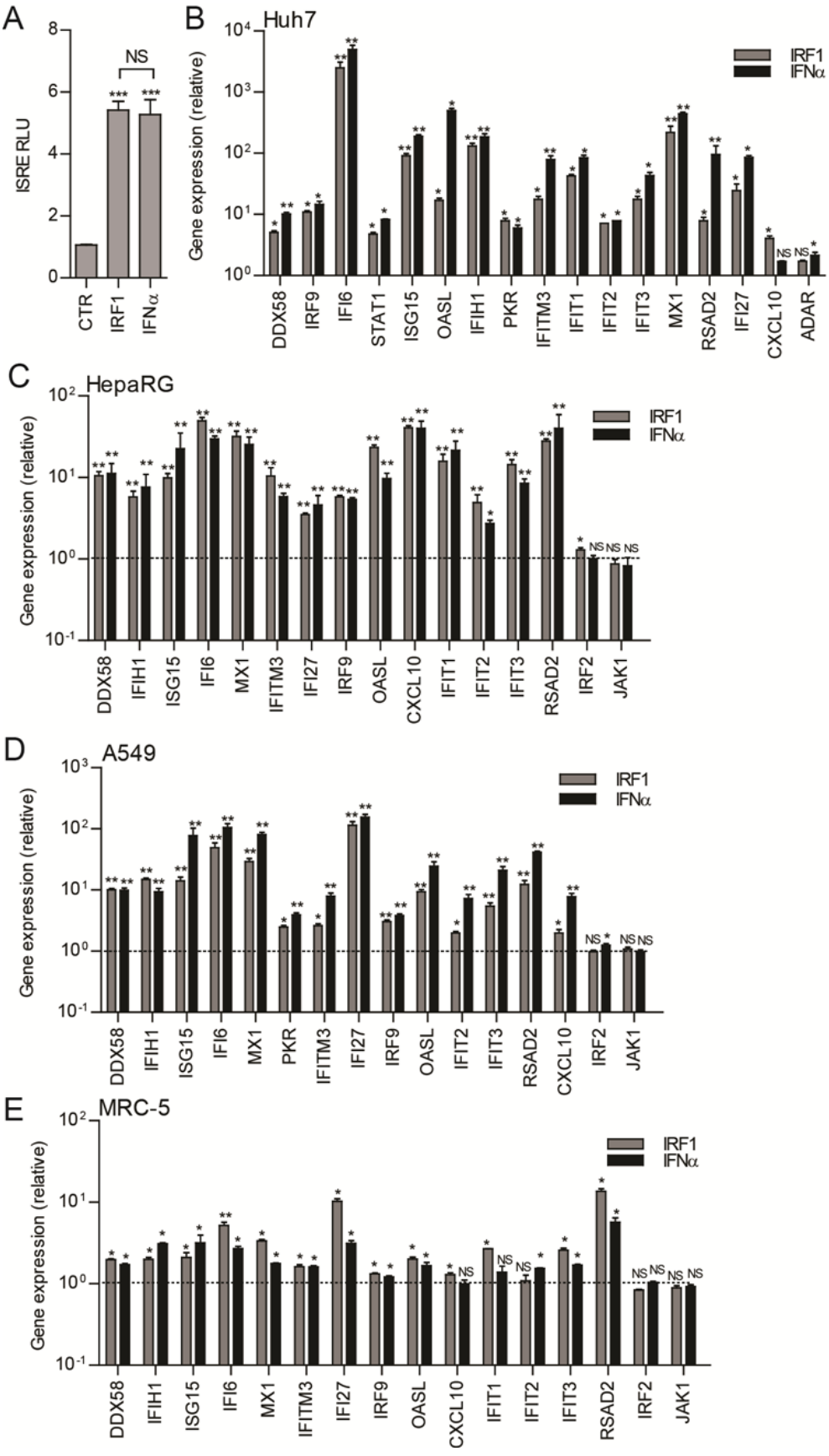

Figure 4. IRF1 activates the expression of ISGs.

A) ISRE promoter-related *firefly* luciferase activity in Huh7-ISRE-Luc model transduced with IRF1 vector or treated with IFNα (1000 IU/mL) for 48 h (n = 4 independent experiments with each of 3 - 4 replicates). B-E) Real-time qRT-PCR analysis of gene expression in Huh7 (B), HepaRG (C), A549 (D), and MRC5 (E) cells transduced with IRF1 or Fluc vector or treated with IFNα (1000 IU/mL) for 48 h (n = 3-5). Data were normalized to GFP (A, CTR, set as 1) or Fluc control (B-E) (set as 1, not shown) and are means ± SEM. *P < 0.05; **P < 0.01; ***P < 0.001; NS, not significant.

Induction of ISGs and anti-HEV of IRF1 relies on STAT1 phosphorylation

JAK1 is the key upstream kinase that dictates STAT1 phosphorylation and the activation of IFN signaling. Activation of STAT1 phosphorylation by IFNα or IRF1 overexpression was almost completely blocked by a pharmacological JAK inhibitor, JAK inhibitor 1 (Fig. 5A). Similarly, JAK inhibitor 1 significantly diminished IRF1- and IFNα-induced ISRE promoter activation (Fig. 5B) and ISG transcription (Fig. 5C, D) without affecting vector delivered IRF1 overexpression (Fig. 5E) and cell viability (Fig. 5F). In line with the abrogation of ISG induction, the anti-HCV and -HEV capability of IRF1 was diminished by JAK inhibitor 1 in an HCV replicon model (Fig. 5G) and in HEV subgenomic and full-length models (Fig. 5H, I). To further validate our observations, another JAK inhibitor, CP-690550 (tofacitinib), was used, and similar results were obtained (Supplemental Fig. S3).

The anti-HEV ability of IRF1 also requires key components of the ISGF3 complex

To further investigate the antiviral ability of IRF1 related to the JAK-STAT pathway, we studied the effects of the ISGF3 complex, which is a downstream element of the JAK-STAT cascade. The ISGF3 complex consists of STAT1, STAT2, and IRF9 and mediates ISG transcription. Gene knockdown of STAT1 (Fig. 6A) significantly promoted HEV replication (Fig. 6B), suggesting a basal defense function of this pathway. When STAT1 was silenced, IRF1- or IFNα-induced ISRE promoter activation was significantly attenuated (Fig. 6C). Consistently, ISG induction as well as anti-HEV effects of IRF1 were significantly attenuated in STAT1-silenced Huh7 cells (Fig. 6D, E). Next, we silenced IRF9, another component of the ISGF3 complex (Fig. 6F). Similarly, HEV replication was also significantly promoted when IRF9 was silenced (Fig. 6G), also suggesting a basal anti-HEV function. Consistently, the depletion of IRF9-attenuated IRF1 induced ISRE promoter activation and ISG expression (Fig. 6H, J). As expected, the antivirals of IRF1 and IFNα were also attenuated (Fig. 6I). These collective results suggest that the ISGF3 complex is necessary for the induction of ISGs and the anti-HEV effect of IRF1.

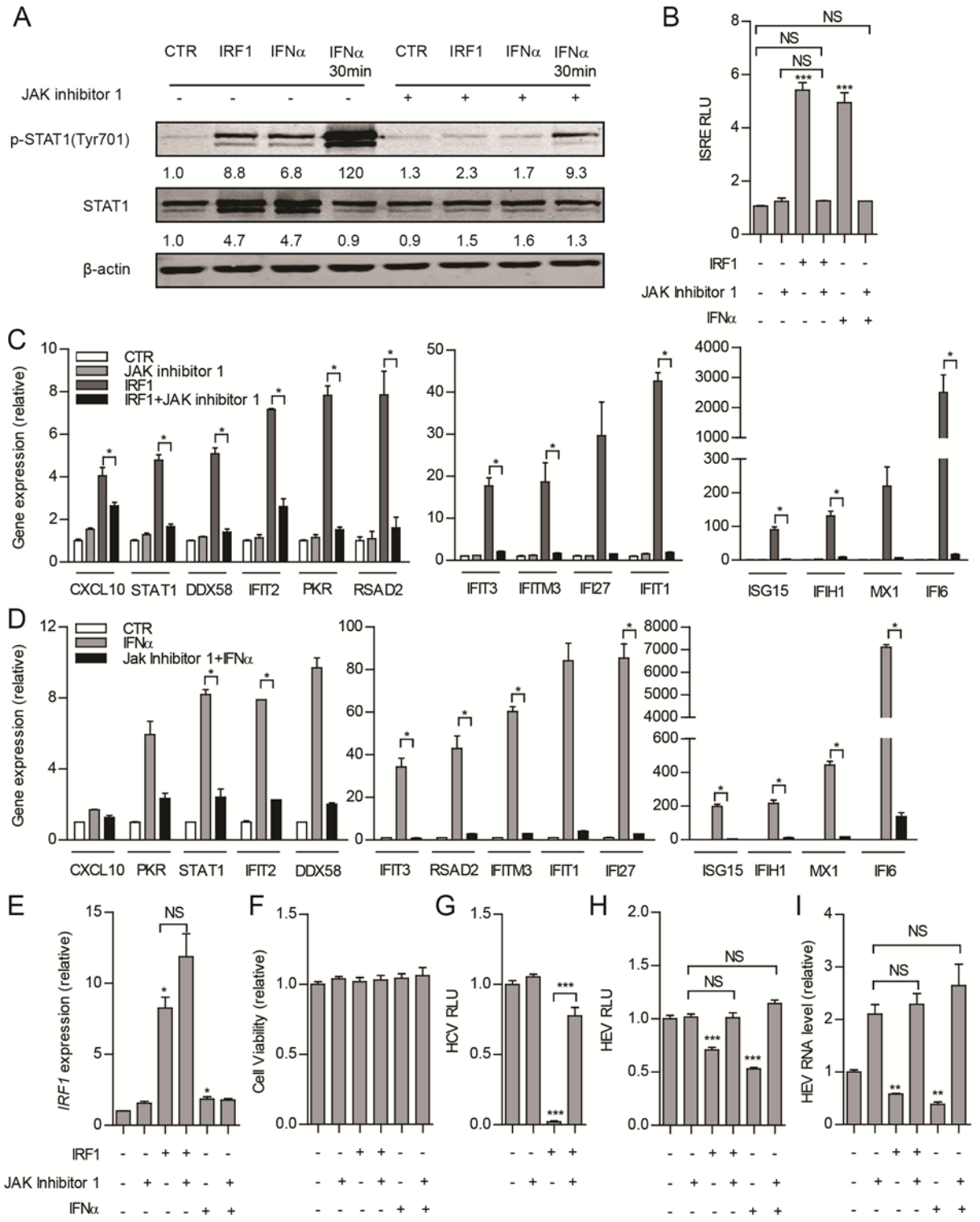

Figure 5. Inhibition of JAK1 diminishes the induction of ISG and the anti-HEV effect of IRF1.

A) Immunoblot analysis of Huh7 cells transduced with IRF1 vector or treated with JAK inhibitor 1 (10 mM) for 48 h or IFNα (1000 IU/mL) for 30 min or 48 h. B) ISRE *firefly* luciferase activity in Huh7-ISRE-Luc model transduced with IRF1 vector or treated with IFNα (1000 IU/mL) or JAK inhibitor 1 (10 mM) for 48 h (n = 4 independent experiments with each of 3 - 4 replicates). C-F) Real-time qRT-PCR analysis of ISG expression (C, n = 6; D, n = 3), IRF1 (E) (n = 4) and MTT assay analysis of cell viability (F) (n = 3 independent experiments with each of 3 - 4 replicates) in an Huh7 cell HEV model transduced with IRF1 vector or treated with IFNα (1000 IU/mL) or JAK inhibitor 1 (10 mM) for 48 h. G-I) HCV viral

replication-related *firefly* luciferase activity in the Huh7-ET-Luc model (G, n = 3 independent experiments with each of 2 - 3 replicates) and HEV-related luciferase activity (H, n = 4 independent experiments with each of 3 - 4 replicates) as well as HEV viral RNA (I, n = 7) in the Huh7-based cell HEV model transduced with IRF1 vector or treated with IFNα (1000 IU/mL) or JAK inhibitor 1 (10 mM) for 48 h. Data were normalized to untreated GFP (B, G) or Fluc (C-F, H, I) control (CTR) (set as 1). Data presented as means ± SEM. *P < 0.05; **P < 0.01; ***P < 0.001; NS, not significant.

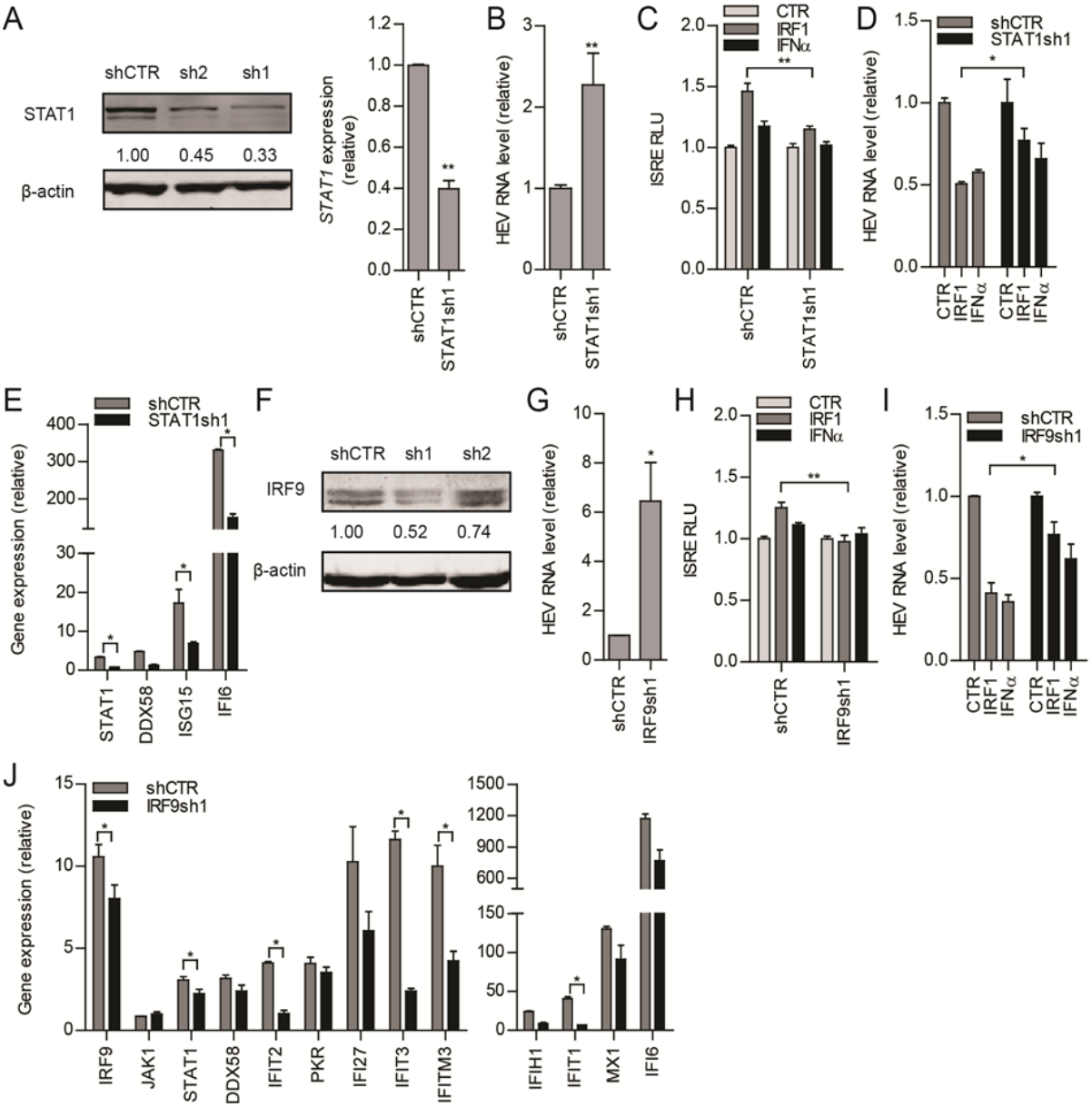

Figure 6. The antiviral function of IRF1 requires key components of the ISGF3 complex.

A) Immunoblot and real-time qRT-PCR analyses (n = 4) of Huh7 cells transduced with lentiviral shRNA vectors that targeting STAT1 or nontargeted control vector shCTR. B) Real-time qRT-PCR analysis of HEV viral RNA in Huh7-p6 model with STAT1 knockdown relative to shCTR (n = 4). Data were normalized to shCTR control (A, B). C) ISRE *firefly* luciferase activity in STAT1 knockdown Huh7-ISRE-Luc cells transduced with IRF1 vector (stock with 100 times dilution) or treated with IFNα (1 IU/mL) (n = 3 independent experiments with each of 4 replicates). D) Real-time qRT-PCR analysis of HEV viral RNA in STAT1-knockdown Huh7-p6 model transduced with IRF1 vector or treated with IFNα (1000 IU/mL) for 48 h (n = 6). Data were normalized to untreated shCTR or STAT1sh1 cells, respectively (both set as 1) (C, D). E) Real-time qRT-PCR analysis of gene expression in STAT1 knockdown or shCTR

cells transduced with IRF1 or Fluc vector for 48 h (n = 4). Data were normalized to shCTR cells that transduced Fluc vector (set as 1, not shown). F) Immunoblot analysis of Huh7 cells transduced with lentiviral shRNA vectors that target IRF9 or nontargeted control vector shCTR. G) Real-time qRT-PCR analysis of HEV viral RNA in Huh7-p6 model with IRF9 knockdown relative to shCTR (n = 4). H) ISRE *firefly* luciferase activity in IRF9 knockdown Huh7-ISRE-Luc model transduced with IRF1 vector (stock with 1003 dilution) or treated with IFNα (1 IU/mL) (n = 3 independent experiments with each of 3 replicates). Data were normalized to untreated shCTR and IRF9sh1 cells (both set as 1). I) Real-time qRT-PCR analysis of HEV viral RNA and gene expression (J) in IRF9 knockdown Huh7-p6 model transduced with IRF1 vector or treated with IFNα (1000 IU/mL) for 48 h (n = 5). Data were normalized to untreated shCTR and IRF9sh1 cells (both set as 1) and are means ± SEM (H-J). *P < 0.05; **P < 0.01; ***P < 0.001; NS, not significant.

The induction of ISGs and the anti-HEV effect of IRF1 overlaps with IFNα but is potentiated by ribavirin

We observed that the patterns of ISG induction by IFNα and IRF1 correlated highly, suggesting a potential overlap of these two anti-HEV mechanisms (Fig. 7A). Gene knockdown of IRF1 did not impair the IFNα-mediated anti-HEV effect (Fig. 7B) and ISG induction (Fig. 7C, D). Furthermore, combined IFNα and IRF1 overexpression did not yield additional induction of STAT1 and IRF1 expression (Fig. 7E, F) or additional anti-HEV activity (Fig. 7G, H). These results suggest that IFNα and IRF1 converged in the JAK-STAT pathway to exert anti-HEV effects.

One study showed that ribavirin potentiates an antiviral IFN response by augmenting ISG induction [29]. Thus, we tested the combined effect of ribavirin and IRF1 overexpression on ISG induction. Consistent with the previous study, we observed that ribavirin alone could up-regulate several ISGs. In contrast to IFNα, ribavirin further promoted IRF1-induced ISG expression including IRF1 in Huh7 cells (Fig. 8A). Furthermore, ribavirin also enhanced the ISG induction and anti-HEV ability of IRF1 in HepaRG, A549, and MRC5 cells (Supplemental Fig. S4A-C). More important, the combination of ribavirin and IRF1 further augmented their anti-HCV and -HEV effects (Fig. 8B-D). Overall, these results indicate that the induction of ISGs and the anti-HEV effect of IRF1 overlaps with IFNα but is potentiated by ribavirin (Fig. 9).

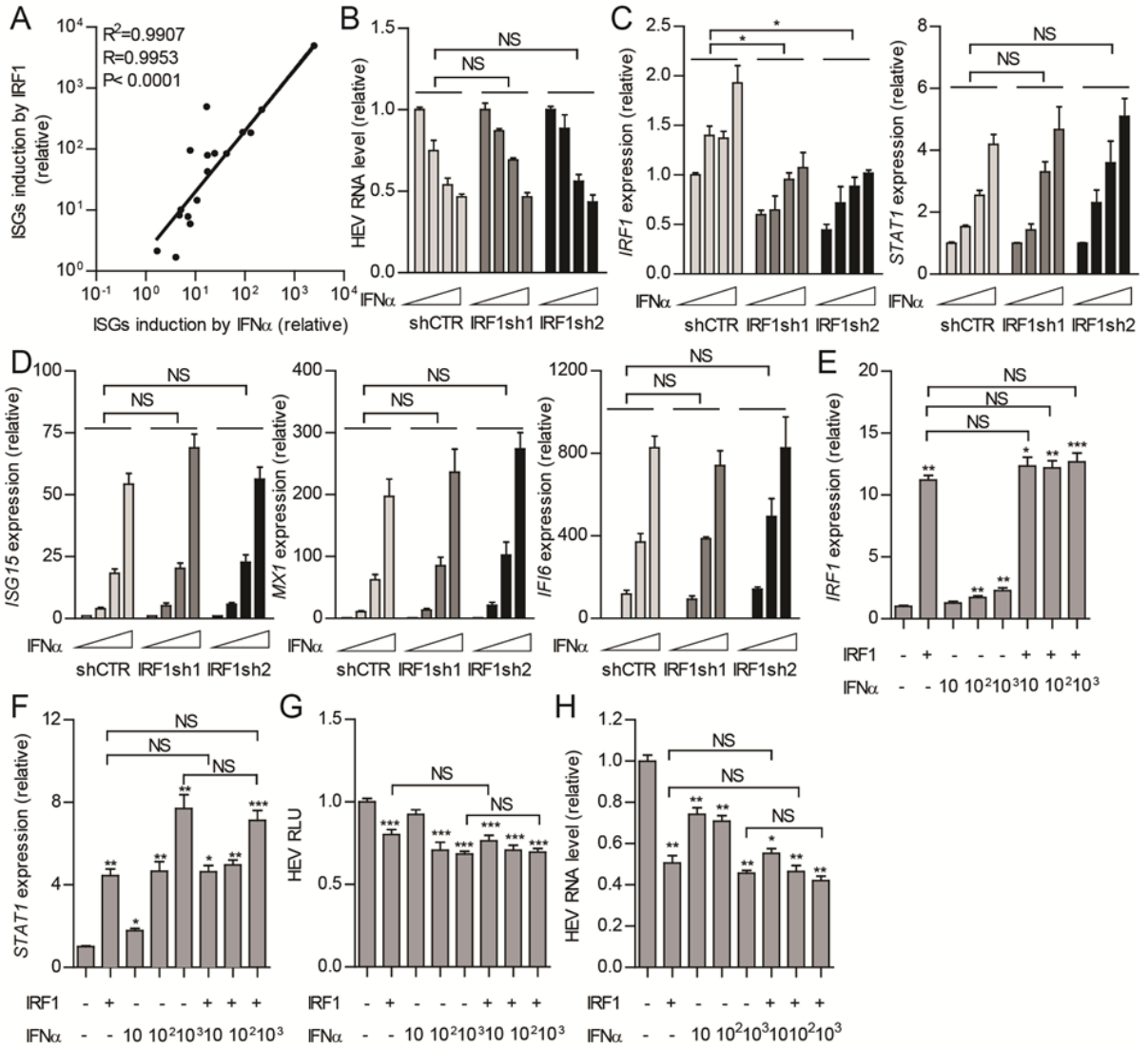

Figure 7. The induction of ISGs and the anti-HEV action of IRF1 overlaps with IFNα.

A) Correlation analysis of ISG expression in Huh7 cells transduced with IRF1 vector or treated with IFNα (1000 IU/mL) for 48 h. Data were normalized to Fluc control (set as 1) and were analyzed by the 2-tailed Pearson correlation method. B) Real-time qRT-PCR analysis of HEV viral RNA in IRF1-knockdown cells treated with IFNα (10, 100, or 1000 IU/mL) for 48 h (shCTR: n = 4; IRF1sh1 and -2: n = 3). Data were normalized to untreated shCTR, IRF1sh1, or IRF1sh2 cells, respectively (all set as 1). C, D) Real-time qRT-PCR analysis of IRF1 and STAT1 (C) and ISG15, MX1, and IFI6 (D) expression in IRF1-knockdown Huh7 cells treated with IFNα (10, 100, or 1000 IU/mL) for 48 h (n = 3). IRF1 expression was normalized to untreated shCTR (set as 1). STAT1, ISG15, MX1, and IFI6 expression was normalized to untreated shCTR, IRF1sh1, and IRF1sh2 cells, respectively (all set as 1). G-H) Real-time qRT-PCR analysis of IRF1 (E, n = 5), STAT1 (F, n = 5), and HEV viral RNA (H, n = 6) expression and HEV-related luciferase activity (G, n = 3 independent experiments with each of 2-4 replicates) in the Huh7-p6-Luc model transduced with IRF1 vector or treated with different doses of IFNα (10, 100, and 1000 IU/mL) for 48 h. Data were normalized to Fluc control without IFNα treatment (set as 1) and are means ± SEM (E-H). *P < 0.05; **P < 0.01; ***P < 0.001; NS, not significant.

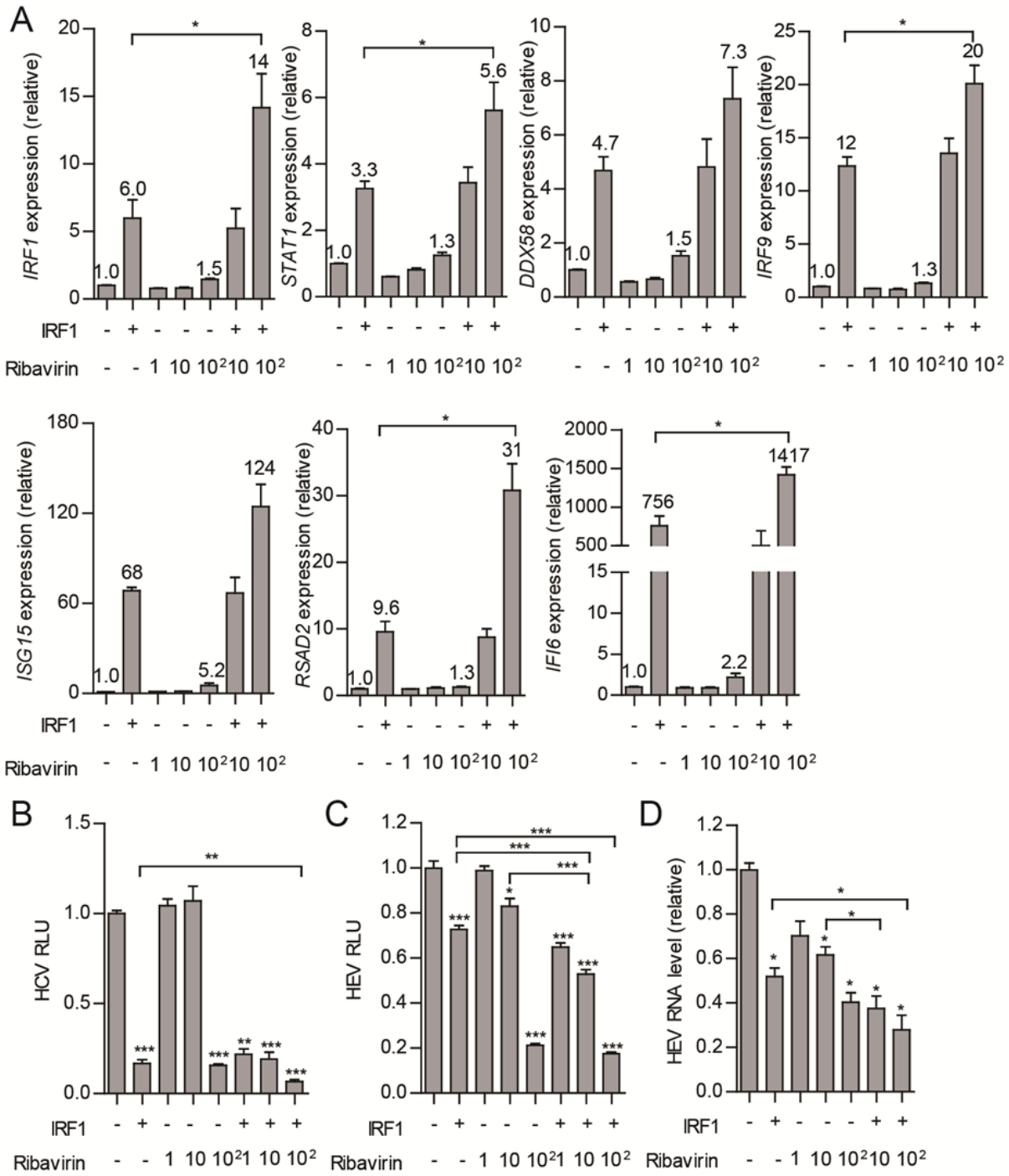

Figure 8. Ribavirin potentiates IRF1-mediated ISG induction and anti-HEV activity.

A) Real-time qRT-PCR analysis of IRF1, STAT1, DDX58, RSAD2, ISG15, IRF9, and IFI6 expression in Huh7 cells transduced with IRF1 vector or treated with ribavirin (1, 10, or 100 mM) for 48 h (n = 5). B) HCV-related luciferase activity in Huh7-ET-Luc model and transduced with IRF1 vector (stock with 503 dilution) or treated with ribavirin (1, 10, or 100 mM) for 48 h (n = 3 independent experiments with each of 4 replicates). C) HEV-related luciferase activity in Huh7-p6-Luc model and transduced with IRF1 vector or treated with ribavirin (1, 10, or 100 mM) for 48 h (n = 3 independent experiments with each of 4 replicates) and real-time qRT-PCR analysis of HEV viral RNA in Huh7-p6 model transduced with IRF1 vector or treated with ribavirin for 48 h (n = 5). Data were normalized to GFP (B) or Fluc (A, C, D) control without ribavirin treatment (set as 1). Data are means ± SEM.*P < 0.05; **P < 0.01; ***P < 0.001; NS, not significant.

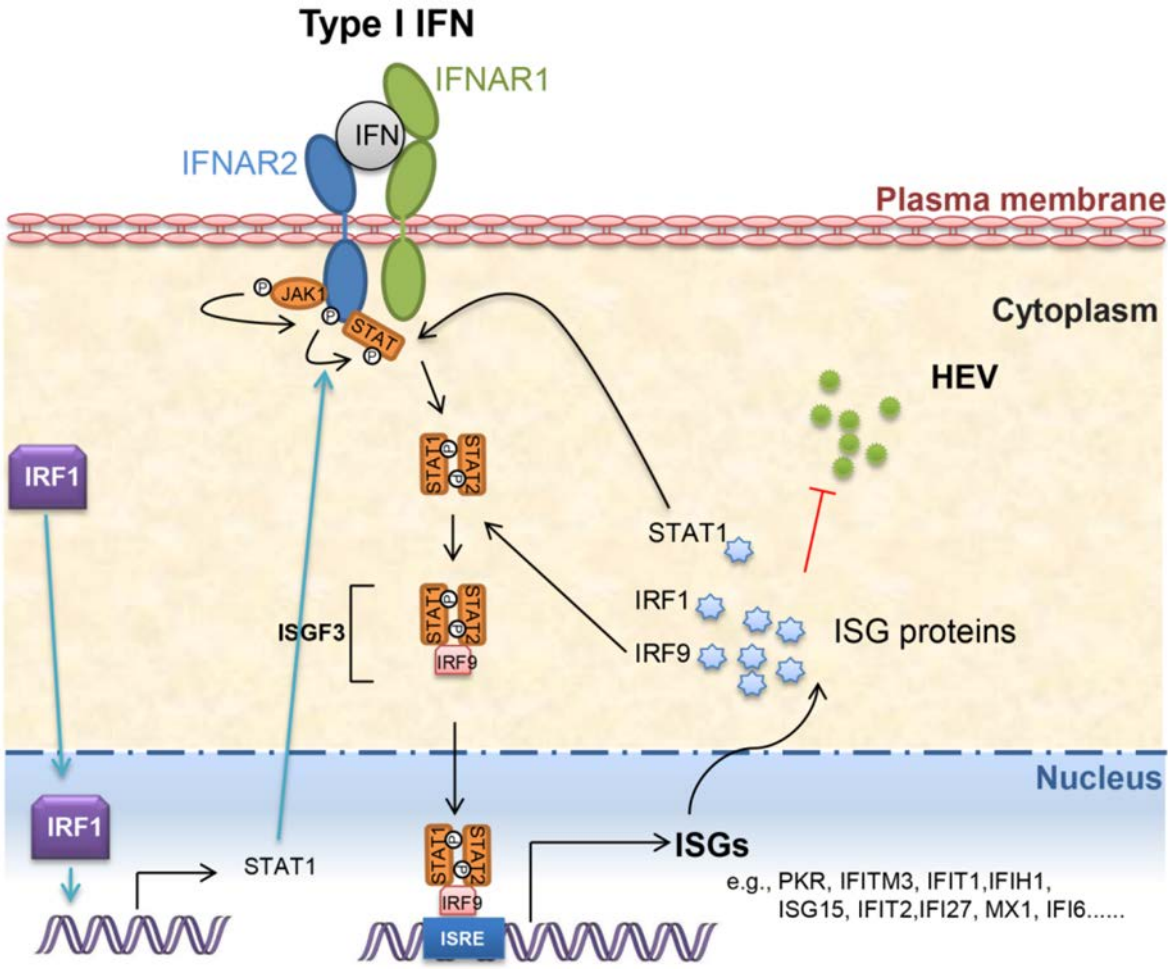

Figure 9. IRF1 restricts HEV replication by activating STAT1 to induce the expression of ISGs.

IRF1 could induce the expression of STAT1. The induction of STAT1 expression further activated the transcription of a panel of downstream antiviral ISGs. The production of these ISGs could inhibit HEV replication.

Discussion

Innate immunity is the frontier in the battle against viral pathogens [30]. The activation of innate immune response relies on the recognition of pathogens by specific pattern recognition receptors (*e.g.,* Toll-like, RIG-I-like, and NOD like receptors) [31], leading to the production of cytokines and chemokines such as IFNs. IFN triggers transcription of hundreds of ISGs through the JAK-STAT pathway. The products of these ISGs ultimately exert antiviral functions [30]. Several recent studies have focused on the characterization of individual ISGs, with respect to their antiviral efficacy and potential mechanism of action [32-34]. Two large-scale screening studies unexpectedly showed that only a small subset of ISGs have antiviral effects and some even have proviral effects on certain viruses [10, 11]. Among more than 380 tested ISGs, IRF1 was one of the strongest antiviral agents against a broad spectrum of

viruses. In this study, we found IRF1 to be basally expressed in liver cells and to confer resistance to HEV infection. Ectopic overexpression of IRF1 effectively inhibits HEV replication, as shown in multiple cellular systems.

Although IRF1 has been reported to induce the expression of some ISGs similar to type I IFNs [10, 11], the exact antiviral mechanism of IRF1 remains largely elusive. It has been reported that IRF1 could act as a transcription factor that activates either IFNβ gene expression in virus infected fibroblasts [24] or IFNα gene expression in uninfected cells [35]. Therefore, we initially hypothesized that the anti-HEV effect of IRF1 may act via the induction of IFN production in the cell model. However, we convincingly demonstrated that HEV cell models including a human hepatoma cell line (Huh7), primary human hepatocyte-like cell line (HepaRG), human lung epithelial carcinoma cell line (A549), and human fetal lung fibroblast cell line (MRC-5) do not produce IFNs upon IRF1 overexpression by both gene expression and functional assays. Our observation in this respect is consistent with a previous study showing that the Huh7 cell line responds to IFN but does not produce IFN [36]. Furthermore, microarray analysis has shown that no IFN genes were up-regulated in IRF1-overexpressing Huh7 cells [11].

IFNα was widely used to treat chronic HBV and HCV infection [28]. In some cases, IFNα was also used to treat chronic HEV infection [9]. In our previous study, we demonstrated that IFNα had moderate and delayed anti-HEV effects in cell culture models and IFNβ/α/γ did not show a notable antiviral effect on HEV replication [37]. Similarly, Todt et al. [38] reported a weak to moderate inhibition of HEV replication by different types of IFNs. Our study demonstrated that IRF1 could effectively inhibit HEV replication without triggering IFN production in host cells. This finding may provide new ideas for developing anti-HEV strategies. Surprisingly, both studies demonstrated that HEV could down-regulate ISG expression induced by different IFN types [37, 38]. These observations suggest that some HEV strategies would subvert host antiviral defenses. Consistently, we observed that IRF1 was induced at the early stage in most cell lines (Supplemental Fig. S2A, B). This result indicates that, after the infection is established, HEV can suppress the immune response elicited by itself.

Given the fact that IRF1 is also a transcription factor and has more than 200 binding sites in the human genome [27], we have explored this scenario to understand its anti-HEV mechanism of action. Indeed, the IRF1 data retrieved from the ChIP-seq database revealed

that IRF1 could directly bind to the promoter region of the STAT1 gene. Consistently, our functional assay demonstrated that IRF1 could drive the transcription of STAT1, resulting in protein expression and phosphorylation Tyr^{701} site, which is an indispensable marker of STAT1 activation. Correspondingly, the IRF1 induced STAT1 phosphorylation leading to the transcription of a series of individual ISGs. We further showed that ISG induction and anti-HEV ability of IRF1 rely heavily on STAT1 phosphorylation. Furthermore, the integrity of the ISFG3 complex is also required. Although previous study has reported the induction of some ISGs in STAT1-deficient fibroblasts by IRF1 [11], this finding may indicate that there are multiple mechanisms mediating the function of IRF1, including STAT1-dependent or -independent mechanisms, probably depending on the cell type and particular circumstances. In this study, we reported a new antiviral mechanism of IRF1 by inducing the expression and phosphorylation of STAT1 without triggering IFN production. This process subsequently activated the JAK-STAT pathway to transcribe antiviral ISGs. It would be interesting to address the relevance of this mechanism in IRF1-mediated effects on other viruses.

Because IRF1 and IFNα converged in the JAK-STAT cascade to drive ISG transcription, we further evaluated the combinatory effects of IFNα and IRF1. As expected, combination of IFNα and IRF1 did not further promote ISG induction and anti-HEV activities. In contrast, IFNα and ribavirin have moderately synergistic anti-HEV effects in 2 HEV cell-culture replication models [39]. As a broad antiviral agent [40], ribavirin can potentiate IFN by augmenting ISG induction in an HCV culture model, which is mediated by a novel mechanism different from the classic IFN or intracellular RNA sensing pathways [29]. In this study, we also tested the combined effects of IRF1 and ribavirin, and ribavirin further enhanced IRF1-induced ISG expression. More important, combination of IRF1 and ribavirin reinforced ISG induction and its anti-HEV effects, although the exact mechanism remains to be further investigated.

In summary, we characterized IRF1 as an important host factor that effectively inhibits HEV replication. Mechanistically, without triggering IFN production in host cells, IRF1 activates gene transcription of STAT1, which subsequently enhances its protein expression and phosphorylation to stimulate antiviral ISG transcription. Furthermore, the induction of ISGs and the anti-HEV effect of IRF1 overlapped IFNα but were potentiated by ribavirin. Thus, this study has shed new light on the molecular insight into an important anti- HEV ISG, which

may help in understanding the complexity of HEV-host interactions and in developing new antiviral strategies.

Acknowledgments

The authors thank Dr. Charles M. Rice (Rockefeller University, New York, NY, USA) for generously providing the overexpressing lentiviral vector; Dr. Suzanne U. Emerson (National Institutes of Health, National Institute of Allergy and Infectious Diseases, Bethesda, MD, USA) for generously providing the plasmids to generate subgenomic and full-length HEV genomic RNA; Prof. Ralf Bartenschlager and Dr. Volker Lohmann (University of Heidelberg, Heidelberg, Germany) for providing the HCV replicon cells, and Dr. Steve Ralph (Griffith University, Southpost, QLD, Australia) for generously providing the full-length STAT1 promoter luciferase plasmids. This research was supported by the European Association for the Study of the Liver (EASL), Sheila Sherlock Fellowship (to Q. P.); The Netherlands Organization for Scientific Research (NWO/ZonMw) Veni Grant 916-13-032) (to Q. P.); the Dutch Digestive Foundation (MLDS) Career Development Grant (CDG) 1304 (to Q. P.); an Daniel den Hoed Foundation Centennial Award Fellowship (to Q. P.), an Erasmus MC Medical Research Advisory Committee (MRace) grant (to Q. P.) and the China Scholarship Council Ph.D. Fellowships Grants 201306300027 (to L. X.), 201206150075 (to X. Z.), 201303250056 (to W. W.), 201207720007 (to Y. W.) and 201307720045 (to Y. Y.). The authors declare no conflicts of interest.

Author contributions

L. Xu contributed to the study concept and design, acquisition of data, analysis and interpretation of data, drafting of the manuscript, and statistical analysis; X. Zhou, W. Wang, Y. Wang, and Y. Yin contributed to acquisition of data and critical revision of the manuscript; L. J. W. van der Laan D. Sprengers, and H. J. Metselaar contributed to study concept and critical revision of the manuscript; M. P. Peppelenbosch contributed to study concept, study supervision and critical revision of the manuscript; and Q. Pan contributed to study concept and design, obtained funding, study supervision, and critical revision of the manuscript.

Supplementary Figures

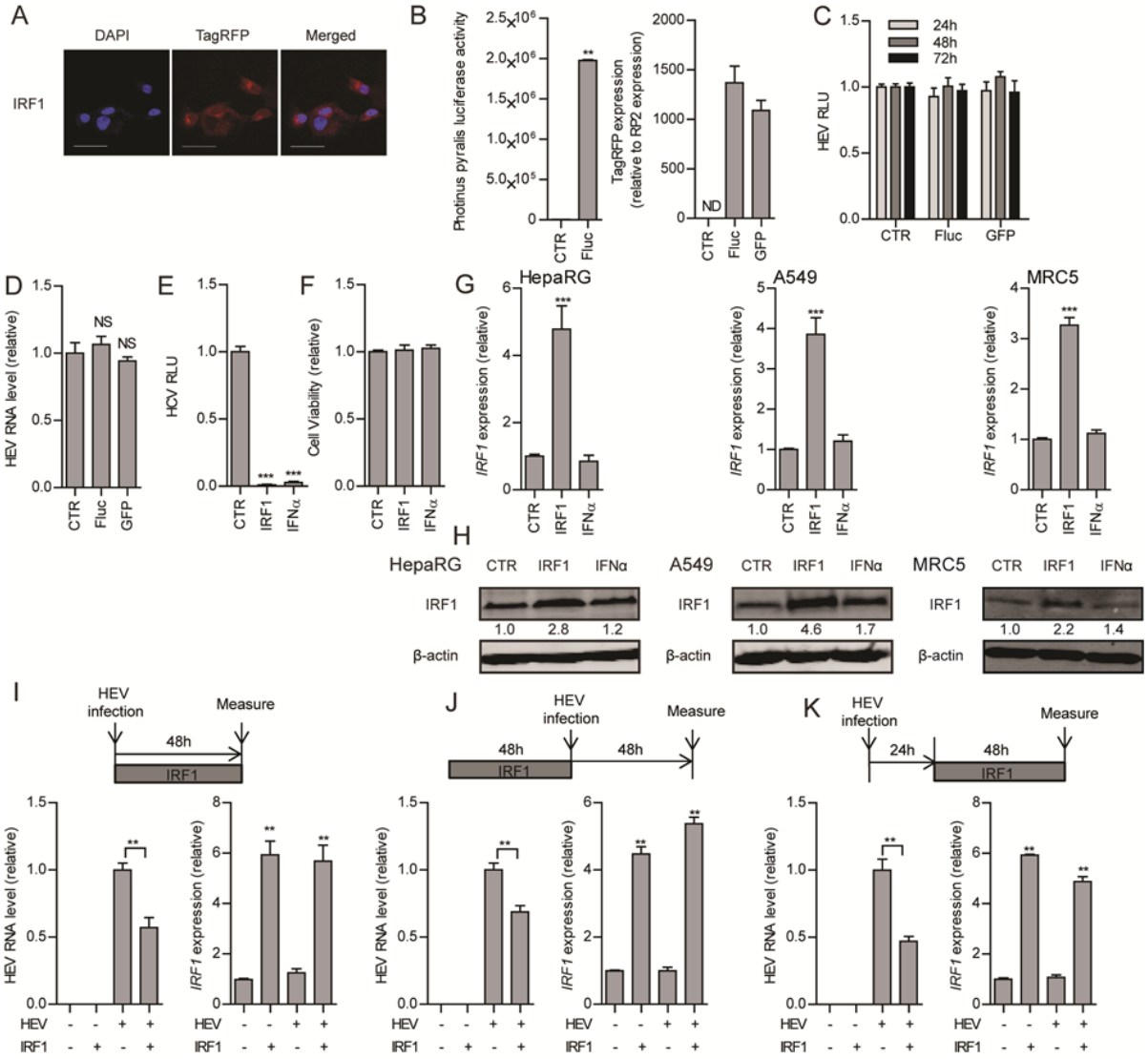

Fig. S1. Over-expression of control vectors does not affect HEV replication.

(A) Fluorescent microscopic analysis of Huh7 cells transduced with TagRFP-IRF1 lentiviral vector for 48 h. Red indicates TagRFP and blue indicates DAPI (Scale bar: 50 μm). (B) *Photinus pyralis* luciferase activity (n = 4-8) and qRT-PCR analysis of TagRFP mRNA expression (n = 3) in Huh7 cells transduced with Fluc, GFP vector or untreated (CTR) for 48 h. HEV viral replication-related *Gaussia* luciferase activity in Huh7-p6-Luc model (C) transduced with GFP, Fluc vector or untreated (CTR) for 24 h, 48 h and 72 h (n = 3 independent experiments with each of 2 - 3 replicates) and qRT-PCR analysis of HEV viral RNA in Huh7-p6 full-length HEV model (D) transduced for 48 h (n = 3). RLU: relative luciferase unit. HCV-related *firefly* luciferase activity in Huh7-ET-Luc model (E) (n = 4 independent experiments with each of 3 - 4 replicates) and MTT assay analysis of cell viability in Huh7 cells (F) (n = 3 independent experiments with each of 3 - 4 replicates) transduced with IRF1, GFP vector or treated with IFNα (1000 IU/mL) for 48 h. qRT-PCR analysis (G, n = 6) or immunoblotting analysis (H) of HepaRG cells, A549 cells and MRC5 cells transduced with IRF1, Fluc vector or treated with IFNα (1000 IU/mL) for 48 h. (I, J, K) qRT-PCR analysis of HEV and IRF1 expression in Huh7 cells transduced with IRF1 or infected by HEV at indicted time point. Date presented as mean ± SEM (*, $P < 0.05$; **, $P < 0.01$; ***, $P < 0.001$; NS, not significant).

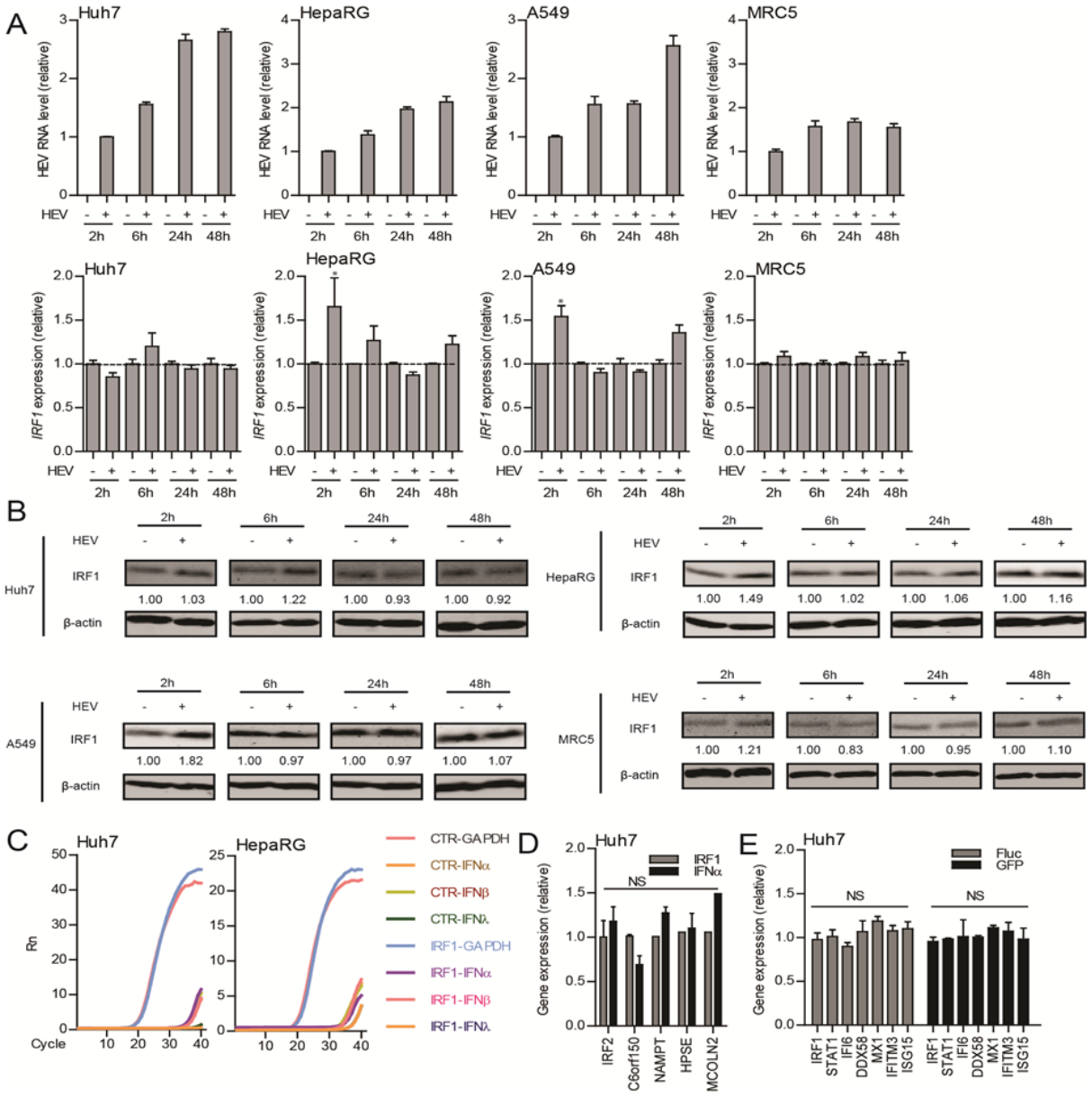

Fig. S2. HEV infection induces IRF1 expression in some cell lines.

qRT-PCR analysis (A, n = 5) and immunoblotting analysis (B) of Huh7, HepaRG, A549 and MRC5 cells infected by HEV for 6 h (For 2 h post infection, cells were incubated with HEV for 2 hours and then cells were lysed). At different time point post HEV infection (2 h, 6 h, 24 h or 48 h post infection), HEV RNA and IRF1 expression level was quantified. HEV RNA level was normalized to 2 h post infection. IRF1 mRNA level and protein level was normalized to un-infected cells at each time point. (C) Plot of qRT-PCR analysis of interferon gene expression in Huh7 and HepaRG cells transduced with IRF1 or Fluc (CTR) vector for 48 h. Rn: Fluorescence signal from the reporter dye normalized to that from the negative control. (D) qRT-PCR analysis of gene expression in Huh7 cells transduced with IRF1 vector or treated with IFNα (1000 IU/mL) for 48 h. (E) qRT-PCR analysis of gene expression in Huh7 cells transduced with GFP, Fluc vector or untreated for 48 h (n = 3). Data was normalized to untreated control (CTR, set as 1, not shown). Date presented as mean ± SEM (*, $P < 0.05$; NS, not significant).

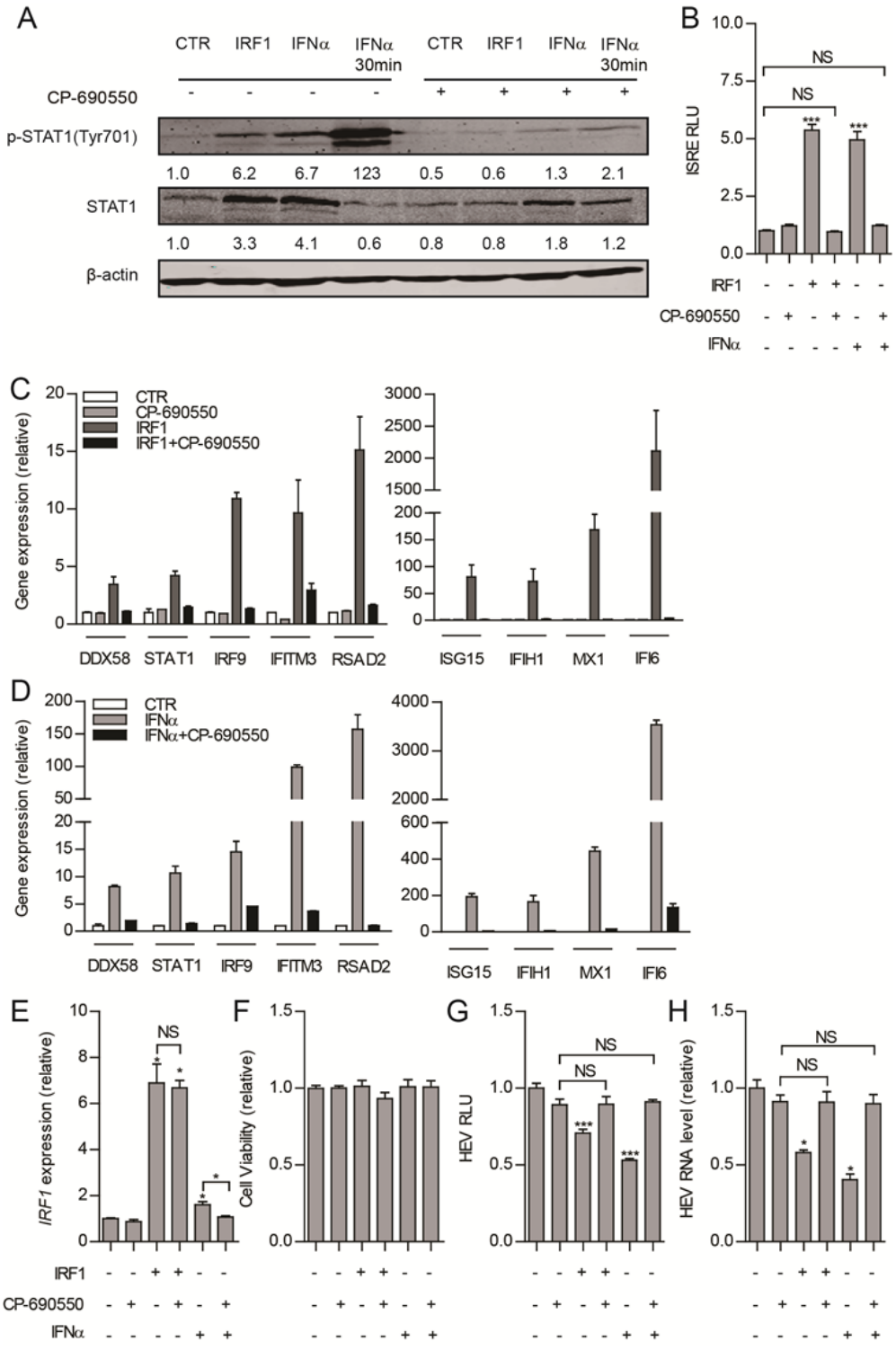

Fig. S3. JAK inhibitor, CP-690550 diminishes the induction of ISG and the anti-HEV effect of IRF1.

(A) Immunoblotting analysis of Huh7 cells transduced with IRF1 vector or treated with CP-690550 (1000 ng/mL) for 48 h or IFNα (1000 IU/mL) for 30 min or 48 h. (B) ISRE *firefly* luciferase activity in Huh7-ISRE-Luc model transduced with IRF1 vector or treated with IFNα (1000 IU/mL) or CP-690550 (1000 ng/mL) for 48 h (n = 4 independent experiments with each of 3 - 4 replicates). qRT-PCR analysis of ISG expression (C, n = 4; D, n = 3), IRF1 (E, n = 5) and MTT assay analysis of cell viability (F, n = 3 independent experiments with each of 3 - 4 replicates) in Huh7 cell HEV model transduced with IRF1 vector or treated with IFNα (1000 IU/mL) or CP-690550 (1000 ng/mL) for 48 h. HEV-related luciferase activity (G, n = 4 independent experiments with each of 4 replicates) and HEV viral RNA (H, n = 6) in Huh7-based cell HEV model transduced with IRF1 vector or treated with IFNα (1000 IU/mL) or CP-690550 (1000 ng/mL) for 48 h. Data was normalized to untreated GFP (B) or Fluc (C, D, E, F and H) control (CTR, set as 1). Date presented as mean ± SEM (*, P < 0.05; **, P < 0.01; ***, P < 0.001; NS, not significant).

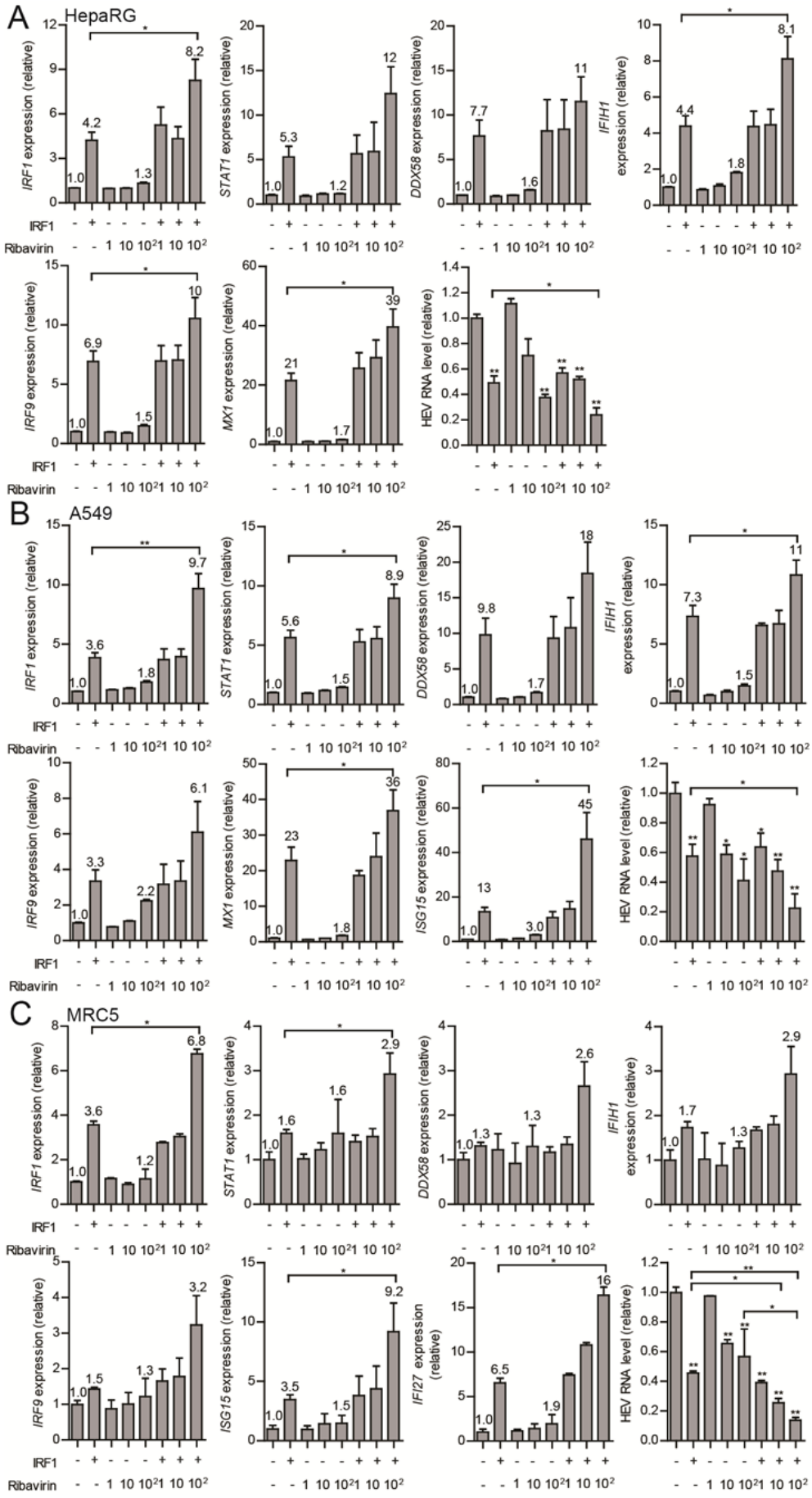

Fig. S4. Ribavirin potentiates IRF1-mediated ISG induction and anti-HEV activity in different cell lines.

qRT-PCR analysis of *IRF1, STAT1, DDX58, IFIH1, ISG15, IRF9, IFI27, MX1* expression and HEV viral RNA level in HepaRG-p6 model (A), A549-p6 model (B) and HEV infected MRC5 cells (C) transduced with IRF1 vector or treated with ribavirin (1, 10 or 100 µM) for 48 h (n = 4-6). Date presented as mean ± SEM (*, P < 0.05; **, P < 0.01; ***, P < 0.001; NS, not significant).

References

1. Dalton, H.R., Hepatitis: hepatitis E and decompensated chronic liver disease. *Nat Rev Gastroenterol Hepatol*, 2012. **9**(8): p. 430-2.
2. Kamar, N., et al., Hepatitis E. *Lancet*, 2012. **379**(9835): p. 2477-88.
3. Behrendt, P., et al., The impact of hepatitis E in the liver transplant setting. *J Hepatol*, 2014. **61**(6): p. 1418-29.
4. Zhou, X., et al., Epidemiology and management of chronic hepatitis E infection in solid organ transplantation: a comprehensive literature review. *Rev Med Virol*, 2013. **23**(5): p. 295-304.
5. Melchjorsen, J., Learning from the messengers: innate sensing of viruses and cytokine regulation of immunity - clues for treatments and vaccines. *Viruses*, 2013. **5**(2): p. 470-527.
6. Sen, G.C., Viruses and interferons. *Annu Rev Microbiol*, 2001. **55**: p. 255-81.
7. Fried, M.W., et al., Peginterferon alfa-2a plus ribavirin for chronic hepatitis C virus infection. *N Engl J Med*, 2002. **347**(13): p. 975-82.
8. Janssen, H.L., et al., Pegylated interferon alfa-2b alone or in combination with lamivudine for HBeAg-positive chronic hepatitis B: a randomised trial. *Lancet*, 2005. **365**(9454): p. 123-9.
9. Peters van Ton, A.M., T.J. Gevers, and J.P. Drenth, Antiviral therapy in chronic hepatitis E: a systematic review. *J Viral Hepat*, 2015. **22**(12): p. 965-73.
10. Schoggins, J.W., et al., Pan-viral specificity of IFN-induced genes reveals new roles for cGAS in innate immunity. *Nature*, 2014. **505**(7485): p. 691-5.
11. Schoggins, J.W., et al., A diverse range of gene products are effectors of the type I interferon antiviral response. *Nature*, 2011. **472**(7344): p. 481-5.
12. Xie, M., et al., Human cytomegalovirus exploits interferon-induced transmembrane proteins to facilitate morphogenesis of the virion assembly compartment. *J Virol*, 2015. **89**(6): p. 3049-61.
13. Gripon, P., et al., Infection of a human hepatoma cell line by hepatitis B virus. *Proc Natl Acad Sci U S A*, 2002. **99**(24): p. 15655-60.
14. Pan, Q., et al., Combined antiviral activity of interferon-alpha and RNA interference directed against hepatitis C without affecting vector delivery and gene silencing. *J Mol Med (Berl)*, 2009. **87**(7): p. 713-22.
15. Pan, Q., et al., Mycophenolic acid augments interferon-stimulated gene expression and inhibits hepatitis C Virus infection in vitro and in vivo. *Hepatology*, 2012. **55**(6): p. 1673-83.
16. Shukla, P., et al., Adaptation of a genotype 3 hepatitis E virus to efficient growth in cell culture depends on an inserted human gene segment acquired by recombination. *J Virol*, 2012. **86**(10): p. 5697-707.
17. Shukla, P., et al., Cross-species infections of cultured cells by hepatitis E virus and discovery of an infectious virus-host recombinant. *Proc Natl Acad Sci U S A*, 2011. **108**(6): p. 2438-43.
18. Dong, C., et al., Suppression of interferon-alpha signaling by hepatitis E virus. *Hepatology*, 2012. **55**(5): p. 1324-32.
19. Debing, Y., et al., A mutation in the hepatitis E virus RNA polymerase promotes its replication and associates with ribavirin treatment failure in organ transplant recipients. *Gastroenterology*, 2014. **147**(5): p. 1008-11 e7; quiz e15-6.
20. Zhou, X., et al., Rapamycin and everolimus facilitate hepatitis E virus replication: revealing a basal defense mechanism of PI3K-PKB-mTOR pathway. *J Hepatol*, 2014. **61**(4): p. 746-54.
21. Engelen, E., et al., Proteins that bind regulatory regions identified by histone modification chromatin immunoprecipitations and mass spectrometry. *Nat Commun*, 2015. **6**: p. 7155.
22. Zhang, Y., et al., Model-based analysis of ChIP-Seq (MACS). *Genome Biol*, 2008. **9**(9): p. R137.
23. Robinson, J.T., et al., Integrative genomics viewer. *Nat Biotechnol*, 2011. **29**(1): p. 24-6.
24. Miyamoto, M., et al., Regulated expression of a gene encoding a nuclear factor, IRF-1, that specifically binds to IFN-beta gene regulatory elements. *Cell*, 1988. **54**(6): p. 903-13.

25. Hornung, V., et al., 5'-Triphosphate RNA is the ligand for RIG-I. *Science*, 2006. **314**(5801): p. 994-7.
26. Frese, M., et al., Hepatitis C virus RNA replication is resistant to tumour necrosis factor-alpha. *J Gen Virol*, 2003. **84**(Pt 5): p. 1253-9.
27. Frontini, M., et al., A ChIP-chip approach reveals a novel role for transcription factor IRF1 in the DNA damage response. *Nucleic Acids Res*, 2009. **37**(4): p. 1073-85.
28. Schneider, W.M., M.D. Chevillotte, and C.M. Rice, Interferon-stimulated genes: a complex web of host defenses. *Annu Rev Immunol*, 2014. **32**: p. 513-45.
29. Thomas, E., et al., Ribavirin potentiates interferon action by augmenting interferon-stimulated gene induction in hepatitis C virus cell culture models. *Hepatology*, 2011. **53**(1): p. 32-41.
30. Schoggins, J.W. and C.M. Rice, Interferon-stimulated genes and their antiviral effector functions. *Curr Opin Virol*, 2011. **1**(6): p. 519-25.
31. O'Neill, L.A. and A.G. Bowie, Sensing and signaling in antiviral innate immunity. *Curr Biol*, 2010. **20**(7): p. R328-33.
32. Jiang, D., et al., Identification of three interferon-inducible cellular enzymes that inhibit the replication of hepatitis C virus. *J Virol*, 2008. **82**(4): p. 1665-78.
33. Brass, A.L., et al., The IFITM proteins mediate cellular resistance to influenza A H1N1 virus, West Nile virus, and dengue virus. *Cell*, 2009. **139**(7): p. 1243-54.
34. Liu, S.Y., et al., Systematic identification of type I and type II interferon-induced antiviral factors. *Proc Natl Acad Sci U S A*, 2012. **109**(11): p. 4239-44.
35. Fujita, T., et al., Induction of the transcription factor IRF-1 and interferon-beta mRNAs by cytokines and activators of second-messenger pathways. *Proc Natl Acad Sci U S A*, 1989. **86**(24): p. 9936-40.
36. Keskinen, P., et al., Impaired antiviral response in human hepatoma cells. *Virology*, 1999. **263**(2): p. 364-75.
37. Zhou, X., et al., Disparity of basal and therapeutically activated interferon signalling in constraining hepatitis E virus infection. *J Viral Hepat*, 2016. **23**(4): p. 294-304.
38. Todt, D., et al., Antiviral Activities of Different Interferon Types and Subtypes against Hepatitis E Virus Replication. *Antimicrob Agents Chemother*, 2016. **60**(4): p. 2132-9.
39. Debing, Y., et al., Ribavirin inhibits in vitro hepatitis E virus replication through depletion of cellular GTP pools and is moderately synergistic with alpha interferon. *Antimicrob Agents Chemother*, 2014. **58**(1): p. 267-73.
40. Feld, J.J. and J.H. Hoofnagle, Mechanism of action of interferon and ribavirin in treatment of hepatitis C. *Nature*, 2005. **436**(7053): p. 967-72.

Chapter 7

Convergent Transcription of Interferon-stimulated Genes by TNF-α and IFN-α Augments Antiviral Activity against HCV and HEV

Wenshi Wang[1], **Lei Xu[1]**, Johannes H. Brandsma[2], Yijin Wang[1], Mohamad S. Hakim[1,3], Xinying Zhou[1], Yuebang Yin[1], Gwenny M. Fuhler[1], Luc J. W. van der Laan[4], C. Janneke van der Woude[1], Dave Sprengers[1], Herold J. Metselaar[1], Ron Smits[1], Raymond A. Poot[1], Maikel P. Peppelenbosch[1] and Qiuwei Pan[1]

[1]Department of Gastroenterology and Hepatology, Postgraduate School Molecular Medicine, Erasmus MC-University Medical Center, Rotterdam, 3015 CE, the Netherlands.

[2]Department of Cell Biology, Medical Genetics Cluster, Erasmus MC-University Medical Center, Rotterdam, 3015 CE, the Netherlands.

[3]Department of Microbiology, Faculty of Medicine, Gadjah Mada University, Yogyakarta, Indonesia.

[4]Department of Surgery, Postgraduate School Molecular Medicine, Erasmus MC-University Medical Center, Rotterdam, 3015 CE, The Netherlands.

Scientific Reports. 2016. 6. 25482.

Abstract

IFN-α has been used for decades to treat chronic hepatitis B and C, and as an off-label treatment for some cases of hepatitis E virus (HEV) infection. TNF-α is another important cytokine involved in inflammatory disease, which can interact with interferon signaling. Because interferon-stimulated genes (ISGs) are the ultimate antiviral effectors of the interferon signaling, this study aimed to understand the regulation of ISG transcription and the antiviral activity by IFN-α and TNF-α. In this study, treatment of TNF-α inhibited replication of HCV by 71 ± 2.4% and HEV by 41 ± 4.9%. Interestingly, TNF-α induced the expression of a panel of antiviral ISGs (2-11 fold). Blocking the TNF-α signaling by Humira abrogated ISG induction and its antiviral activity. Chip-seq data analysis and mutagenesis assay further revealed that the NF-κB protein complex, a key downstream element of TNF-α signaling, directly binds to the ISRE motif in the ISG promoters and thereby drives their transcription. This process is independent of interferons and JAK-STAT cascade. Importantly, when combined with IFN-α, TNF-α works cooperatively on ISG induction, explaining their additive antiviral effects. Thus, our study reveals a novel mechanism of convergent transcription of ISGs by TNF-α and IFN-α, which augments their antiviral activity against HCV and HEV.

Introduction

Cytokines orchestrate cellular communication in an autocrine, juxtacrine, or paracrine fashion through binding to distinct families of receptors, triggering specific immune responses against invading pathogens. The interferon (IFN)-mediated innate immune response is probably the most prominent response and provides a robust first defense line. Among different types of interferons, IFN-α (a type I member) has been used for decades to treat chronic hepatitis B or C infection in the clinic [1]. When stimulated by its cognate ligand, interferon receptors respond by the activation of kinases of the Janus family (JAKs), which in turn phosphorylate tyrosine residues in the intracellular tail of the interferon receptors. These phosphotyrosines serve as docking sites for recruitment and phosphorylation of the Signal Transducers and Activators of Transcription (STAT) family, which provokes STAT1 and STAT2 dimerization and subsequent binding to interferon regulatory factor 9 (IRF9) to form the IFN-stimulated gene factor 3 (ISGF3) complex. The ISGF3 complex translocates into the nucleus, and binds to specific promotor elements denoted as interferon signaling response elements (ISREs) and thus mediate the transcription of so-called interferon-stimulated genes (ISGs). ISGs are the ultimate antiviral effectors of the interferon signaling.

It is generally believed that ISGs are predominantly induced by interferons. However, ISGs are still up-regulated in embryonic fibroblasts from IFN alpha/beta receptor knockout mouse upon infection of West Nile virus [2]. These observations suggest the existence of alternative mechanisms of regulating ISG transcription. But these non-canonical mechanisms remain largely unknown.

Tumor necrosis factor alpha (TNF-α) is another important cytokine that mediates host response to infections. TNF-α/TNFR interactions can play decisive roles in the outcome of a number of viral infections, contributing to virus control or immune mediated pathology [3]. Deregulation of TNF-α is associated with many pathological conditions, including various types of arthritis and inflammatory bowel disease (IBD) [4]. TNF-α inhibitors have been successfully used in the clinic to treat these chronic immune-mediated diseases [5]. However, patients receiving TNF-α inhibitors are often at high risk of viral infections [6]. Treatment with TNF-α inhibitors have been reported to increase reactivation of concurrent chronic hepatitis B and potentially increase hepatitis C virus (HCV) replication [7], further supporting the importance of TNF-α in defending the human body against viral infections. Interestingly,

several previous studies reported crosstalk between TNF-α and the antiviral interferon signaling and ISG expression in the setting of vesicular stomatitis virus [8], hepatitis C virus (HCV) [9], respiratory virus [10] and poxvirus infections [11].

However, the exact antiviral mechanisms of TNF-α and how it cooperates with the interferon signaling remain largely elusive, thus prompting us to explore their molecular basis. Here we report that TNF-α alone was sufficient to induce the expression of ISGs and to exert antiviral activity against HCV and hepatitis E virus (HEV). This is through the activation of the NF-κB signaling but independent of the canonical interferon pathway. Surprisingly, we found a consensus DNA binding sequence between the NF-κB and ISRE motif with bioinformatics analysis. Functional assays revealed that the NF-κB complex is able to bind to the ISRE motif and directly activates the transcription of antiviral ISGs. Combination of TNF-α with IFN-α further boosts the induction of ISGs and results in augmented antiviral activity against HCV and HEV. Thus, this study identified a non-canonical mechanism of driving antiviral ISG transcription, which provides the molecular basis for the antiviral action of TNF-α and its additive antiviral effect with interferon.

Results

TNF-α activates ISG transcription and exerts antiviral activity against HCV and HEV

TNF-α is involved in host responses to a variety of pathogen invasions, including HCV and HEV infections [9, 12]. To assess the direct effects of TNF-α on HCV and HEV replication, we employed a human hepatocyte cell line, i.e. Huh7, transfected with a HCV or HEV replicon luciferase as reporters. In parallel, Huh7 cells constitutively expressing a non-secreted *firefly* luciferase under control of the human phosphoglycerate kinase (PGK) promoter (LV-PGK-Luc) were also used for normalization of nonspecific effects on luciferase signals. Both HCV and HEV replicon luciferase activity were significantly inhibited by treatment of cells with TNF-α (Fig. 1A, B). For instance, 100 ng/mL TNF-α inhibited HCV to 29 ± 2.4% ($n = 5$, $P < 0.001$), HEV to 59 ± 4.9% ($n = 5$, $P < 0.01$) at 72 hrs.

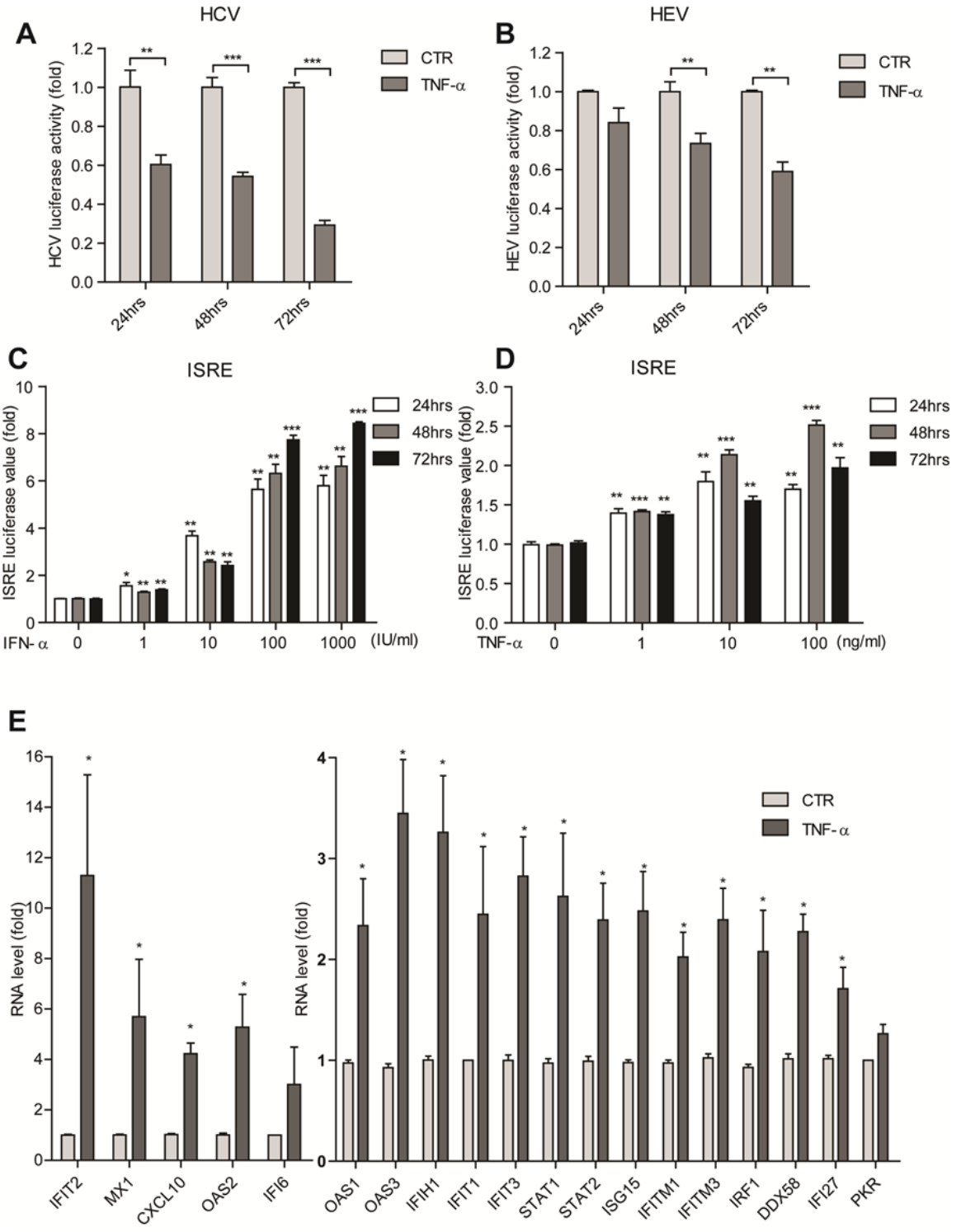

Figure 1: TNF-α activates ISG transcription and exerts antiviral activity against HCV and HEV.

(A) In the Huh7 cell-based subgenomic HCV replicon, treatment with recombinant human TNF-α (100 ng/mL) inhibited HCV replication-related luciferase activity as measured at 3 different time points (n = 5). **(B)** Same as **(A)** for the Huh7 cell-based subgenomic HEV replicon model. **(C)** In the Huh7 cell-based ISRE luciferase reporter cells, treatment with IFN-α resulted in a dose-dependent induction of ISRE-related luciferase activity (n = 3 independent experiments with 2 - 3 replicates each). **(D)** Same as **(C)** for TNF-α. **(E)** Expression profile of 20 antiviral ISGs in Huh7 cells as measured by qRT-PCR. Most ISGs were highly up-regulated with TNF-α treatment (n = 5). Data presented as mean ± SD (*P < 0.05; **P < 0.01; ***P < 0.001).

Since TNF-α has been reported to interacts with interferon signaling and ISGs are the ultimate antiviral effectors of the interferon cascade, we thus attempted to investigate whether TNF-α alone has any effect on ISG transcription. Based on the knowledge that interferon induces ISG expression via the activation of the ISRE motifs within the promoters of ISGs, a Huh7 cell line stably harboring a ISRE-driven luciferase reporter was used [13]. As expected, IFN-α treatment induced a strong transactivation of ISRE-driven luciferase value (Fig. 1C). Surprisingly, TNF-α stimulation also provoked a strong transactivation of the ISRE transcription elements (Fig. 1D). This interesting result prompted us to investigate the relative expression level of a panel of well-studied antiviral ISGs by qRT-PCR. Consistently, treatment of TNF-α provoked the induction of most tested ISGs, ranging from 1.7 to 11.3 fold increase (Fig. 1E). These data demonstrate that TNF-α transactivates the ISRE motif, resulting in the induction of ISGs, which in turn mediate the antiviral effects of TNF-α against HCV and HEV.

Activation of ISRE transcription by TNF-α does not require interferon production

The fact that TNF-α can induce ISGs inspired us to investigate the straightforward possibility that TNF-α merely triggers the production of interferons. Interferon regulatory factor 1 (IRF1) was demonstrated to be important in a TNF-α triggered IFN-β autocrine loop in primary macrophage cells [14]. To dissect whether a similar mechanism exist in our experiment system, we first studied the potential involvement of IRF1. Lentiviral vector was used to overexpress IRF1 in Huh7 based ISRE-driven luciferase reporter cells and the successful overexpression of IRF1 was confirmed at both mRNA and protein levels (Fig. 2A, B). IRF1 overexpression significantly increased ISRE-regulated luciferase activity (Fig. 2C). Surprisingly, the combination of IRF1 overexpression and TNF-α induced a strong additive ISRE activation (Fig. 2C). Furthermore, stable IRF1 knockdown by lentiviral RNAi (Fig. 2D, E) had no significant effect on TNF-α induced ISRE activation (Fig. 2F). In addition, the involvement of another interferon regulatory factor, IRF7, was also examined via loss-of-function assay. TNF-α induced ISRE activation was not affected even upon the efficient IRF7 knockdown (Supplementary Figure 1A-C). These results suggest that TNF-α triggered ISRE activation is independent of IRF1 and IRF7.

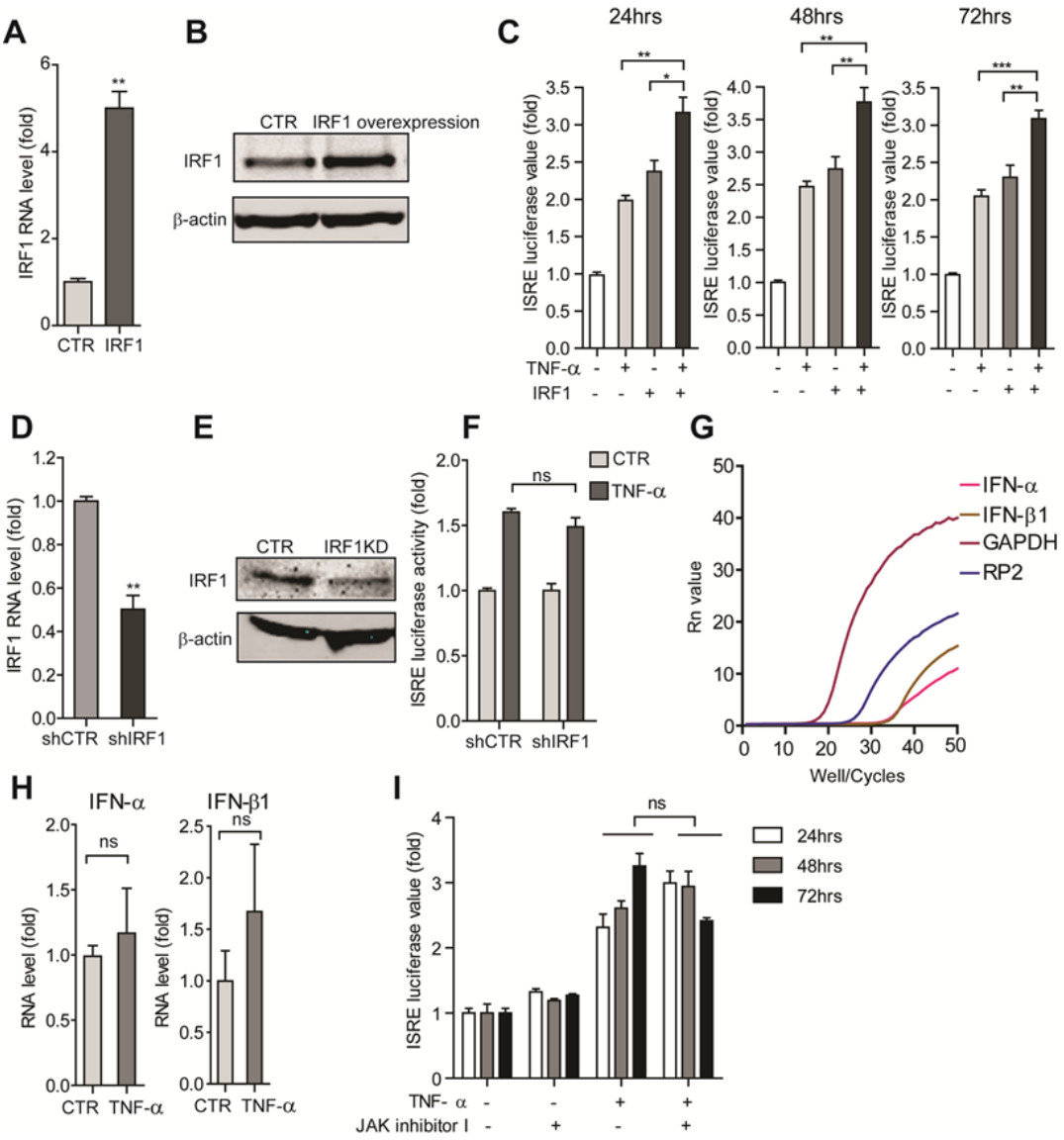

Figure 2: Activation of ISRE transcription by TNF-α does not require interferon production and the JAK-STAT signaling.

(**A**) qRT-PCR analysis of IRF1 overexpression by lentiviral vectors in the Huh7 based ISRE luciferase reporter cells. Compared to the control vector transduced cells, the IRF1 lentiviral vector showed strong IRF1 induction on RNA level. (**B**) Western blot analysis confirmed the successful overexpression of IRF1 by lentiviral vectors in the Huh7 based ISRE luciferase reporter cells. (**C**) In the Huh7 cell-based ISRE luciferase reporter cells, the combination of IRF1 overexpression and TNF-α induced a strong additive ISRE activation as measured at 3 different time points (n = 5). (**D**) qRT-PCR analysis of IRF1 knockdown by lentiviral shRNA vectors in the Huh7 based ISRE luciferase reporter cells. Compared to the control vector transduced cells, the IRF1 shRNA treated clones showed strong reduction of IRF1 RNA levels. (**E**) Western blot analysis confirmed the successful knockdown of IRF1 by lentiviral shRNA vectors in the Huh7 based ISRE luciferase reporter cells. (**F**) Knockdown of IRF1 in Huh7 based ISRE luciferase reporter cells did not block TNF-α induced ISRE-related luciferase activation (n = 4). (**G**) The relative IFN-α and β1 expression levels in Huh7 cells were determined by qRT-PCR. GAPDH and RP2 served as internal reference genes. (**H**) IFN-α and β1 expression levels in Huh7 cells were not up-regulated upon TNF-α treatment as measured by qRT-PCR (n = 6). (**I**) JAK inhibitor I (5 μM) did not abrogate TNF-α induced ISRE-related luciferase activation (n = 3 independent experiments with 2 - 3 replicates each). Data presented as mean ± SD (*P < 0.05; **P < 0.01; ***P < 0.001; ns, not significant).

We next investigated the effects of TNF-α on gene expression of type I interferons. As determined by qRT-PCR, the constitutive expression levels of IFN-α and β1 in Huh7 cells are rather low, compared to the reference genes GAPDH and RP2 (Fig. 2G). Moreover, TNF-α treatment did not significantly increase IFN-α and IFN-β1 mRNA levels (Fig. 2H). This is consistent with a previous study showing that the Huh7 cell line responds to interferon but does not produce interferon [15]. These data collectively indicate that activation of ISRE transcription by TNF-α does not require interferon production in our model system.

TNF-α induced ISRE activation is independent of the JAK-STAT signaling

Classically, ISGs are induced by interferons via the JAK-STAT signaling. Following receptor activation by interferons, JAK1 phosphorylates STAT1 and Tyrosine kinase 2 (TYK2) phosphorylates STAT2. This provokes STAT1 and STAT2 dimerization and subsequent binding to IRF9 to form the ISGF3 complex. The ISGF3 complex translocates into the nucleus, binds to the ISRE motif [5'-CAGTTTCACTTTCC-3'] and drives the transcription of ISGs (Supplementary Figure 2A). To test whether activation of ISRE by TNF-α require JAK-STAT signaling, we first examined the role of JAKs. Strikingly, neither JAK inhibitor (an inhibitor of JAK1, JAK2, JAK3 and TYK2) nor Bayer-18 (a selective TYK2 inhibitor) abrogated TNF-α induced ISRE activation (Fig. 2I and Supplementary Figure 2B). Consistently, TNF-α induced ISG expression was not affected by the treatment of JAK inhibitor I (Supplementary Figure 2D). In contrast, both IFN-α induce ISRE activation and ISG expression were largely blocked by JAK inhibitor I (Supplementary Figures 2C and 3A). Interestingly, the selective TYK2 inhibitor, Bayer-18, did not significantly affect IFN-α induced ISRE activation (Supplementary Figure 2C). This is consistent with a previous study, showing that TYK2 plays a restricted role in IFN-α signaling [16].

Furthermore, to see if TNF-α treatment has any effect on STATs activation and translocation, we examined the phosphorylation status of STAT1 at amino acid 701 (Y701P) and STAT2 at amino acid 690 (Y690), which are indispensable signature of STAT1 and STAT2 activation, respectively. WB results showed TNF-α treatment had no effects on the phosphorylation of both STAT1 and STAT2 at indicated sites (Fig. 3A, B). Confocal microscopy analysis also confirmed that IFN-α induced the activation and nuclear translocation of STAT1 and STAT2 via the phosphorylation at indicated sites, while TNF-α had no effects (Fig. 3C, D). To further exclude a role of STAT1 in TNF-α induced ISRE activation, lentiviral RNAi was used

to knockdown STAT1. The stable STAT1 knockdown (Fig. 3E, F) had no effect on both TNF-α induced ISRE activation and ISG expression (Fig. 3G, H). Collectively, TNF-α triggered ISRE activation is totally independent of STAT1.

In addition, the role of IRF9 was also verified, which is a key downstream element of interferon pathway. IRF9 was up-regulated and translocated into cell nucleus upon IFN-α stimulation, whereas TNF-α stimulation did not induce the translocation of IRF9 into cell nucleus (Supplementary Figure 3B). These results collectively demonstrate that TNF-α induced ISRE activation is independent of the JAK-STAT signaling.

TNF-α activates ISRE via TNF receptor 1

TNF receptor (TNFR) is the important upstream component in TNF-α induced signaling transduction. TNF acts through two receptors, TNFR1 and TNFR2. TNFR1 is the major signaling receptor for TNF-α and is expressed by all human tissues, while TNFR2 is mostly expressed in immune cells and mediates limited biological responses [17]. In light of the fact that TNF-α is capable of activating ISG transcription, we sought to determine whether this action of TNF-α was mediated via TNFR. For this, the ISRE reporter cell line was transduced with integrating lentiviral RNAi vectors to silence TNFR1, resulting in a profound down-regulation of TNFR1 expression (Fig. 4A). As expected, IFN-α induced ISRE activation was not influenced (Fig. 4B), but TNF-α induced ISRE luciferase activity was largely abrogated in TNFR1 knockdown cells when compared to control cells (Fig. 4C). Consistently, the induction of ISGs by TNF-α was also blocked by TNFR1 knockdown (Supplementary Figure 4A).

To further confirm these results, the clinically widely used drug for rheumatoid arthritis patients and Crohn's disease, Humira (adalimumab), was used. Humira binds specifically to TNF-α and blocks its interaction with TNF receptors. As expected, Humira effectively blocks TNF-α induced activation of NF-κB luciferase activity (Fig. 5A), NF-κB activity being a well-known downstream effect of TNF-α receptor ligation. Importantly, both TNF-α induced ISRE luciferase activity and ISG expression were also abrogated by Humira treatment (Fig. 5B, C). This effect was not limited to Huh7 cells, but also observed in a human lung cell line, A549 (Supplementary Figure 4B). More relevantly, Humira totally abolished TNF-α mediated antiviral effect against HCV and HEV (Fig. 5D, E), providing a possible explanation for the high risk of infection in patients treated with TNF-α inhibitors. Next, we collected serum samples from anti-TNF-α treatment naive Crohn's disease patients

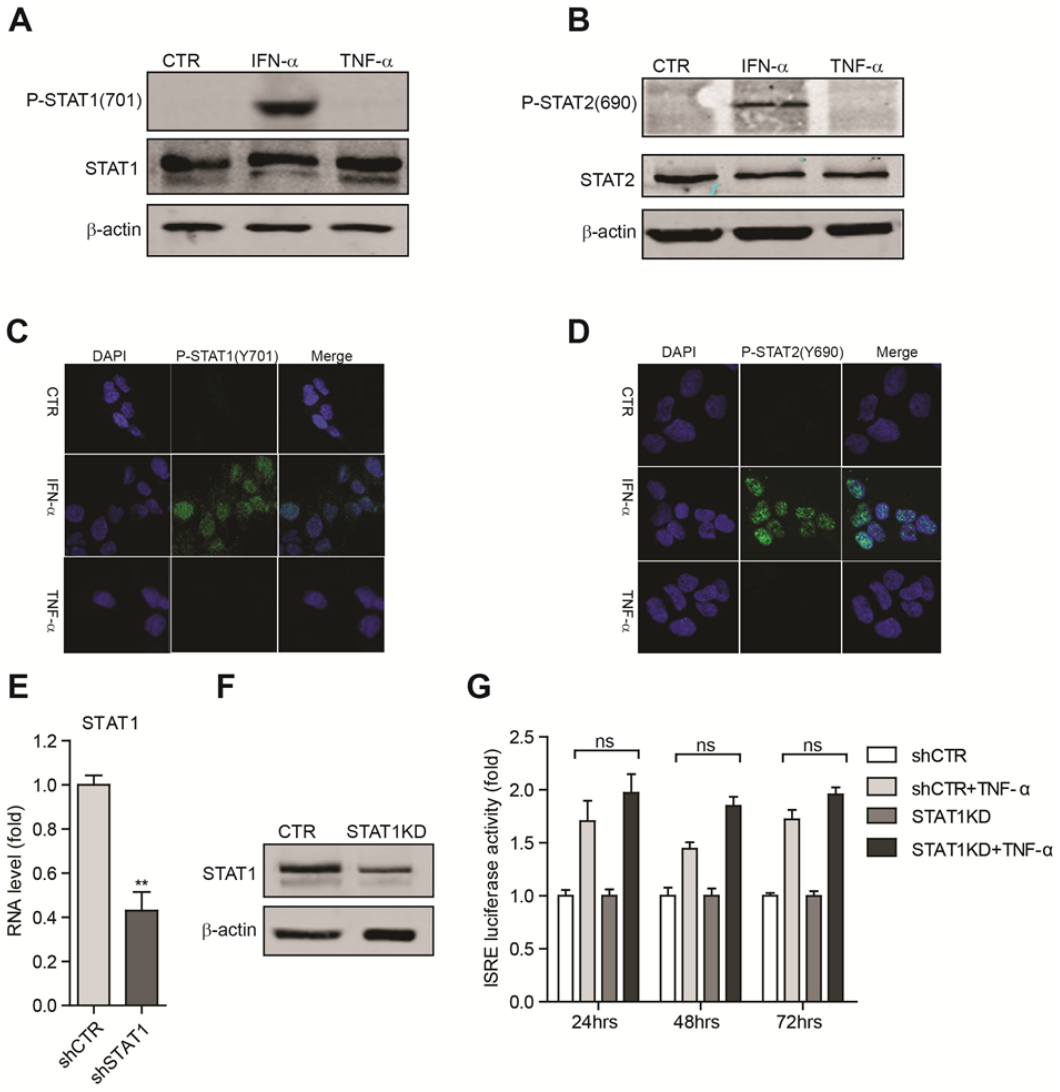

Figure 3: TNF-α activates ISRE in a STAT1 independent manner.

(**A**) Western blot analysis of total STAT1 and phosphorylated STAT1 (Y701P) protein levels under the treatment of TNF-α (100 ng/mL), IFN-α (1000 IU/mL). (**B**) Same as (**A**) for the detection of total STAT2 and phosphorylated STAT2 (Y690P) protein levels under the treatment of TNF-α, IFN-α. (**C**) Confocal microscopy analysis of phosphorylated STAT1 (Y701P) localization in Huh7 cells treated with IFN-α or TNF-α. STAT1 was phosphorylated and translocated to the nucleus upon IFN-α, but not TNF-α treatment. Phosphorylated STAT1 (Y701P) antibody (green). Nuclei were visualized by DAPI (blue). (**D**) Same as (**C**) for the detection and localization of phosphorylated STAT2 (Y690P). (**E**) qRT-PCR confirmed the successful STAT1 knockdown by lentiviral shRNA vectors in the Huh7 based ISRE luciferase reporter cells. (**F**) Western blot analysis confirmed the successful knockdown of STAT1 by lentiviral shRNA vectors in the Huh7 based ISRE luciferase reporter cells. (**G**) STAT1 knockdown had no significant influence on TNF-α induced ISRE-related luciferase activation as measured at 3 different time points (n = 3 independent experiments with 2 -3 replicates each). (**H**) STAT1 knockdown exerts no effect on TNF-α induced ISG expression as measured by qRT-PCR (n = 3).

and measured the serum TNF-α levels by ELISA. 3 serum samples with high TNF-α levels were selected to treat Huh7 based ISRE-driven luciferase reporter cells (Fig. 5F). Consistently, all 3 serum samples exerted higher ISRE activity compared to control serum sample (Fig. 5F, right). Furthermore, Humira decreased the serum induced ISRE activity (Supplementary Figure 4C). More interestingly, serum samples with higher TNF-α levels inhibited HCV-related luciferase activity compared to control serum sample (Supplementary Figure 4D). Collectively, these results demonstrate that TNF-α acts via its receptor to activate ISG transcription and exerts antiviral activity, which can be blocked by clinically used TNF-α inhibitor.

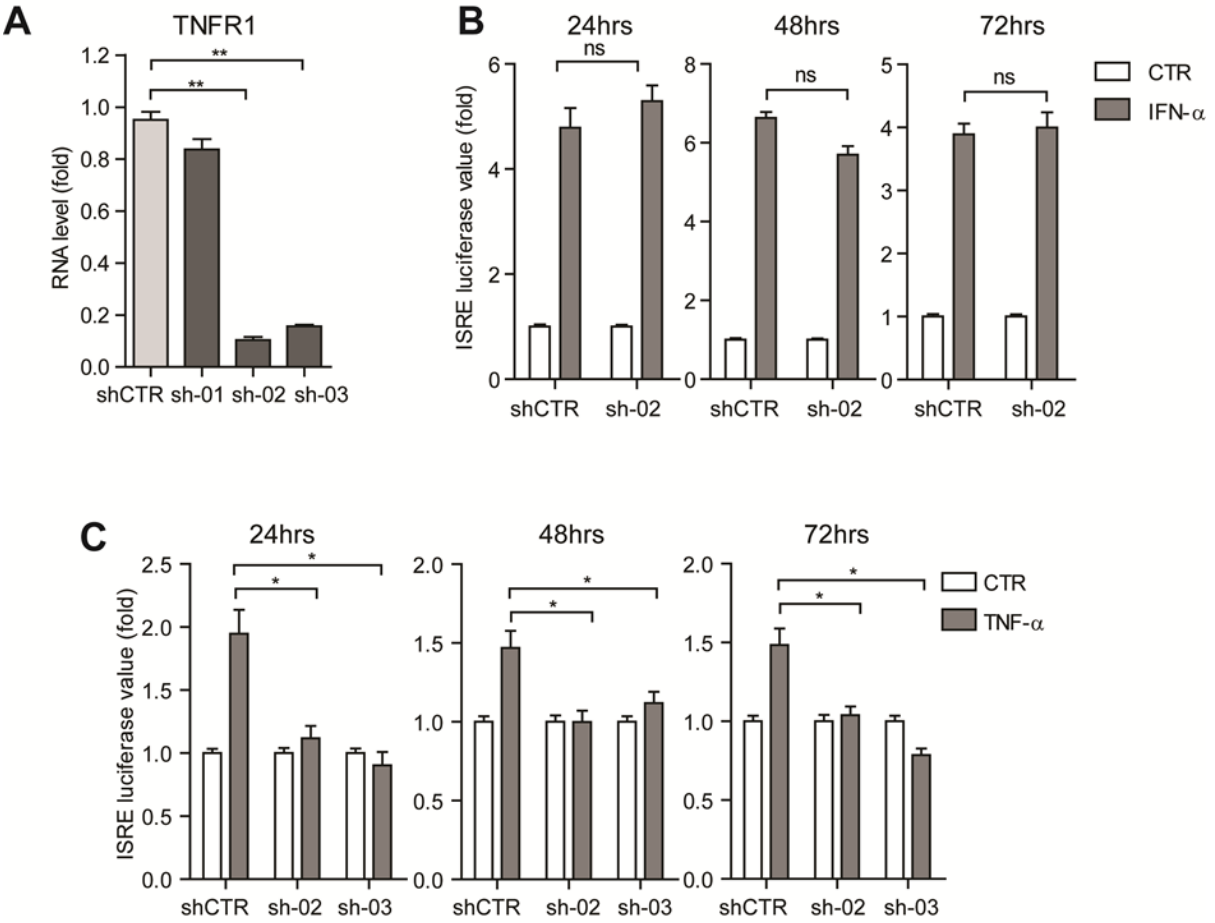

Figure 4: TNF-α activates ISRE via TNF receptor I.

(**A**) qRT-PCR analysis of TNFR1 knockdown by lentiviral shRNA vectors in the Huh7 based ISRE luciferase reporter cells. Compared to the control vector transduced cells, the two shRNA treated clones (sh-02 and sh-03) showed strong reduction of TNFR1 RNA levels. (**B**) TNFR1 knockdown had no significant influence on IFN-α induced ISRE-related luciferase activation as measured at 3 different time points (n = 3 independent experiments with 2 - 3 replicates each). (**C**) TNFR1 knockdown blocked TNF-α induced ISRE-related luciferase activation as measured at 3 different time points (n = 3 independent experiments with 2 - 3 replicates each).

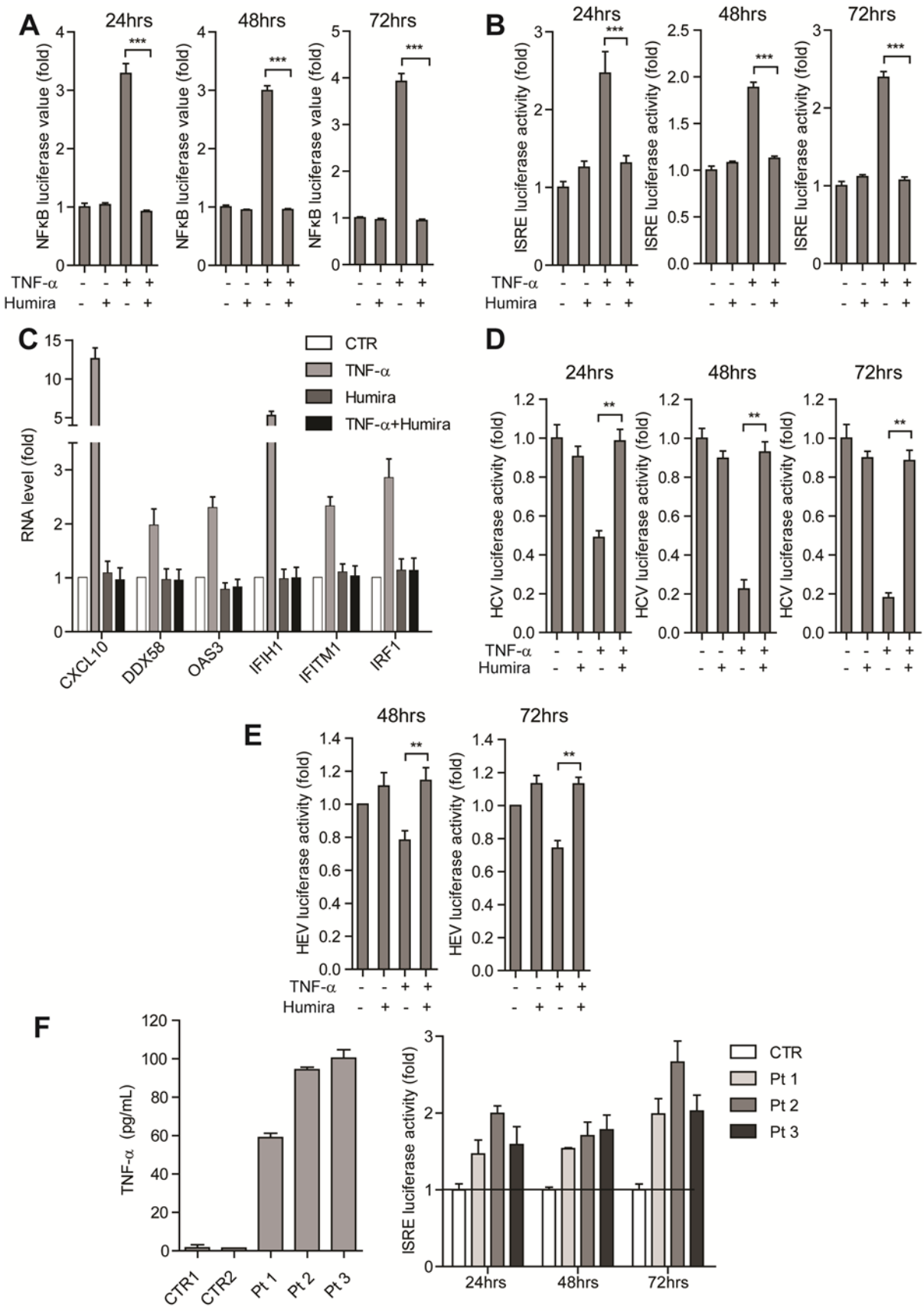

Figure 5: Both TNF-α induced ISG expression and antiviral activity against HCV and HEV were abrogated by its inhibitor Humira.

(**A**) In the Huh7 cell-based NF-κB luciferase reporter cells, the TNF-α inhibitor, Humira, abrogated TNF-α induced NF-κB-related luciferase activation as measured at 3 different time points (n = 3 independent experiments with 2 - 3 replicates each). (**B**) Same as (**A**) for the Huh7 cell-based ISRE luciferase reporter cells. (**C**) In Huh7 cells, the TNF-α inhibitor, Humira, abrogated TNF-α induced ISG expression as measured by qRT-PCR (n = 4). (**D**) In the Huh7 cell-based subgenomic HCV replicon, Humira abrogated the TNF-α induced anti-HCV effect as measured at 3 different time points (n = 3 independent experiments with 2 - 3 replicates each). (**E**) Same as (**D**) for Huh7 cell-based subgenomic HEV replicon. (**F**) TNF-α levels in serum samples collected from anti-TNF-α treatment naive Crohn's disease patients were measured by ELISA kit (left). Serum samples with higher TNF-α levels showed stronger ISRE-related luciferase activity compared with control serum as measured at 3 different time points. Data presented as mean ± SD. (*P < 0.05; **P < 0.01; ***P < 0.001; ns, not significant).

TNF-α mediates the activation of ISRE through NF-κB signaling

Activation of NF-κB signaling is one of the most important canonical responses to the stimulation of TNF-α. Following TNF receptor activation by TNF-α, inhibitor of kappa B (IκB) proteins undergo phosphorylation dependent ubiquitination and degradation, resulting in the activation and translocation of NF-κB dimers into the cell nucleus. In the cell nucleus, NF-κB dimers bind to the specific NF-κB motifs, [5'-GGGAA/CTTTCC-3'], within the promoter regions driving the expression of NF-κB target genes (Supplementary Figure 5A). Because some studies have reported that TNF-α can also increase the transcriptional activity of activator protein-1 (AP-1) in some specific cell types [18, 19], we thus created Huh7 based stable NF-κB or AP-1 driven luciferase reporter cell lines, respectively. As shown in Supplementary Figure 5B, stimulation with TNF-α led to strong activation of NF-κB luciferase activity, but no significant effect on AP-1 activity. Therefore, we only focused on NF-κB signaling for the following investigation.

The NF-κB complex is the endpoint of its signal transduction, which comprises the heterodimeric RelA (P65)-P50 complex. Indeed, unstimulated cells display little nuclear RelA, but the RelA protein level in the cell nucleus was substantially elevated following TNF-α stimulation (Fig. 6A). Thus, to dissect the role of the RelA (P65)-P50 complex in TNF-α induced ISRE activation, the Huh7 ISRE reporter cell line was transduced with integrating lentiviral RNAi vectors to silence RelA (P65), resulting in profound down-regulation of RelA expression (Fig. 6B). Consistently, TNF-α induced ISRE luciferase activity and ISG expression was largely demolished in RelA knockdown cells when compared with control cells (Fig. 6C, D). On the contrary, IFN-α induced ISRE activation was not affected (Fig. 6E). Thus, NF-κB signaling appears to be essential for TNF-α mediated ISRE activation.

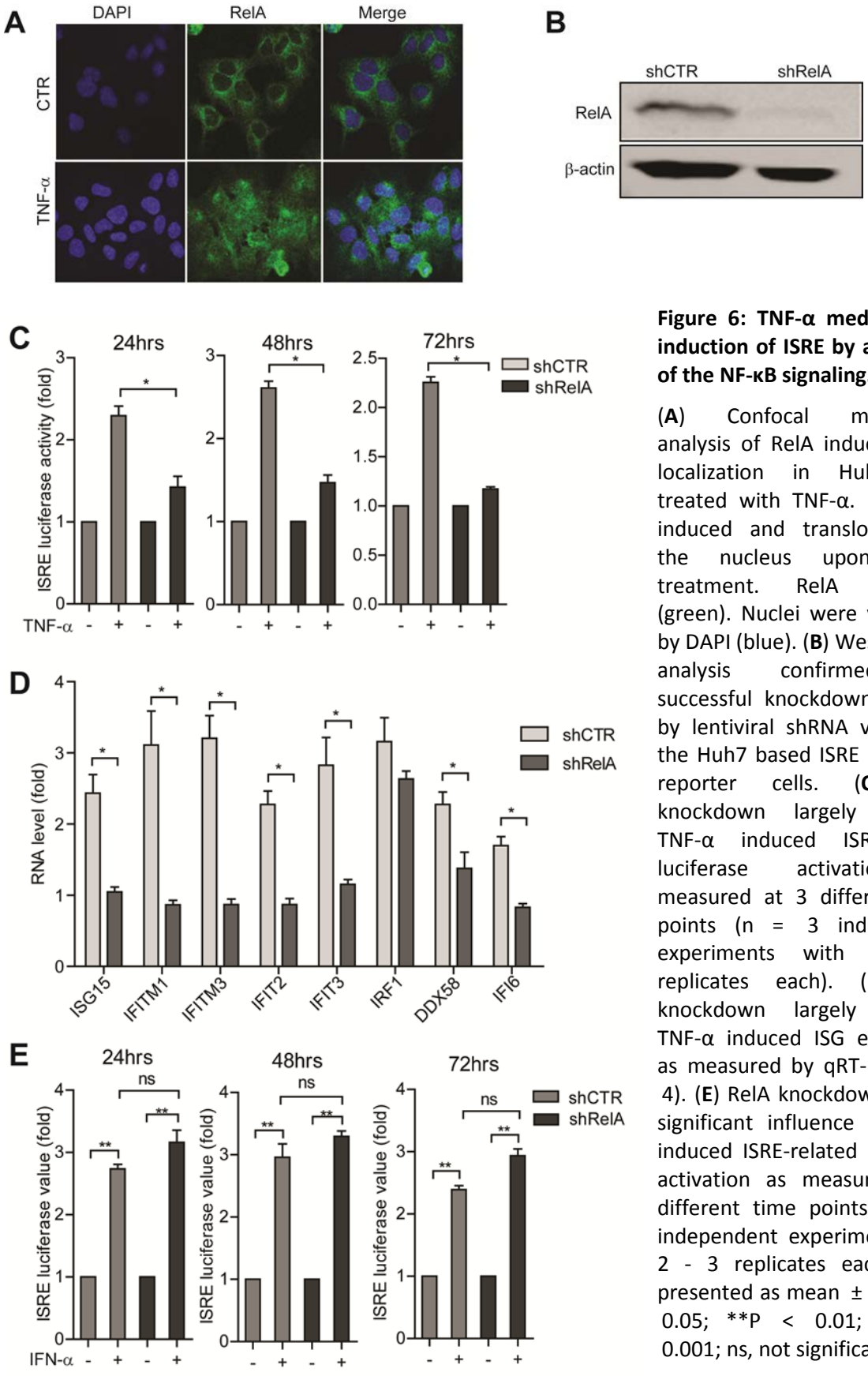

Figure 6: TNF-α mediates the induction of ISRE by activation of the NF-κB signaling.

(**A**) Confocal microscopy analysis of RelA induction and localization in Huh7 cells treated with TNF-α. RelA was induced and translocated to the nucleus upon TNF-α treatment. RelA antibody (green). Nuclei were visualized by DAPI (blue). (**B**) Western blot analysis confirmed the successful knockdown of RelA by lentiviral shRNA vectors in the Huh7 based ISRE luciferase reporter cells. (**C**) RelA knockdown largely blocked TNF-α induced ISRE-related luciferase activation as measured at 3 different time points (n = 3 independent experiments with 2 - 3 replicates each). (**D**) RelA knockdown largely blocked TNF-α induced ISG expression as measured by qRT-PCR (n = 4). (**E**) RelA knockdown has no significant influence on IFN-α induced ISRE-related luciferase activation as measured at 3 different time points (n = 3 independent experiments with 2 - 3 replicates each). Data presented as mean ± SD (*P < 0.05; **P < 0.01; ***P < 0.001; ns, not significant).

The NF-κB complex directly binds to ISRE and drives its transcriptional activity

Upon TNF-α stimulation and signaling activation, the transcription factor complex, NF-κB, can directly bind to a sequence specific motif [5'-GGGAA/CTTTCC-3'] to promote target gene transcription [13, 20-22]. The puzzling role of NF-κB in the transactivation of ISRE led us to perform an *in silico* analysis comparing the ISRE motif and the NF-κB DNA binding site. Surprisingly, we identified a partial consensus sequence region in common within these two motifs (Fig. 7A). We thus hypothesized that NF-κB might bind to this consensus sequence within the ISRE motif to drive transcription of corresponding ISGs. To test this hypothesis, we retrieved genome wide RelA and STAT1 (positive control) ChIP-seq data from the ENCODE ChIP-seq Experiment Matrix database. ChIP-seq datasets were processed and analyzed. Confirming our hypothesis, we found that RelA showed a similar genome-wide binding pattern with STAT1. For a large cohort of genes, RelA overlapped with STAT1 in their gene binding site (Fig. 7B, left). To be more specifically, we further analyzed the RelA and STAT1 binding sites that were within 1 kb of a transcription start site. This region is frequently located at the site of the promoter. Consistently, RelA still overlaps with STAT1 in the specific binding sites near gene transcription start sites. Since most genes bound and regulated by STAT1 are ISGs, this indicates that RelA also possesses the ability to bind and regulate a large cohort of ISGs. Then we analyzed RelA binding on a list of well-established antiviral ISGs. Convincingly, RelA shows strong and specific binding on the promoters of indicated ISGs, while the rabbit-IgG (negative control) shows no significant binding (Fig. 7C). To further confirm that NF-κB binds to the consensus sequence within the ISRE motif to drive corresponding ISG transcription, we mutated the consensus nucleotide sequence within the ISRE motif based on the lentiviral transcriptional reporter vector expressing the *firefly* luciferase gene driven by multiple ISREs. In theory, RelA will not be able to bind to this mutant ISRE sequence (Supplementary Figure 6). Huh7 cells were transduced with this vector to create a stable reporter cell line. As expected, TNF-α failed to activate this mutated ISRE (Fig. 7D). Hence, NF-κB can directly bind to the ISRE motif and activate its transcriptional activity.

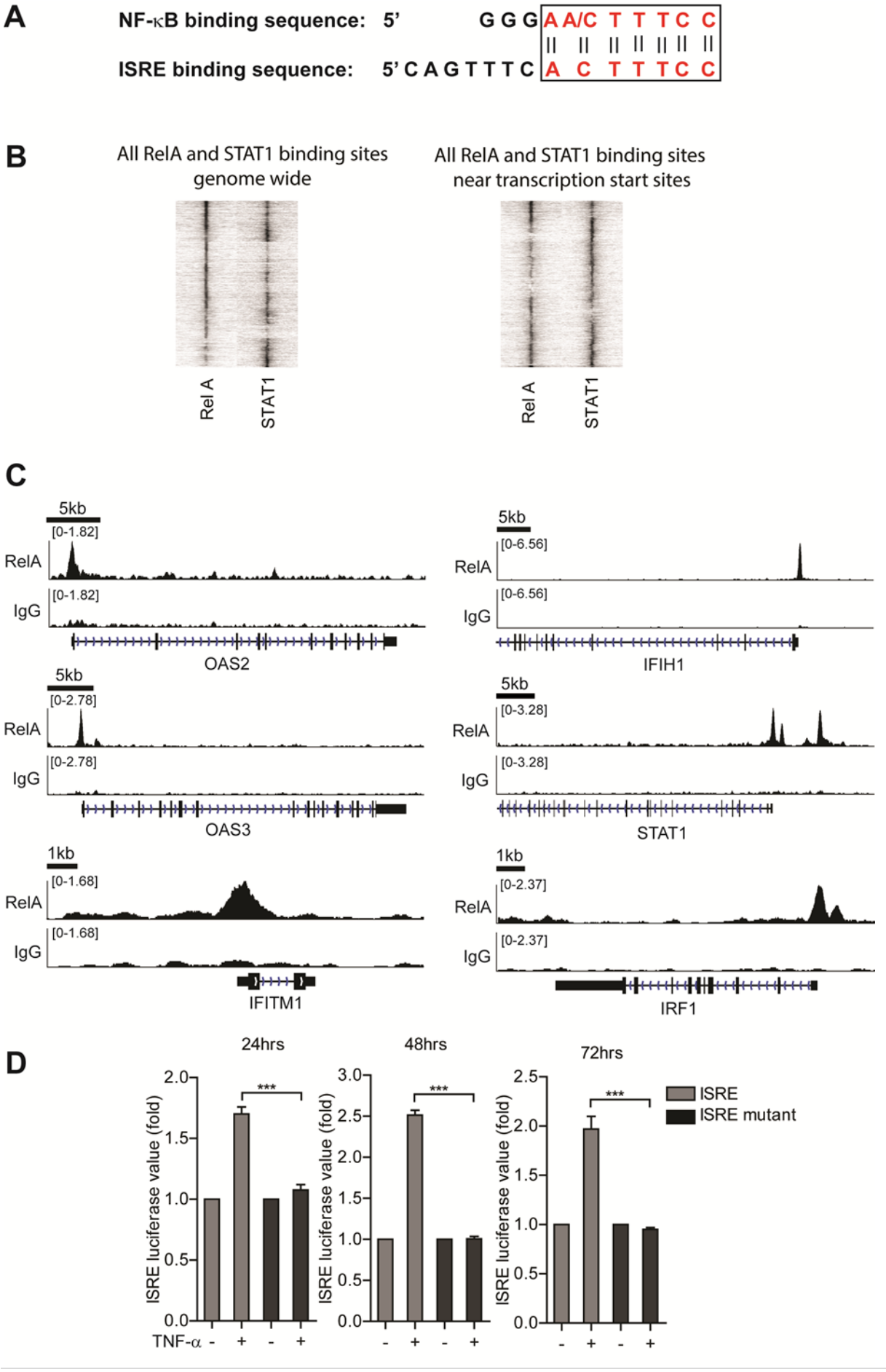
A
NF-κB binding sequence: 5' G G G A A/C T T T C C
ISRE binding sequence: 5' C A G T T T C A C T T T C C
B
All RelA and STAT1 binding sites genome wide
All RelA and STAT1 binding sites near transcription start sites
Rel A
STAT1
Rel A
STAT1
C
5kb
[0-1.82]
RelA
[0-1.82]
IgG
OAS2
5kb
[0-6.56]
RelA
[0-6.56]
IgG
IFIH1
5kb
[0-2.78]
RelA
[0-2.78]
IgG
OAS3
5kb
[0-3.28]
RelA
[0-3.28]
IgG
STAT1
1kb
[0-1.68]
RelA
[0-1.68]
IgG
IFITM1
1kb
[0-2.37]
RelA
[0-2.37]
IgG
IRF1
D
24hrs
48hrs
72hrs
ISRE luciferase value (fold)
***
ISRE
ISRE mutant
TNF-α - + - +

Figure 7: The NF-κB complex directly binds to ISRE and drives its transcriptional activity.

(A) NF-κB and ISRE sequence specific binding regions. Their consensus nucleotides are labeled in red color, and the consensus region is enclosed by the rectangular box. (B) Heatmaps display the normalized ChIP-seq reads representing the binding intensity of STAT1 and RelA. Displayed are 8 kb regions centered on the summits of significant STAT1 and/or RelA binding sites. The heatmap are clustered for the STAT1 and RelA binding signal based on the central 0.5 kb of the heatmap. left) Heatmaps of all significant STAT1 and RelA binding sites (n = 13367). right) Heatmap of all significant STAT1 and RelA binding sites that are within 1 kb of a transcription start site (n = 4545). (C) Binding of RelA to the promoters of the indicated ISGs. Sequence reads from anti-RelA ChIP-seq or rabbit-IgG-control were plotted relative to chromosomal position. Genome location of corresponding ISGs is shown beneath the track signaling. RelA shows strong and specific binding on the promoters of indicated ISGs, while the rabbit-IgG, serving as negative control, shows no significant binding. (D) In the Huh7 cell-based mutant ISRE luciferase reporter cells, TNF-α did not induce mutant ISRE related luciferase activation as measured at 3 different time points (n = 3 independent experiments with 2–3 replicates each). Data presented as mean ± SD (*P < 0.05; **P < 0.01; ***P < 0.001; ns, not significant).

TNF-α cooperates with IFN-α in ISG induction and antiviral action

Because of the distinct signaling cascades that finally converge the transcription of antiviral ISGs by TNF-α and interferons, we further investigated the combinatory effects of TNF-α with IFN-α on ISG induction and antiviral action. Thus, we quantified the expression levels of a list of well-known antiviral ISGs in the Huh7 cell line with treatment of TNF-α, IFN-α or a combination thereof. Both TNF-α and IFN-α can induce significant up-regulation of tested ISGs, and their combination resulted in a strong additive induction of ISGs (Fig. 8A).

Consistent with a previous publication [23], our results of ISG antiviral assay (Supplementary Figure 7) again highlight the important antiviral role of ISGs. Thus, the cooperation in ISG induction prompted us to test whether an additive antiviral effect can be achieved with the combination of TNF-α and IFN-α. Hence, we employed the Huh7 cell line based HCV or HEV replicon luciferase reporter as the cell models for the test. As shown in Fig. 8B and 8C, the combination of TNF-α and IFN-α resulted in additive antiviral effects in both HCV and HEV replicon models. Thus, TNF-α cooperates with IFN-α in ISG induction, explaining their additive antiviral effects against HCV and HEV as we observed.

Discussion

TNF-α is a cytokine within the TNF superfamily, which acts as a central mediator of inflammation and immune regulations. Although TNF-α was first noted for its role in the killing of tumor cells [24], it has pleiotropic functions that include the inflammatory response and host resistance to pathogens. Indeed, numerous studies have demonstrated the

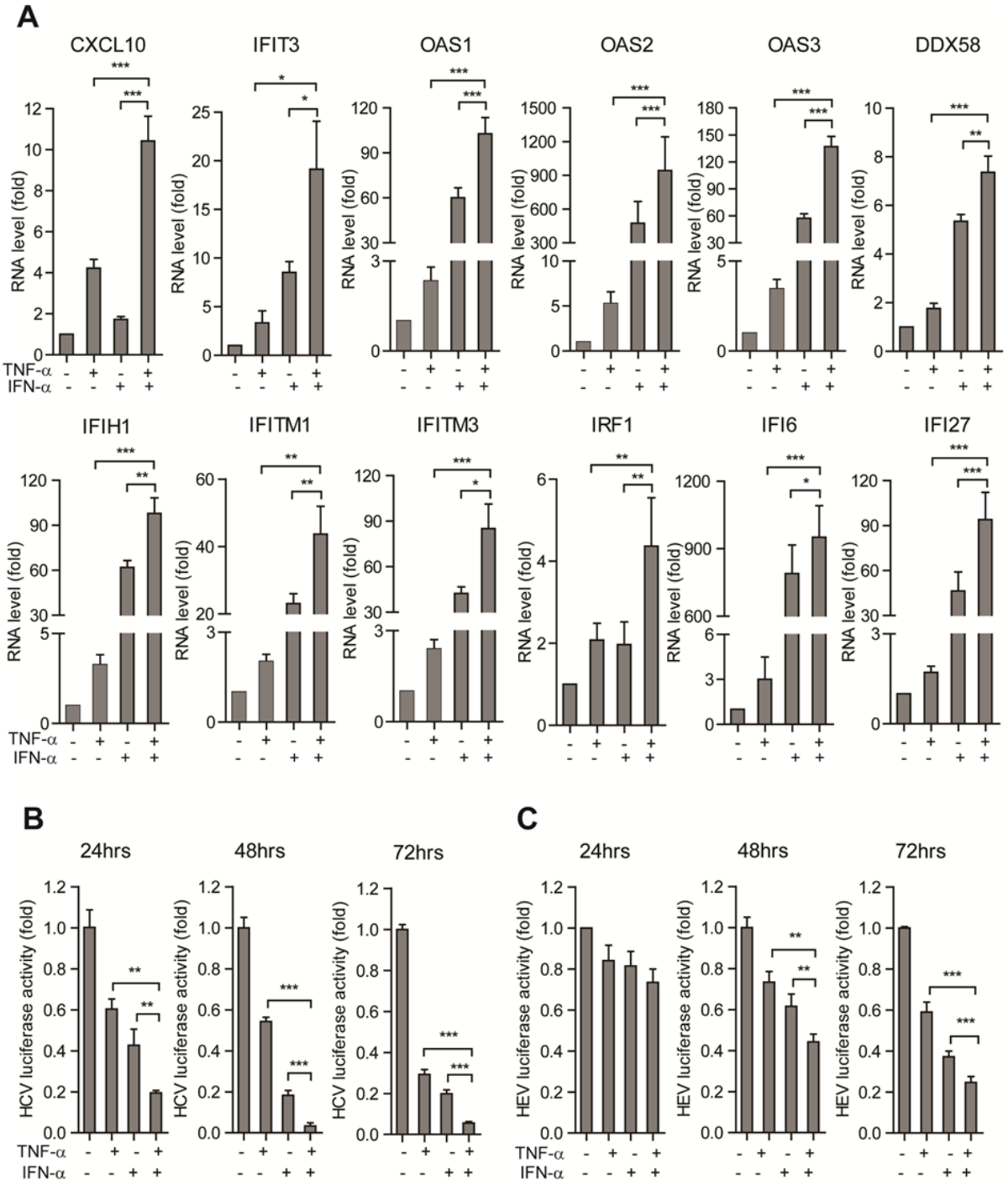

Figure 8: TNF-α cooperates with IFN-α in ISG induction and antiviral action.

(A) In the Huh7 cells, the combination of TNF-α and IFN-α induced a strong additive ISG expression compared with treatment of either TNF-α or IFN-α alone as measured by qRT-PCR (n = 6). (B) In the Huh7 cell-based subgenomic HCV replicon model, the combination of TNF-α and IFN-α induced a strong additive anti-HCV effect compared with treatment of either TNF-α or IFN-α alone as measured at 3 different time (n = 3 independent experiments with 2 - 3 replicates each). (C) Same as (B) for the Huh7 cell-based subgenomic HEV replicon model.

importance of TNF-α in protection against pathogens, including *Mycobacterium tuberculosis, Cryptococcus neoformans*, vesicular stomatitis virus, encephalomyocarditis virus, herpes

simplex virus, influenza virus and hepatitis B virus [25-29]. Disordered TNF-α regulation may have a significant negative role in inflammation and pathogenesis. Based on this, TNF-α antagonists have been proven to be highly effective in the treatment of certain inflammatory diseases, such as rheumatoid arthritis [30], psoriatic arthritis [31], juvenile rheumatoid arthritis [32], and Crohn's disease [33]. Several TNF-α inhibitors have been approved for the treatment of these inflammatory illnesses by the US Food and Drug Administration (FDA). Contradictory, many studies have demonstrated an increased risk of opportunistic infections and difficulty in clearing infections once they develop in patients treated with TNF-α inhibitors, such as HBV or HCV infection [34-36]. Our experimental results showing that clinically used anti-TNF-α inhibitors can totally abrogate the antiviral activity of TNF-α appear to support those clinical observations and highlight the primary role of TNF-α in host defense against infections.

As a first line defense, TNF-α and type I interferons are induced by microbial stimuli and mediate innate immune responses. Despite the fact that cells at sites of infection are continuously exposed to both cytokines, the interactions between TNF-α and interferons remain under investigated [37]. Although previous studies have reported that TNF-α interacts with antiviral interferon signaling and regulates ISG expression in the setting of different virus infections [8-10], the molecular mechanisms behind these interactions have not been delineated. In this study, we demonstrated that the activation of NF-κB signaling by TNF-α was able to directly transactivate the ISRE motif, resulting in the induction of antiviral ISGs. This whole process is independent of IFN production and the canonical JAK-STAT cascade, but relies on TNF-α induced NF-κB activity. NF-κB is a homo- or heterodimeric complex formed by the Rel-like domain-containing proteins: RelA (P65), RelB, c-Rel, P50 and P52 and the heterodimeric RelA (P65)-P50 complex appear to be the most abundant one. The dimers bind to the sequence specific NF-κB response element in the promoter region of their target genes to regulate transcription. To our surprise, *in silico* analysis discovered a consensus nucleotide sequence shared by the ISRE motif and NF-κB DNA binding site. ChIP-seq data analysis reveals RelA (P65) can directly bind to the promoter region of a large cohort of ISGs. Our loss-of-function and mutagenesis assay further confirmed that NF-κB could directly drive ISRE-controlled gene transcription. Since NF-κB is also the key downstream effector of most Toll-like receptors (TLR), this novel mechanism may also partially explain the antiviral

activities of TLR agonists in clinic, such as the TLR7 agonists, which are being therapeutically targeted and explored for HCV treatment in clinic trial [38].

More excitingly, TNF-α not only activates antiviral ISGs transcription, but also cooperates with IFN-α, explaining the additive antiviral outcome of their combination. This highlights the important facts that different cytokines orchestrate innate immune responses by activating signaling cascades to protect against infection efficiently.

In conclusion, we revealed a novel antiviral mechanism of TNF-α. TNF-α, via the activation of NF-κB cascade, can drive the transcription of antiviral ISGs through direct binding of ISREs. This antiviral mechanism may provide clues for tackling the high rise of infections caused by TNF-α inhibitor treatment in patients. More interestingly, TNF-α also acts cooperatively with IFN-α in antiviral ISGs induction to exert additive antiviral effects. These findings not only provide new clues for understanding virus-host interactions but also assign a novel function of the canonical NF-κB pathway.

Materials and Methods

The HCV subgenomic replicon comprised Huh7 cells containing a subgenomic HCV bicistronic replicon (1389/NS3-3 V/LucUbiNeo-ET) linked to the *firefly* luciferase reporter gene were maintained with 250 μg/mL G418 (Sigma, Zwijndrecht, the Netherlands). The HEV subgenomic model was based on Huh7 cells containing the subgenomic HEV sequence (Kernow-C1 p6/luc) coupled to a *Gaussia* luciferase reporter gene. Lentiviral pLK.O knockdown vectors (Sigma-Aldrich) targeting IRF1, TNFR1, RelA were obtained from the Erasmus Biomics Center and produced in HEK293T cells as previously described [39]. The use of serum samples from IBD patients was approved by the Medical Ethical Committee of the Erasmus Medical Center (Medisch Ethische Toetsings Commissie Erasmus MC), and the informed consent was obtained from all subjects. All methods were carried out in accordance with the approved guidelines. For more details, see Supplementary Information.

Acknowledgements

The authors gratefully thank Dr. Suzanne U. Emerson (National Institute of Allergy and Infectious Diseases, NIH, USA) for generously providing the plasmids to generate subgenomic HEV genomic RNA; Prof. Ralf Bartenschlager and Dr. Volker Lohmann (University of Heidelberg, Germany) for providing the HCV replicon cells; Prof. Dr. Charles M. Rice (the Rockefeller University) providing the overexpression lentiviral vector. The authors also

would like to acknowledge the ENCODE Experiment Matrix for providing the RelA and STAT1 ChIP-seq dataset. This research is supported by the European Association for the Study of the Liver (EASL) for a Sheila Sherlock Fellowship (to Q. Pan), the Netherlands Organization for Scientific Research (NWO/ZonMw) for a VENI grant (No. 916-13-032) (to Q. Pan), the Dutch Digestive Foundation (MLDS) for a career development grant (No. CDG 1304) (to Q. Pan), the Daniel den Hoed Foundation for a Centennial Award fellowship (to Q. Pan), the Erasmus MC Mrace grant (to Q. Pan), the China Scholarship Council for funding PhD fellowships to W. Wang (201303250056), Y. Wang (201207720007), X. Zhou (201206150075), Y. Yin (201307720045) and L. Xu (201306300027) and Indonesia Endowment Fund for Education (LPDP) PhD fellowship to Mohamad S. Hakim.

Supplementary Materials and Methods

Reagents

Recombinant human TNF-α (Peprotech, USA) and human IFN-α (Thermo Scientific, the Netherlands) was dissolved in PBS. Stocks of JAK inhibitor 1 (Santa Cruz Biotech, CA) and Bayer-18 (Synkinase, China) were dissolved in DMSO with a final concentration of 5 mg/mL. Antibodies phospho-STAT1 (Tyr701) (58D6, #9167), STAT1 (#9172), RelA (P65) (C22B4, #4764), IRF1 (D5E4), IRF7 (D2A1J), Anti-rabbit IgG(H+L), F(ab') 2 Fragment (Alexa Fluor 488 conjugate) and Anti-mouse IgG (H+L), F(ab')2 Fragment (Alexa Fluor® 488 Conjugate) were purchased from Cell Signaling Technology. IRF9 antibody was obtained from LSBio (Life Span BioSciences, Inc.). β-actin, STAT2 (sc-476), phospho-STAT2 (Tyr690) were purchased from Santa Cruz Biotechnology; anti-rabbit or anti-mouse IRDye-conjugated antibodies were used as secondary antibodies for western blotting (Stressgen, Victoria, BC, Canada).

Cell models

The HCV subgenomic replicon comprised Huh7 cells containing a subgenomic HCV bicistronic replicon (1389/NS3-3V/LucUbiNeo-ET) linked to the *firefly* luciferase reporter gene were maintained with 250 μg/mL G418 (Sigma, Zwijndrecht, the Netherlands). The HEV subgenomic model was based on Huh7 cells containing the subgenomic HEV sequence (Kernow-C1 p6/luc) coupled to a *Gaussia* luciferase reporter gene. Luciferase normalization cells (LV-PGK-Luc) were generated by transducing Huh7 cells with a lentiviral vector expressing the *firefly* luciferase gene under control of the human phosphoglycerate kinase

(PGK) promoter. ISRE, NF-κB, AP-1 luciferase reporter cells were generated by transducing Huh7 cells with lentiviral vectors expressing the *firefly* luciferase gene under the control of the promoters containing the ISRE, NF-κB, AP-1 motifs, respectively (System Biosciences).

Gene knockdown or overexpression by lentiviral vectors

Lentiviral pLKO.1 knockdown vectors (Sigma-Aldrich) targeting IRF1, IRF7, STAT1, TNFR1, RelA (P65) were obtained from the Erasmus Biomics Center and produced in HEK293T cells. After a pilot study, the shRNA vectors exerting optimal gene knockdown were selected. Stable gene knockdown cells were generated after lentiviral vector transduction and puromycin (2 μg/mL; Sigma) selection. IRF1, IFI6 and DDX58 lentiviral overexpression vectors were a kind gift from Prof. Charles M. Rice, the Rockefeller University [23]. Meanwhile, two control vectors expressing reporter genes *Photinus pyralis* luciferase (Fluc) or Green fluorescent protein (GFP) were also used.

Measurement of luciferase activity

For *Gaussia* luciferase analysis, the activity of secreted luciferase in the cell culture medium was measured by BioLux® *Gaussia* Luciferase Flex Assay Kit (New England Biolabs) according to the manufacturer's instructions. For *firefly* luciferase, luciferin potassium salt (100 mM; Sigma) was added to cells and incubated for 10 min at 37 °C The luciferase activity was quantified with a LumiStar Optima luminescence counter (BMG Lab Tech, Offenburg, Germany).

Quantitative real-time polymerase chain reaction

RNA was isolated with a Machery-NucleoSpin RNA II kit (Bioke, Leiden, The Netherlands) and quantified using a Nanodrop ND-1000 (Wilmington, DE, USA). cDNA was synthesized from total RNA using a cDNA Synthesis Kit (TAKARA BIO INC). The cDNA of all detected genes was amplified for 50 cycles and quantified with a SYBR-Green-based real-time PCR (Applied Biosystems) according to the manufacturer's instructions. GAPDH and RP2 were considered as reference genes to normalize gene expression. All the primer sequences are included in Supplemental Table 2.

Western Blot Assay

Cultured cells were lysed in Laemmli sample buffer containing 0.1 M DTT and heated 5 mins at 95 °C, followed by loading onto a 10% sodium dodecyl sulfate polyacrylamide gel and

separation by electrophoresis. After 90 mins running at 120 V, proteins were electrophoretically transferred onto a polyvinylidene difluoride membrane (Invitrogen) for 1.5 hrs with an electric current of 250 mA. Subsequently, the membrane was blocked with a mixture of 2.5 mL blocking buffer (Odyssey) and 2.5 mL phosphate-buffered saline containing 0.05% Tween 20. It was followed by overnight incubation with primary antibodies (1: 1 000) at 4 °C. The membrane was washed 3 times followed by incubation for 1 h with IRDye-conjugated secondary antibody (1: 5 000). After washing 3 times, protein bands were detected with the Odyssey 3.0 Infrared Imaging System.

Enzyme-linked immunosorbent assay (ELISA)

Serum samples were collected and stored at -80 °C. TNF-α level was measured by an ELISA kit (eBioscience, USA) according to manufacturer's instructions. The absorbance was measured at 450 nm in an automatic microplate reader. Results were calculated based on a standard curve.

Confocal laser electroscope assay

Huh7 cells were seeded on glass coverslips. After 12 hrs, cells were washed with PBS, fixed in 4% PBS-buffered formalin for 10 mins and blocked with tween-milk-glycine medium (PBS, 0.05% tween, 5 g/L skim milk and 1.5 g/L glycine). Samples were incubated with primary antibodies overnight at 4 °C. Subsequently, samples were incubated with 1:1 000 dilutions of the anti-mouse IgG (H+L), F(ab')2 Fragment (Alexa Fluor® 488 Conjugate) or anti-rabbit IgG(H+L), F(ab') 2 Fragment (Alexa Fluor 488 conjugate) secondary antibodies. Nuclei were stained with DAPI (4, 6-diamidino-2-phenylindole; Invitrogen). Images were detected using confocal electroscope.

ChIP-seq data analysis

ChIP-seq datasets for STAT1 in Gm12878 cells and RelA in the TNFα stimulated Gm12878 cells were retrieved from the ENCODE database. ChIP-seq datasets were processed and mapped to hg38 reference genome as described [40]. ChIP-seq datasets with multiple replicates were merged. MACS 1.4.2 was used for peak calling and for the generation of binding profiles [41]. MACS was run with -p 1e-10, using the mock control of TNF-α stimulated cell as control dataset for both the STAT1 and RelA ChIP-seq. Heatmaps were generated based on a unified peak list. If the centers of two binding regions reported by MACS were

100 bp or less apart, they were unified to a single binding region. Heatmaps were normalized for each individual factor by calculating the RPM based on the sum of all reads displayed by the heatmap. RPM was log2 transformed and manhattan clustering was performed. The heatmap images were generated in R. The sequencing profiles were generated in the IGV browser [42].

Construction of mutant ISRE reporter cell line

Based on the sequence specific ISRE motif, a mutant version of ISRE was designed and synthesized (Forward: 5'-*aattc*AGTTTCGTCAAGTCTTTCAGTTTCGTCAAGTCTTTCAGTTTCGTCAAGTCTTTCAGTTTCGTCAAGTCTTT*a*-3'; Reverse: 5'-*ctagt*AAAGACTTGACGAAACTGAAAGACTTGACGAAACTGAAAGACTTGACGAAACTGAAAGACTTGACGAAACT*g*-3'), which shows no consensus sequence with the NF-κB motif. EcoRI and SpeI sites are included (shown in italics) to facilitate directional cloning into the pGreenFire Lenti-Reporter vector (System Biosciences). The recombinant plasmid was verified by restriction enzyme digestion and DNA sequencing. Stable mutant ISRE reporter cells were generated after lentiviral vector transduction and puromycin (2 μg/mL; Sigma) selection.

Statistical analysis

All results were presented as mean ± SD. Comparisons between groups were performed with Mann-Whitney test. Differences were considered significant at a P value less than 0.05.

Ethics Statement

The use of serum samples from IBD patients was approved by the Medical Ethical Committee of the Erasmus Medical Center (Medisch Ethische Toetsings Commissie Erasmus MC). The volunteers or patients agreed to participate by written informed consent.

Supplementary Figure and Figure Legends

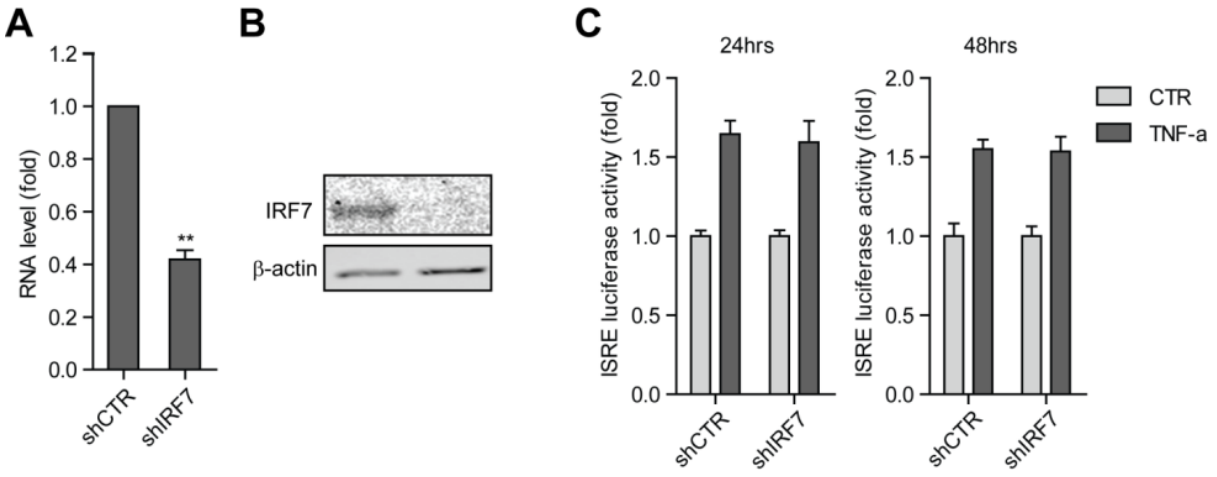

Figure S1. TNF-α induced ISRE activation is independent of IRF7.

(A) qRT-PCR analysis of successful IRF7 knockdown by lentiviral shRNA vectors in the Huh7 based ISRE luciferase reporter cells. (B) Western blot analysis confirmed the successful knockdown of IRF7 by lentiviral shRNA vectors in the Huh7 based ISRE luciferase reporter cells. (C) IRF7 knockdown had no significant influence on TNF-α induced ISRE-related luciferase activation as measured at 2 different time points (n = 3 independent experiments with 2 - 3 replicates each).

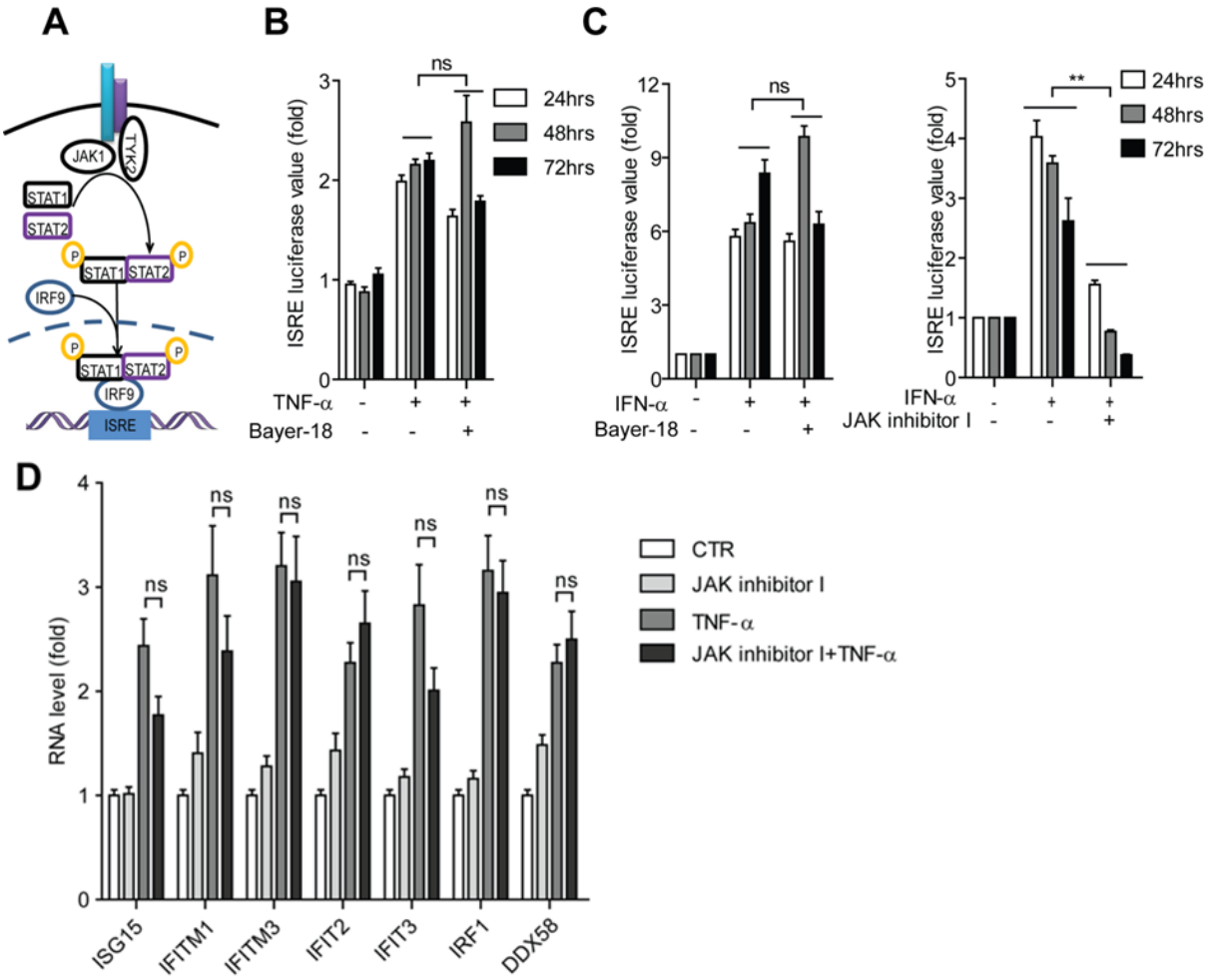

Figure S2. TNF-α induced ISRE activation is independent of interferon and the JAK-STAT signaling.

(A) Illustration of key elements in IFN-α induced JAK-STAT signaling pathway. (B) The selective TYK2 inhibitor, Bayer-18, did not abrogate TNF-α induced ISRE-related luciferase activation (n = 3 independent experiments with 2- 3 replicates each). (C) In Huh7 based ISRE luciferase cells, TYK2 selective inhibitor, Bayer-18, did not exert significant effect on IFN-α (1000 IU/mL) induced ISRE-luciferase activity (left), while JAK inhibitor I (10 μM) abrogated IFN-α (1000 IU/mL) induced ISRE luciferase activity as measured at 24, 48 and 72 hrs (n = 3 independent experiments with 2 - 3 replicates each). (D) JAK inhibitor I exerts no significant influence on TNF-α induced ISG expression as measured by qRT-PCR. (n = 4).

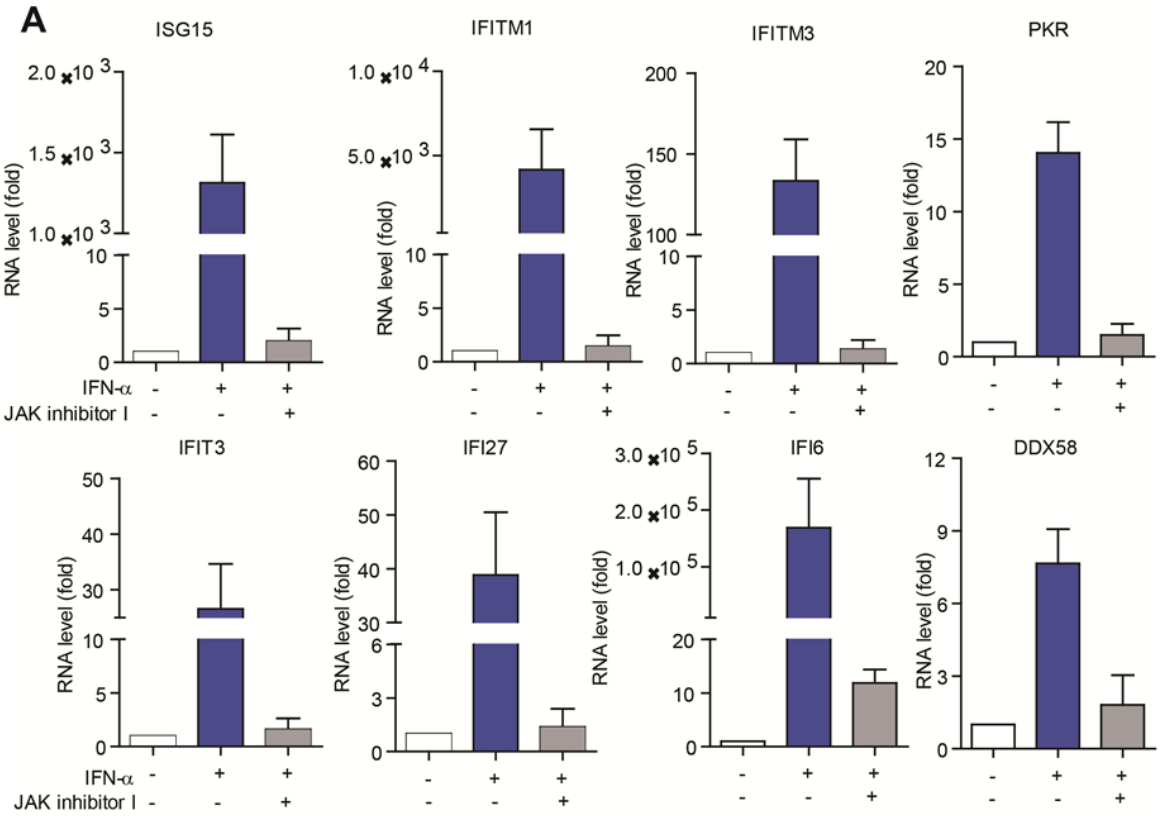

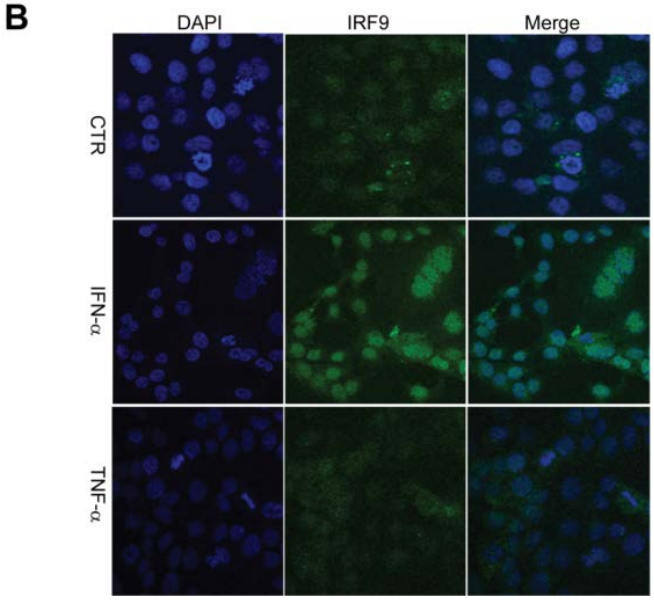

Figure S3. IFN-α induced ISRE activation depends on the JAK-STAT signaling.

(A) In Huh7 cells, JAK inhibitor I (10 μM) abrogated IFN-α (1000 IU/mL) induced ISG expression as measured by qRT-PCR. (B) Confocal microscopy analysis of IRF9 localization in Huh7 cells treated with IFN-α or TNF-α. IRF9 was induced and translocated to the nucleus upon IFN-α, but not TNF-α treatment. IRF9 antibody (green). Nuclei were visualized by DAPI (blue).

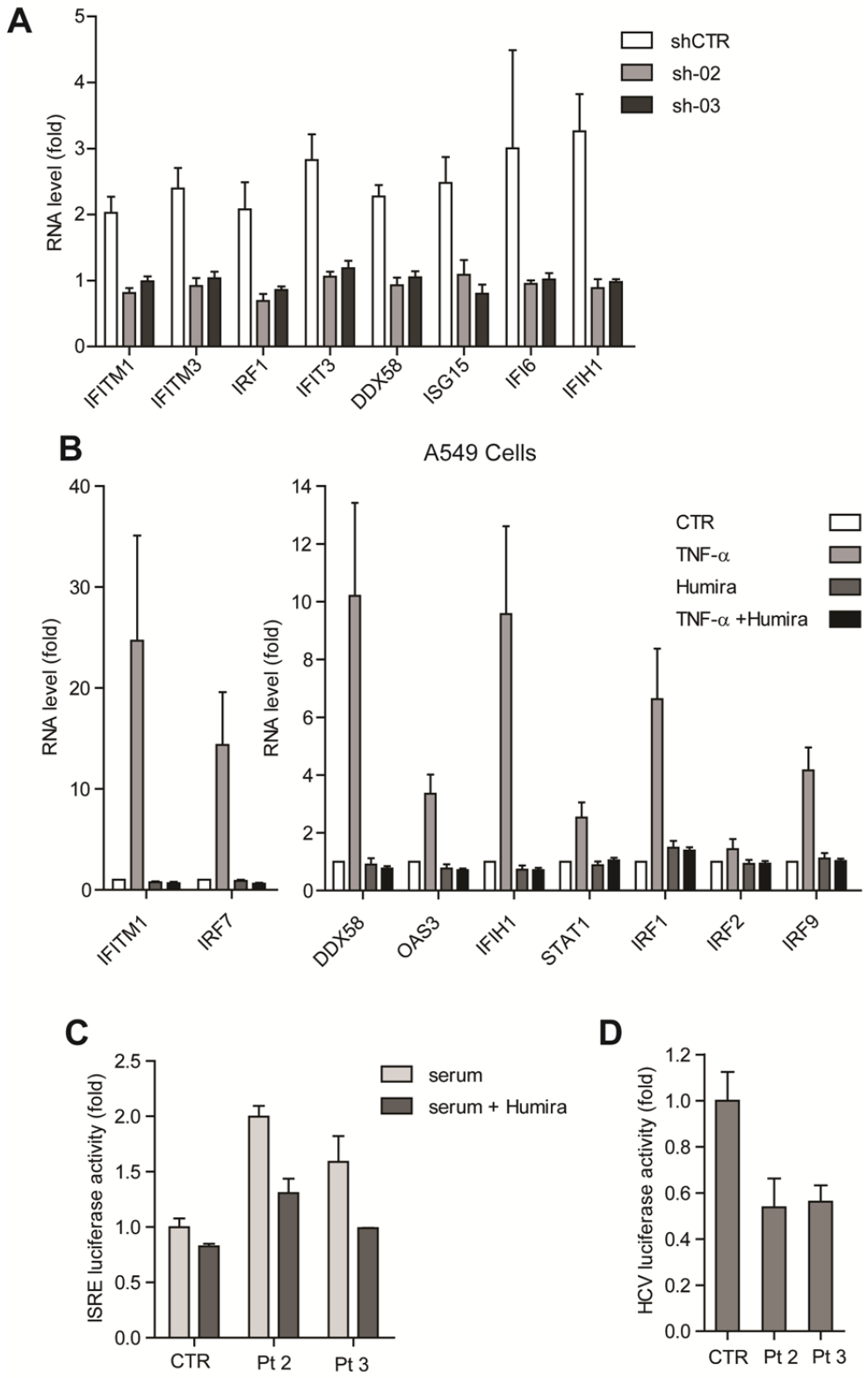

Figure S4. TNF-α activates ISRE via TNF receptor.

(A) TNFR1 knockdown blocked TNF-α induced ISG expression as measured by qRT-PCR (n = 4). (B) In A549 cells, TNF-α inhibitor, Humira, abrogated TNF-α induced ISG expression as measured by qRT-PCR (n = 4). (C) Humira decreased serum samples (with higher TNF-α levels) induced ISRE-related luciferase activity. (D) Serum samples with higher TNF-α levels inhibited HCV-related luciferase activity compared with control serum.

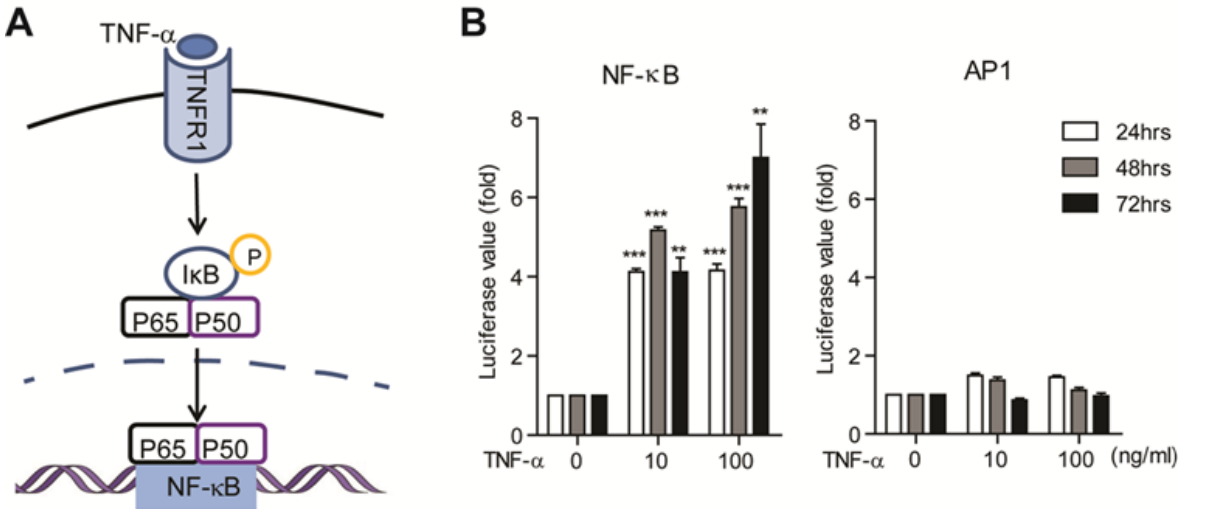

Figure S5. TNF-α efficiently activate NF-κB signaling pathway.

(A) Illustration of key elements in TNF-αinduced NF-κB signaling pathway. (B) In the Huh7 cell-based NF-κB or AP1 luciferase reporter cells, TNF-α dose-dependently induced activation of NF-κB-related luciferase activity, while no significant effect on AP1-related luciferase activity as measured at 3 different time points (n = 3 independent experiments with 2 - 3 replicates each).

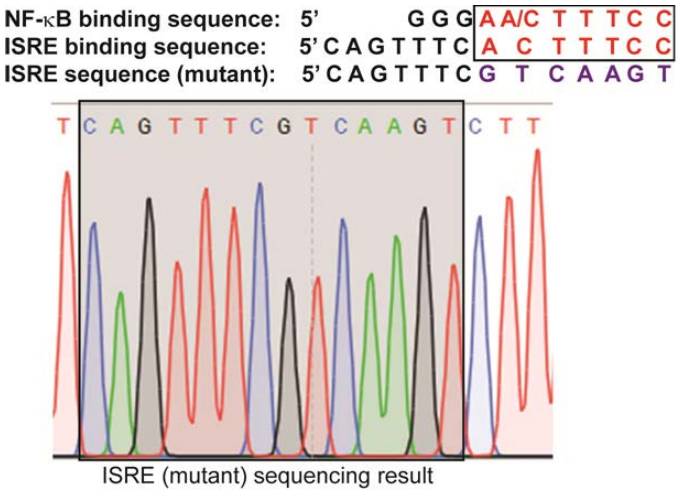

Figure S6. The nucleotide sequence of NF-κB, ISRE and the ISRE mutant binding regions.

Their consensus nucleotides are labeled in red color, and the consensus region is marked in a rectangular box. The mutated nucleotides are shown in purple color. The ISRE (mutant) sequencing result is shown in the illustration below.

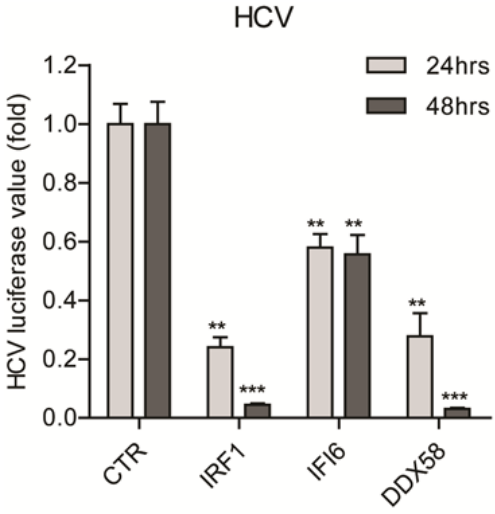

Fig. S7. ISG, *e.g.* IRF1, IFI6 or DDX58 exerts strong antiviral effect against HCV.

Huh7 cell based HCV replicon luciferase reporter was transduced with integrating lentiviral vectors to overexpress ISG, *e.g.* IRF1, IFI6 or DDX58, showing strong antiviral potency against HCV.

References

1. Lin, F.C. and H.A. Young, Interferons: Success in anti-viral immunotherapy. *Cytokine Growth Factor Rev*, 2014. **25**(4): p. 369-76.
2. Pulit-Penaloza, J.A., S.V. Scherbik, and M.A. Brinton, Type 1 IFN-independent activation of a subset of interferon stimulated genes in West Nile virus Eg101-infected mouse cells. *Virology*, 2012. **425**(2): p. 82-94.
3. Mbanwi, A.N. and T.H. Watts, Costimulatory TNFR family members in control of viral infection: outstanding questions. *Semin Immunol*, 2014. **26**(3): p. 210-9.
4. Brenner, D., H. Blaser, and T.W. Mak, Regulation of tumour necrosis factor signalling: live or let die. *Nat Rev Immunol*, 2015. **15**(6): p. 362-74.
5. Nielsen, O.H., New strategies for treatment of inflammatory bowel disease. *Front Med (Lausanne)*, 2014. **1**: p. 3.
6. Murdaca, G., et al., Infection risk associated with anti-TNF-alpha agents: a review. *Expert Opin Drug Saf*, 2015. **14**(4): p. 571-82.
7. Pompili, M., et al., Tumor necrosis factor-alpha inhibitors and chronic hepatitis C: a comprehensive literature review. *World J Gastroenterol*, 2013. **19**(44): p. 7867-73.
8. Mestan, J., et al., Antiviral activity of tumour necrosis factor. Synergism with interferons and induction of oligo-2',5'-adenylate synthetase. *J Gen Virol*, 1988. **69 (Pt 12)**: p. 3113-20.
9. Lee, J., et al., TNF-alpha Induced by Hepatitis C Virus via TLR7 and TLR8 in Hepatocytes Supports Interferon Signaling via an Autocrine Mechanism. *PLoS Pathog*, 2015. **11**(5): p. e1004937.
10. Fink, K., et al., IFNbeta/TNFalpha synergism induces a non-canonical STAT2/IRF9-dependent pathway triggering a novel DUOX2 NADPH oxidase-mediated airway antiviral response. *Cell Res*, 2013. **23**(5): p. 673-90.
11. Bartee, E., et al., The addition of tumor necrosis factor plus beta interferon induces a novel synergistic antiviral state against poxviruses in primary human fibroblasts. *J Virol*, 2009. **83**(2): p. 498-511.
12. Devhare, P.B., et al., Analysis of antiviral response in human epithelial cells infected with hepatitis E virus. *PLoS One*, 2013. **8**(5): p. e63793.
13. Colin, L., et al., The AP-1 binding sites located in the pol gene intragenic regulatory region of HIV-1 are important for viral replication. *PLoS One*, 2011. **6**(4): p. e19084.
14. Yarilina, A., et al., TNF activates an IRF1-dependent autocrine loop leading to sustained expression of chemokines and STAT1-dependent type I interferon-response genes. *Nat Immunol*, 2008. **9**(4): p. 378-87.
15. Keskinen, P., et al., Impaired antiviral response in human hepatoma cells. *Virology*, 1999. **263**(2): p. 364-75.
16. Shimoda, K., et al., Tyk2 plays a restricted role in IFN alpha signaling, although it is required for IL-12-mediated T cell function. *Immunity*, 2000. **13**(4): p. 561-71.
17. Tartaglia, L.A., et al., The two different receptors for tumor necrosis factor mediate distinct cellular responses. *Proc Natl Acad Sci U S A*, 1991. **88**(20): p. 9292-6.
18. Westwick, J.K., et al., Tumor necrosis factor alpha stimulates AP-1 activity through prolonged activation of the c-Jun kinase. *J Biol Chem*, 1994. **269**(42): p. 26396-401.
19. Yin, Y., et al., JNK/AP-1 pathway is involved in tumor necrosis factor-alpha induced expression of vascular endothelial growth factor in MCF7 cells. *Biomed Pharmacother*, 2009. **63**(6): p. 429-35.
20. Wan, F. and M.J. Lenardo, Specification of DNA binding activity of NF-kappaB proteins. *Cold Spring Harb Perspect Biol*, 2009. **1**(4): p. a000067.
21. Hess, J., P. Angel, and M. Schorpp-Kistner, AP-1 subunits: quarrel and harmony among siblings. *J Cell Sci*, 2004. **117**(Pt 25): p. 5965-73.

22. Van Lint, C., A. Burny, and E. Verdin, The intragenic enhancer of human immunodeficiency virus type 1 contains functional AP-1 binding sites. *J Virol*, 1991. **65**(12): p. 7066-72.
23. Schoggins, J.W., et al., A diverse range of gene products are effectors of the type I interferon antiviral response. *Nature*, 2011. **472**(7344): p. 481-5.
24. Carswell, E.A., et al., An endotoxin-induced serum factor that causes necrosis of tumors. *Proc Natl Acad Sci U S A*, 1975. **72**(9): p. 3666-70.
25. Flynn, J.L., et al., Tumor necrosis factor-alpha is required in the protective immune response against Mycobacterium tuberculosis in mice. *Immunity*, 1995. **2**(6): p. 561-72.
26. Huffnagle, G.B., et al., Afferent phase production of TNF-alpha is required for the development of protective T cell immunity to Cryptococcus neoformans. *J Immunol*, 1996. **157**(10): p. 4529-36.
27. Mestan, J., et al., Antiviral effects of recombinant tumour necrosis factor in vitro. *Nature*, 1986. **323**(6091): p. 816-9.
28. Seo, S.H. and R.G. Webster, Tumor necrosis factor alpha exerts powerful anti-influenza virus effects in lung epithelial cells. *J Virol*, 2002. **76**(3): p. 1071-6.
29. Tzeng, H.T., et al., Tumor necrosis factor-alpha induced by hepatitis B virus core mediating the immune response for hepatitis B viral clearance in mice model. *PLoS One*, 2014. **9**(7): p. e103008.
30. Furst, D.E., et al., Adalimumab, a fully human anti tumor necrosis factor-alpha monoclonal antibody, and concomitant standard antirheumatic therapy for the treatment of rheumatoid arthritis: results of STAR (Safety Trial of Adalimumab in Rheumatoid Arthritis). *J Rheumatol*, 2003. **30**(12): p. 2563-71.
31. Mease, P.J., et al., Etanercept in the treatment of psoriatic arthritis and psoriasis: a randomised trial. *Lancet*, 2000. **356**(9227): p. 385-90.
32. Lovell, D.J., et al., Etanercept in children with polyarticular juvenile rheumatoid arthritis. Pediatric Rheumatology Collaborative Study Group. *N Engl J Med*, 2000. **342**(11): p. 763-9.
33. Present, D.H., et al., Infliximab for the treatment of fistulas in patients with Crohn's disease. *N Engl J Med*, 1999. **340**(18): p. 1398-405.
34. Kim, S.Y. and D.H. Solomon, Tumor necrosis factor blockade and the risk of viral infection. *Nat Rev Rheumatol*, 2010. **6**(3): p. 165-74.
35. Vigano, M., et al., Anti-TNF drugs in patients with hepatitis B or C virus infection: safety and clinical management. *Expert Opin Biol Ther*, 2012. **12**(2): p. 193-207.
36. Shale, M.J., et al., Review article: chronic viral infection in the anti-tumour necrosis factor therapy era in inflammatory bowel disease. *Aliment Pharmacol Ther*, 2010. **31**(1): p. 20-34.
37. Yarilina, A. and L.B. Ivashkiv, Type I interferon: a new player in TNF signaling. *Curr Dir Autoimmun*, 2010. **11**: p. 94-104.
38. Gearing, A.J., Targeting toll-like receptors for drug development: a summary of commercial approaches. *Immunol Cell Biol*, 2007. **85**(6): p. 490-4.
39. Pan, Q., et al., Combined antiviral activity of interferon-alpha and RNA interference directed against hepatitis C without affecting vector delivery and gene silencing. *J Mol Med (Berl)*, 2009. **87**(7): p. 713-22.
40. Engelen, E., et al., Proteins that bind regulatory regions identified by histone modification chromatin immunoprecipitations and mass spectrometry. *Nat Commun*, 2015. **6**: p. 7155.
41. Zhang, Y., et al., Model-based analysis of ChIP-Seq (MACS). *Genome Biol*, 2008. **9**(9): p. R137.
42. Robinson, J.T., et al., Integrative genomics viewer. *Nat Biotechnol*, 2011. **29**(1): p. 24-6.

Chapter 8

Unphosphorylated ISGF3 Drives Constitutive Expression of Interferon-stimulated Genes to Protect Against Viral Infections

Wenshi Wang[1], Yuebang Yin[1], **Lei Xu[1]**, Junhong Su[2], Fen Huang[2], Yijin Wang[1], Patrick P C Boor[1], Kan Chen[1], Wenhui Wang[1], Wanlu Cao[1], Xinying Zhou[1], Pengyu Liu[1], Luc J. W. van der Laan[3], Jaap Kwekkeboom[1], Maikel P. Peppelenbosch[1] and Qiuwei Pan[1]

[1]Department of Gastroenterology and Hepatology, Postgraduate School Molecular Medicine, Erasmus MC-University Medical Center, Rotterdam, the Netherlands

[2]Medical Faculty, Kunming University of Science and Technology, Kunming, PR China

[3]Department of Surgery, Postgraduate School Molecular Medicine, Erasmus MC-University Medical Center, Rotterdam, the Netherlands

Science Signaling. 2017. In Press.

Abstract

Interferon-stimulated genes (ISGs) are antiviral effectors that are efficiently induced by interferons (IFNs) via the formation of a tripartite transcription factor ISGF3 (IRF9, phosphorylated STAT1 and STAT2). However, we found that IFN-independent ISG expression was detectable in immortalized cell lines, primary intestinal and liver organoids, and liver tissues. We report that the constitutive expression of ISGs was mediated by the unphosphorylated ISGF3 (U-ISGF3) complex, which was formed by IRF9 together with unphosphorylated STAT1 and STAT2. Under homeostatic conditions, the nuclear localization of endogenous STAT1, STAT2, and IRF9 was observed. Analysis of a chromatin immunoprecipitation–sequencing (ChIP-seq) dataset revealed that STAT1 specifically bound to the promoters of ISGs even in the absence of IFNs. Knockdown of STAT1, STAT2, or IRF9 by RNA interference (RNAi) led to the decreased expression of a range of ISGs in Huh7.5 cells, which was confirmed in mouse embryonic fibroblasts (MEFs) from STAT1-/-, STAT2-/-, or IRF9-/- mice. Furthermore, decreased ISG expression was accompanied by the increased replication of hepatitis C virus (HCV) and hepatitis E virus (HEV). Conversely, simultaneous overexpression of all of the ISGF3 components, but not any single factor, induced the expression of ISGs and inhibited viral replication. However, no phosphorylated STAT1 and STAT2 was detected. Substitution of wild-type STAT1 with a phosphorylation-deficient mutant had comparable effect on IFN-independent expression of ISGs or antiviral activity, suggesting that ISGF3 works in a phosphorylation-independent manner. These data suggest that the U-ISGF3 complex is both necessary and sufficient for constitutive ISG expression and antiviral immunity under homeostatic conditions.

Keywords: U-ISGF3; HCV; HEV; basal ISG; transcription

Introduction

Interferon-stimulated genes (ISGs) are hardwired within genomes and provide a robust first line of defense against invading pathogens. Canonically, following pathogen invasion and interferon (IFN) stimulation, IFN receptors respond with activation of the Janus kinases JAK1 and TYK2, which in turn phosphorylate tyrosine residues in the intracellular tail of the IFN receptors. Subsequently, STAT1 and STAT2 are phosphorylated, which provokes dimerization and subsequent binding to interferon regulatory factor 9 (IRF9) to form the IFN-stimulated gene factor 3 (ISGF3) complex. The ISGF3 complex translocates into the nucleus, and binds to specific promotor elements denoted as IFN-stimulated response elements (ISREs), leading to the rapid transcriptional activation of hundreds of ISGs. This leads to an effective antiviral state against positive-, negative-, and double-stranded RNA viruses, DNA viruses, and intracellular bacteria and parasites [1]. Interestingly, an IFN regulated non-canonical mechanism of ISG transcription was recently reported. When cells are continuously exposed to a low amount of exogenous interferon, unphosphorylated ISGF3 (U-ISGF3), formed by interferon induced IRF9 and unphosphorylated STAT1 and STAT2, leads to steady-state increased expression of a subset of ISGs [2].

In the absence of interferon activation, constitutive ISG expression is also critical in determining cellular susceptibility to viral infection [3]. Inefficient replication of influenza A virus has been reported in human bronchial epithelial cells (BEAS-2B) with a higher expression level of basal ISGs, compared with other respiratory epithelial cell lines [4]. Similar observation was reported with regard to reovirus replication in cardiac myocytes [5, 6]. Conversely, abnormal regulation of basal ISG expression is associated with adverse consequences in patients. Patients with chronic hepatitis C virus (HCV) infection who have abnormally high levels of basal ISG expression in the liver are prone to poor sustained virologic response (SVR) to pegylated IFN-α and ribavirin therapy [7, 8]. Abnormally high expression levels of basal ISGs have been reported to promote tumor growth, and confer resistance to chemotherapy and radiotherapy [9, 10]. Thus, the question as to the mechanisms maintaining and determining the level of constitutive ISG expression is of utmost importance.

Here, we report that under homeostatic status, nuclear localization of endogenous STAT1, STAT2 and IRF9 were observed in cell lines, 3-D cultured primary intestinal and liver organoids, and liver tissues. In the absence of interferons, constitutive ISG expression is

mediated by endogenous U-ISGF3 complex, formed by IRF9, and unphosphorylated STAT1 and STAT2. This process is totally independent of IFN production and the upstream elements of IFN signaling, but effectively confers resistance of host cells to HCV and HEV infections. Thus, the endogenous U-ISGF3 complex is both necessary and sufficient for sustaining constitutive ISG transcription and antiviral immunity in host cells under homeostatic condition.

Results

Constitutive ISG transcription is independent of IFN production

The profile of constitutive ISG expression in human liver tissue, 3D-cultured primary human liver and intestinal organoids (fig. S1A), and three different cell lines (Huh7.5, Caco2, and A549) was quantified by quantitative reverse-transcription polymerase chain reaction (qRT-PCR) analysis. ISG expression was readily detectable in all tested models under homeostatic conditions (Fig. 1, A and B). This finding was further confirmed by the quantification of the gene copy numbers of four representative ISGs, as normalized to the corresponding plasmid template using a standard curve calculation method (Fig. 1C and fig. S1B).

The classical role of IFN in the induction of ISG expression prompted us to investigate the potential involvement of IFN in our system. Thus, we collected conditioned medium from these cultured cells (after 48 hours) and added to a transcriptional reporter system that mimics IFN response with a luciferase reporter gene that was driven by multiple ISREs (ISRE-Luc). Cell culture medium from all three cell lines failed to stimulate any response in the ISRE-luc model(Fig. 1D). Consistently, the conditioned medium failed to stimulate ISG expression in Huh7.5 cells (fig. S1C). In addition, conditioned culture medium was also used to perform a functional assay on the IFN sensitive HCV-replicon model, Huh7.5-HCV-luc; however, we found that the culture media did not affect HCV replication (Fig. 1E). JAK1 is the key upstream component that drives the activation of IFN signaling. IFN-α-stimulated STAT1 phosphorylation and ISG expression were blocked by a pharmacological JAK inhibitor, JAK inhibitor I (fig. S2, A and B). However, JAK inhibitor I did not decrease constitutive ISG expression in Huh7.5, Caco2, or A549 cells (Fig. 1F and fig. S2, C and D). Together, these data suggest that constitutive ISG expression is independent of IFN production.

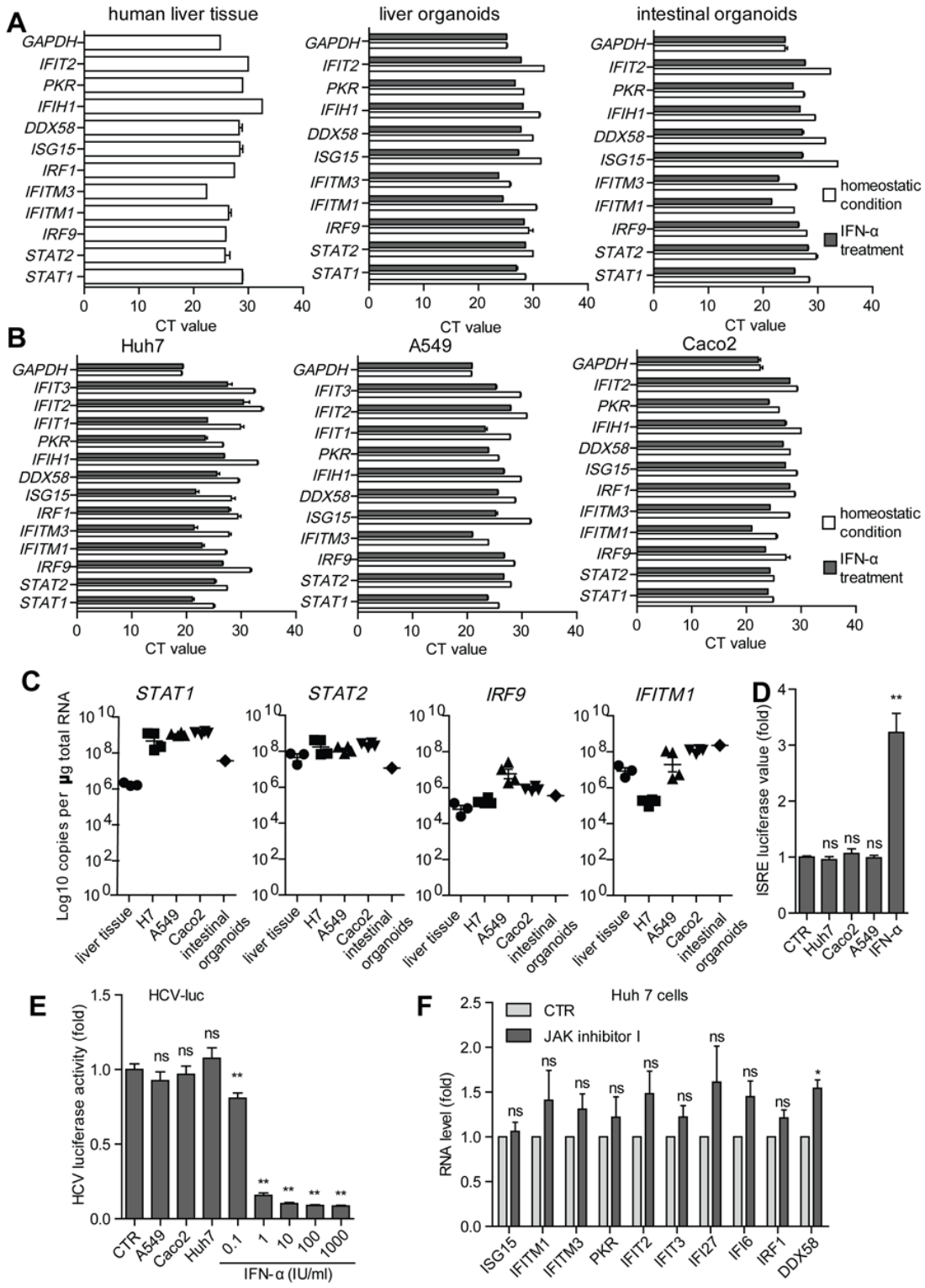

Figure 1. Cell sustains basal ISG transcription independent of interferon production.

(**A** and **B**) Total RNA was extracted from human liver tissue samples, primary human liver organoids, human intestinal organoids (A), and from Huh7.5 cells, A549 cells, and Caco2 cells (B). The relative abundances of mRNAs of the indicated ISGs were quantified by qRT-PCR. Human liver organoids, intestinal organoids, Huh7.5 cells, A549 cells, and Caco2 cells treated for 24 hours with IFN-α (1000 IU/ml) served as the positive controls for ISG expression. *GAPDH* was used as reference gene. Data are means ± SEM from three independent experiments. (**C**) The gene copy numbers of the four indicated ISGs were quantified relative to the appropriate plasmid templates using a standard curve

calculation method. Data are means ± SEM from three independent experiments. (**D**) Huh7.5-ISRE-luccells were left untreated or were treated for 24 hours with conditioned medium from Huh7.5, Caco2, or A549 cells or with IFN-α (10 IU/ml) as a positive control. ISRE luciferase values were then measured and the fold-increase in activity relative to that of untreated cells was determined. Data are means ± SEM from three independent experiments. (**E**) HCV viral replication-related firefly luciferase activity was measured upon the treatment of Huh7.5-HCV-luc cells with conditioned medium from Huh7.5, Caco2, or A549 cells. As a positive control, the cells were treated with the indicated range of concentrations of IFN-α. Data are means ± SEM from three independent experiments. (**F**) Huh7.5 cells were treated with vehicle (CTR) or with 5 μM JAK inhibitor I for 24 hours before being subjected to qRT-PCR analysis of the relative abundances of the indicated mRNAs. Data are means ± SEM of four independent experiments. **P* < 0.05; ***P* < 0.01; ns, not significant.

STAT1, STAT2, and IRF9 are required for constitutive ISG transcription and they constrain HCV and HEV replication

Upon IFN stimulation, STAT1 is a vital transcription factor to drive ISG transcription. Thus, we first examined the role of STAT1 in basal ISG transcription under homeostatic conditions. Because nuclear localization is a primary determinant for the transcriptional function of STAT1, we investigated the cellular location of endogenous STAT1. We found that the staining of endogenous STAT1 protein in both cytoplasm and nucleus was apparent. in human and mouse liver tissue samples as determined by immunohistochemistry (IHC) (Fig. 2A). Consistently, the cellular localization of STAT1 was similar in primary human liver and intestinal organoids and in three different cell lines (Fig. 2, B to E, fig. S3, A and B). To investigate whether STAT1 in the cell nucleus could bind to the promoter regions of ISGs, we retrieved genome-wide STAT1 ChIP-seq data (GSE31477) from the ENCODE ChIP-seq Experiment Matrix database and Gene Expression Omnibus [11]. The STAT1 ChIP-seq datasets were then processed and analyzed. Even without IFN stimulation, STAT1 showed specific binding peaks on the promoter regions of a large cohort of ISGs (186 out of 350 ISGs analyzed), including IRF1, IRF9, STAT1, and ISG15 (Fig. 2F), whereas rabbit immunoglobulin G (IgG, which was the negative control) showed no specific binding peak.

To further investigate the role of STAT1 in basal ISG expression, Huh7.5 cells were transduced with an integrating lentiviral vector expressing STAT1-specific short hairpin RNA (shRNA), which resulted in a marked decrease in STAT1 abundance (Fig. 3A). Knockdown of endogenous STAT1 led to the decreased expression of 13 out of 14 tested ISGs, with inhibitory efficiency ranging from 30 to 90% (Fig. 3B). In addition, we performed experiments with mouse embryonic fibroblasts (MEFs) from wild-type (WT) and STAT1$^{-/-}$

mice to examine the effect of STAT1 on ISG expression (Fig. 3, C and D). We found that the abundances of ISG mRNAs were reduced in STAT1$^{-/-}$ MEFs compared to those in WT MEFs (Fig. 3E). Furthermore, shRNA mediated STAT1 knockdown increased viral replication of HCV (2.2-fold) (Fig. 3F) and HEV (1.7-fold) (Fig. 3G) compared to its shRNA control in Huh7.5-based HCV-luc and HEV-luc models. In contrast, over-expression of STAT1 did not substantially affect ISG expression or viral replication (Fig. 3, H to J), suggesting that STAT1, although important for such responses, does not work alone.

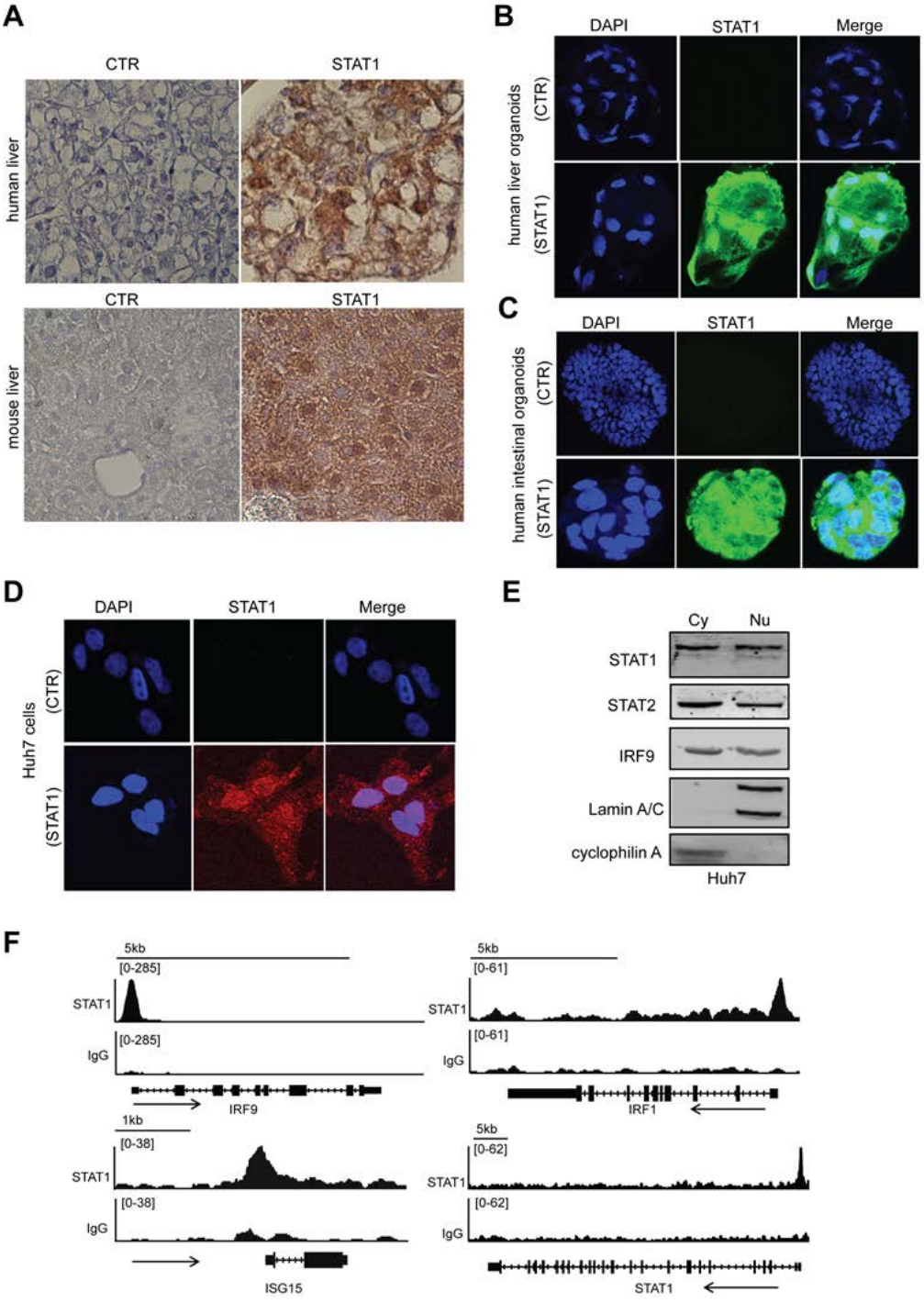

Figure 2. A substantial fraction of endogenous STAT1 is localized in the nucleus and binds to ISG promoters under homeostatic conditions.

(**A**) Representative immunohistochemical staining analysis of the cellular localization of endogenous STAT1 in cells in human (top) and mouse (bottom) liver sections. As a negative control (CTR), primary antibody against STAT1 was replaced with PBS containing 0.05% Tween. Images are representative of three independent experiments. (**B** to **D**) Confocal laser electroscope analysis of endogenous STAT1 localization in human liver organoids (B), human intestinal organoids (C), and Huh7.5 cells (D). STAT1 is shown in green in organoids and in red in Huh7.5 cells. Nuclei were visualized by DAPI (blue). As a negative control (CTR), primary antibody against STAT1 was replaced with PBS containing 0.05% Tween. Images are representative of multiple organoids or cells from three independent experiments. (**E**) Huh7.5 cell lysates were fractionated into cytoplasmic (Cy) and nuclear (Nu) fractions and then were analyzed by Western blotting with antibodies against the indicated proteins. Cyclophilin A and Lamin A/C were used as cytosolic and nuclear markers, respectively. Western blots are representative of three independent experiments. (**F**) The ChIP-seq dataset for STAT1 (GSE31477) was retrieved from the ENCODE database. Binding profiles of endogenous STAT1 to the promoter regions of the indicated ISGs. Sequence reads from anti-STAT1 antibody or rabbit-IgG-control ChIP-seq data were plotted relative to chromosomal position. The genome locations of the corresponding ISGs are shown beneath the track signaling.

Next, we examined the involvement of STAT2. Under homeostatic conditions, STAT2 was abundantly present in both the cytoplasm and nuclei of human liver tissue, human liver organoids, human intestinal organoids, and cell lines (Fig. 4, A to D). Furthermore, knockdown of STAT2 by lentiviral shRNA (Fig. 4E) led to the decreased expression of ISGs (10 out of 12 tested ISGs), ranging from a 30 to 70% decrease (Fig. 4F). MEFs from $STAT2^{-/-}$ mice (Fig. 4G) had reduced amounts of many ISG mRNAs compared to those in WT MEFs (Fig. 4H). ShRNA mediated STAT2 knockdown increased replication of HCV (1.5-fold) (Fig. 4I) and HEV (1.6-fold) (Fig. 4J) compared to its shRNA control in Huh7.5-based HCV-luc and HEV-luc models. However, overexpression of STAT2 did not affect either ISG expression or viral replication (Fig. 4, K to M), mirroring the results obtained from experiments with overexpressed STAT1.

Finally, the role of IRF9 was also investigated. Substantial nuclear localization of IRF9 was observed in human and mouse liver tissues (Fig. 5A), human liver organoids (Fig. 5B), human intestinal organoids (Fig. 5C), and Huh7.5 cells (Fig. 5D). Knockdown of endogenous IRF9 by lentiviral vector based IRF9-specific shRNA (Fig. 5E) resulted in decreased ISG expression in Huh7.5 cells (Fig. 5F). Consistently, compared with WT MEFs, $IRF9^{-/-}$ MEFs (Fig. 5G) had reduced amounts of ISG mRNAs under homeostatic conditions (Fig. 5H). ShRNA mediated IRF9 knockdown increased replication of both HCV (3.8-fold) (Fig. 5I) and HEV (1.8-fold) (Fig. 5J) compared to its shRNA control in Huh7.5-based HCV-luc and HEV-luc models. Over-expression of IRF9 in Huh7.5 cells had no effect on ISG expression (Fig. 5K).

Whereas overexpression of IRF9 in these cells inhibited HCV replication (Fig. 5L), it had no effect on HEV replication (Fig. 5M). The idea that the reduced replication of HCV was ISG-independent was supported by the observation that over-expression of IRF9 in Caco2 cells had no substantial effect on either ISG expression or rotavirus replication (fig. S3, C and D). Together, these results suggest that STAT1, STAT2, and IRF9 are all required and likely cooperate to regulate the basal expression of ISGs.

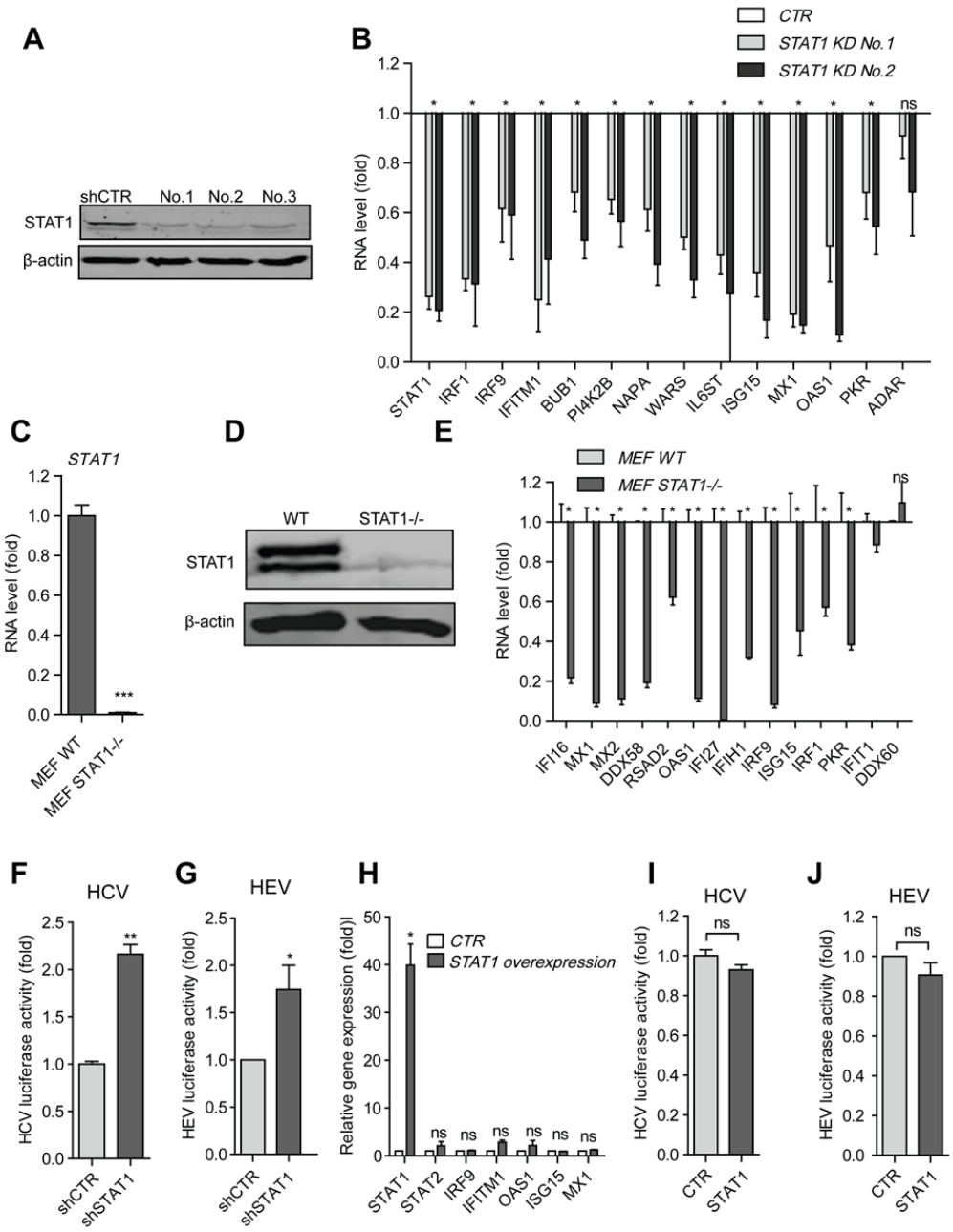

Figure 3. STAT1 is required for sustaining the basal expression of ISGs and constraining viral replication

(**A**) Huh7.5 cells were transduced with lentiviruses expressing control shRNA (shCTR) or three different STAT1-targeting shRNAs. After the puromycin selection for two weeks, cells were analyzed by Western blotting with antibodies against the indicated proteins. Western blots are representative

of three independent experiments. (**B**) Huh7.5 cells expressing control shRNA or the indicated STAT1-specific shRNAs were analyzed by qRT-PCR to determine the relative abundances of the indicated mRNAs. Data are means ± SEM of four independent experiments. (**C**) WT and STAT1$^{-/-}$ MEFs were analyzed by qRT-PCR to determine the relative abundance of *STAT1* mRNA. Data are means ± SEM of four independent experiments. (**D**) WT and STAT1$^{-/-}$ MEFs were analyzed by Western blotting with antibodies against the indicated proteins. Western blots are representative of three independent experiments. (**E**) WT and STAT1$^{-/-}$ MEFs were subjected to qRT-PCR analysis of the relative abundance of the indicated mRNAs. Data are means ± SEM of three independent experiments. (**F**) HCV replicon positive Huh7.5 cells were transduced with lentiviruses expressing control or STAT1-specific shRNAs before being subjected to a HCV replication–related luciferase activity. Data are means ± SEM of three independent experiments. (**G**) HEV replicon positive Huh7.5 cells were transduced with lentiviruses expressing control or STAT1-specific shRNAs before being subjected to a HEV replication–related luciferase activity. Data are means ± SEM of three independent experiments. (**H**) Huh7.5 cells transduced with lentivirus expressing control or STAT1-specific shRNA were subjected to qRT-PCR analysis of the relative abundances of the indicated mRNAs. Data are means ± SEM of three independent experiments. (**I** and **J**) HCV replicon positive (I) and HEV replicon positive (J) Huh7.5 cells transduced with control lentivirus or with lentivirus expressing STAT1 were subjected to qRT-PCR analysis of the relative abundances of the indicated mRNAs. Data are means ± SEM of three independent experiments. **P* < 0.05; ***P* < 0.01; ****P* < 0.001; ns, not significant.

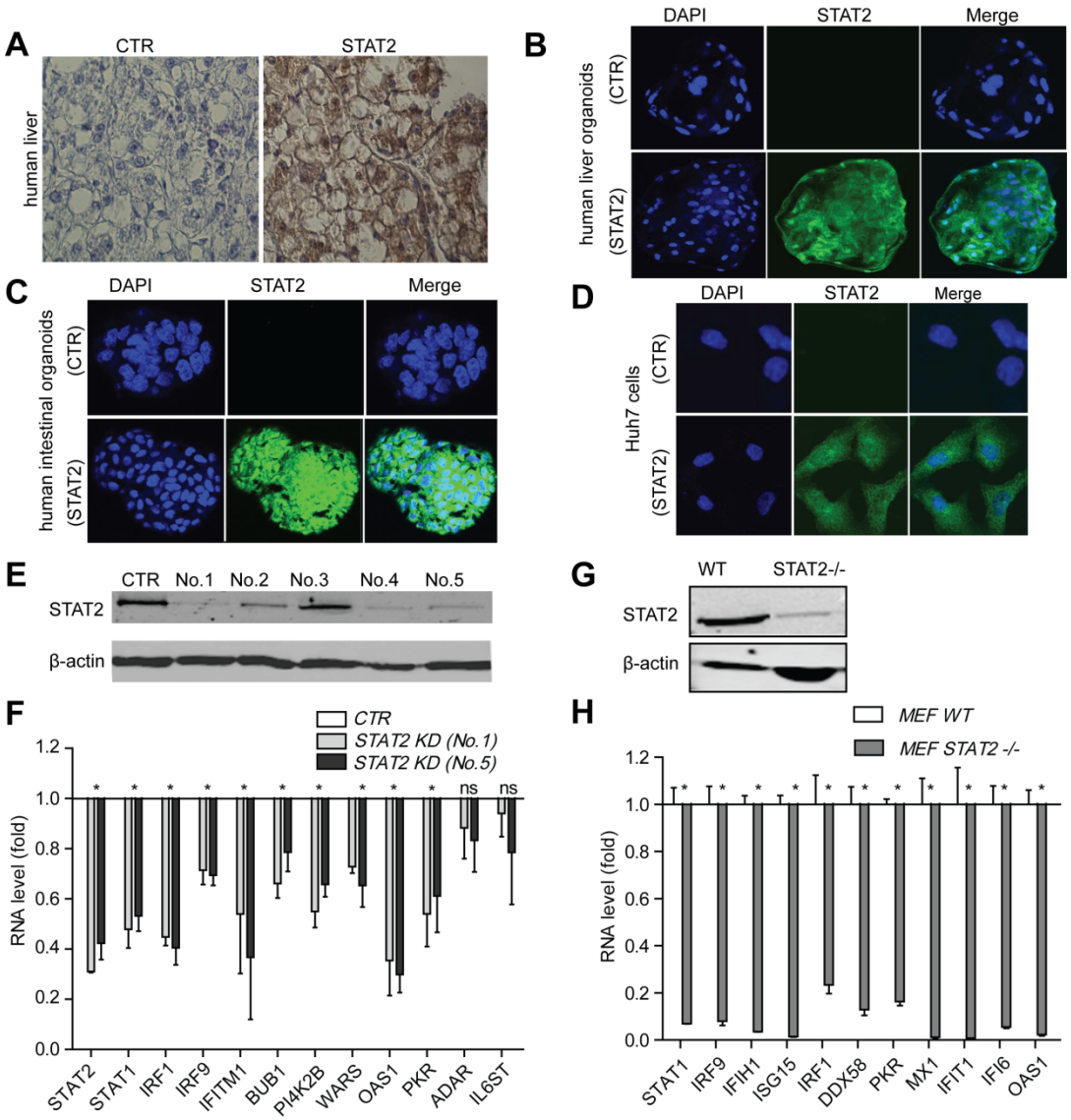

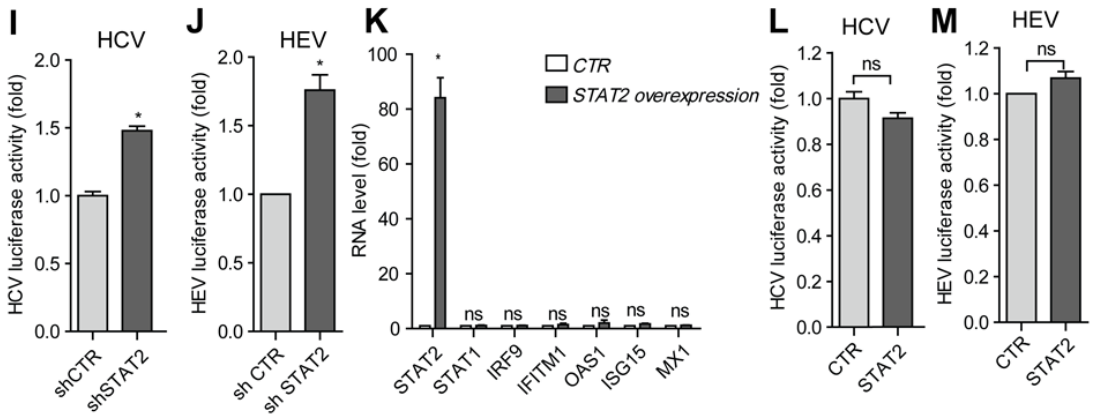

Figure 4. STAT2 is essential for sustaining the basal expression of ISGs and constraining viral replication.

(**A**) Immunohistochemical staining of the cellular localization of endogenous STAT2 in cells from human liver tissue. As a negative control, primary antibody against STAT2 was replaced with PBS containing 0.05% Tween. Images are representative of three independent experiments. (**B** to **D**) Confocal laser electroscope analysis of the cellular localization of endogenous STAT2 in human liver organoids (B), human intestinal organoids (C), and Huh7.5 cells (D). STAT2 antibody staining is shown in green, whereas nuclei were visualized by DAPI (blue). As a negative control, primary antibody against STAT2 was replaced with PBS containing 0.05% Tween. Images are representative of multiple organoids or cells from three independent experiments. (**E**) Huh7.5 cells transduced with lentiviruses expressing control shRNA or the indicated STAT2-specific shRNAs were analyzed by Western blotting with antibodies against the indicated proteins. Western blots are representative of three independent experiments. (**F**) Huh7.5 cells expressing control shRNA or the indicated STAT2-specific shRNAs were analyzed by qRT-PCR to determine the relative abundances of the indicated mRNAs. Data are means ± SEM of four independent experiments. (**G**) WT and $STAT2^{-/-}$ MEFs were analyzed by Western blotting with antibodies against the indicated proteins. Western blots are representative of three independent experiments. (**H**) WT and $STAT2^{-/-}$ MEFs were subjected to qRT-PCR analysis of the relative abundance of the indicated mRNAs. Data are means ± SEM of three independent experiments. (**I** and **J**) HCV replicon positive (I) and HEV replicon positive (J) Huh7.5 cells were transduced with lentiviruses expressing control or STAT2-specific shRNAs before being subjected to assays of viral replication–related luciferase activity. Data are means ± SEM of three independent experiments. (**K**) Huh7.5 cells transduced with control lentivirus or with lentivirus expressing STAT2 were subjected to qRT-PCR analysis of the relative abundances of the indicated mRNAs. Data are means ± SEM of three independent experiments. (**L** and **M**) HCV-positive (L) and HEV-positive (M) Huh7.5 cells transduced with control lentivirus or with lentivirus expressing STAT2 were subjected to qRT-PCR analysis of the relative abundances of the indicated mRNAs. Data are means ± SEM of three independent experiments. **P* < 0.05; ***P* < 0.01; ns, not significant.

STAT1, STAT2, and IRF9 function as the U-ISGF3 complex to drive ISG expression and exert antiviral effects against HCV and HEV

Because STAT1, STAT2, and IRF9 alone were all necessary, but not sufficient, to drive constitutive ISG expression, we investigated whether these three factors in combination functioned as the ISGF3 complex independently of activation by exogenous IFN. Thus, we over-expressed STAT1, STAT2, and IRF9 in Huh7.5 cells through lentiviral transduction (Fig. 6

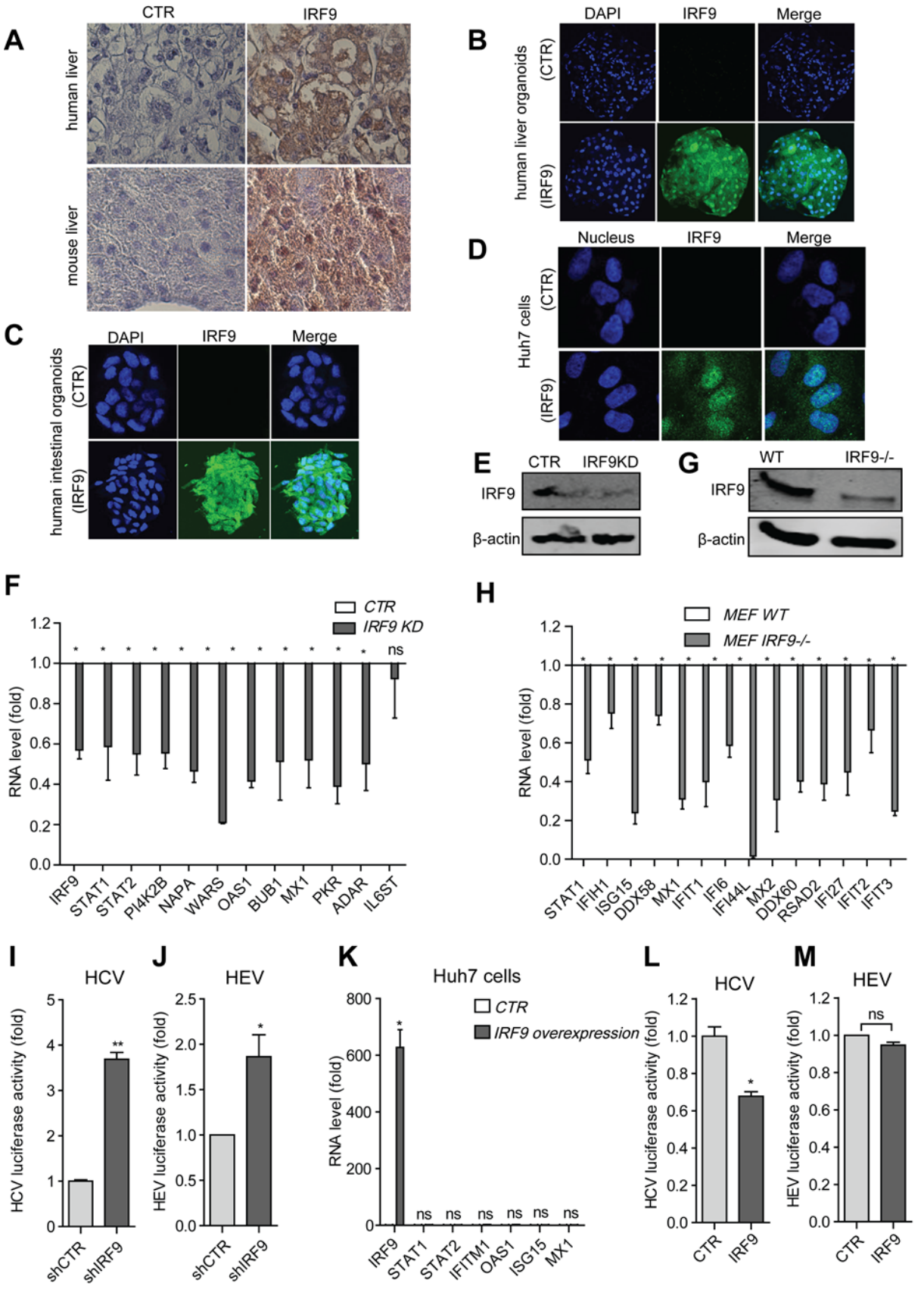

Figure 5. IRF9 is also required for the basal expression of ISGs and for limiting viral replication.

(**A**) Immunohistochemical staining of the cellular localization of endogenous IRF9 in cells from human (top) and mouse (bottom) liver tissue. As a negative control, primary antibody against IRF9 was

replaced with PBS containing 0.05% Tween. Images are representative of three independent experiments. (**B** to **D**) Confocal laser electroscope analysis of the cellular localization of endogenous IRF9 in human liver organoids (B), human intestinal organoids (C), and Huh7.5 cells (D). IRF9 antibody staining is shown in green, whereas nuclei were visualized by DAPI (blue). As a negative control, primary antibody against IRF9 was replaced with PBS containing 0.05% Tween. Images are representative of multiple organoids or cells from three independent experiments. (**E**) Huh7.5 cells transduced with lentiviruses expressing control shRNA or IRF9-specific shRNAs were analyzed by Western blotting with antibodies against the indicated proteins. Western blots are representative of three independent experiments. (**F**) Huh7.5 cells expressing control shRNA or IRF9-specific shRNAs were analyzed by qRT-PCR to determine the relative abundances of the indicated mRNAs. Data are means ± SEM of four independent experiments. (**G**) WT and IRF9$^{-/-}$ MEFs were analyzed by Western blotting with antibodies against the indicated proteins. Western blots are representative of three independent experiments. (**H**) WT and IRF9$^{-/-}$ MEFs were subjected to qRT-PCR analysis of the relative abundance of the indicated mRNAs. Data are means ± SEM of three independent experiments. (**I** and **J**) HCV-positive (I) and HEV-positive (J) Huh7.5 cells were transduced with lentiviruses expressing control or IRF9-specific shRNAs before being subjected to assays of viral replication–related luciferase activity. Data are means ± SEM of three independent experiments. (**K**) Huh7.5 cells transduced with control lentivirus or with lentivirus expressing IRF9 were subjected to qRT-PCR analysis of the relative abundances of the indicated mRNAs. Data are means ± SEM of three independent experiments. (**L** and **M**) HCV-positive (L) and HEV-positive (M) Huh7.5 cells transduced with control lentivirus or with lentivirus expressing IRF9 were subjected to qRT-PCR analysis of the relative abundances of the indicated mRNAs. Data are means ± SEM of three independent experiments. **P* < 0.05; ***P* < 0.01; ns, not significant.

A), which led to a substantial antiviral effect and induction of ISG expression (Fig. 6, B to D), as compared to the over-expression of any one of the three factors alone. These data suggest that the integrity of the ISGF3 complex is necessary for these effects.

To rule out any interference by endogenous WT STAT1 or STAT2 (should any be present in the cells) and to further confirm the role of ISGF3, we overexpressed STAT1, STAT2, and IRF9 in U3A cells (which are STAT1-deficient) and U6A cells (which are STAT2-deficient) (fig. S4, A to D) [12], which led to a substantial induction of ISG expression in both cell types (fig. S4, B and D), mirroring the results observed in Huh7.5 cells. STAT1 phosphorylated at Tyr^{701} (pSTAT1-Tyr^{701}) and STAT2 phosphorylated at Tyr^{690} (pSTAT2-Tyr^{690}) were undetectable even when either protein was overexpressed (Fig. 6A), which suggests that ISGF3 complex occurs through a phosphorylation-independent mechanism. Indeed, no pSTAT1-Tyr^{701} or pSTAT2-Tyr^{690} was detected in either human or mouse liver tissue samples by IHC (Fig. 6E and fig. S4E) or in three individual liver tissue samples that were examined by Western blotting (Fig. 6F). The same observation was also made by examining human liver organoids (Fig. 6G), intestinal organoids (fig. S4, F to H), and Huh7.5 cells (Fig. 6H). Furthermore, overexpression of a mutant STAT1 (Y701F-STAT1), which cannot be phosphorylated at Tyr^{701} [13], together with STAT2 and IRF9 in Huh7.5 cells led to a

comparable potency of antiviral effect and ISG induction (Fig. 6, I to K). This was further confirmed in U3A cells (fig. S4, I and J).

In addition to the tyrosine phosphorylation sites in STAT1 and STAT2, phosphorylation of the sites Ser^{708} and Ser^{727} in STAT1 correlates with ISG expression [14, 15]. However, we were unable to detect pSTAT1-Ser^{727} in either Huh7.5 cells (fig. S4K) or human liver tissue samples (fig. S4L). Generally, STAT1 or STAT2 is phosphorylated by specific kinases upon cellular stimulation (for example, by IFNs). Furthermore, pSTAT1 and pSTAT2 proteins undergo dephosphorylation. Thus, the phosphorylation and dephosphorylation processes are coordinated to maintain the phosphorylation states of these proteins to an extent that achieves a balance between their beneficial, antiviral actions and their detrimental, proinflammatory effects. Consequently, the inhibition of phosphatases would alter this balance, resulting in increased amounts of pSTAT1 and pSTAT2 and to the greater induction of ISG expression (fig. S5A) [16]. Thus, we performed experiments with the phosphatase inhibitor NSC87877 (which has IC_{50} values of 0.318 μM for SHP-2, 0.355 μM for SHP-1, and 1.691 μM for PTP1B) to specifically inhibit the key phosphatases involved in pSTAT1 and pSTAT2 dephosphorylation at both tyrosines and serines [16-18]. However, we found that NSC87877 had no effect on basal ISG expression in either Huh7.5 cells or Caco2 cells (Fig. 7A and fig. S5B). NSC87877 also had no effect on ISG expression induced by the simultaneous over-expression of STAT1, STAT2, and IRF9 (Fig. 7B). Together, these data suggest that STAT1, STAT2, and IRF9 function as part of U-ISGF3 to drive ISG expression, which leads to antiviral effects.

The basal expression of particular ISGs is enhanced in chemotherapy-resistant cancer cells and in chronic HCV patients who are resistant to IFN therapy; however, under these conditions, pSTAT1 is almost undetectable [2, 19]. Thus, we overexpressed Y701F-STAT1, STAT2, and IRF9 together in Huh7.5 cells and examined the basal expression of several ISGs that were previously identified as potential makers to predict responsiveness to IFN therapy in patients chronically infected with HCV [7, 8]. As expected, the expression of all of these ISGs was increased upon overexpression of the components of the U-ISGF3 (fig. S5C). Note that IFNs stimulate the expression of antiviral ISGs and of negative regulatory ISGs to avoid excessive IFN responses [20]. We found that the expression of four of five of these negative regulatory ISGs was also enhanced upon overexpression of U-ISGF3 (fig. S5D).

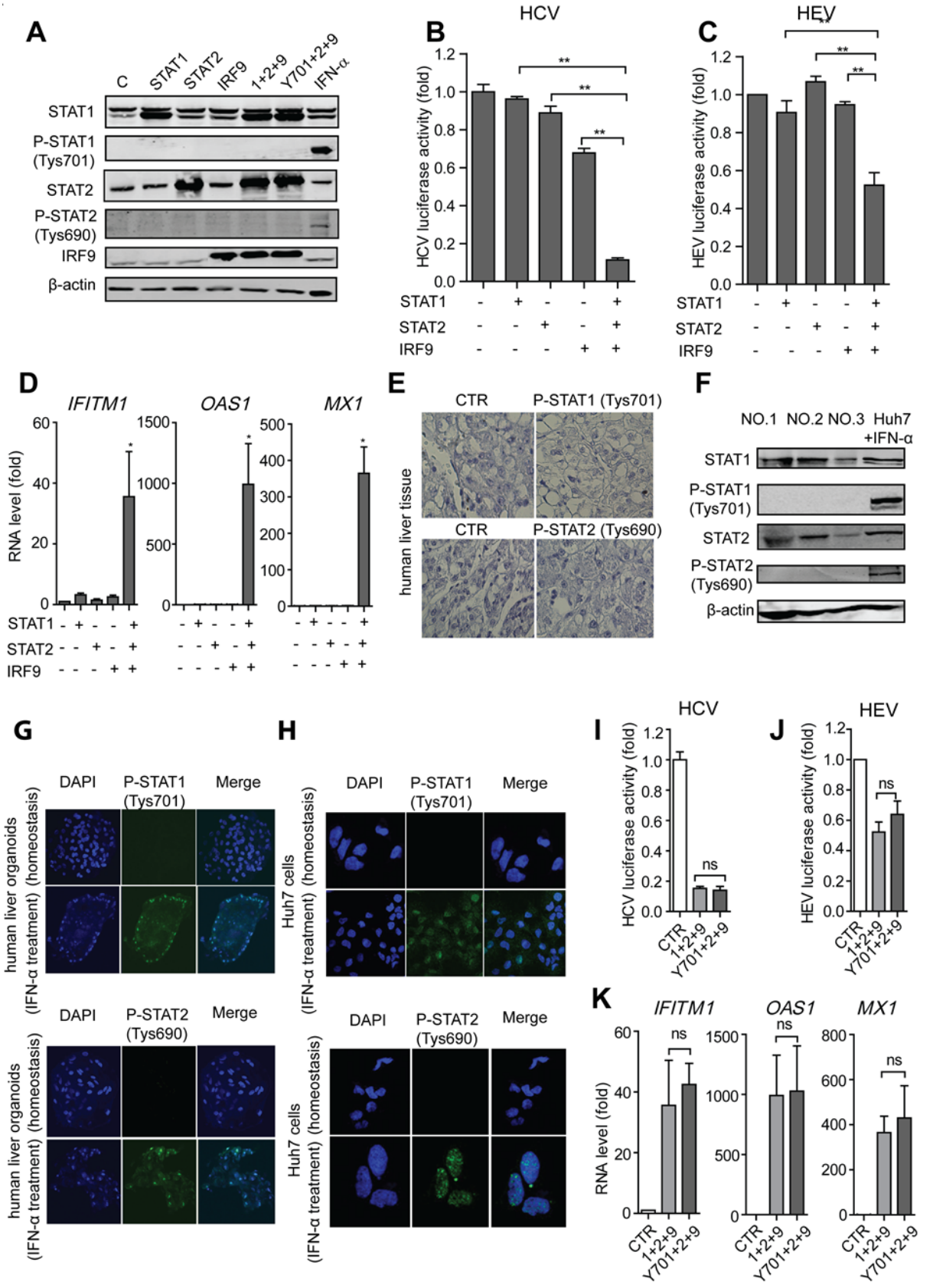

Figure 6. U-ISGF3 stimulates the expression of ISGs and constrains viral replication.

Huh7.5 cells were transduced with control lentivirus (C) or with lentiviruses expressing the indicated proteins before being subjected to Western blotting analysis with antibodies against the indicated proteins. As a positive control for the detection of pSTAT1 and pSTAT2, Huh7.5 cells were treated

with IFN-α for 30min. Western blots are representative of three independent experiments. (**B** and **C**) HCV-positive (B) and HEV-positive (C) Huh7.5 cells were transduced with control lentivirus or with lentiviruses expressing the indicated proteins before being subjected to assays of viral replication–related luciferase activity. Data are means ± SEM of three independent experiments. (**D**) Huh7.5 cells were transduced with control lentivirus or with lentiviruses expressing the indicated proteins before being subjected to qRT-PCR analysis of the relative abundances of the indicated mRNAs. Data are means ± SEM of three independent experiments. (**E**) Representative immunohistochemical analysis of pSTAT1-Tyr^{701} and pSTAT2-Tyr^{690} in human liver tissue samples. Neither protein was detected. As negative controls (CTR), the primary antibodies were replaced with PBS containing 0.05% Tween. (**F**) Samples from three individual human liver samples were analyzed by Western blotting with antibodies against the indicated proteins. As a positive control for pSTAT proteins, Huh7.5 cells were treated with IFN-α for 30 min. Western blots are representative of three independent experiments. (**G** and **H**) Confocal laser electroscope analysis of pSTAT1-Tyr^{701} (top) and pSTAT2-Tyr^{690} (bottom) in human liver organoids (G) and Huh7.5 cells (H). The pSTAT1 and pSTAT2 proteins are shown in green, whereas nuclei were visualized by DAPI (blue). Human liver organoids or Huh7.5 cells treated with IFN-α for 30 min served as the corresponding positive controls. Images are representative of multiple organoids or cells from three individual experiments. (**I** and **J**) HCV-positive (I) and HEV-positive (J) Huh7.5 cells transduced with control lentivirus or lentiviruses expressing WT or Y701F mutant STAT1 together with STAT2 and IRF9 were subjected to assays of viral replication–related luciferase activity. Data are means ± SEM of three independent experiments. (**K**) Huh7.5 cells transduced with control lentivirus or lentiviruses expressing WT or Y701F mutant STAT1 together with STAT2 and IRF9 were subjected to qRT-PCR analysis of the relative abundances of the indicated mRNAs. Data are means ± SEM of three independent experiments. **P* < 0.05; ***P* < 0.01; ns, not significant.

U-ISGF3 drives ISG transcription without stimulating IFN production

To further dissect whether the U-ISGF3–induced expression of ISGs was independent of IFN production, we measured the basal abundances of mRNAs of several IFNs, including *IFNA*, *IFNB*, *IFNG*, *IL29*, and *IL28A* (fig. S5E). The abundances of *IFNA* and *IFNB*mRNAs were not statistically significantly increased by the overexpression of STAT1, STAT2, or IRF9 alone or in combination (Fig. 7, C and D), whereas the mRNAs encoding *IFNG*, *IL29*, and *IL28A* were undetectable with or without overexpression of the U-ISGF3 components (fig. S5E). To further confirm the lack of IFN production, we collected the conditioned medium of these cells (fig. S5F) and performed functional assays. Conditioned culture medium from any of the overexpressing Huh7.5 cells was unable to stimulate an IFN response in an ISRE reporter assay (fig. 7E). Consistently, treatment of Huh7.5 cells with these conditioned media had no effect on ISG expression (fig. S5G). These data suggest that the U-ISGF3–induced expression of ISGs is IFN-independent.

U-ISGF3 drives ISG expression independently of the upstream components of the IFN signaling pathway

IFNs are mainly produced by so-called IFN-producing cells (IPCs). In our study, we included three types of well-known IPCs, human plasmacytoid dendritic cells (pDCs), myeloid dendritic cells (mDCs), and T cells to demonstrate the classical IFN-dependent mechanisms of ISG transcription and antiviral action. As expected, these IPCs produced IFNs to activate the JAK-STAT pathway, drive ISG transcription, and exert antiviral activity. These effects were specifically blocked by JAK inhibitor I (fig. S6). Therefore, upon IFN stimulation, the intact JAK-STAT signaling pathway is a prerequisite for the formation of its downstream transcription factor complex, ISGF3, which drives the expression of ISGs (fig. S7A). To dissect the involvement of its upstream elements in basal ISG transcription, we knocked down either IFN-αR1 or IFN-λR1 in Huh7.5 cells by lentiviral shRNA (Fig. 7F). Efficient knockdown of IFN-αR1 or IFN-λR1 had no effect on constitutive ISG expression (Fig. 7G). In addition, knockdown of endogenous JAK1 in Huh7.5 cells (Fig. 7, H and I) did not inhibit the constitutive expression of ISGs (Fig. 7J). This finding was further confirmed in experiments with Caco2 cells (fig. S7, B to D). Conversely, collective overexpression of STAT1, STAT2, and IRF9 by lentiviral transduction in IFN-αR1-, IFN-λR1-, or JAK1-knockdown Huh7.5 cells showed comparable ISG induction ability compared with control lentiviral vector (Fig. 7K). These results suggest that U-ISGF3 drives the basal expression of ISGs independently of the upstream elements of the IFN signaling pathway.

Discussion

ISGs are the ultimate antiviral effectors of the IFN signaling. They function either by targeting different steps of the viral life cycle or by reinforcing host defense by further activation of ISG expression [1, 21]. Classically, upon IFN stimulation, STAT1 and STAT2 are phosphorylated, leading to the association with IRF9 to form the transcription factor complex ISGF3. Phosphorylated ISGF3 translocates into cell nucleus and binds to the promoter regions of ISGs to activate the transcription of these hundreds of ISGs. However, when cells are continuously exposed to a low level of exogenous interferon, unphosphorylated ISGF3 (U-ISGF3), formed by interferon stimulated IRF9 and unphosphorylated STAT1 and STAT2, can also lead to increased expression of a subset of ISGs [2]. Importantly, both regulatory mechanisms require the activation by IFN.

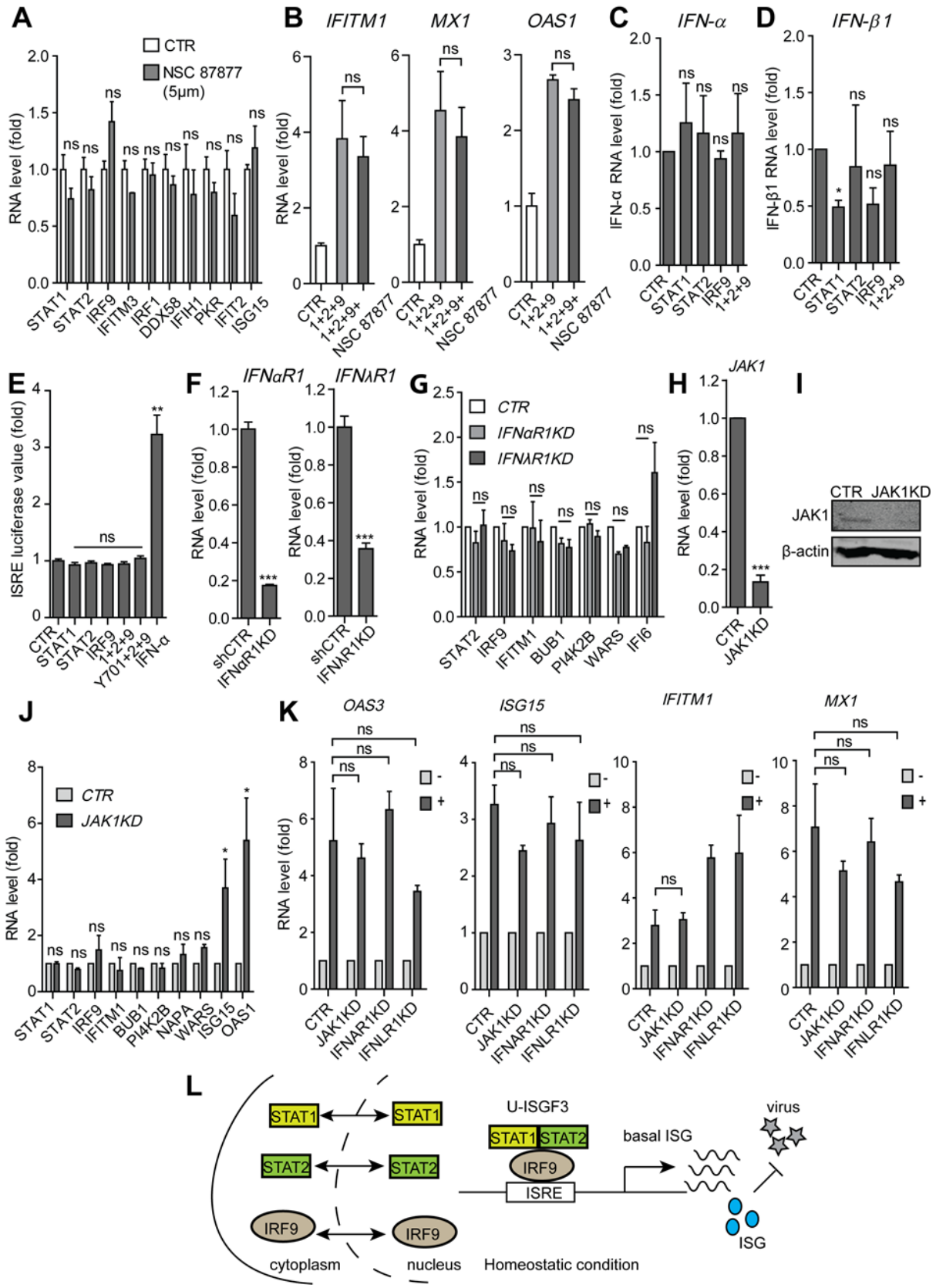

Figure 7. U-ISGF3 stimulates the expression of ISGs independently of IFN production and the upstream elements of the IFN signaling pathway

(**A**) Huh7.5 cells were left untreated (CTR) or were treated with 5 μM NSC87877 (phosphatase inhibitor) before the cells were subjected to qRT-PCR analysis of the relative abundances of the

indicated mRNAs. Data are means ± SEM of three independent experiments. (**B** to **D**) Huh7.5 cells were transduced with control lentivirus or with lentiviruses expressing STAT1, STAT2, and IRF9, individually or in combination, before being treated with vehicle or NSC87877. The cells were then subjected to qRT-PCR analysis of the relative abundances of the indicated mRNAs for ISGs (B), *IFNA* (C), and *IFNB* (D). Data are means ± SEM of three independent experiments. (**E**) Huh7.5 cells transduced with lentiviruses expressing the indicated proteins were cultured for 48 hours before the cell culture medium was collected and used to treat an ISRE luciferase reporter cell line. As a positive control, culture medium was collected from cells treated with IFN-α (10 IU/ml). Data are means ± SEM of three independent experiments. (**F**) Huh7.5 cells transduced with lentiviruses expressing control shRNA, *IFNAR1*-specific shRNA, or *IFNLR1*-specific shRNA were analyzed by qRT-PCR to determine the extent of knockdown of the indicated mRNAs. Data are means ± SEM of three independent experiments. (**G**) Huh7.5 cells transduced with lentiviruses expressing control shRNA, *IFNAR1*-specific shRNA, or *IFNLR1*-specific shRNA were analyzed by qRT-PCR to determine the relative abundances of the indicated mRNAs. Data are means ± SEM of three independent experiments. (**H** and **I**) Huh7.5 cells transduced with lentiviruses expressing control or JAK1-specific shRNAs were analyzed by qRT-PCR to determine the extent of knockdown of JAK1 mRNA (H) or by Western blotting with antibodies against the indicated proteins (I). Data in (H) are means ± SEM of three independent experiments. Western blots are representative of three independent experiments. (**J**) Huh7.5 cells transduced with lentiviruses expressing control or JAK1-specific shRNAs were analyzed by qRT-PCR to determine the relative abundances of the indicated mRNAs. Data are means ± SEM of three independent experiments. (**K**) Huh7.5 cells were transduced with lentiviruses expressing control shRNA or shRNAs specific for JAK1, IFNAR, or IFNLR. After the puromycin selection, they were not (-) or were (+) transduced with lentiviruses expressing STAT1, STAT2, and IRF9. The cells were then subjected to qRT-PCR analysis of the relative abundances of the indicated mRNAs. Data are means ± SEM of three independent experiments. **P* < 0.05; ***P* < 0.01; ns, not significant. (**L**) Illustration of the mechanism of basal expression of ISGs under homeostatic conditions. Unphosphorylated STAT1, STAT2, and IRF9 shuttle between the cytoplasm and the nucleus. When these three components are present in the nucleus, they function as the constitutively active transcription factor complex U-ISGF3 to sustain the basal expression of ISGs. The products of these expressed ISGs confer protection to the cell from viral infection.

Classically, IFNs are mainly produced by so-called IFN-producing cells (IPCs) These IPCs produced IFNs to activate the JAK-STAT pathway, drive ISG transcription, and exert antiviral activity. Huh7.5Huh7.5Here, we highlighted the existence of an IFN-independent mechanism that sustains the constitutive expression of IFN-encoding genes. We found that constitutive ISG expression was mediated by the endogenous U-ISGF3 complex. This regulatory mechanism was independent of IFN production and the upstream elements of IFN signaling, but conferred the cells with resistance against viral infections (Fig. 7L). Thus, these data suggest that both IFN-dependent and -independent antiviral mechanisms co-exist and work cooperatively.

As a critical element in determining cellular susceptibility to viral infection, constitutively expressed ISGs also determine the rapid response and intensity of cellular antiviral activity. Because many ISGs are key components of antiviral pathways, their basal expression is necessary for the quick activation of these signaling pathways upon ligand

engagement. Taking the JAK-STAT pathway as a typical example, because the key components of this cascade are present in the cell under homeostatic conditions, the synthesis of new protein components of this pathway in response to stimulation with IFN is not required. Therefore, activation of this signaling pathway can rapidly occur, resulting in a timely and effective way of controlling invading pathogens. Furthermore, most of the necessary components of the JAK-STAT pathway are encoded by ISGs.

In particular circumstances, deficiency of a single ISG can lead to compromised immunity following virus infection. Mice genetically deficient for STAT1, STAT2 or IRF9 developed persistent virus infection or even lethal disease in response to virus invasion, including those provoked by choriomeningitis virus, respiratory syndrome coronavirus and vesicular stomatitis virus [22-25]. In contrast, cells maintaining relatively higher levels of baseline ISGs show stronger resistance against virus infection. Nevertheless, the abnormal regulation of constitutive ISG expression is closely associated with treatment outcome in cancer or chronic HCV patients. Chronic hepatitis C patients with abnormally high levels of ISG expression in the liver at baseline poorly respond to pegylated IFN-α/ribavirin therapy [7, 8]. In cancer patients, abnormally high expression of ISGs promotes tumor growth, metastasis, and confers resistance to chemotherapy and radiation [9, 10]. Thus, constitutive ISGs at requisite levels are vital to prepare the host cells into a “combat ready” or “pre-arming” mode, but also determine the treatment responses in particular diseases in patients. In conclusion, we have demonstrated that endogenous U-ISGF3 function as the constitutive transcription factor to sustain basal ISG transcription, conferring cell resistance against virus infection. In contrast, the absence of U-ISGF3 can lead to decreased ISG expression at baseline, being susceptible to virus infection.

Supplementary Materials and Methods

Study approval

The animal study was approved by the institutional animal ethics committee (Dier Experimenten Commissie). Human intestinal or liver tissues were obtained from patients during surgical resection. The patients agreed to participate by written informed consent, and the study was approved by the Medical Ethical Committee of the Erasmus Medical Center (Medisch Ethische Toetsings Commissie Erasmus MC).

Reagents

Human IFN-α (Thermo Scientific) was dissolved in phosphate-buffered saline (PBS) before use. Antibody against pSTAT1-Tyr^{701} (58D6; rabbit monoclonal; #9167) was obtained from Cell Signaling Technology. Antibodies against STAT1 (rabbit polyclonal; sc-592), STAT2 (rabbit polyclonal; SC-476), pSTAT2-Tyr^{690} (rabbit polyclonal; sc-21689-R), pSTAT1-Ser^{727} (rabbit polyclonal; sc-16570-R), ISGF-3γ p48 (H-143; rabbit polyclonal; sc-365893), and β-actin were purchased from Santa Cruz Biotechnology. Anti-rabbit or anti-mouse IRDye-conjugated secondary antibodies were obtained from LI-COR Biosciences. Stocks of JAK inhibitor 1 and NSC87877 (Santa Cruz Biotechnology) were dissolved in DMSO at a concentration of 10 mM.

3-D primary human intestinal or liver organoids models

Human intestinal crypt isolation and primary human intestinal organoids culture was described previously [26]. Human liver cell isolation and primary human liver organoids culture was described accordingly [27].

Cell models

Huh7.5 cells (a human hepatoma cell line), Caco2 cells (a human epithelial colorectal adenocarcinoma cell line), and A549 cells (a human alveolar basal epithelial cell line) were cultured in Dulbecco's modified Eagle medium (DMEM, Lonza Biowhittaker) complemented with 10% (v/v) fetal calf serum (FCS, Hyclone), 100 IU/ml penicillin, and 100 µg/ml streptomycin. Wild-type (WT) MEFs and MEFs from STAT1$^{-/-}$ [28] and STAT2$^{-/-}$ [29] mice were generously provided by Prof. Andrea Kröger (Helmholtz Centre for Infection Research) and Christian Schindler (Columbia University, NY), respectively. IRF9$^{-/-}$ mice and the corresponding WT MEFs [30] [30] were generously provided by K. Mossman (McMaster University, Canada). STAT1-deficient (U3A) and STAT2-deficient (U6A) cell lines were kindly provided by G. R. Stark (Lerner Research Institute). Huh7.5 cells expressing the HCV subgenomic replicon containing a subgenomic HCV bicistronic replicon (1389/NS3-3V/LucUbiNeo-ET) linked to the firefly *luciferase* reporter gene were maintained in Dulbecco's modified Eagle medium (DMEM) complemented with 10% (v/v) fetal calf serum, 100 IU/ml penicillin, and 100 µg/ml streptomycin and 250 µg/ml G418 (Sigma) [31]. The HEV subgenomic model: Huh7.5 cells containing the subgenomic HEV sequence (Kernow-C1 p6/luc) coupled to a Gaussia luciferase reporter gene [32, 33]. Luciferase normalization cells (Huh7.5-norm) were generated by transducing Huh7.5 cells with a lentiviral vector expressing the firefly *luciferase* gene under the control of the human *phosphoglycerate*

kinase (*PGK*) promoter. For the ISRE reporter model, Huh7.5 cells were transduced with a lentiviral transcriptional reporter system that expressed the firefly *luciferase* gene driven by a promoter containing multiple ISRE promoter elements (SBI Systems Biosciences), and luciferase activity was used as a reporter of ISRE promoter activation [34, 35]. Human plasmacytoid dendritic cells (pDCs), myeloid dendritic cells (mDCs), and T cells were purified from the buffy coats of healthy blood donors and were cultured in round-bottom, 96-well plates [36]. Culture medium of these cells was harvested after 48 hours and served as conditioned medium for further experiments. For simian rotavirus experiments, SA11, a well-characterized and broadly used laboratory strain of the virus, was used to inoculate the Caco2 cell line as a rotavirus infection model [26].

Gene knockdown or overexpression by lentiviral vectors

Lentiviral pLKO knockdown vectors (Sigma-Aldrich) expressing shRNAs targeting IFN-αR1, IFN-λR1, JAK1, STAT1, STAT2, or IRF9 and their appropriate controls were obtained from the Erasmus Biomics Center and were produced in HEK 293T cells. After a pilot study, those shRNA-expressing vectors that exerted optimal gene knockdown were selected. These shRNA sequences are listed in table S1. Stable gene knockdown cells were generated after lentiviral vector transduction and selection in medium containing puromycin (3 μg/ml; Sigma). The pTRIP.CMV.IVSb.ISG.ires.TagRFP–based STAT1, STAT2, and IRF9 overexpression lentiviral vectors were a kind gift from C. M. Rice (Rockefeller University) [37]. Control vectors expressing green fluorescent protein (GFP) was also used. The pLV-tetO-CMV-SV40-Puro-LoxP–based lentiviral vectors expressing WT STAT1 or the Y701F-STAT1 mutant (which cannot be phosphorylated) were kindly provided by G. R. Stark (Lerner Research Institute) [13]. Lentiviral pseudoparticles were generated as described previously [13, 37]. Ultracentrifugation was used to achieve high-titer lentiviruses with superior transduction efficiency.

Measurement of luciferase activity

For *Gaussia* luciferase analysis, the activity of secreted luciferase in the cell culture medium was measured with the BioLux *Gaussia* Luciferase Flex Assay Kit (New England Biolabs) according to the manufacturer's instructions. For firefly luciferase assays, luciferin potassium salt (100 mM; Sigma) was added to the cells and incubated for 10 min at 37°C. Luciferase activity was then quantified with a LumiStar Optima luminescence counter (BMG Lab Tech).

Quantitative RT-PCR analysis

RNA was isolated with a Machery-NucleoSpin RNA II kit (Bioke) and quantified with a Nanodrop ND-1000 spectrophotometer (Wilmington). All RNA samples were adjusted to a concentration of 62.5 ng/µL. RNA (500 ng) was used as template for the generation of complementary DNA (cDNA) with the reverse transcription system (TAKARA BIO INC). The cDNA (10 ng/well) of all detected genes was amplified for 50 cycles and quantified with a SYBRGreen-based real-time PCR system (Applied Biosystems) according to the manufacturer's instructions. *GAPDH* was considered as reference gene to normalize gene expression. Relative gene expression (based on mRNA abundance) was normalized to that of *GAPDH* using the formula: $2^{-\Delta\Delta CT}$ ($\Delta\Delta CT = \Delta CT_{sample} - \Delta CT_{control}$) [38]. All of the primer sequences are included in table S2.

Quantification of gene copy numbers

To generate a template with which to quantify ISG copy number under basal conditions, vectors containing the corresponding ISG genes were used. A series of dilutions, from 10^{-2} to 10^{-10}, were prepared and then were amplified and quantified by qRT-PCR to generate a standard curve. The standard curve was generated by plotting the log of the copy number against the cycle threshold (CT) value (fig. S1A). Copy numbers were calculated with the following equation: Copy number (molecules/µg) = (1 µg/0.01 µg) × [concentration (ng/µL) × 6.022×10^{23} (molecules/mol)] / [length of amplicon × 640 (g/mol) × 10^{9} (ng/g)].

Nuclear extraction and Western blotting analysis

Nuclear and cytoplasmic proteins were extracted with the nuclear and cytoplasmic protein extraction kit (Active Motif) according to the manufacturer's instructions. All samples were lysed in Laemmli sample buffer containing 0.1 M DTT and heated for 5 min at 95°C, which was followed by loading the samples onto a 10% sodium dodecyl sulfate polyacrylamide gel (SDS-PAGE) and separation by electrophoresis. After 90 min running at 120 V, proteins were electrophoretically transferred onto a polyvinylidene difluoride (PVDF) membrane (Invitrogen) for 1.5 hours with an electric current of 250 mA. Subsequently, the membrane was blocked with a mixture of 2.5 ml of blocking buffer (Odyssey) and 2.5 ml of PBS containing 0.05% Tween 20. This was followed by overnight incubation with the appropriate primary antibody (at a 1:1000 dilution) at 4°C. The membrane was washed three times, which was followed by incubation for 1 hour with IRDye-conjugated secondary antibody (1:

5000). After the membrane was washed three times, protein bands were detected with the Odyssey 3.0 Infrared Imaging System.

IFN production assay

Huh7.5 cells were seeded into 6-well plates at a density of 10×10^4 cells per well and then were transduced with lentiviruses expressing STAT1, STAT2, or IRF9 singly or in combination at 37°C. Forty-eight hours later, the lentiviral particles were removed and the cells were washed three times with PBS. The culture medium was refreshed and the transduced cells were cultured for another 48 hours. The culture medium was subsequently collected and added to an ISRE luciferase reporter cell line that is sensitive to IFNs. The conditioned medium was also used to treat Huh7.5 cells for 24 hours, which was followed by quantification of ISG expression by qRT-PCR analysis.

Confocal laser electroscope assay

Cells were seeded on glass coverslips. After 12 hours, the cells were washed with PBS, fixed in 4% PBS-buffered formalin for 10 min, and blocked with Tween-milk-glycine medium [PBS, 0.05% Tween, skim milk (5 g /L), and glycine (1.5 g/L)]. Samples were incubated with primary antibodies overnight at 4 °C. The samples were then incubated with anti-mouse IgG (H+L), F(ab')2 Fragment (Alexa Fluor 488 conjugate), or anti-rabbit IgG(H+L), F(ab') 2 Fragment (Alexa Fluor 488 conjugate) secondary antibodies (each at a 1:1000 dilution). Nuclei were stained with DAPI (4,6-diamidino-2-phenylindole; Invitrogen). Images were detected with confocal electroscope (lens: 40 ×, software: ZenLightEdition).

Immunohistochemistry (IHC)

Paraffin-embedded liver tissue sections were deparaffinized in xylene, rehydrated in graded alcohols, and rinsed once in PBS containing 0.05% Tween. After antigen retrieval, 1.5% H_2O_2 was used to block endogenous peroxidase for 10 min at room temperature. The slides were incubated in 5% milk blocking solution, which was followed by overnight incubation with primary antibody at a 1:200 dilution before the tissue sections were then counterstained with hematoxylin. As a negative control, the primary antibody was replaced with PBS containing 0.05% Tween.

ChIP-seq data analysis

The ChIP-seq dataset for STAT1 (GSE31477) was retrieved from the ENCODE database. ChIP-seq datasets were processed and mapped to the hg19 reference genome as described previously [11]. ChIP-seq datasets with multiple replicates were merged. MACS 1.4.2 software was used for peak-calling and for the generation of binding profiles [39]. If the centers of two binding regions reported by MACS were 100 bp or less apart, then they were unified to a single binding region. The sequencing profiles were generated in the IGV browser [40].

Statistical analysis

All results were presented as means ± SEM. Comparisons between groups were performed with the Mann-Whitney test. Differences were considered to be statistically significant when $P < 0.05$.

Supplementary Figures

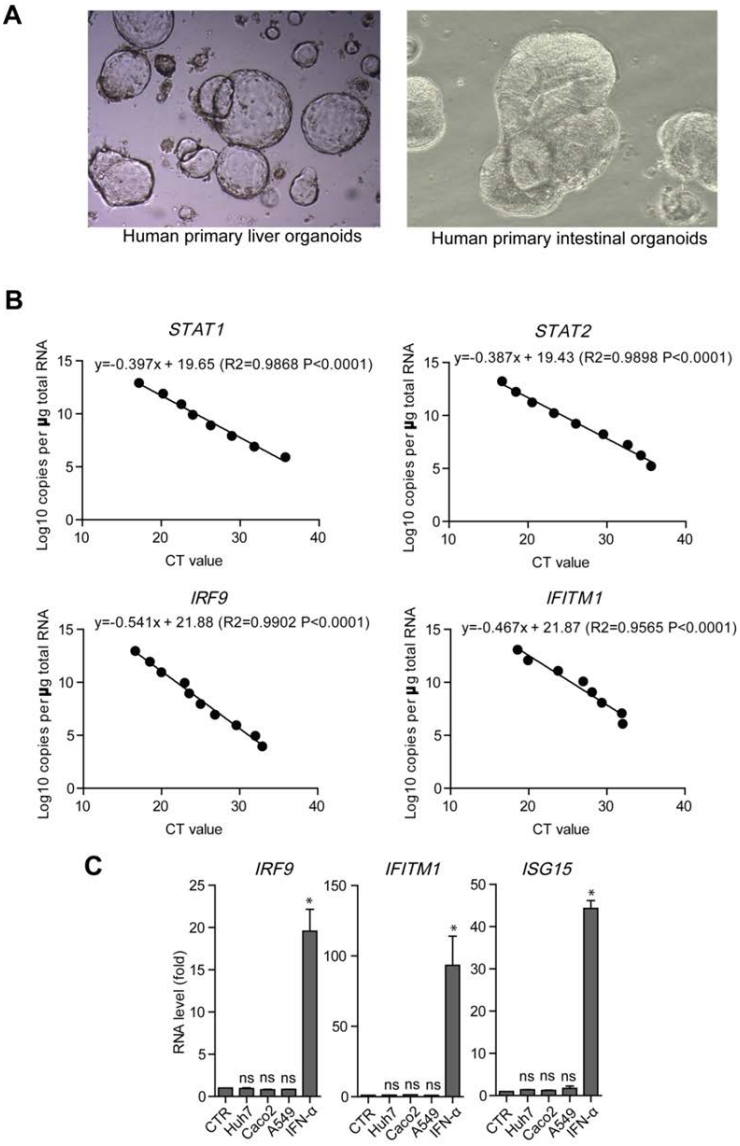

Fig. S1. Cells sustain basal ISG expression under homeostatic conditions.

(**A**) Representative microscopy image of cultured human primary liver organoids (left) and intestinal organoids (right). (**B**) Standard curve for quantifying ISG genes copy numbers. Plasmids containing the corresponding ISG genes (*STAT1*, *STAT2*, *IRF9*, and *IFITM1*) were used. The plasmids were extracted, followed by a series of dilutions, from 10^{-2} to 10^{-10}, were prepared and then were amplified and quantified by qRT-PCR. Standard curve was generated by plotting the cycle threshold (CT) value with regard to the log copy number. (**C**) With the treatment of Huh7, Caco2, A549 conditioned medium or IFN-α (10 IU/ml, positive control) for 24 hours, the expression levels of *IRF9*, *IFITM1*, and *ISG15* in Huh7 cells were quantified by qRT-PCR (n = 3 independent experiments). **P* < 0.05; ***P* < 0.01; ns, not significant.

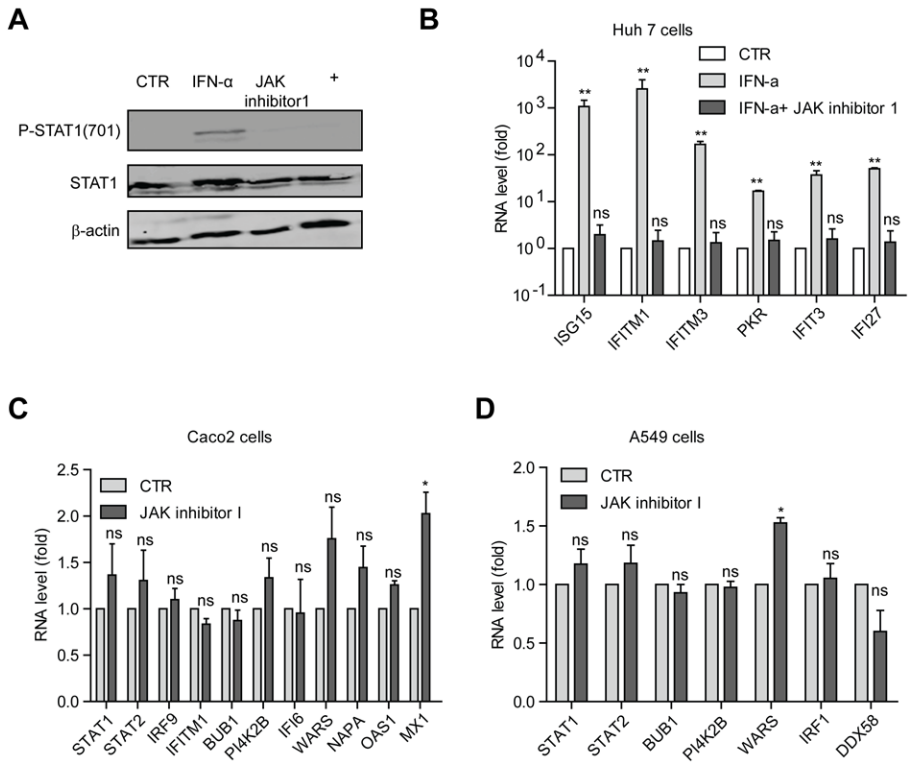

Fig. S2. Sustained basal ISG expression is independent of IFN production.

(**A**) Representative Western blotting analysis (from three experiments) of total STAT1 and pSTAT1 (Tyr701) protein levels under the treatment of IFN-α (1000IU/ml), JAK inhibitor I (5uM) or the combination. (**B**) Huh7.5 cells were treated with IFN-α (1000IU/ml), 5 μM JAK inhibitor I or their combination for 24 hours before being subjected to qRT-PCR analysis of the relative abundances of the indicated mRNAs. (n = 3 independent experiments). (**C**) Caco2 cells were treated with 5 μM JAK inhibitor I for 24 hours before being subjected to qRT-PCR analysis of the relative abundances of the indicated mRNAs (n = 3 independent experiments). (**D**) Same as (C) for A549 cells (n = 3 independent experiments).

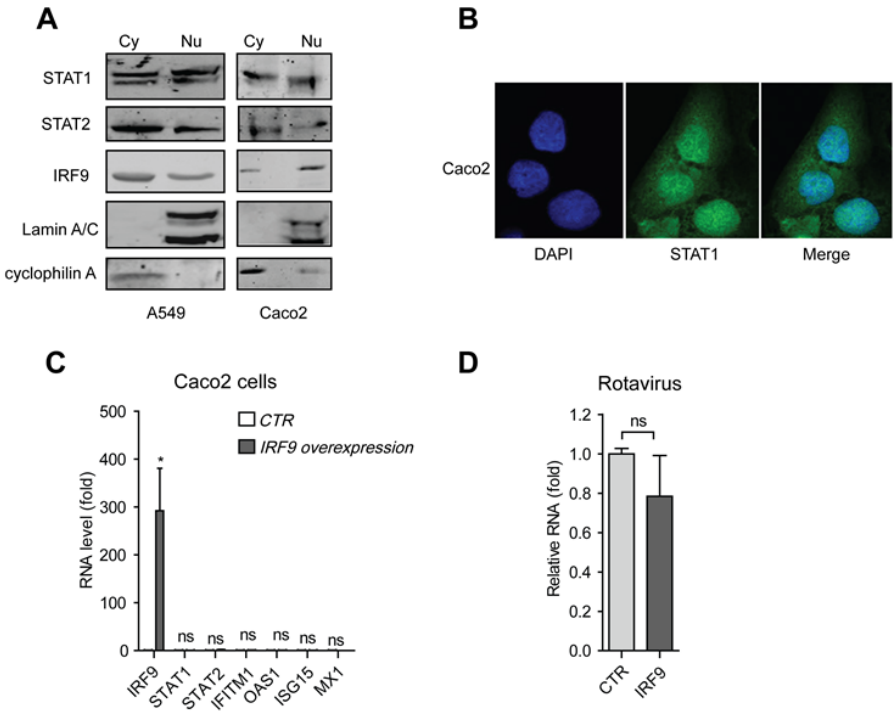

Fig. S3. STAT1, STAT2, and IRF9 are required for constitutive ISG expression.

(**A**) A549 and Caco2 cell lysates were fractionated into cytoplasmic (Cy) and nuclear (Nu) fractions and then were analyzed by Western blotting with antibodies against the indicated proteins. Cyclophilin A and Lamin A/C were used as cytosolic and nuclear markers, respectively. Western blots are representative of three independent experiments. (**B**) Confocal laser electroscope analysis of endogenous STAT1 localization in Caco2 cells. STAT1 is shown in green. Nuclei were visualized by DAPI (blue). Images are representative of multiple cells from three independent experiments.. (**C**) Caco2 cells transduced with control lentivirus or with lentivirus expressing IRF9 were subjected to qRT-PCR analysis of the relative abundances of the indicated mRNAs. (n = 3 independent experiments). (**D**) Rotavirus positive Caco2

cells transduced with control lentivirus or with lentivirus expressing IRF9 were subjected to qRT-PCR analysis of the relative abundances of the indicated mRNAs. (n = 3 independent experiments). *P < 0.05; **P < 0.01; ns, not significant.

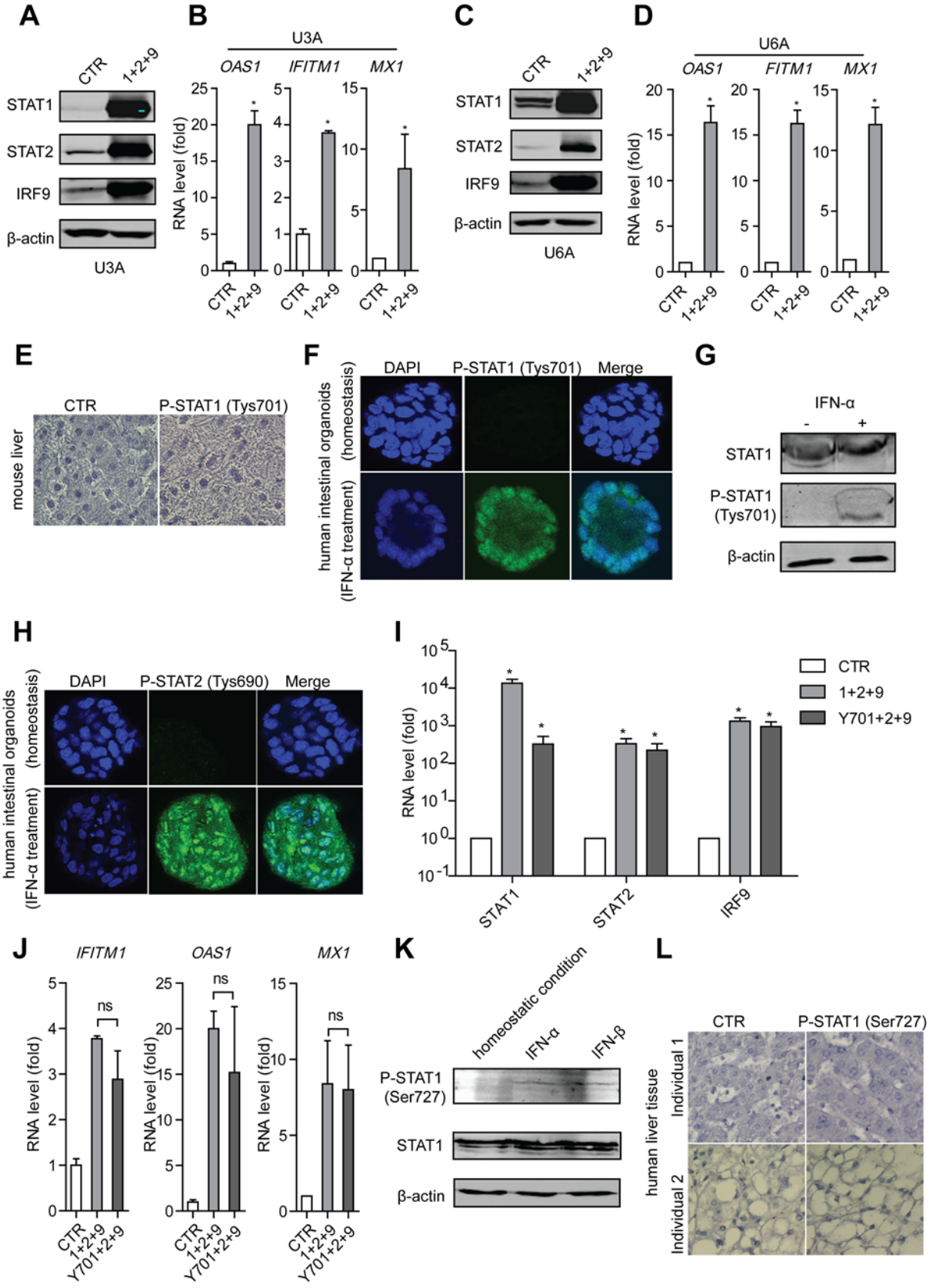

Fig. S4. The overexpression of U-ISGF3 leads to increased ISG expression.

(**A**) STAT1 mutant cells (U3A) were transduced with control lentivirus or with lentivirus expressing STAT1, STAT2 and IRF9 before being subjected to Western blotting analysis with antibodies against the indicated proteins. Western blots are representative of three independent experiments.Western blotting (**B**) U3A cells were transduced with control lentivirus or with lentiviruses expressing the indicated proteins before being subjected to qRT-PCR analysis of the relative abundances of the indicated mRNAs. Data are means ± SEM of three independent experiments. (**C**) Same as (A) for U6A cells. (**D**) Same as (B) for U6A cells. (**E**) Representative immunohistochemical analysis of pSTAT1-Tyr^{701} in mouse liver tissue samples. As negative control, primary antibody against pSTAT1-Tyr^{701} was replaced with PBS plus Tween 0.05%. (**F** and **G**) Confocal laser electroscope analysis (F) and Western blotting analysis (G) of pSTAT1-Tyr^{701} in human intestinal organoids (from three experiments). Human intestinal organoids treated with IFN-α for 30 min served as the corresponding positive control. (**H**) Confocal laser electroscope analysis of pSTAT2-Tyr^{690}) in human intestinal organoids. Human intestinal organoids treated with IFN-α for 30 min served as the positive control. Images are representative of multiple organoids from three individual experiments. (**I**) RT-PCR confirmed the successful over-expression of STAT1, Y701F-STAT1, STAT2 or IRF9 in U3A cells (n = 3 independent experiments). (**J**) In U3A cells, over-expression of Y701F-STAT1 together with STAT2 and IRF9 led to a comparable ISG induction compared with its wild type (n = 3 independent experiments). (**K**) Representative Western blotting analysis (from three experiments) of pSTAT1 (Ser^{727}) in Huh7 cells under the homeostatic condition. Huh7 cells treated with IFN-α, IFN-β (100IU/ml, 16 hours) served as positive controls. (**L**) Representative immunohistochemical staining (from three experiments) analysis of pSTAT1 (Ser^{727}) in human liver tissue samples from two individuals. Neither of them was detected. As negative control, primary antibody against pSTAT1 (Ser^{727}) was replaced with PBS plus Tween 0.05%. *P < 0.05; **P < 0.01; ns, not significant.

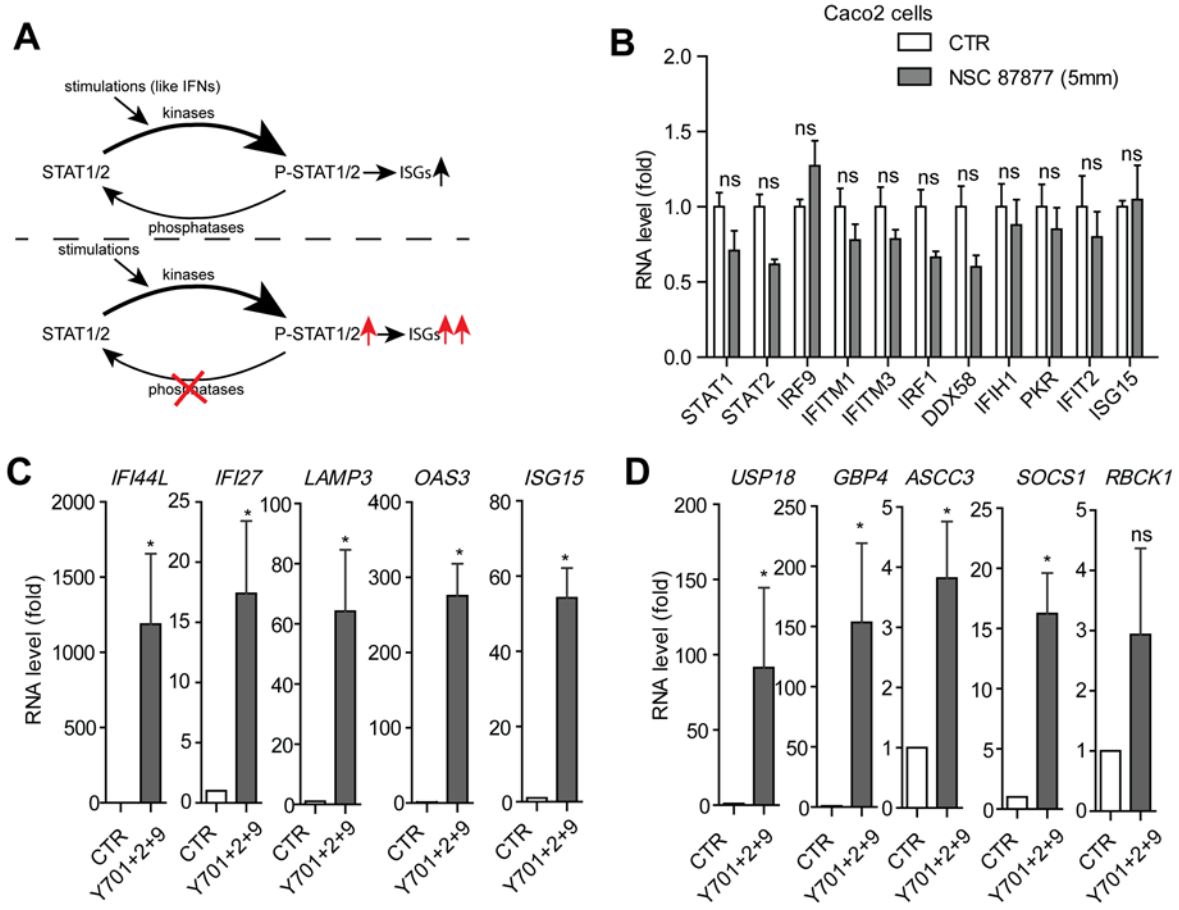

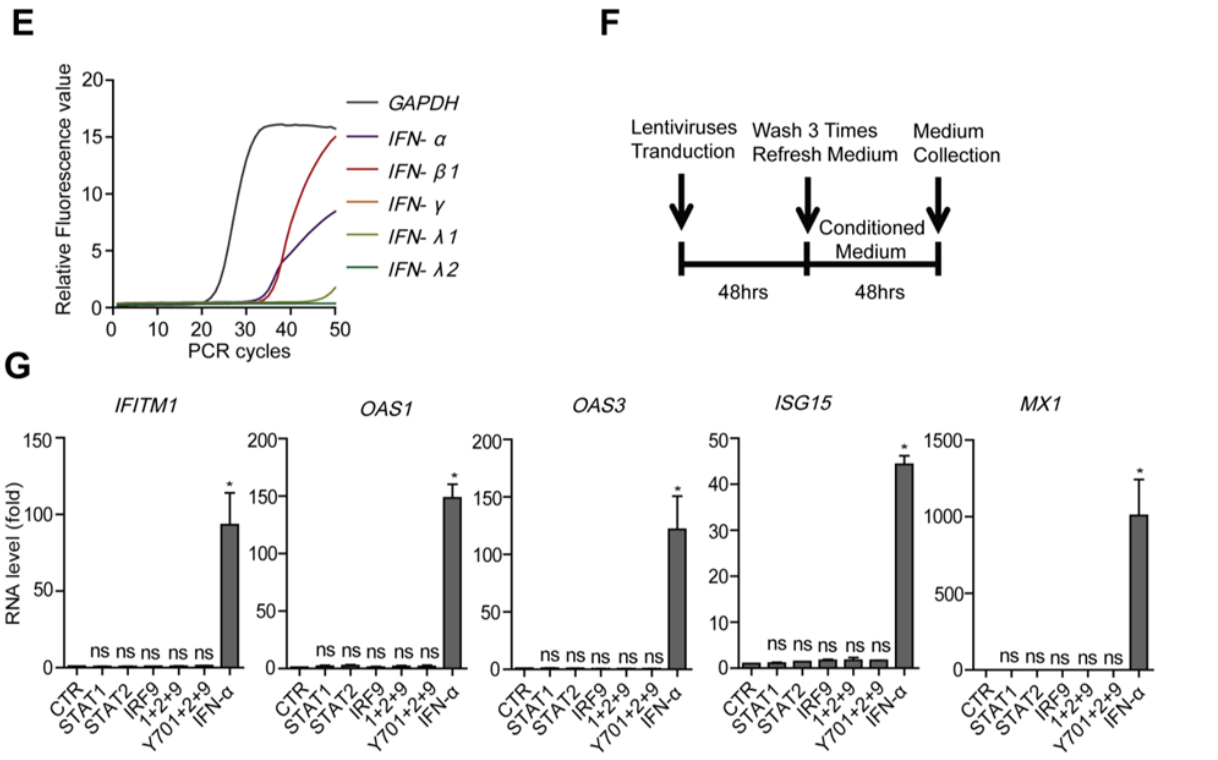

Fig. S5. U-ISGF3 stimulates ISG expression independently of IFN production.

(**A**) The regulation of phosphorylation process of STAT1/2 was illustrated. Upon stimulations (e.g. by IFNs), STAT1/2 get phosphorylated by specific kinases. Importantly, phosphorylated STAT1/2 undergo dephosphorylation process. Thus, the phosphorylation and dephosphorylation process coordinate to maintain the phosphorylation level at a balanced state, which balances its beneficial antiviral versus detrimental proinflammatory effects. Consequently, the inhibition of phosphatases will alter the balanced state, leading to higher levels of phosphorylated STAT1/2 and a much stronger induction of ISGs. (**B**) Caco2 cells were left untreated (CTR) or were treated with 5 μM NSC87877 (phosphatase inhibitor) before the cells were subjected to qRT-PCR analysis of the relative abundances of the indicated mRNAs. (n = 3 independent experiments). (**C**) and (**D**) Huh7.5 cells transduced with control lentivirus or with lentivirus expressing Y701F-STAT1, STAT2 and IRF9 were subjected to qRT-PCR analysis of the relative abundances of the indicated mRNAs. (n = 3 independent experiments). (**E**) The basal expression levels of several interferons, including *IFNA, IFNB1, IFNG, IL29*, *IL28A*, and the reference gene (*GAPDH*) were evaluated by qRT-PCR. (**F**) Schematic illustration of the production of conditioned medium (supernatant). (**G**) Huh7.5 cells were treated with conditioned medium from Huh7.5 cells with over-expression of STAT1, STAT2, IRF9 or their combination were subjected to qRT-PCR analysis of the relative abundances of the indicated mRNAs. IFN-α (10 IU/ml) serves as positive control (n = 3 independent experiments).

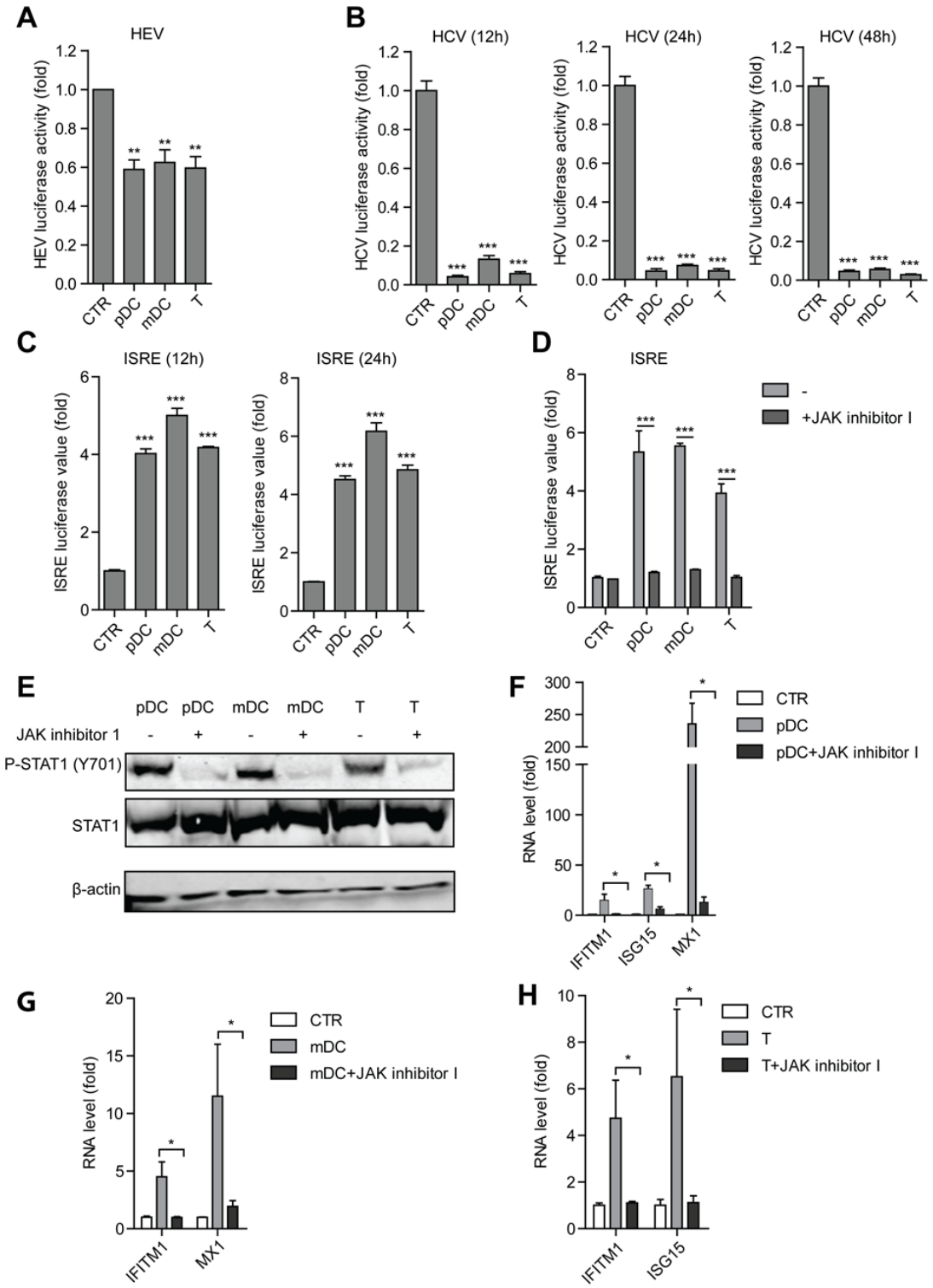

Fig. S6. IPCs produce IFNs to activate the JAK-STAT pathway, thus stimulating ISG expression and antiviral activity.

(**A**) HEV viral replication-related firefly luciferase activity was measured upon the treatment of conditioned medium from pDC, mDC and T cells for 48 hours Data are means ± SEM of two or three replicates from three independent experiments. (**B**) HCV viral replication-related firefly luciferase activity was measured at 3 different time points (12 hours, 24 hours and 48 hours) upon the treatment of conditioned medium from pDC, mDC and T cells Data are means ± SEM of two or three replicates from three independent experiments. (**C**) ISRE luciferase value was measured at 2 different time points (12 hours and 24 hours) after the treatment of conditioned medium from pDC, mDC and

T cells Data are means ± SEM of two or three replicates from three independent experiments. (**D**) Huh7.5-ISRE-luc cells were treated with conditioned medium from pDC, mDC and T cells without (-) or with JAK inhibitor I (5 µM) for 24 hours ISRE luciferase values were then measured and the fold-increase in activity relative to that of untreated cells was determined. Data are means ± SEM of two or three replicates from three independent experiments. (**E**) Representative Western blotting analysis (from three experiments) of total STAT1 and pSTAT1(Tyr701) in Huh7.5 cells treated with conditioned medium (from pDC, mDC and T cells). (**F**) Huh7.5 cells were treated with conditioned medium (from pDC) without or with JAK inhibitor I (5 µM) for 24 hours before subjected to qRT-PCR analysis of the relative abundances of the indicated mRNAs. (n = 3 independent experiments). (**G** and **H**) Same as (F) for conditioned medium from mDC (G) and T (H) cells. **P* < 0.05; ***P* < 0.01; ****P* < 0.001; ns, not significant.

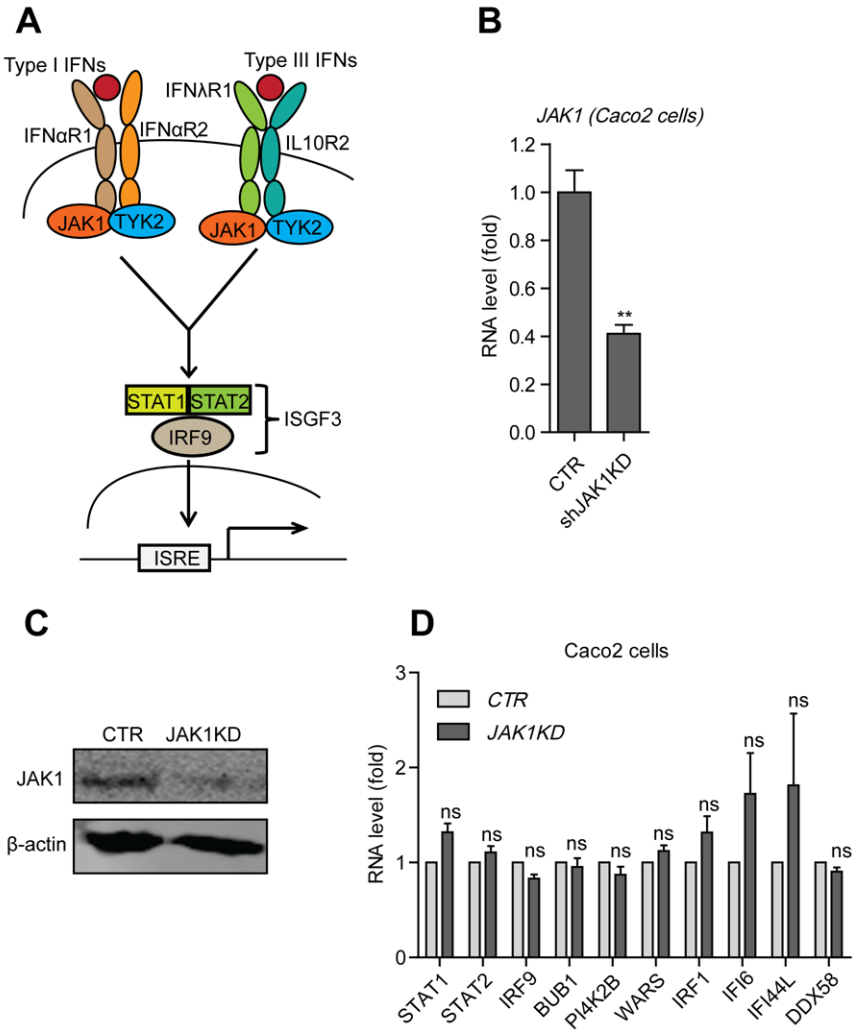

Fig. S7. U-ISGF3 stimulates ISG expression independently of upstream elements of the IFN signaling pathway.

(**A**) Illustration of type I and III IFN signaling pathways. (**B** and **C**) Caco2 cells transduced with lentiviruses expressing control or JAK1-specific shRNAs were analyzed by qRT-PCR to determine the extent of knockdown of JAK1 mRNA (B) or by Western blotting with antibodies against the indicated proteins (C). Data in (B) are means ± SEM of three independent experiments. Western blots are representative of three independent experiments. (**D**) Caco2 cells transduced with lentiviruses expressing control or JAK1-specific shRNAs were analyzed by qRT-PCR to determine the relative abundances of the indicated mRNAs. Data are means ± SEM of three independent experiments. (n = 3 independent experiments). **P* < 0.05; ***P* < 0.01; ns, not significant.

Acknowledgments

The authors gratefully thank S. U. Emerson (National Institute of Allergy and Infectious Diseases, NIH, USA) for generously providing the plasmids to generate subgenomic HEV genomic RNA; R. Bartenschlager and V. Lohmann (University of Heidelberg, Germany) for providing the HCV replicon cells; C. M. Rice (Rockefeller University) for providing the STAT1, STAT2, and IRF9 lentiviral vectors; G. R. Stark (Lerner Research Institute) for providing the WT STAT1 and Y701F-STAT1 lentiviral vectors and the U3A and U6A cells; A. Kröger (Helmholtz Centre for Infection Research) for providing the WT and $STAT1^{-/-}$ MEFs; C. Schindler (Columbia University, NY) for providing $STAT2^{-/-}$ MEFs; and K. Mossman (McMaster University, Canada) for providing primary WT and $IRF9^{-/-}$ MEFs. The authors also would like to acknowledge the ENCODE Experiment Matrix for providing the STAT1 ChIP-seq dataset.

Funding sources

This research was supported by The Netherlands Organization for Scientific Research (NWO/ZonMw) for VENI grant No. 916-13-032 to Q.P., the Dutch Digestive Foundation (MLDS) for a career development grant (No. CDG 1304) to Q.P., the Daniel den Hoed Foundation for a Centennial Award fellowship (to Q.P.), the European Association for the Study of the Liver (EASL) for a Sheila Sherlock Fellowship (to Q.P.), and the China Scholarship Council for funding Ph.D. fellowships to W.W. (201303250056), Y.Y. (201307720045), L.X. (201306300027), Y.W. (201207720007), and X.Z. (No. 201206150075).

References

1. Schneider, W.M., M.D. Chevillotte, and C.M. Rice, Interferon-stimulated genes: a complex web of host defenses. *Annu Rev Immunol*, 2014. **32**: p. 513-45.
2. Cheon, H., et al., IFNbeta-dependent increases in STAT1, STAT2, and IRF9 mediate resistance to viruses and DNA damage. *EMBO J*, 2013. **32**(20): p. 2751-63.
3. Cho, H., et al., Differential innate immune response programs in neuronal subtypes determine susceptibility to infection in the brain by positive-stranded RNA viruses. *Nat Med*, 2013. **19**(4): p. 458-64.
4. Seng, L.G., et al., High basal expression of interferon-stimulated genes in human bronchial epithelial (BEAS-2B) cells contributes to influenza A virus resistance. *PLoS One*, 2014. **9**(10): p. e109023.
5. Zurney, J., K.E. Howard, and B. Sherry, Basal expression levels of IFNAR and Jak-STAT components are determinants of cell-type-specific differences in cardiac antiviral responses. *J Virol*, 2007. **81**(24): p. 13668-80.
6. Stewart, M.J., et al., Basal and reovirus-induced beta interferon (IFN-beta) and IFN-beta-stimulated gene expression are cell type specific in the cardiac protective response. *J Virol*, 2005. **79**(5): p. 2979-87.
7. Dill, M.T., et al., Interferon-induced gene expression is a stronger predictor of treatment response than IL28B genotype in patients with hepatitis C. *Gastroenterology*, 2011. **140**(3): p. 1021-31.
8. Sarasin-Filipowicz, M., et al., Interferon signaling and treatment outcome in chronic hepatitis C. *Proc Natl Acad Sci U S A*, 2008. **105**(19): p. 7034-9.
9. Khodarev, N.N., B. Roizman, and R.R. Weichselbaum, Molecular pathways: interferon/stat1 pathway: role in the tumor resistance to genotoxic stress and aggressive growth. *Clin Cancer Res*, 2012. **18**(11): p. 3015-21.
10. Luszczek, W., et al., Combinations of DNA methyltransferase and histone deacetylase inhibitors induce DNA damage in small cell lung cancer cells: correlation of resistance with IFN-stimulated gene expression. *Mol Cancer Ther*, 2010. **9**(8): p. 2309-21.
11. Consortium, E.P., An integrated encyclopedia of DNA elements in the human genome. *Nature*, 2012. **489**(7414): p. 57-74.
12. McKendry, R., et al., High-frequency mutagenesis of human cells and characterization of a mutant unresponsive to both alpha and gamma interferons. *Proc Natl Acad Sci U S A*, 1991. **88**(24): p. 11455-9.
13. Cheon, H. and G.R. Stark, Unphosphorylated STAT1 prolongs the expression of interferon-induced immune regulatory genes. *Proc Natl Acad Sci U S A*, 2009. **106**(23): p. 9373-8.
14. Perwitasari, O., et al., Inhibitor of kappaB kinase epsilon (IKK(epsilon)), STAT1, and IFIT2 proteins define novel innate immune effector pathway against West Nile virus infection. *J Biol Chem*, 2011. **286**(52): p. 44412-23.
15. Ooi, E.L., et al., Novel antiviral host factor, TNK1, regulates IFN signaling through serine phosphorylation of STAT1. *Proc Natl Acad Sci U S A*, 2014. **111**(5): p. 1909-14.
16. Wu, T.R., et al., SHP-2 is a dual-specificity phosphatase involved in Stat1 dephosphorylation at both tyrosine and serine residues in nuclei. *J Biol Chem*, 2002. **277**(49): p. 47572-80.
17. Myers, M.P., et al., TYK2 and JAK2 are substrates of protein-tyrosine phosphatase 1B. *J Biol Chem*, 2001. **276**(51): p. 47771-4.
18. Eriksen, K.W., et al., Deficient SOCS3 and SHP-1 expression in psoriatic T cells. *J Invest Dermatol*, 2010. **130**(6): p. 1590-7.
19. Sung, P.S., et al., Roles of unphosphorylated ISGF3 in HCV infection and interferon responsiveness. *Proc Natl Acad Sci U S A*, 2015. **112**(33): p. 10443-8.
20. Porritt, R.A. and P.J. Hertzog, Dynamic control of type I IFN signalling by an integrated network of negative regulators. *Trends Immunol*, 2015. **36**(3): p. 150-60.

21. Schoggins, J.W. and C.M. Rice, Interferon-stimulated genes and their antiviral effector functions. *Curr Opin Virol*, 2011. **1**(6): p. 519-25.
22. Hofer, M.J., et al., Mice deficient in STAT1 but not STAT2 or IRF9 develop a lethal CD4+ T-cell-mediated disease following infection with lymphocytic choriomeningitis virus. *J Virol*, 2012. **86**(12): p. 6932-46.
23. Li, W., et al., IRF7-dependent type I interferon production induces lethal immune-mediated disease in STAT1 knockout mice infected with lymphocytic choriomeningitis virus. *J Virol*, 2014. **88**(13): p. 7578-88.
24. Zornetzer, G.A., et al., Transcriptomic analysis reveals a mechanism for a prefibrotic phenotype in STAT1 knockout mice during severe acute respiratory syndrome coronavirus infection. *J Virol*, 2010. **84**(21): p. 11297-309.
25. Meraz, M.A., et al., Targeted disruption of the Stat1 gene in mice reveals unexpected physiologic specificity in the JAK-STAT signaling pathway. *Cell*, 1996. **84**(3): p. 431-42.
26. Yin, Y., et al., Modeling rotavirus infection and antiviral therapy using primary intestinal organoids. *Antiviral Res*, 2015. **123**: p. 120-31.
27. Huch, M., et al., Long-term culture of genome-stable bipotent stem cells from adult human liver. *Cell*, 2015. **160**(1-2): p. 299-312.
28. Nandakumar, R., et al., Hepatitis C virus replication in mouse cells is restricted by IFN-dependent and -independent mechanisms. *Gastroenterology*, 2013. **145**(6): p. 1414-23 e1.
29. Park, C., et al., Immune response in Stat2 knockout mice. *Immunity*, 2000. **13**(6): p. 795-804.
30. Kimura, T., et al., Essential and non-redundant roles of p48 (ISGF3 gamma) and IRF-1 in both type I and type II interferon responses, as revealed by gene targeting studies. *Genes Cells*, 1996. **1**(1): p. 115-24.
31. Pan, Q., et al., Combined antiviral activity of interferon-alpha and RNA interference directed against hepatitis C without affecting vector delivery and gene silencing. *J Mol Med (Berl)*, 2009. **87**(7): p. 713-22.
32. Shukla, P., et al., Adaptation of a genotype 3 hepatitis E virus to efficient growth in cell culture depends on an inserted human gene segment acquired by recombination. *J Virol*, 2012. **86**(10): p. 5697-707.
33. Shukla, P., et al., Cross-species infections of cultured cells by hepatitis E virus and discovery of an infectious virus-host recombinant. *Proc Natl Acad Sci U S A*, 2011. **108**(6): p. 2438-43.
34. Wang, W., et al., Convergent Transcription of Interferon-stimulated Genes by TNF-alpha and IFN-alpha Augments Antiviral Activity against HCV and HEV. *Sci Rep*, 2016. **6**: p. 25482.
35. Pan, Q., et al., Mycophenolic acid augments interferon-stimulated gene expression and inhibits hepatitis C Virus infection in vitro and in vivo. *Hepatology*, 2012. **55**(6): p. 1673-83.
36. Pedroza-Gonzalez, A., et al., Tumor-infiltrating plasmacytoid dendritic cells promote immunosuppression by Tr1 cells in human liver tumors. *Oncoimmunology*, 2015. **4**(6): p. e1008355.
37. Schoggins, J.W., et al., A diverse range of gene products are effectors of the type I interferon antiviral response. *Nature*, 2011. **472**(7344): p. 481-5.
38. Livak, K.J. and T.D. Schmittgen, Analysis of relative gene expression data using real-time quantitative PCR and the 2(-Delta Delta C(T)) Method. *Methods*, 2001. **25**(4): p. 402-8.
39. Zhang, Y., et al., Model-based analysis of ChIP-Seq (MACS). *Genome Biol*, 2008. **9**(9): p. R137.
40. Robinson, J.T., et al., Integrative genomics viewer. *Nat Biotechnol*, 2011. **29**(1): p. 24-6.

Chapter 9

Requirement of The Eukaryotic Translation Initiation Factor 4F Complex in Hepatitis E Virus Replication

Xinying Zhou[1], **Lei Xu[1]**, Yijin Wang[1], Wenshi Wang[1], Dave Sprengers[1], Herold J. Metselaar[1], Maikel P. Peppelenbosch[1] and Qiuwei Pan[1]

[1]Department of Gastroenterology and Hepatology, Erasmus MC-University Medical Center, Rotterdam, Netherlands

Antiviral Research. 2015. 124: 11-9.

Abstract

Hepatitis E virus (HEV) infection, one of the foremost causes of acute hepatitis, is becoming a health problem of increasing magnitude. As other viruses, HEV exploits elements from host cell biochemistry, but we understand little as to which components of the human hepatocellular machinery are perverted for HEV multiplication. It is, however, known that the eukaryotic translation initiation factors 4F (eIF4F) complex, the key regulator of the mRNA-ribosome recruitment phase of translation initiation, serves as an important component for the translation and replication of many viruses. Here we aim to investigate the role of three subunits of the eIF4F complex: eukaryotic translation initiation factor 4A (eIF4A), eukaryotic translation initiation factor 4G (eIF4G) and eukaryotic translation initiation factor 4E (eIF4E) in HEV replication. We found that efficient replication of HEV requires eIF4A, eIF4G and eIF4E. Consistently, the negative regulatory factors of this complex: programmed cell death 4 (PDCD4) and eIF4E-binding protein 1 (4E-BP1) exert anti-HEV activities, which further illustrates the requirement for eIF4A and eIF4E in supporting HEV replication. Notably, phosphorylation of eIF4E induced by MNK1/2 activation is not involved in HEV replication. Although ribavirin and interferon-α (IFN-α), the most often-used off-label drugs for treating hepatitis E, interact with this complex, their antiviral activities are independent of eIF4E. In contrast, eIF4E silencing provokes enhanced anti-HEV activity of these compounds. Thus, HEV replication requires eIF4F complex and targeting essential elements of this complex provides important clues for the development of novel antiviral therapy against HEV.

Keywords: Eukaryotic translation initiation factor 4F complex; Hepatitis E virus; IFN-α; Ribavirin; eIF4E-binding protein 1

Introduction

Hepatitis E virus (HEV), a single-strand-positive RNA virus classified within the genus *Hepevirus* in the family *Hepeviridae*, represents the most common cause of acute viral hepatitis [1]. Like all viruses, HEV is completely dependent on the translational machinery of host cells to synthesize the viral proteins essential for its productive infection [2]. The host protein synthesis machinery commandeered by viruses has major impact on viral protein synthesis and genome replication [3], but little is known regarding how HEV uses host translational machinery for its life-cycle.

As a heterotrimeric protein complex, eukaryotic translation initiation factor 4F (eIF4F) mediates recruitment of ribosomes to mRNA and is the rate-limiting step for cap-dependent translation in viruses and cells under most circumstances. Functions of the constituent proteins of eIF4F include delivery of an RNA helicase eukaryotic initiation translation factor 4A (eIF4A) to the 5' region, bridging mRNA and ribosome by eukaryotic initiation translation factor 4G (eIF4G) scaffolding protein and recognition of the mRNA 5' cap structure by eukaryotic initiation translation factor 4E (eIF4E) cap-binding protein [4]. Not surprisingly, all these translation initiation factors are required for various types of viruses during their translation and replication [2, 5-7]. In addition, eIF4E phosphorylation is induced by the eIF4G-associated kinase MNK1 to facilitate eIF4F assembly [8]. This process of translational control has been reported to be critical for the efficient viral infection [2, 9, 10]. Furthermore, other cellular regulatory proteins of eIF4F complex such as eukaryotic translation initiation factor 4B (eIF4B) [11], programmed cell death 4 (PDCD4) [12] and eIF4E-binding protein 1 (4E-BP1) have been reported vital for viral protein synthesis [13-15]. HEV, however, has not been investigated in this context and it is currently unknown whether the virus requires eIF4F complex for efficient replication.

Interestingly, the eIF4F complex can interact with antiviral regimens, such as ribavirin or interferon-α (IFN-α), which are the classical standard therapy of chronic hepatitis C but also as off-label drugs for treating individual HEV cases or small case series [16, 17]. Ribavirin can directly bind to eIF4E and compete for 5' cap mRNA binding [18, 19], whereas some regulatory factors of eIF4F complex are involved in interferon mediated antiviral immune response [20, 21]. In absence, however, of information as to requirement of HEV for elements of the host translational machinery it is impossible to make statements whether ribavirin

exerts its anti-HEV action through inhibition of the eIF4F complex or whether alternative mechanisms are involved.

The lack of knowledge as to the requirements made by HEV on the hepatocellular host cell machinery with respect to translation of viral gene products represents a major gap in our understanding of the biology of this virus and hampers design of rational treatment. Therefore, this study has investigated the role of the eIF4F complex and its regulatory factors in HEV replication, as well as their potential involvements in the anti-HEV actions of ribavirin and IFN-α.

Materials and methods

Reagents

Compound GCP57380 as Mnk1 inhibitor (> 98% purity) was purchased from Abcam Biochemicals (UK). Ribavirin was purchased from Sigma-Aldrich (St Louis, MO). Human IFN-α (Thermo Scientific, the Netherlands) was dissolved in PBS. Doxycycline hyclate (≥ 98% TLC) was purchased from Sigma-Aldrich (St Louis, MO). Stocks of Jak inhibitor I (Santa Cruz Biotech, Santa Cruz, CA) was dissolved in DMSO (Sigma-Aldrich, St Louis, MO) with a final concentration of 5 mg/mL. Antibodies including total-eIF4E, phosphor-eIF4E, total-4E-BP1 (Cell Signaling Technology, Netherlands) and β-actin (Santa Cruz Biotech, Santa Cruz, CA); anti-rabbit or anti-mouse IRDye-conjugated secondary antibodies (Stressgen, Glandford Ave, Victoria, BC, Canada) were also used.

Cell culture and cell models

Naïve or vector transduced Huh7 cells was established from a hepatocellular carcinoma, immortalized mouse embryonic fibroblasts (MEFs) derived from wild-type and 4E-BP1 knock-out (4E-BP1$^{-/-}$) mice (kind gifts from E.N. Fish's lab), eIF4E-S209A MEFs containing an eIF4E mutation in which eIF4E cannot be phosphorylated (kind gift from Dr. Sonenberg's lab, McGill University) were cultured in Dulbecco's modified Eagle medium (DMEM) (Invitrogen-Gibco, Breda, the Netherlands) complemented with 10% v/v fetal calf serum (Hyclone, Lonan, Utah), 100 IU/mL penicillin, 100 mg/mL streptomycin and 2 mM L-glutamine (Invitrogen-Gibco). Authentication of cell line was performed at the Department of Pathology, Erasmus MC and regular testing for mycoplasma contamination was performed at the Laboratory of Gastroenterology and Hepatology, Erasmus MC.

HEV genomic RNA was generated from a plasmid construct containing the full-length HEV genome (Kernow-C1 p6 clone, GenBank Accession Number JQ679013) or a construct containing subgenomic HEV sequence coupled with a *Gaussia* luciferase reporter gene (p6-Luc), using the Ambion MESSAGE MACHINE *in vitro* RNA transcription Kit (Life Technologies Corporation) [22, 23]. The human hepatoma 7 (Huh7) cells were collected and centrifuged for 5 min, 1500 rpm, 4 °C. Supernatant was removed and washed with 4 mL Opti-MEM by centrifuging for 5 min, 1500 rpm, 4 °C. The cell pellet was re-suspended in 100 µL Opti-MEM and mixed with p6 full-length HEV RNA or p6-Luc subgenomic RNA. Electroporation was performed with the Bio-Rad's electroporation systems using the protocol of a designed program (240 V, pulse length 0.5, number 1 and cuvette 4 mm) [22]. All cells were grown at 37 °C, 5% CO_2, and 100% humidity.

Gene knockdown and overexpression by lentiviral vector

Lentiviral vectors of shRNA (Sigma-Aldrich) targeting eIF4A, eIF4G, eIF4B, PDCD4, eIF4E, 4E-BP1 and controls were obtained from the Erasmus Center for Biomics and produced in HEK 293T cells as previously described [24]. Three types of control vectors have been tested on HEV replication (CTR1: Control that will not activate the RNAi pathway because the vector does not contain an shRNA insert, CTR2: Control that will activate RISC and the RNAi pathway, but does not target any human or mouse genes. The short hairpin sequence contains 5 bp mismatches and scrambled sequences to any known human or mouse gene, CTR3: Control contains shRNA sequence that targets GFP reporter that is not expressed in our cell lines. Since no off-target effect was observed (Supplementary Figure 1), the most advanced shRNA control vector targeting GFP (GFP is not expressed in our cell lines) was used in this study as control (shCTR). After a pilot study, the shRNA vectors exerting optimal gene knockdown were selected. To generate gene knockdown cells, Huh7 cells were transduced with lentiviral vectors. Since the knockdown vectors also express a puromycin resistance gene, transduced cells were subsequently selected by adding 3 µg/mL puromycin to the cell culture medium. Overexpression of 4E-BP1 lentivector (AddGene) was a kind gift from Dr. Sonenberg's lab, McGill University. To generate overexpression cells, Huh7 cells were transduced with lentiviral vectors and doxycycline was used to add in the 4E-BP1 overexpression cell lines as the stimulation factor.

Quantitative real-time polymerase chain reaction

RNA was isolated with a Machery-Nucleo Spin RNA II kit (Bioke, Leiden, Netherlands) and quantified using a Nanodrop ND-1000 (Wilmington, DE, USA). cDNA was prepared from total RNA using a cDNA Synthesis Kit (TAKARA BIO INC). The cDNA was quantified with a SYBR Green-based real-time PCR (MJ Research Opticon, Hercules, CA, USA) according to the manufacturer's instructions. GAPDH or β-actin was considered as reference gene to normalize gene expression. The HEV primer sequences were 5'-ATTGGCCAGAAGTTGGTTTTCAC-3' (sense) and 5'-CCGTGGCTATAATTGTGGTCT-3' (antisense).

Western blot assay

Proteins in cell lysates were heated 5 min at 95 °C followed by loading onto a 10 - 15% sodium dodecyl sulphate-polyacrylamide gel (SDS-PAGE) and separated by electrophoresis. After 90 min running at 100 V, proteins were electrophoretically transferred onto a polyvinylidenedifluoride (PVDF) membrane (Invitrogen) for 1.5 hrs with an electric current of 250 mA. Subsequently, the membrane was blocked with blocking buffer. It was followed by incubation with rabbit t-eIF4E, p-eIF4E, t-4E-BP1 (1: 1 000) antibodies overnight at 4 °C. The membrane was washed 3 times followed by incubation for 1 hrs with anti-rabbit or anti-mouse IRDye-conjugated secondary antibodies (LI-COR Biosciences, Lincoln, USA) (1: 5 000) at room temperature. Blots were assayed for β-actin content as standardization of sample loading, scanned, and quantified by Odyssey infrared imaging (Li-COR Biosciences, Lincoln, NE, USA). Results were visualized and quantitated with Odyssey 3.0 software.

Measurement of luciferase activity

For *Gaussia* luciferase, the activity of secreted luciferase in the cell culture medium was measured by BioLux® *Gaussia* Luciferase Flex Assay Kit (New England Biolabs). For *firefly* luciferase, luciferin potassium salt (100 mM, Sigma) was added to cells and incubated for 30 min at 37 °C. Both *Gaussia* and *firefly* Luciferase activity was quantified with a LumiStar Optima luminescence counter (BMG LabTech, Offenburg, Germany).

Statistical analysis

All results were presented as mean ± SEM. Comparisons between groups were performed with Mann-Whitney test. Differences were considered significant at a p value less than 0.05 *or 0.01 **.

Results

Requirements of eIF4A and eIF4G for efficient HEV replication

Most of cellular and viral mRNAs rely on cap-dependent mRNA translation. The canonical mechanism of initiation commences with recognition of 5' end m^7GpppN cap structure by the eIF4F complex formed by the DEAD-box helicase eIF4A, the scaffolding protein eIF4G and the cap recognition factor eIF4E [25]. Among these initiation factors, eIF4A is a subunit in charge of unwinding of secondary structure within the leader sequence of mRNA, while large scaffolding subunit eIF4G is associated with many other translation initiation factors [7]. Because of the important roles of both eIF4A and eIF4G subunits reported in translation and replication of many viruses, we investigated their roles in HEV replication.

Firstly, we evaluated the role of the DEAD-box RNA helicase eIF4A by using RNAi-based gene loss-of-function approach. Two out of four (sheIF4A-1 and sheIF4A-2) shRNAs targeting eIF4A showed significant reduction of its mRNA level in Huh7 cells, compared with a control shRNA targeting GFP (shCTR) (Figure 1A). Consistently, their protein levels were also down-regulated without affecting the expression of eIF4G and eIF4E, which suggested a successful knockdown of eIF4A (Figure 1B). No cytotoxicity has been observed in these cells as measured by MTT assay (Supplementary Figure 2A). Silencing of eIF4A resulted in significant decrease of cellular HEV RNA level by 63.1% ± 8.6% and 57.6% ± 13.8% (mean ± SEM, n = 4, $P < 0.05$) after three days inoculation of HEV particles, respectively (Figure 1C). Next, knockdown of scaffold protein eIF4G by four shRNAs were also performed in Huh7 cells. Two clones (sheIF4G-1 and sheIF4G-4) showed efficient down-regulation of eIF4G at both mRNA level and protein level, but did not influence the protein level of eIF4A or eIF4E (Figure 1D and 1E). No cytotoxicity was observed in these knockdown cells (Supplementary Figure 2B). Correspondingly, HEV RNA levels was significantly reduced by 36.1% ± 10.6% and 33.8% ± 11.0% (mean ± SEM, n = 4, $P < 0.05$) in both eIF4G knockdown cells, respectively, compared to shCTR cells (Figure 1F). These results demonstrate that both eIF4A and eIF4G are required for efficient HEV replication.

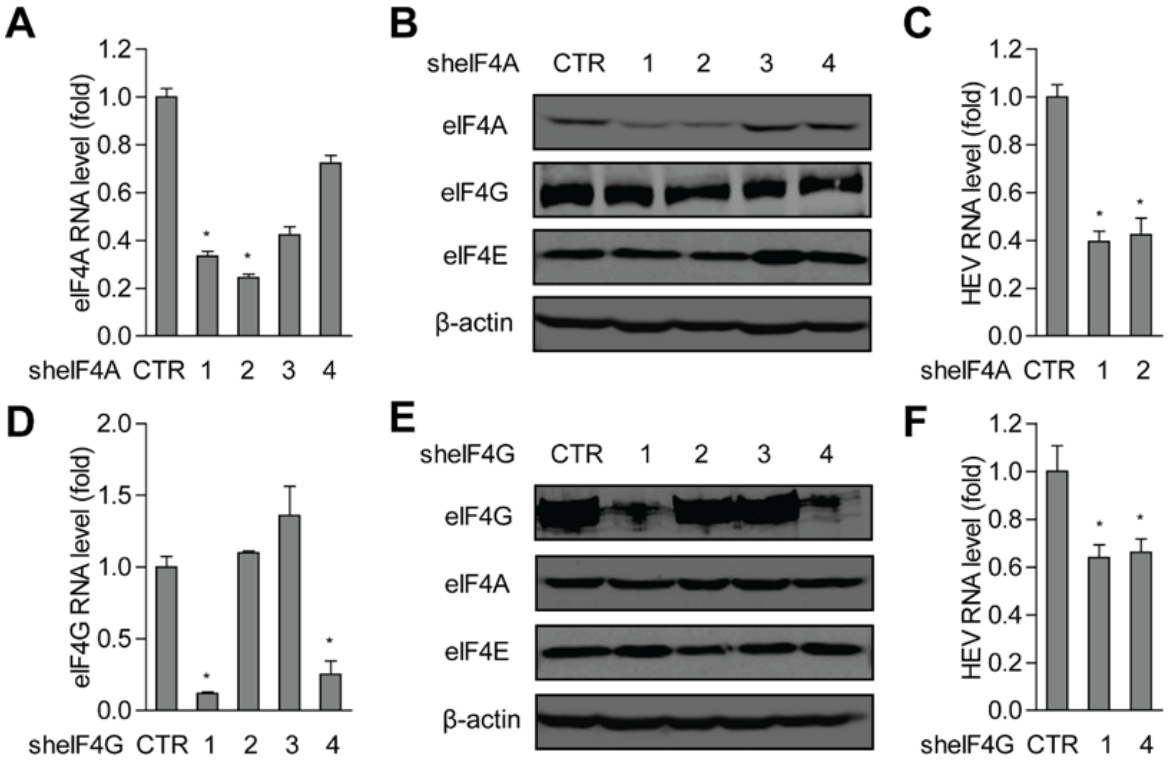

Figure 1. Requirements of eIF4A and eIF4G for HEV replication.

Knockdown of eIF4A and eIF4G by lentiviral shRNA vectors were performed in Huh7 cells. Compared with the control vector transduced cells, the sheIF4A clone 1 and 2 (A and B) or the sheIF4G clone 1 and 4 (D and E) showed potent gene silencing at mRNA level and protein level. Correspondingly, knockdown of eIF4A (C) and eIF4G (F) resulted in significant increase of cellular HEV RNA level (Mean ± SEM, n = 4). * $P < 0.05$.

PDCD4, the negative regulatory factor of eIF4A, restricts HEV replication

Given the fact that the function of eIF4A is regulated by multiple cellular factors, we first investigated the effect of its activator eIF4B that can increase the helicase activity of eIF4A. Knockdown of eIF4B by two out of four shRNA clones (sheIF4B-2 and sheIF4B-3) resulted in significant down-regulation of eIF4B expression (Figure 2A), but has no significant influence on cellular HEV RNA level (Figure 2B).

We next examined a negative regulatory factor of eIF4A, PDCD4, which prevents the binding of eIF4A to eIF4G and thereby inhibits the initiation of translation [26], To assess the effect of PDCD4 on HEV replication, lentiviral shRNA vectors were used to stably knockdown its expression in Huh7 cells. Potent down-regulation of PDCD4 mRNA and protein expression of two clones (shPDCD4-1 and shPDCD4-3) (Figure 2C and 2D) resulted in a significant increase of HEV RNA after inoculation of HEV particles for three days (Figure 2E). No cytotoxicity was observed in knockdown cells (Supplementary Figure 2C). These results are

consistent with the finding that eIF4A supports HEV replication and inhibiting the function of eIF4A by PDCD4 in turn suppresses HEV replication.

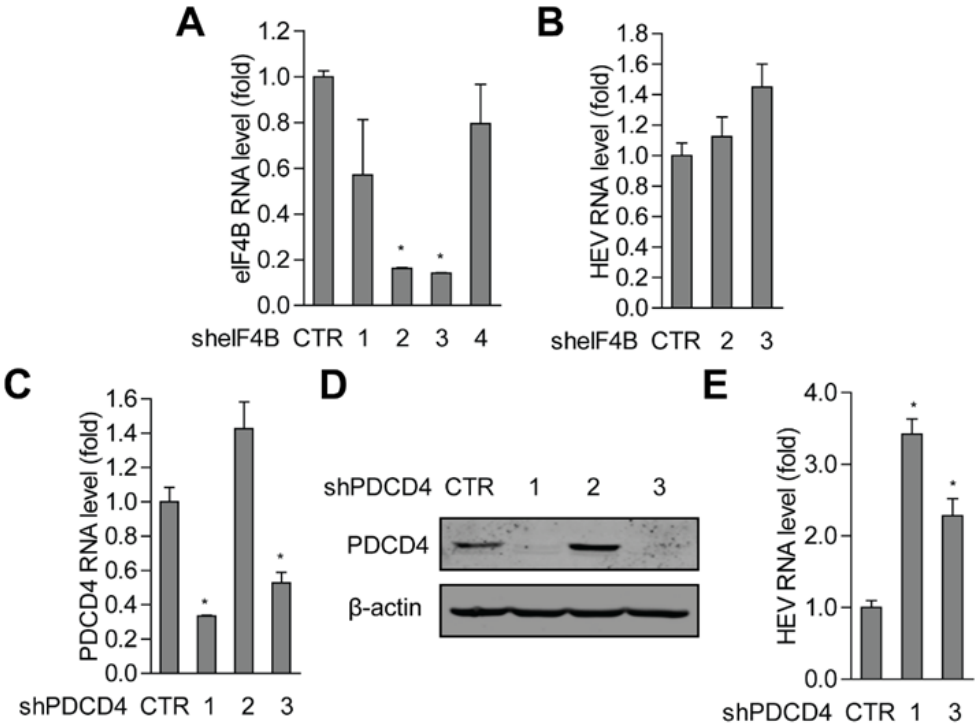

Figure 2. The regulatory factors of eIF4A, PDCD4 but not eIF4B, restricted HEV replication.

(A) Clone 2 and 3 Knockdown of eIF4B by lentiviral shRNA vectors exerted significant down-regulation of eIF4B at mRNA level. (B) Silencing of eIF4B did not influence HEV replication during 72 hrs inoculation of viral particles. mRNA level (C) and protein level (D) of PDCD4 were significantly reduced in clone 1 and 3. (E) HEV RNA level were dramatically increased when silencing PDCD4 in clone 1 and 3. (Mean ± SEM, n = 4). * $P < 0.05$.

eIF4E is also required for efficient HEV replication

eIF4E, the least abundant component of the eIF4F complex, is a rate-limiting factor for translation [27], To investigate the role of eIF4E in HEV replication, its expression was silenced by RNAi. Two out of five shRNAs targeting eIF4E exerted potent knockdown at both protein (Figure 3A) and mRNA levels (Figure 3B). No off-target effect was observed on protein expression of eIF4G or eIF4A (Figure 3A), or on genes such as CyA, CyB, 4E-BP1 and mTOR, which are known to affect HEV replication as previously shown [28, 29] (Supplementary Figure 3). MTT assay showed no cytotoxicity of eIF4E silencing in cells (Supplementary Figure 2D). Accordingly, inoculation of HEV led to reduction by 44% ± 12% and 41% ± 25% (mean ± SEM, n = 5, $P < 0.05$) in viral RNA level in these two knockdown cells compared to shCTR cells (Figure 3C). We observed similar effect in MEFs (Figure 3D and 3E), further confirming that eIF4E plays an important role in HEV replication.

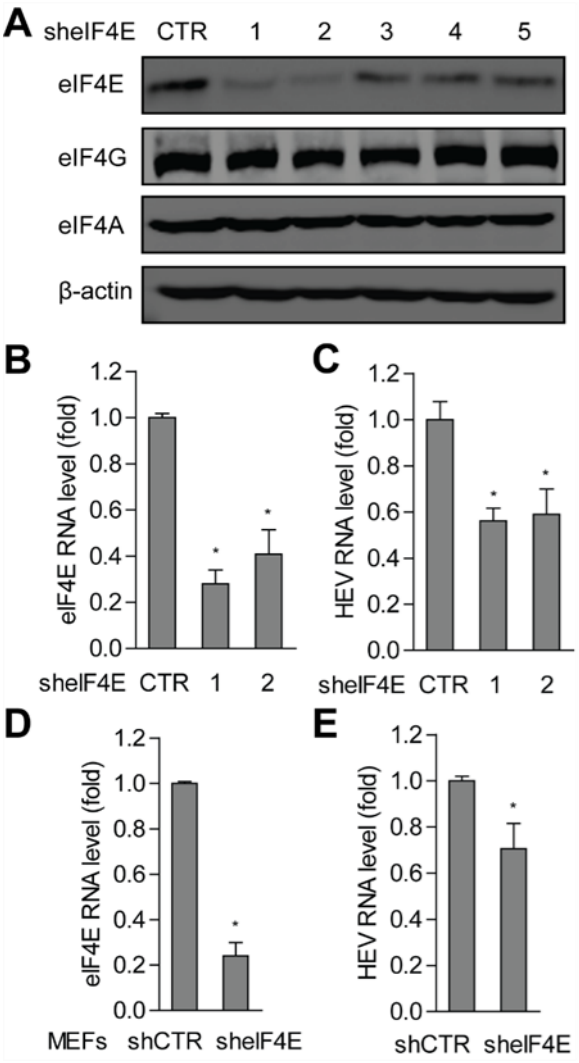

Figure 3. eIF4E supports HEV replication.

Knockdown of human eIF4E by five lentiviral shRNA vectors were performed in Huh7 cells. Clone 1 and 2 exhibited a potent down-regulation of eIF4E at protein (A) and mRNA (B) levels. β-actin served as an internal reference. (C) Correspondingly, these two clones of eIF4E knockdown inhibited HEV replication. (D) Knockdown of mouse eIF4E by lentiviral shRNA vector was applied in MEFs showed a significant decrease at eIF4E mRNA level. (E) HEV RNA level was significantly reduced with eIF4E silencing in MEFs. (Mean ± SEM, n = 4). * $P < 0.05$.

Phosphorylation is not required for eIF4E to support HEV replication

Ser209 phosphorylation has been shown to be required for the oncogenic potential of eIF4E [30]. To examine whether this is also important in the context of HEV infection, Huh7 cells harboring the HEV subgenomic replicon or the full-length genome were treated with 10-100 μM CGP57380, a well-characterized inhibitor of MNK. MNK is the only known physiologic kinase that phosphorylates eIF4E (Ser209 site) [31]. This compound potently inhibited eIF4E-S209 phosphorylation without effect on total eIF4E protein level (Figure 4A). However, CGP57380 had no effect on HEV replication in both luciferase replicon model (Figure 4B) and infectious model (Figure 4C). To further confirm the function of phosphorylation of eIF4E, MEFs cultured from mice with S209A mutation were used. This mutation targeting the conserved phosphorylation site for MNK1/2 kinase with serine-to-alanine completely abolished phosphorylation of eIF4E at Ser209 without effect on total eIF4E (Figure 4D).

Consistently, no significant effect was observed on HEV replication between mutated and wild type MEFs (Figure 4E). These data suggest that phosphorylation of eIF4E is dispensable for HEV replication.

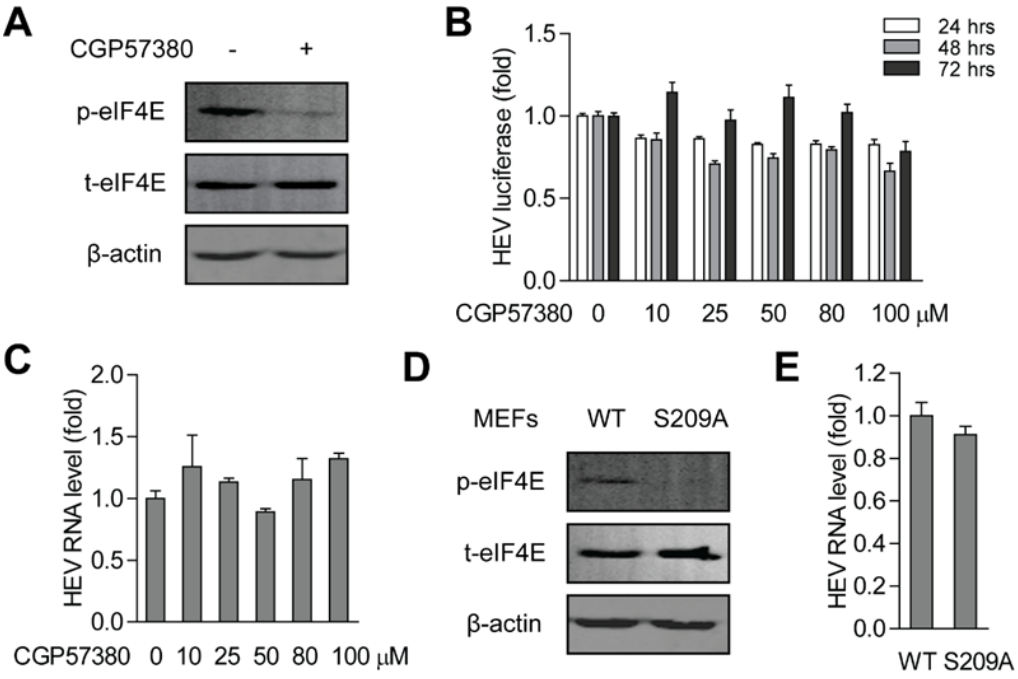

Fig. 4. eIF4E phosphorylation did not significantly affect HEV replication.

(A) Treatment with MNK1/2 inhibitor CGP57380 of 100 μM dramatically decreased the phosphorylation of eIF4E, but not total eIF4E protein shown by Western blot assay. β-actin served as an internal reference. 10 - 100 μM CGP57380 did not significantly affected viral replication-related luciferase activity during the three days (B) and viral RNA level in Huh7-p6 infectious model for 48 hrs (C). (D) MEFs of S209A mutation abolished phosphorylation of eIF4E at Ser209 shown by Western blot assay. β-actin served as an internal reference. (E) Inhibition of phosphorylation in S209A MEFs did not significantly influence HEV replication. (Mean ± SEM, n = 4).

HEV replication is inhibited by the eIF4E suppressor, 4E-BP1

eIF4E can be released by 4E-BP1 hyperphosphorylation with elimination of translational repression [21]. For a more detailed characterization of the role of eIF4E suppressor 4E-BP1 in HEV infection, we employed both loss- and gain-of-function approaches in Huh7 cells. Using lentiviral RNAi technique, 4E-BP1 was dramatically down-regulated at both protein and mRNA levels (Figure 5A). Accordingly, 48 hrs inoculation of HEV resulted in 2.6 ± 1.2 fold (mean ± SEM, n = 4, $P < 0.05$) increase of viral RNA in 4E-BP1 knockdown Huh7 cells, compared with the mock knockdown cells (Figure 5A). In contrast, using an inducible overexpression lentiviral vector, 4E-BP1 expression was drastically up-regulated at both protein and mRNA levels with treatment of dose dependent doxycycline, which resulted in significant reduction of HEV RNA by 59% ± 17% (mean ± SEM, n = 4, $P < 0.05$) (Figure 5B).

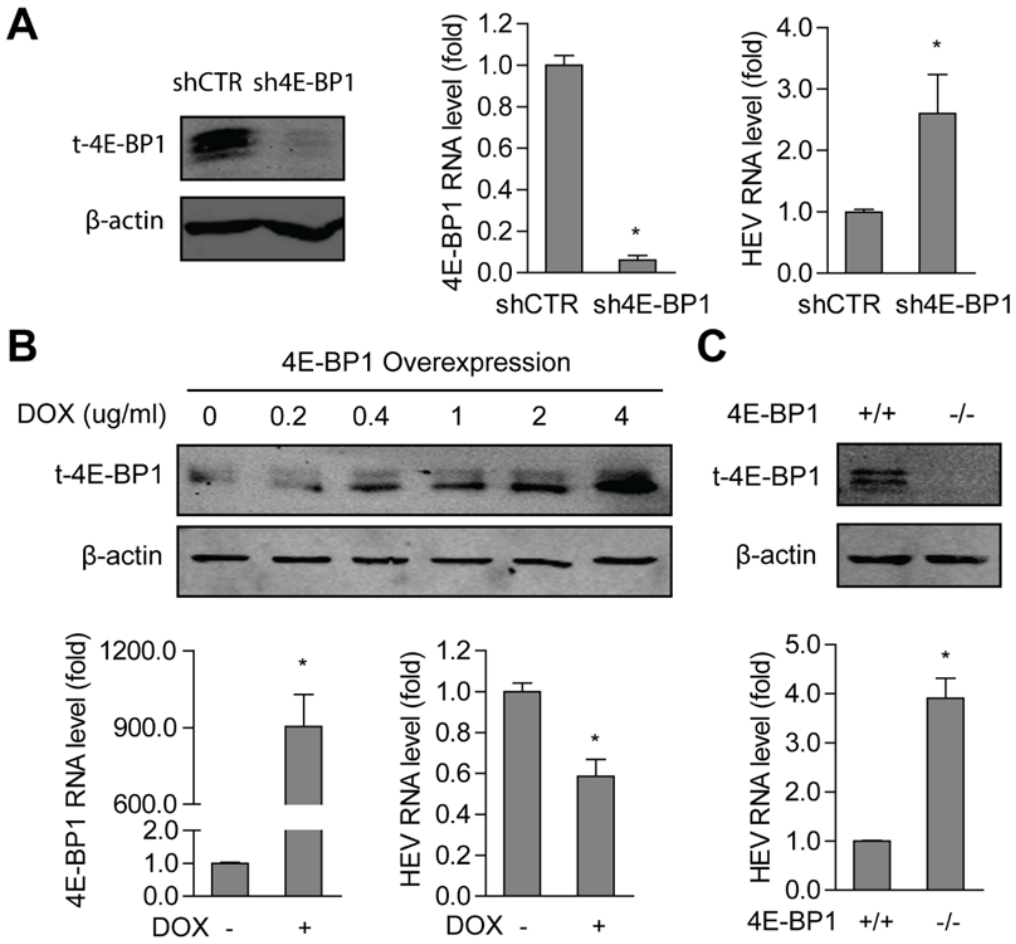

Figure 5. The eIF4E suppressor, 4E-BP1, limited HEV replication.

(A) Efficient silencing of 4E-BP1 at protein level was detected by Western blot assay. β-actin served as an internal reference. Similarly, 4E-BP1 was significantly down-regulated at mRNA level (Mean ± SEM, n = 7). Correspondingly, inoculation of HEV resulted in significant increase of viral RNA in 4E-BP1 knockdown Huh7 cells, compared with the mock knockdown cells (Mean ± SEM, n = 4). (B) 4E-BP1 was drastically up-regulated at protein level when the overexpression cell lines were treated with different concentrations of doxycycline for 24 hrs. β-actin served as an internal reference. Similarly, mRNA levels of 4E-BP1 was dramatically increased after treatment of 4 μg/mL doxycycline for 24 hrs. (Mean ± SEM, n = 5). Correspondingly, 4E-BP1 overexpression cell line with treatment of 4 μg/mL doxycycline for 24 hrs resulted in significant reduction of HEV RNA level (Mean ± SEM, n = 4). (C). MEFs derived from 4E-BP1 knockout (4E-BP1$^{-/-}$) mice presented an efficient silencing of 4E-BP1 at protein level compared to WT MEFs, leading to significant increase of HEV RNA level (Mean ± SEM, n = 4). * $P < 0.05$.

To further validate 4E-BP1 function in HEV infection, MEFs cultured from 4E-BP1 knockout mice were studied. Western blot assay showed a complete knockout of 4E-BP1 at protein level (Figure 5C). Accordingly, 48 hrs inoculation of HEV led to 3.9 ± 0.8 fold (mean ± SEM, n = 4, $P < 0.05$) increase of cellular HEV RNA level in 4E-BP1 knockout MEFs (4E-BP1$^{-/-}$) compared to wild type MEFs (4E-BP1$^{+/+}$) (Figure 5C). Hence, these data supported a role of 4E-BP1 in constraining HEV replication.

The anti-HEV activities of ribavirin and IFN-α are independent of eIF4E

Ribavirin is a well-known inhibitor of eIF4E [18]. To evaluate whether the anti-HEV activity of ribavirin is mediated by the inhibition of eIF4E, both shCTR and sheIF4E-1 cells with HEV inoculation were used for the treatments of 6.25, 12.5, 25, 50, 100 μM ribavirin for 48 hrs. Comparable IC_{50} in shCTR and sheIF4E cells were found with the range between 12.5-25 μM (Figure 6A).

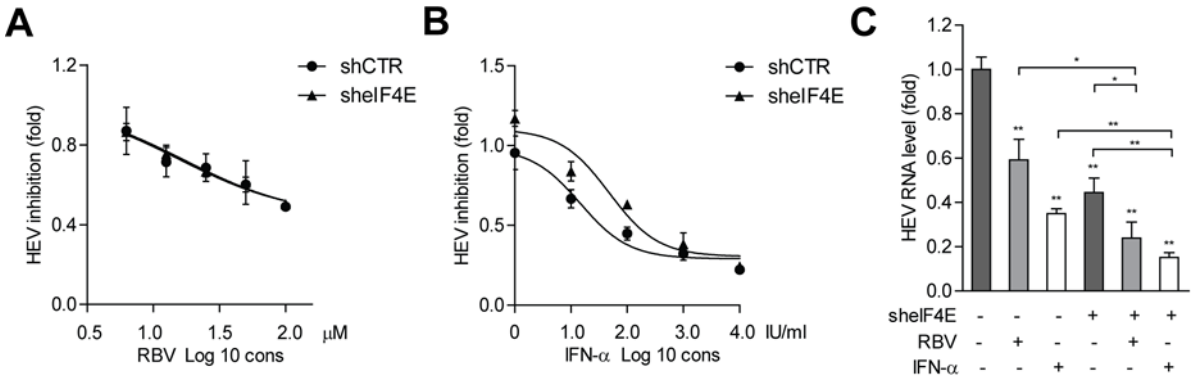

Figure 6. The anti-HEV activities of ribavirin and IFN-α is independent of eIF4E.

(A) IC_{50} of RBV was with the range between 12.5 - 25 μM: 15.67 μM in shCTR cells and 17.24 μM in sheIF4E cells and (B) IFN-α was with the range between 10 - 50 IU/mL: 14.55 IU/mL in shCTR cells and 47.75 IU/mL in sheIF4E cells). (C) 25 μM ribavirin and 1000 IU/mL IFN-α were treated in shCTR and sheIF4E cells. HEV RNA level was detected by qRT-PCR after 72 hrs inoculation of viral particle. (Mean ± SEM, n = 4 - 8). * $P < 0.05$. ** $P < 0.01$.

The antiviral activity of IFN-α has also been associated to the regulation of translation initiation factors in particular circumstances [20, 21]. To further assess whether eIF4E could mediate the anti-HEV activity of IFN-α, treatments of 1, 10, 100, 1000, 10000 IU/mL IFN-α on HEV in both shCTR and sheIF4E-1 cells for 48 hrs has been performed. Comparable IC_{50} of IFN-α were observed with the range between 10-50 IU/mL in shCTR and sheIF4E cells (Figure 6B). Furthermore, as expected, HEV replication were significantly inhibited with treatment of 25 μM ribavirin and 1000 IU/mL IFN-α for 48 hrs. However, the anti-HEV effects of ribavirin and IFN-α were further enhanced by eIF4E knockdown (Figure 6C). In addition, no clear cytotoxicity was observed in both shCTR and sheIF4E cells (Supplementary Figure 4A and 4B). These results indicated that the antiviral effects of ribavirin and IFN-α are independent of eIF4E, although silencing of eIF4E could already inhibit HEV replication.

Discussion

Most of the viruses can only encode restricted numbers of proteins and therefore they heavily rely on the host cellular machinery and their ingredients to accomplish the virus life-

cycles [3]. Recent studies show that translation initiation mechanisms especially eIF4F complex is employed by many viruses as a primary target for cap-dependent translational control to confer advantages to generate progeny [32]. Three proteins: RNA helicase eIF4A, scaffolding protein eIF4G and cap binding protein eIF4E, which are components of the eIF4F complex, are related to the efficient translation and replication of various viruses [2, 5, 7]. It is, however, unknown to what extent HEV requires elements from the translation initiation complex. Our study was aimed to provide more insight in this area of HEV biology, also with the explicit goal to provide directions for the development of rational treatment of HEV-related disease. Our study demonstrated a requirement of the eIF4F complex for efficient HEV replication (Figure 1 and 3).

Among all three subunits of the eIF4F complex, eIF4E is the main regulatory nexus involved in the complex formation and has impact on many types of viral infections [3], including on HEV as we showed in this study. One of the mechanisms by which eIF4E takes control of complex formation and translation initiation process is via phosphorylation on serine 209 carried out by MNK1/2 [3]. Stimulation of eIF4E phosphorylation is correlated with facilitated translation and replication of some viruses [2, 9, 30]. In contrast, we found that S209 phosphorylation is not required for eIF4E to support HEV replication (Figure 4). Another regulatory mechanism of eIF4E is exerted via 4E-BP1, a small-molecular-weight repressor of 5' capped mRNA translation, which has also been implicated in host defense against viral infection [15]. In apparent agreement, we show that 4E-BP1 can inhibit HEV replication (Figure 5). 4E-BP1 is a phosphoprotein that binds to eIF4E depending on its phosphorylation status. 4E-BP1 hyperphosphorylation results in releasing eIF4E to form the functional eIF4F complex. Conversely, 4E-BP1 hypophosphorylation allows binding of this protein to eIF4E and counteracts the formation of eIF4F complex [3]. Therefore, without this hijacking of eIF4E in a 4E-BP1-deficient context, eIF4E can still exert its pro-HEV activity (as we have shown in Supplementary Figure 5). Similarly, the eIF4A suppressor PDCD4 can also restrict HEV replication (Figure 2). PDCD4 sequesters eIF4A from the eIF4E-eIF4G complex, resulting in repressed translation of mRNAs [12] and thus modulates replication of various viruses [13, 14]. Apparently this notion also holds true in the biology of HEV infection.

Despite the absence of proven medications for treating HEV, ribavirin, IFN-α, or the combination have been use as off-label antiviral drugs to treat individual HEV cases or small case series [16]. The antiviral effect of interferons and their signaling pathways have been

attributed to effects in the 4E-BP1 cascade [15, 20]. However, loss- or gain-function of 4E-BP1 had no significant effects on the expression of IFN-α and -β (Supplementary Figure 6A) and no effect on phosphorylation of STAT1, the key element of interferon signaling transduction (Supplementary Figure 6B). Furthermore, the effect of 4E-BP1 on HEV is independent of JAK-STAT cascades (Supplementary Figure 6C). Conversely, the anti-HEV effect of IFN-α is also independent of 4E-BP1 (Supplementary Figure 6D). Although ribavirin directly binds to eIF4E and competes for 5' cap mRNA binding [18, 19], the anti-HEV activity of ribavirin is also independent of eIF4E in our experimental system (Figure 6). Instead, loss of eIF4E exerts additive anti-HEV effect of IFN-α or ribavirin and suggests that treatments aimed at targeting the translation initiation complex in conjunction with IFN-α or ribavirin have significant promise.

In conclusion, we revealed that cap dependent translation machinery plays a critical role in help with efficient HEV replication. The translational suppressors PDCD4 and 4E-BP1 are important antiviral factors in restraining HEV infection (Figure 7). Thus, these results have shed new light on virus-host interactions and provided new avenue for potential antiviral drug development against HEV infection.

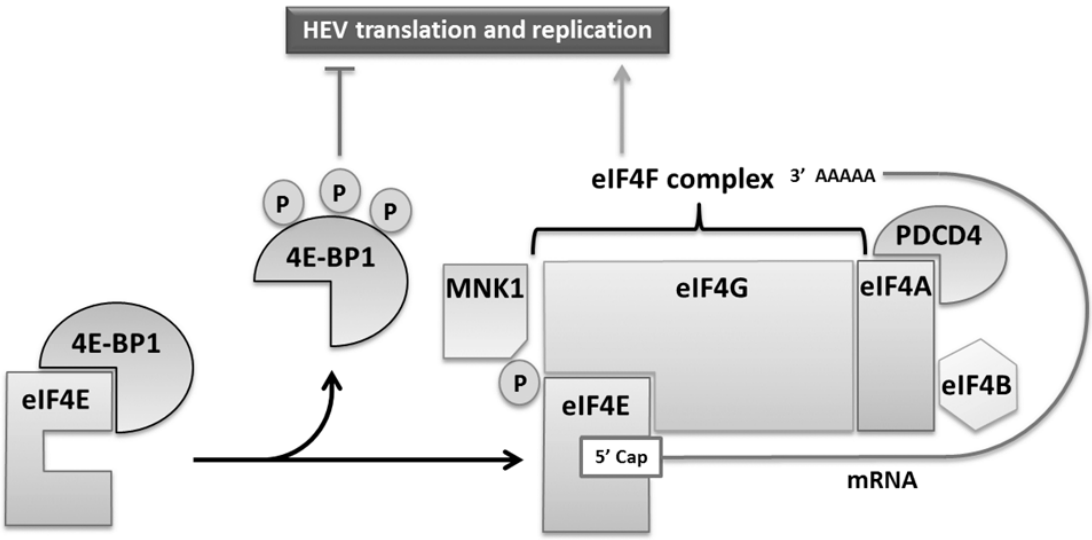

Figure 7. Schematic illustration of the involvement of the eIF4F complex in HEV replication.

Three subunits of eIF4F complex: eIF4A, eIF4G and eIF4E play important roles in efficient HEV replication. Furthermore, HEV replication is limited by the cap dependent translational suppressors, PDCD4 and 4E-BP1, but is not influenced by eIF4E phosphorylation induced by MNK1/2 kinase activation.

Supplementary Figures and Tables

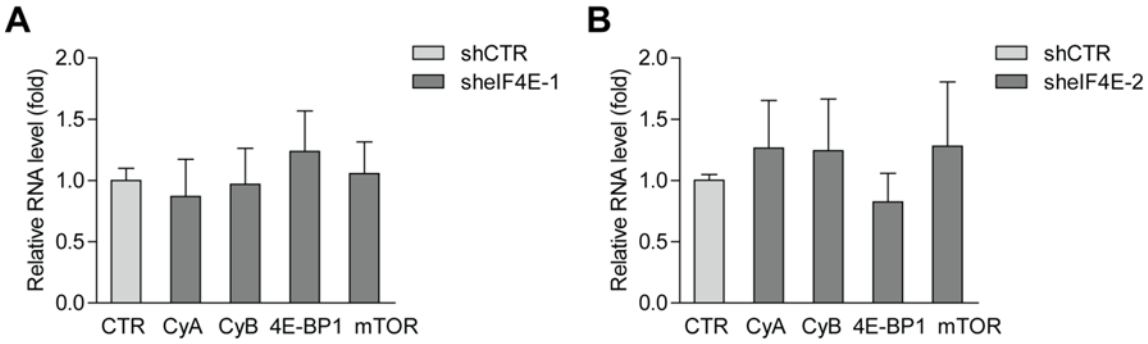

Supplementary Figure 1.

eIF4E knockdown did not significant affect off-target genes expression in Huh7 cells. CyA, CyB, 4E-BP1 and mTOR mRNA levels were not influenced in sheIF4E-1 (A) and sheIF4E-2 cells (B). (Mean ± SEM, n = 3).

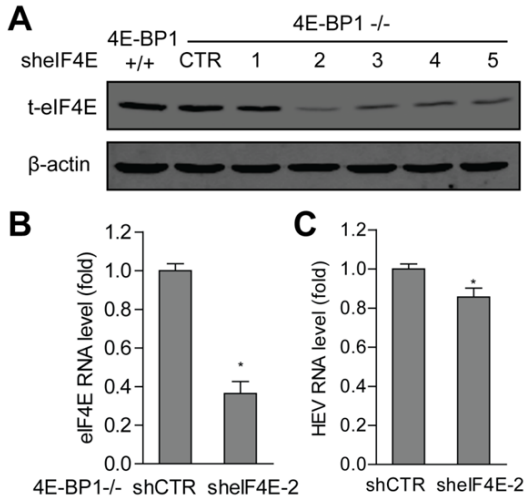

Supplementary Figure 2.

eIF4E is required for efficient HEV replication in 4E-BP1$^{-/-}$ knockout MEFs. Clone sheIF4E-2 of mouse eIF4E knockdown showed a potent eIF4E silencing at protein (A) and mRNA levels (B). β-actin served as an internal reference in Western blot assay. (C) HEV RNA level was significantly reduced in sheIF4E-2 MEFs deficient of 4E-BP1. (Mean ± SEM, n = 4). * $P < 0.05$.

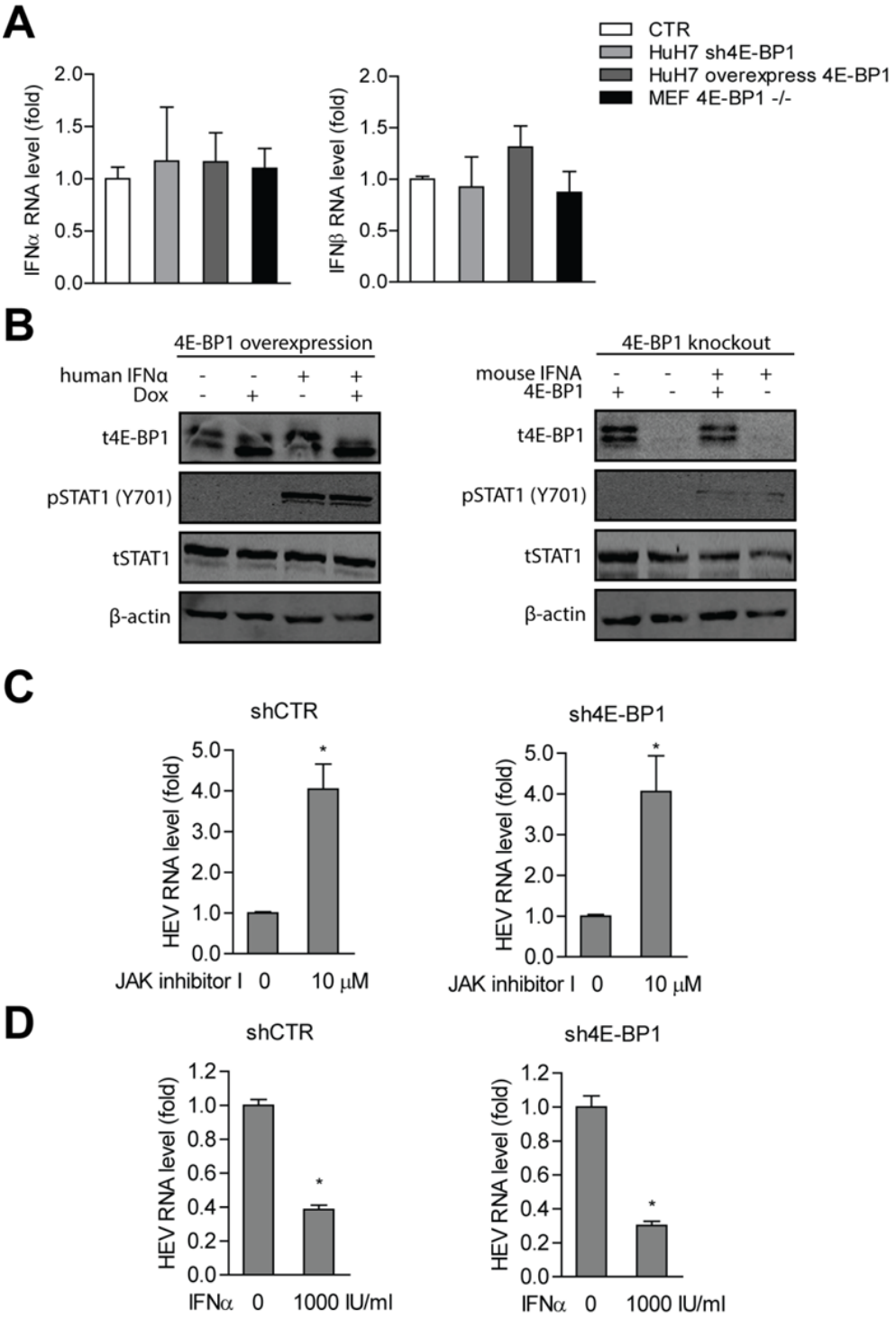

Supplementary Figure 3.

(A) IFN-α and -β production were not influenced by 4E-BP1 expression in Huh7 cells and MEFs. (B) IFN-α induced phosphorylation of STAT1, which represents key elements in antiviral JAK-STAT1 cascades, showed no difference in 4E-BP1 overexpression Huh7 cells and 4E-BP1 knockout MEFs by Western blot assay. β-actin served as an internal reference. 4E-BP1 did not mediate the pro-HEV effects of Jak inhibitor I (C) and anti-HEV effects of IFN-α (D) for 48 hrs. (Mean ± SD, n = 4).

References

1. Kamar, N., et al., Hepatitis E virus infection. *Clin Microbiol Rev*, 2014. **27**(1): p. 116-38.
2. Walsh, D. and I. Mohr, Phosphorylation of eIF4E by Mnk-1 enhances HSV-1 translation and replication in quiescent cells. *Genes Dev*, 2004. **18**(6): p. 660-72.
3. Montero, H., R. Garcia-Roman, and S.I. Mora, eIF4E as a control target for viruses. *Viruses*, 2015. **7**(2): p. 739-50.
4. Gingras, A.C., B. Raught, and N. Sonenberg, eIF4 initiation factors: effectors of mRNA recruitment to ribosomes and regulators of translation. *Annu Rev Biochem*, 1999. **68**: p. 913-63.
5. George, A., et al., Hepatitis C virus NS5A binds to the mRNA cap-binding eukaryotic translation initiation 4F (eIF4F) complex and up-regulates host translation initiation machinery through eIF4E-binding protein 1 inactivation. *J Biol Chem*, 2012. **287**(7): p. 5042-58.
6. Ventoso, I., et al., HIV-1 protease cleaves eukaryotic initiation factor 4G and inhibits cap-dependent translation. *Proc Natl Acad Sci U S A*, 2001. **98**(23): p. 12966-71.
7. de Breyne, S., et al., In vitro studies reveal that different modes of initiation on HIV-1 mRNA have different levels of requirement for eukaryotic initiation factor 4F. *FEBS J*, 2012. **279**(17): p. 3098-111.
8. Walsh, D., M.B. Mathews, and I. Mohr, Tinkering with translation: protein synthesis in virus-infected cells. *Cold Spring Harb Perspect Biol*, 2013. **5**(1): p. a012351.
9. Royall, E., et al., Murine norovirus 1 (MNV1) replication induces translational control of the host by regulating eIF4E activity during infection. *J Biol Chem*, 2015. **290**(8): p. 4748-58.
10. Walsh, D., et al., Regulation of the translation initiation factor eIF4F by multiple mechanisms in human cytomegalovirus-infected cells. *J Virol*, 2005. **79**(13): p. 8057-64.
11. Harms, U., et al., eIF4B, eIF4G and RNA regulate eIF4A activity in translation initiation by modulating the eIF4A conformational cycle. *Nucleic Acids Res*, 2014. **42**(12): p. 7911-22.
12. Dennis, M.D., L.S. Jefferson, and S.R. Kimball, Role of p70S6K1-mediated phosphorylation of eIF4B and PDCD4 proteins in the regulation of protein synthesis. *J Biol Chem*, 2012. **287**(51): p. 42890-9.
13. Wang, S., et al., Influenza A virus-induced degradation of eukaryotic translation initiation factor 4B contributes to viral replication by suppressing IFITM3 protein expression. *J Virol*, 2014. **88**(15): p. 8375-85.
14. Damania, P., et al., Hepatitis B virus induces cell proliferation via HBx-induced microRNA-21 in hepatocellular carcinoma by targeting programmed cell death protein4 (PDCD4) and phosphatase and tensin homologue (PTEN). *PLoS One*, 2014. **9**(3): p. e91745.
15. Kaur, S., et al., Regulatory effects of mammalian target of rapamycin-activated pathways in type I and II interferon signaling. *J Biol Chem*, 2007. **282**(3): p. 1757-68.
16. Zhou, X., et al., Epidemiology and management of chronic hepatitis E infection in solid organ transplantation: a comprehensive literature review. *Rev Med Virol*, 2013. **23**(5): p. 295-304.
17. Kamar, N., et al., Ribavirin for chronic hepatitis E virus infection in transplant recipients. *N Engl J Med*, 2014. **370**(12): p. 1111-20.
18. Kentsis, A., et al., Ribavirin suppresses eIF4E-mediated oncogenic transformation by physical mimicry of the 7-methyl guanosine mRNA cap. *Proc Natl Acad Sci U S A*, 2004. **101**(52): p. 18105-10.
19. De la Cruz-Hernandez, E., et al., Ribavirin as a tri-targeted antitumor repositioned drug. *Oncol Rep*, 2015. **33**(5): p. 2384-92.
20. Burke, J.D., et al., Antiviral effects of interferon-beta are enhanced in the absence of the translational suppressor 4E-BP1 in myocarditis induced by Coxsackievirus B3. *Antivir Ther*, 2011. **16**(4): p. 577-84.

21. Nehdi, A., et al., Deficiency in either 4E-BP1 or 4E-BP2 augments innate antiviral immune responses. *PLoS One*, 2014. **9**(12): p. e114854.
22. Shukla, P., et al., Adaptation of a genotype 3 hepatitis E virus to efficient growth in cell culture depends on an inserted human gene segment acquired by recombination. *J Virol*, 2012. **86**(10): p. 5697-707.
23. Shukla, P., et al., Cross-species infections of cultured cells by hepatitis E virus and discovery of an infectious virus-host recombinant. *Proc Natl Acad Sci U S A*, 2011. **108**(6): p. 2438-43.
24. Pan, Q., et al., Combined antiviral activity of interferon-alpha and RNA interference directed against hepatitis C without affecting vector delivery and gene silencing. *J Mol Med (Berl)*, 2009. **87**(7): p. 713-22.
25. Sonenberg, N. and A.G. Hinnebusch, Regulation of translation initiation in eukaryotes: mechanisms and biological targets. *Cell*, 2009. **136**(4): p. 731-45.
26. Pelletier, J., et al., Targeting the eIF4F translation initiation complex: a critical nexus for cancer development. *Cancer Res*, 2015. **75**(2): p. 250-63.
27. Mohr, I. and N. Sonenberg, Host translation at the nexus of infection and immunity. *Cell Host Microbe*, 2012. **12**(4): p. 470-83.
28. Han, J., et al., SPF rabbits infected with rabbit hepatitis E virus isolate experimentally showing the chronicity of hepatitis. *PLoS One*, 2014. **9**(6): p. e99861.
29. Zhou, X., et al., Rapamycin and everolimus facilitate hepatitis E virus replication: revealing a basal defense mechanism of PI3K-PKB-mTOR pathway. *J Hepatol*, 2014. **61**(4): p. 746-54.
30. Panda, S., et al., A unique phosphorylation-dependent eIF4E assembly on 40S ribosomes co-ordinated by hepatitis C virus protein NS5A that activates internal ribosome entry site translation. *Biochem J*, 2014. **462**(2): p. 291-302.
31. Kyriakis, J.M., In the beginning, there was protein phosphorylation. *J Biol Chem*, 2014. **289**(14): p. 9460-2.
32. Bushell, M. and P. Sarnow, Hijacking the translation apparatus by RNA viruses. *J Cell Biol*, 2002. **158**(3): p. 395-9.

Chapter 10

Inhibition of Hepatitis E Virus Replication by Proteasome Inhibitor is Nonspecific

Lei Xu[1], Xinying Zhou[1], Maikel P. Peppelenbosch[1] and Qiuwei Pan[1]

[1]Department of Gastroenterology and Hepatology, Erasmus MC-University Medical Center, Rotterdam, Netherlands

Archives of Virology. 2015. 160(2):435-439.

Abstract

The ubiquitin proteasome system plays important role in virus infection. A previous study showed that the proteasome inhibitor MG132 could potentially affect hepatitis E virus (HEV) replication. In this study, we found that MG132 could inhibit HEV and hepatitis C virus (HCV) replication-related luciferase activity in subgenomic models. Furthermore, treatment with MG132 in a HEV infectious model resulted in a dramatic reduction in the intracellular level of HEV RNA. Surprisingly, MG132 concurrently inhibited the expression of a luciferase gene used as a control as well as a wide range of host genes. Consistently, the total cellular RNA and protein content was concurrently reduced by MG132 treatment, suggesting a nonspecific antiviral effect.

Keywords: Ubiquitin proteasome system; MG132; Hepatitis E virus

Introduction

The ubiquitin proteasome system (UPS), which serves as a major pathway for protein degradation and modification in eukaryotic cells, can be utilized by many types of viruses [1-3]. Previous studies have demonstrated that UPS can regulate viral RNA-dependent RNA polymerase (RdRp), which mediates viral RNA synthesis [1, 4-6]. In addition, UPS can also regulate ubiquitylation and degradation of some viral structural proteins [7-9] and thus represents a potential antiviral target.

Hepatitis E virus (HEV) is a single-strand positive-sense RNA virus that belongs to the family Hepeviridae. It is a small non-enveloped virus with a 7.2-kb RNA genome, which is capped at the 5' termini and polyadenylated at the 3' termini [10]. Outbreaks of hepatitis E occur periodically throughout the developing world. It typically causes an acute and self-limiting infection, but fulminant hepatitis and high mortality (reaching 25 %) have been described in cases of pregnant women. In the western world, HEV mainly affects immunocompromised patients with a high risk of developing chronic hepatitis [11]. However, no proven medication is available to treat hepatitis E. A recent study reported potent antiviral effects of a well-known proteasome inhibitor, MG132, against HEV [12]. In a Renilla-luciferase-coupled HEV replication model, the authors showed that treatment with MG132 resulted in dramatic reduction of HEV-related luciferase activity [12]. These important findings have inspired us to further evaluate the effects of MG132 in two HEV cell culture models.

Materials and methods

In this study, two human hepatoma cell line (Huh7)-based HEV cell culture models were employed: a subgenomic HEV replicon containing *Gaussia* luciferase reporter (p6- Luc) in which the accumulation of secreted luciferase serves as a reporter for HEV replication, and a full-length infectious model (p6) in which Huh7 cells were electroporated with full-length HEV genomic RNA (Kernow-C1 p6 clone, GenBank accession number JQ679013) [13]. Two *firefly* luciferase cell models were also used: a cell line for normalization in which stable expression of luciferase is driven by a phosphoglycerate kinase (PGK) promoter (Huh7-PGK) and a hepatitis C virus (HCV, also a single-strand positive-sense RNA virus) subgenomic cell culture model (Huh7-ET) [14]. The *Gaussia* luciferase and *firefly* luciferase activity were

measured as described previously [13] using a LumiStar Optima luminescence counter (BMG Lab Tech, Offenburg, Germany). MTT assays were performed as described previously [15]. The absorbance of each well was read using a microplate absorbance reader (Bio-Rad) at a wavelength of 490 nm. RNA was isolated using a Macherey-Nagel NucleoSpin RNA II Kit (Bioke, Leiden, The Netherlands) and quantified using a NanoDrop ND-1000 (Thermo, DE, USA). cDNA was prepared from total RNA using a cDNA Synthesis Kit (Takara Bio Inc.). HEV, GAPDH, RP2 (human retinitis pigmentosa 2), CyA (cyclophilin A), CyB (cyclophilin B), CD81 (cluster of differentiation 81) and IMPDH2 (inosine-5'-monophosphate dehydrogenase 2) were quantified by SYBR-Green-based real-time PCR. The HEV primer sequences were 5'-ATTGGCCAGAAGTTGGTTTTCAC-3' (sense) and 5' -CCGTGGCTATAATTGTGGTCT-3'(anti-sense), the primer sequences for the housekeeping gene GAPDH were 5' -TGTCCCCACCCCCAATGTATC-3' (sense) and 5' -CTCCGATGCCTGCTTCACTACCTT-3'(antisense), and the primers for the housekeeping gene RP2 were 5'-CCCATTAAACTCCAAGGCAA-3' (sense) and 5'- AAGCTGAGGATGCTCAAAGG-3' (antisense). The primer sequences for CyA were 5'-GGCAAATGCTGGACCCAACACA-3'(antisense) and 5'-TGCTGGTCTTGCCATTCCTGGA-3' (sense), and the primers for CyB were 5'- AACGCAGGCAAAGACACCAACG-3' (antisense) and 5'- TCTGTCTTGGTGCTCTCCACCT-3' (sense). The primers for CD81 were 5' -CTGCTTTGACCACCTCAGTGCT-3' (antisense) and 5'-TGGCAGCAATGCCGATGAGGTA-3' (sense), and the primers for IMPDH2 were 5' -AGTGGCTCCATCTGCATTACGC-3' (antisense) and 5' -GGATTCCTCCATCAGCAATGACC-3' (sense). For Western blot, 100,000 cells were seeded in a 6-well plate and treated with MG132 for 48 h. Cell lysates (300 µL) were heated for 5 minutes at 95 °C followed by loading 30 µL of sample onto a 10 % sodium dodecyl sulfate polyacrylamide gel and separating by electrophoresis. Mouse β-actin antibody (1: 1000) was used as primary antibody. For SDS-PAGE, after electrophoresis for 90 min at 120 V, the gel was stained in Coomassie brilliant blue solution and distained.

Results

Consistent with a previous study [12], treatment with 1 µM and 10 µM MG132 did not significantly impair cellular metabolic activity or viability as determined by MTT assay after 24 h (Fig. 1A) and 48 h (Fig. 1B), although a minor inhibitory effect was observed when cells were treated with 10 µM MG132 for 48 h. As expected, treatment with 1 µM MG132 potently inhibited HEV-replication-related *Gaussia* luciferase activity in the p6-Luc model (Fig.

1) after 24 h and 48 h. Furthermore, we tested this proteasome inhibitor in the Huh7-based hepatitis C virus subgenomic model (Huh7-ET). Consistently, MG132 inhibited HCV-coupled *firefly* luciferase activity (Fig. 1). Surprisingly, when Huh7-PGK cells were treated with MG132, the control *firefly* luciferase activity driven by the PGK promoter was also potently inhibited (Fig. 1). These results raised concerns regarding the specificity of the effect of MG132 on viral replication.

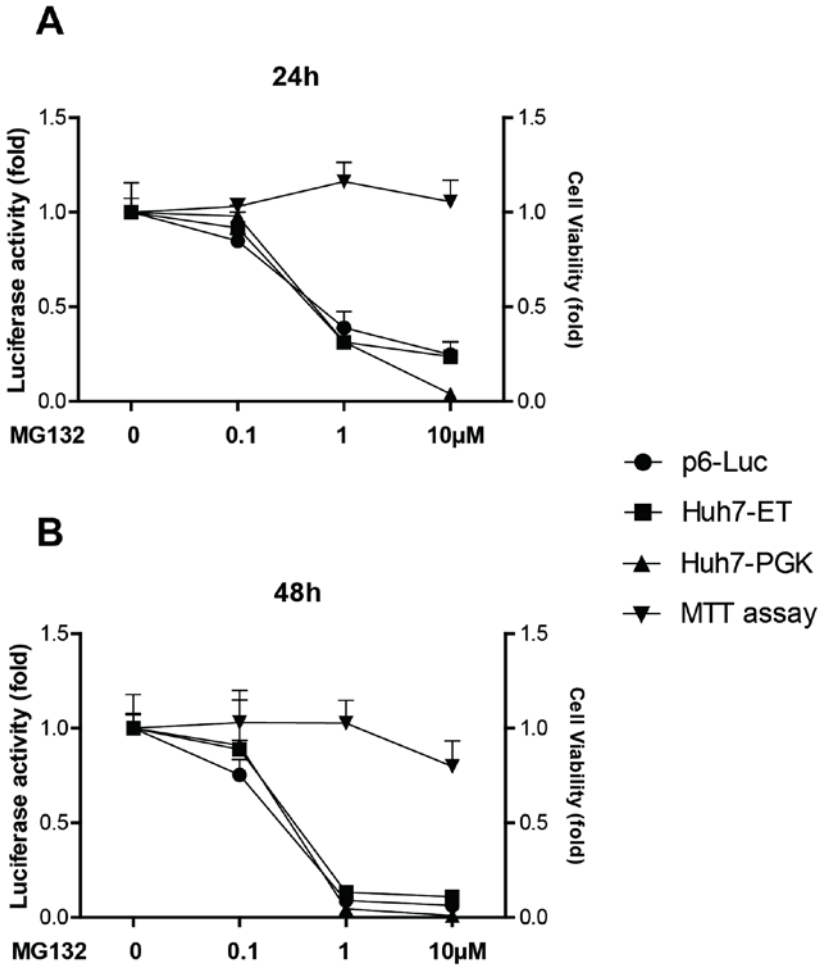

Fig. 1 Nonspecific effects of the proteasome inhibitor MG132 on luciferase activity.

Treatment with MG132 after 24 h (A) and 48 h (B) resulted in dramatic reduction of luciferase activity in subgenomic HEV replicon (p6-Luc) (mean ± SD, n = 12), HCV replicon (Huh7- ET) (mean ± SD, n = 4) and Huh7 cells constantly expressing a control luciferase gene under the control of the PGK promoter (Huh7- PGK) (mean ± SD, n = 4). MG132 treatment did not strongly affect cellular metabolic activity or viability, as determined by MTT assay (OD490 value) (mean ± SD, n = 4), although a minor inhibitory effect was observed after treatment at 10 μM for 48 h

To investigate further, the HEV infectious model (p6) was treated with MG132 for 48 h. The relative levels of HEV viral RNA and two host reference genes (GAPDH and RP2) were quantified by SYBR-based qRT-PCR. As shown in Fig. 2A, treatment with 1 or 10 μM MG132 resulted in a significant decrease in intracellular HEV RNA by 32 ± 19% and 76 ± 24% (mean ± SD, n=6, $p < 0.01$), respectively. Strikingly, the expression levels of two references genes, GAPDH and RP2 were concurrently decreased. In addition, the expression of four other host genes that we tested, CyA, CyB, CD81 and IMPDH2, also decreased simultaneously (Fig. 2B). These results confirm that the effect of MG132 is nonspecific.

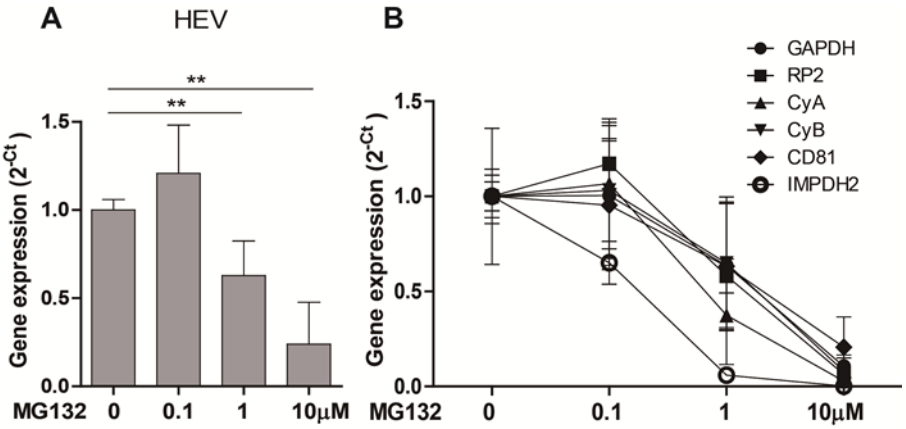

Fig. 2 Significantly decrease in HEV viral RNA levels after MG132 treatment.

(A) and (B) The expression of two reference genes (GAPDH, RP2) and four host genes (CyA, CyB, CD81 and IMPDH2) were concurrently inhibited by treatment with MG132. Relative gene expression was quantified by qRT-PCR. Data are presented as 2^{-Ct} and normalized to the untreated control (mean ± SD, n = 6). **P < 0.01

Next, we measured the RNA concentration and total protein content of the cells after MG132 treatment and we found that MG132 treatment (1 μM and 10 μM) drastically reduced the total cellular RNA content (Fig. 3A). Furthermore, cells that were treated with MG132 and lysed showed reduced cellular protein expression. As shown in Fig. 3B, the protein level of internal reference b-actin was decreased after treatment with 1 μM and 10 μM MG132, and the total protein content was also reduced (Fig. 3C). However, the effects of MG132 at the protein level were less profound than that at the RNA level. These results suggest that MG132 inhibits expression and translation of a broad range of genes rather than having a specific effect on viral infection.

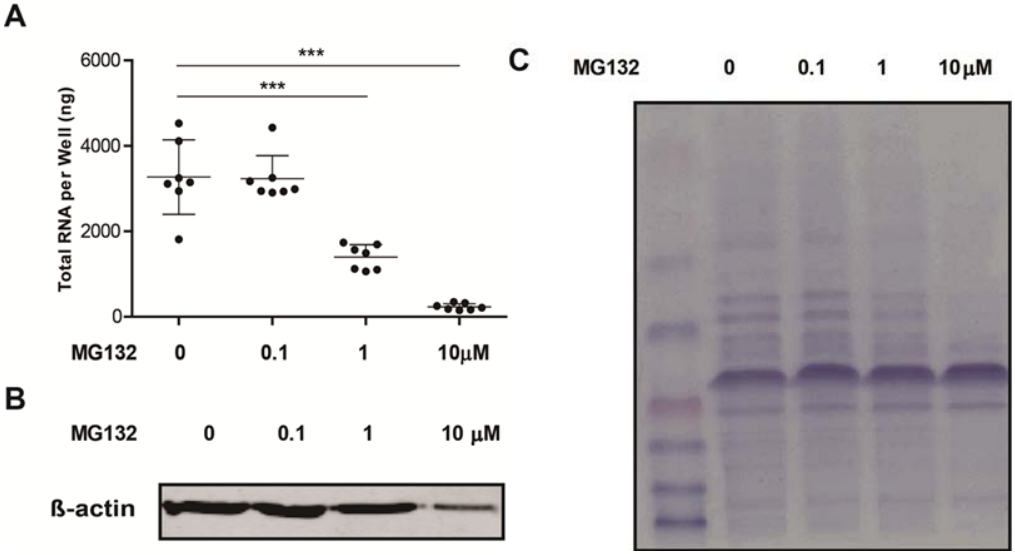

Fig. 3 Decrease in cellular RNA and protein content after MG132 treatment.

Total intracellular RNA in cells was dramatically reduced by MG132 treatment after 48 h. RNA concentration was determined using a NanoDrop 2000 spectrophotometer (mean ± SD, n = 7). (B) Protein expression of internal reference β-actin was inhibited by MG132 (in particular with 10 μM) treatment after 48 h. The same volumes of cell lysates were loaded, and the protein level was determined by Western blot. (C) Total intracellular protein was reduced by MG132 treatment (in particular with 10 μM) after 48 h. The same volumes of cell lysate were loaded, and the gel was stained in Coomassie brilliant blue solution and distained. **P < 0.01 ***P < 0.001

Discussion

There is substantial evidence suggesting that the cellular UPS is associated with viral infection. RdRp, the essential enzyme for viral replication, can be regulated by UPS in turnip yellow mosaic virus (TYMV) [1], Sindbis virus [4], hepatitis A virus (HAV) [5] and HCV [6] infections. Virus-encoded proteases cleave viral polyprotein proteolytically but can also mediate the processing of many host proteins [16]. Mature 3C proteases of HAV and encephalomyocarditis virus (EMCV) have been shown to be subject to rapid, ubiquitin-mediated protein degradation [17, 18]. As a combat strategy, some viral proteases have been shown to contain de-ubiquitinating enzyme activity. Papain-like cysteine proteases of SARS coronavirus [19], HEV [20] and foot-and-mouth disease virus (FMDV) [21] have the ability to hydrolyze ubiquitinating substrates. Therefore, modulating the UPS represents as a potential antiviral strategy.

Treatment with the proteasome inhibitor MG132 has been shown to decrease the titer of porcine circovirus type 2 (PCV2) at an early stage of infection [22]. Treatment with MG132 has also been shown to decrease the activity of *Renilla* luciferase expressed from an HEV replicon [12]. However, our study raised concerns regarding the specificity of the effect of MG132 on HEV replication. Although we confirmed the inhibitory effects on luciferase activity in both the HEV and HCV replicon models, MG132 also inhibited constitutively expressed luciferase in control cells. Furthermore, in the full-length HEV model, although MG132 treatment reduced HEV RNA levels, it also simultaneously inhibited the expression of reference genes and other host genes. We further demonstrated that MG132 dramatically decreases the levels of total intracellular RNA and protein, which explains its nonspecific effect on viral infection.

It is not surprising that inhibition of this system could exert variety of effects on cell physiology, since the UPS plays an essential role in the processing of cellular proteins. Proteasomes promptly degrade ubiquitylated proteins [23], and some of these proteins are important mediators of cell-cycle progression and apoptosis [24]. MG132 has been shown to

induce the expression of death receptor 5 (DR5), a receptor for tumor necrosis factor-related apoptosis-inducing ligand (TRAIL), resulting in enhanced sensitivity to TRAIL-induced apoptosis in cancer cells [25, 26]. Thus, inhibition of this major intracellular protein degradation pathway could nonspecifically affect viral infection, but we do not fully exclude that UPS may also specifically modulate certain viruses [2].

In summary, this study demonstrated that inhibition of HEV infection by the proteasome inhibitor MG132 is nonspecific. Thus, we should be careful in interpreting data regarding the effects and mechanisms of proteasome inhibitors on viral infection. Although proteasome inhibitors are in the preclinical phase of testing as anticancer agents [24, 27], we would call for caution in developing proteasome-targeted antiviral therapies.

Abbreviations

UPS: Ubiquitin proteasome system; HEV: Hepatitis E virus; HCV: Hepatitis C virus; RdRp: RNA-dependent RNA polymerase; PGK: Phosphoglycerate kinase; TYMV: Turnip yellow mosaic virus; HAV: Hepatitis A virus; RP2: Human retinitis pigmentosa 2; CyA: Cyclophilin A; CyB: Cyclophilin B; CD81: Cluster of differentiation 81; IMPDH2: Inosine-5'-monophosphate dehydrogenase 2

Acknowledgments

The authors would like to thank Dr. Suzanne U. Emerson (National Institute of Allergy and Infectious Diseases, NIH, USA) for generously providing the plasmids to generate subgenomic and full-length HEV genomic RNA. The authors also thank the Netherlands Organization for Scientific Research (NWO/ZonMw) for a VENI grant (No. 916-13-032), the European Association for the Study of the Liver (EASL) for a Sheila Sherlock Fellowship, the Dutch Digestive Foundation (MLDS) for a career development grant (No. CDG 1304), the Daniel den Hoed Foundation for a Centennial Award grant (to Q. Pan), and the China Scholarship Council for funding PhD fellowships for L. Xu (201306300027) and X. Zhou (No. 201206150075).

References

1. Camborde, L., et al., The ubiquitin-proteasome system regulates the accumulation of Turnip yellow mosaic virus RNA-dependent RNA polymerase during viral infection. *Plant Cell*, 2010. **22**(9): p. 3142-52.
2. Choi, A.G., et al., The ubiquitin-proteasome system in positive-strand RNA virus infection. *Rev Med Virol*, 2013. **23**(2): p. 85-96.
3. Isaacson, M.K. and H.L. Ploegh, Ubiquitination, ubiquitin-like modifiers, and deubiquitination in viral infection. *Cell Host Microbe*, 2009. **5**(6): p. 559-70.
4. de Groot, R.J., et al., Sindbis virus RNA polymerase is degraded by the N-end rule pathway. *Proc Natl Acad Sci U S A*, 1991. **88**(20): p. 8967-71.
5. Losick, V.P., et al., Signals in hepatitis A virus P3 region proteins recognized by the ubiquitin-mediated proteolytic system. *Virology*, 2003. **309**(2): p. 306-19.
6. Gao, G. and H. Luo, The ubiquitin-proteasome pathway in viral infections. *Can J Physiol Pharmacol*, 2006. **84**(1): p. 5-14.
7. Yuksek, K., et al., Ubiquitin-independent degradation of hepatitis C virus F protein. *J Virol*, 2009. **83**(2): p. 612-21.
8. Shirakura, M., et al., E6AP ubiquitin ligase mediates ubiquitylation and degradation of hepatitis C virus core protein. *J Virol*, 2007. **81**(3): p. 1174-85.
9. Fan, Z., et al., SARS-CoV nucleocapsid protein binds to hUbc9, a ubiquitin conjugating enzyme of the sumoylation system. *J Med Virol*, 2006. **78**(11): p. 1365-73.
10. Kamar, N., et al., Hepatitis E. *Lancet*, 2012. **379**(9835): p. 2477-88.
11. Zhou, X., et al., Epidemiology and management of chronic hepatitis E infection in solid organ transplantation: a comprehensive literature review. *Rev Med Virol*, 2013. **23**(5): p. 295-304.
12. Karpe, Y.A. and X.J. Meng, Hepatitis E virus replication requires an active ubiquitin-proteasome system. *J Virol*, 2012. **86**(10): p. 5948-52.
13. Zhou, X., et al., Rapamycin and everolimus facilitate hepatitis E virus replication: revealing a basal defense mechanism of PI3K-PKB-mTOR pathway. *J Hepatol*, 2014. **61**(4): p. 746-54.
14. Pan, Q., et al., Mycophenolic acid augments interferon-stimulated gene expression and inhibits hepatitis C Virus infection in vitro and in vivo. *Hepatology*, 2012. **55**(6): p. 1673-83.
15. Wang, Y., et al., Calcineurin inhibitors stimulate and mycophenolic acid inhibits replication of hepatitis E virus. *Gastroenterology*, 2014. **146**(7): p. 1775-83.
16. Lloyd, R.E., Translational control by viral proteinases. *Virus Res*, 2006. **119**(1): p. 76-88.
17. Gladding, R.L., et al., Evaluation of the susceptibility of the 3C proteases of hepatitis A virus and poliovirus to degradation by the ubiquitin-mediated proteolytic system. *Biochem Biophys Res Commun*, 1997. **238**(1): p. 119-25.
18. Lawson, T.G., et al., Identification and characterization of a protein destruction signal in the encephalomyocarditis virus 3C protease. *J Biol Chem*, 1999. **274**(14): p. 9904-80.
19. Barretto, N., et al., The papain-like protease of severe acute respiratory syndrome coronavirus has deubiquitinating activity. *J Virol*, 2005. **79**(24): p. 15189-98.
20. Karpe, Y.A. and K.S. Lole, Deubiquitination activity associated with hepatitis E virus putative papain-like cysteine protease. *J Gen Virol*, 2011. **92**(Pt 9): p. 2088-92.
21. Wang, D., et al., The leader proteinase of foot-and-mouth disease virus negatively regulates the type I interferon pathway by acting as a viral deubiquitinase. *J Virol*, 2011. **85**(8): p. 3758-66.
22. Cheng, S., et al., The ubiquitin-proteasome system is required for the early stages of porcine circovirus type 2 replication. *Virology*, 2014. **456-457**: p. 198-204.
23. Rock, K.L., et al., Inhibitors of the proteasome block the degradation of most cell proteins and the generation of peptides presented on MHC class I molecules. *Cell*, 1994. **78**(5): p. 761-71.

24. Adams, J., The proteasome: a suitable antineoplastic target. *Nat Rev Cancer*, 2004. **4**(5): p. 349-60.
25. Yoshida, T., et al., Proteasome inhibitor MG132 induces death receptor 5 through CCAAT/enhancer-binding protein homologous protein. *Cancer Res*, 2005. **65**(13): p. 5662-7.
26. He, Q., Y. Huang, and M.S. Sheikh, Proteasome inhibitor MG132 upregulates death receptor 5 and cooperates with Apo2L/TRAIL to induce apoptosis in Bax-proficient and -deficient cells. *Oncogene*, 2004. **23**(14): p. 2554-8.
27. Elliott, P.J., T.M. Zollner, and W.H. Boehncke, Proteasome inhibition: a new anti-inflammatory strategy. *J Mol Med (Berl)*, 2003. **81**(4): p. 235-45.

Chapter 11

Summary and Discussion

The interferon (IFN)-mediated cellular response is thought to be the first line of antiviral barrier [1-3]. The production of IFN is usually triggered by viral infection [4]. IFN exert its antiviral function by activating the expression a large number of IFN-stimulated genes (ISGs) [3, 5]. Generally, the transcription of these ISGs is provoked via the JAK-STAT pathway. However, recent studies demonstrated the other non-canonical mechanisms are also involved in the regulation of ISG transcription. In **Chapter 2**, we comprehensively reviewed the canonical and non-canonical regulation mechanisms of ISG transcription. In this review, we first reviewed the classical pathway that regulates ISG transcription. We also discussed non-canonical regulation of ISG expression that involved some unique pathways or complex, such as non-canonical ISGF3 complex, STAT5-CrkL complex and nucleotide synthesis pathway. We hope our review will expand our understanding of the ISG transcription regualtion and provide some clues for the development of new antiviral strategies. In our previous study, we have shown the inhibition of nucleotide synthesis leads to the expression of some ISGs independent of JAK-STAT pathway, although the exact mechanism is still unclear [6]. Interestingly, we now are conducting a large-scale screening of an FDA-approved drug library to identify molecular that have the ability to enhance IFN induced ISG transcription, several nucleotide synthesis inhibitors were identified (our unpublished data). This may have important clinical implication to develop new antiviral drugs. Host cells have the ability to sense the invasion of viruses through pattern recognition receptors (PRRs) to produce IFNs [3, 4]. Therefore, the innate antiviral immune response is largely mediated by IFN production. In **Chapter 3,** we highlighted the IFN-independent mechanisms of many ISGs. Many important antiviral ISGs have the ability to activate the ISG transcription without the involvement of IFN production. Some ISGs which are believed exert their antiviral function via the IFN production have direct antiviral abilites. Hence, we feel that although massive researches have been done in the ISG/IFN field, this is still a largely unknown area and further effects should be taken.

Hepatitis E virus (HEV) infection is the leading cause of acute viral hepatitis worldwide [7]. Although its infection is usually a self-limiting disease for common people, gt1 (genotype 1) HEV infection have severe outcomes in pregnant women and gt3 HEV infection could develop to chronic infection in certain patients [8-11]. The current anti-HEV therapy is mainly consistent by IFN-α and ribavirin, which is learned from anti-HCV or anti-HBV treatment [7, 12-14]. Both of IFN-α and ribavirin have proven their efficacy *in vitro* and *in vivo*

[15-19]. However, treatment failure was observed in some cases of chronic patients treated with ribavirin and this seems due to some mutations in the viral genome [20-23]. Hence, we moved focus on the natural antiviral regimen, IFNs. In **Chapter 4**, we first screened many human cytokines and chemokines for their anti-HEV potential and found most of them exert minor anti-HEV activity, expect for IFN-α. We further revealed that HEV replication level is much higher in cells that have a defected JAK-STAT pathway. This observation further highlighted the vital role of JAK-STAT cascade in defending HEV infection. We also noticed that the antiviral activity of IFN-α against HEV is much lower compare to HCV but the underlying mechanism remains unknown. IFN exerts its antiviral function via the activation of a large number of Interferon-stimulated genes (ISGs) [3, 5, 24]. The antiviral potential of each individual ISG against different viruses has been profiled in different studies [5, 24-27]. However, little is known about regarding HEV infection.

In **Chapter 5,** by using the overexpression approach [5, 24], we profiled many important human ISGs for their anti-HEV ability. RIG-I, MDA5 and IRF1 were identified as potent anti-HEV ISGs in two different HEV culture models. In this chapter, we main focus on the antiviral mechanism of RIG-I, which is a pattern recognition receptors (PRRs) that recognized viral RNA, especially viral RNA has a triphosphate signature at its 5' end [28]. The antiviral potential of this ISG against HEV was further validated in different HEV culture systems. Interestingly, manually delivery the natural ligand of RIG-I 5'pppRNA into cytoplasm induced a strong antiviral immune response that inhibits HEV replication. This finding has a great clinical significance that provides an idea to develop new therapies for HEV treatment. Interestingly, we found RIG-I play important role in IFN induced ISG transcription. The lacking of RIG-I will attenuates IFN-initiated ISG expression while the overexpression of RIG-I enhances ISG expression. It is general believed that RIG-I exert its antiviral action by the induction of IFN production [4]. In this chapter, we revealed a non-canonical antiviral mechanism of RIG-I against HEV infection that independent IFN production. RIG-I overexpression causes the phosphorylation of STAT1 without triggering the IFN production. Furthermore, the RIG-I activated ISGs can be divided into 2 groups, one group totally depends on the JAK-STAT pathway and the other is not. However, some issues such as how STAT1 is phosphorylated by RIG-I without IFN production and how RIG-I activate ISGs independent of JAK-STAT pathways are not totally elucidated. In **Chapter 6,** we continue to investigate the antiviral mechanism of another identified anti-HEV ISG, IFN regulatory factor 1 (IRF1). IRF1 is an

important ISG that has been proved have broad antiviral ability against different kinds of DNA and RNA virus [5, 24]. IRF1 is also a transcription factor that leads to IFN-β expression [29]. However, in this study, we reveal that without triggering IFN expression, IRF1 still exert strong anti-HEV ability by activating the transcription of a wide range of ISGs. We further revealed that the antiviral and ISG induction ability of IRF1 is enhanced by ribavirin. Taken together, both studies demonstrated that many ISGs have non-canonical antiviral mechanisms. For instance, both IRF1 and RIG-I are known to exert their effect via IFN production, but our studies added new antiviral mechanisms to these genes, as we discussed in **Chapter 3**.

As we reviewed in **Chapter 2**, the transcription of ISG is usually regulated by the classical JAK-STAT pathway, but many non-canonical pathways are also involved in the regulation of ISG transcription. Besides IFN-α, TNF-α (Tumor Necrosis Factor-alpha) is also an important antiviral cytokine and its downstream pathway NF-κB pathway plays essential roles in regulating the expression of inflammatory cytokines [30]. In **Chapter 7**, we investigated the antiviral ability of TNF-α against HEV infection and its role in regulating ISG transcription. We first demonstrated that TNF-α exerts potent antiviral ability against HEV and HCV. We also noticed that TNF-α have the ability to activate ISG transcription. With this interesting observation, we focused on the mechanism that how TNF-α induces ISG expression. We first rule out the possibility that TNF-α induces ISG expression through the production of IFN or JAK-STAT signaling. Next, we found the TNF-α activates ISG transcription via its canonical downstream pathway, NF-κB. Different kinds of techniques were employed to answer the question that how NF-κB pathway activate ISG transcription. We surprisingly demonstrated that RelA (P65), the subunit of NF-κB, have the ability to directly bind to the promoter region of many ISGs. Our following observation found that the combination of TNF-α and IFN-α exert additive effects in ISG induction and HCV/HEV inhibition. This further support the notion that TNF-α activates ISG transcription independent IFN-JAK-STAT pathway. Without the present of IFNs, many ISGs are constitutive expressed, which may confer a rapid and direct resistance to viral infection [31]. However, how the host cells maintaining this constitutive expression of ISGs is still not clear. In **Chapter 8** we reported a novel mechanism that the unphosphorylated ISGF3 (U-ISGF3) complex drives the constitutive expression of ISGs in homeostatic condition. This novel U-ISGF3 complex consists by unphosphorylated STAT1 and STAT2 together with IRF9. Deletion

any element of this U-ISGF3 complex leads the decreased expression of ISGs and increased HCV and HEV replication. In contrast, overexpression all these three parts together induced ISG expression and inhibited viral replication. Interestingly, overexpression any part alone cannot reproduce the induction of ISG or the inhibition of virus. Of note, overexpression all these three parts does not found any phosphorylation of STAT1 or STAT2, suggesting this U-ISGF3 functions in a manner independent of phosphorylation. The study on this novel antiviral mechanism expands our knowledge in the mechanisms that regulate ISG transcription. As we reviewed in **Chapter 2**, more canonical and non-canonical regulatory mechanisms of the ISG expression will be studied in the future. All these canonical and non-canonical mechanisms coordinately regulate the vast host antiviral web that centered at ISG.

All viruses rely on the host translational machinery to complete their life cycles [32]. HEV is a positive single-stranded RNA virus, which means once HEV infects host cells, the viral RNA can be directly translated like mRNA. However, until now, little is now about how the host translational machinery involved in the replication of HEV. Most cellular mRNA and viral RNA use the cap-dependent mRNA translation system that initiated via the eIF4F complex. The eIF4F complex consists by eIF4A (Eukaryotic Translation Initiation Factor 4A), eIF4G and eIF4E [33]. In **Chapter 9**, we found all these three subunits are required for HEV replication. Meanwhile, after depleting the negative regulator of this pathway, a higher level of HEV replication was observed. This further support the notion the HEV replication required this eIF4F complex. Although ribavirin was reported has the ability bind to the eIF4E to act as an inhibitor of this complex [34], we observed that ribavirin inhibit HEV replication in an eIF4E independent manner. The inhibition of HEV translation may serve as a potential target for developing new treatments against HEV infection. In **Chapter 9**, we have demonstrated the host translation system has great an impact for HEV replication, it is reasonable to assume that protein degradation may also play important role in regulating HEV replication. The ubiquitin proteasome system (UPS) are the main pathway for protein degradation and also used by virus [35]. In a previous study, it was reported that the ubiquitin-proteasome system is necessary during HEV replication and proteasome inhibitor MG132 inhibits viral replication [36]. In line with this study, **in Chapter 10**, we also observed the inhibition effect of this MG132 against HEV replication. However, our following study revealed that HCV-couple luciferase activity, cellular RNA and protein content were also affected by this inhibitor, indicating the non-specific function of this proteasome inhibitor.

References

1. **Xu, L.**, et al., Noncanonical Antiviral Mechanisms of ISGs: Dispensability of Inducible Interferons. *Trends Immunol*, 2017. **38**(1): p. 1-2.
2. Wang, W., et al., Transcriptional Regulation of Antiviral Interferon-Stimulated Genes. *Trends Microbiol*, 2017.
3. Schneider, W.M., M.D. Chevillotte, and C.M. Rice, Interferon-stimulated genes: a complex web of host defenses. *Annu Rev Immunol*, 2014. **32**: p. 513-45.
4. Goubau, D., S. Deddouche, and C. Reis e Sousa, Cytosolic sensing of viruses. *Immunity*, 2013. **38**(5): p. 855-69.
5. Schoggins, J.W., et al., A diverse range of gene products are effectors of the type I interferon antiviral response. *Nature*, 2011. **472**(7344): p. 481-5.
6. Wang, Y., et al., Cross Talk between Nucleotide Synthesis Pathways with Cellular Immunity in Constraining Hepatitis E Virus Replication. *Antimicrob Agents Chemother*, 2016. **60**(5): p. 2834-48.
7. Debing, Y., et al., Update on Hepatitis E Virology:Implications for Clinical Practice. *J Hepatol*, 2016.
8. Kumar, A., et al., Association of cytokines in hepatitis E with pregnancy outcome. *Cytokine*, 2014. **65**(1): p. 95-104.
9. Dalton, H.R., J.G. Hunter, and R.P. Bendall, Hepatitis E. *Curr Opin Infect Dis*, 2013. **26**(5): p. 471-8.
10. Kamar, N., et al., Hepatitis E. *Lancet*, 2012. **379**(9835): p. 2477-88.
11. Hakim, M.S., et al., The global burden of hepatitis E outbreaks: a systematic review. *Liver Int*, 2016.
12. Peters van Ton, A.M., T.J. Gevers, and J.P. Drenth, Antiviral therapy in chronic hepatitis E: a systematic review. *J Viral Hepat*, 2015. **22**(12): p. 965-73.
13. Janssen, H.L., et al., Pegylated interferon alfa-2b alone or in combination with lamivudine for HBeAg-positive chronic hepatitis B: a randomised trial. *Lancet*, 2005. **365**(9454): p. 123-9.
14. Debing, Y. and J. Neyts, Antiviral strategies for hepatitis E virus. *Antiviral Res*, 2014. **102**: p. 106-18.
15. Kamar, N., et al., Pegylated interferon-alpha for treating chronic hepatitis E virus infection after liver transplantation. *Clin Infect Dis*, 2010. **50**(5): p. e30-3.
16. Kamar, N., et al., Ribavirin for chronic hepatitis E virus infection in transplant recipients. *N Engl J Med*, 2014. **370**(12): p. 1111-20.
17. Debing, Y., et al., Ribavirin inhibits in vitro hepatitis E virus replication through depletion of cellular GTP pools and is moderately synergistic with alpha interferon. *Antimicrob Agents Chemother*, 2014. **58**(1): p. 267-73.
18. Zhou, X., et al., Disparity of basal and therapeutically activated interferon signalling in constraining hepatitis E virus infection. *J Viral Hepat*, 2016. **23**(4): p. 294-304.
19. Todt, D., et al., Antiviral activity of different interferon (sub-) types against hepatitis E virus replication. *Antimicrob Agents Chemother*, 2016.
20. Debing, Y., et al., Hepatitis E virus mutations associated with ribavirin treatment failure result in altered viral fitness and ribavirin sensitivity. *J Hepatol*, 2016. **65**(3): p. 499-508.
21. Todt, D., et al., Mutagenic Effects of Ribavirin on Hepatitis E Virus-Viral Extinction versus Selection of Fitness-Enhancing Mutations. *Viruses*, 2016. **8**(10).
22. Todt, D., et al., In vivo evidence for ribavirin-induced mutagenesis of the hepatitis E virus genome. *Gut*, 2016. **65**(10): p. 1733-43.
23. Lhomme, S., et al., Mutation in the Hepatitis E Virus Polymerase and Outcome of Ribavirin Therapy. *Antimicrob Agents Chemother*, 2016. **60**(3): p. 1608-14.
24. Schoggins, J.W., et al., Pan-viral specificity of IFN-induced genes reveals new roles for cGAS in innate immunity. *Nature*, 2014. **505**(7485): p. 691-5.

25. Kane, M., et al., MX2 is an interferon-induced inhibitor of HIV-1 infection. *Nature*, 2013. **502**(7472): p. 563-6.
26. Kane, M., et al., Identification of Interferon-Stimulated Genes with Antiretroviral Activity. *Cell Host Microbe*, 2016. **20**(3): p. 392-405.
27. Liu, Z., et al., The interferon-inducible MxB protein inhibits HIV-1 infection. *Cell Host Microbe*, 2013. **14**(4): p. 398-410.
28. Weber, M., et al., Incoming RNA virus nucleocapsids containing a 5'-triphosphorylated genome activate RIG-I and antiviral signaling. *Cell Host Microbe*, 2013. **13**(3): p. 336-46.
29. Miyamoto, M., et al., Regulated expression of a gene encoding a nuclear factor, IRF-1, that specifically binds to IFN-beta gene regulatory elements. *Cell*, 1988. **54**(6): p. 903-13.
30. Wang, W., et al., Convergent Transcription of Interferon-stimulated Genes by TNF-alpha and IFN-alpha Augments Antiviral Activity against HCV and HEV. *Sci Rep*, 2016. **6**: p. 25482.
31. Cho, H., et al., Differential innate immune response programs in neuronal subtypes determine susceptibility to infection in the brain by positive-stranded RNA viruses. *Nat Med*, 2013. **19**(4): p. 458-64.
32. Montero, H., R. Garcia-Roman, and S.I. Mora, eIF4E as a control target for viruses. *Viruses*, 2015. **7**(2): p. 739-50.
33. Sonenberg, N. and A.G. Hinnebusch, Regulation of translation initiation in eukaryotes: mechanisms and biological targets. *Cell*, 2009. **136**(4): p. 731-45.
34. Kentsis, A., et al., Ribavirin suppresses eIF4E-mediated oncogenic transformation by physical mimicry of the 7-methyl guanosine mRNA cap. *Proc Natl Acad Sci U S A*, 2004. **101**(52): p. 18105-10.
35. Isaacson, M.K. and H.L. Ploegh, Ubiquitination, ubiquitin-like modifiers, and deubiquitination in viral infection. *Cell Host Microbe*, 2009. **5**(6): p. 559-70.
36. Karpe, Y.A. and X.J. Meng, Hepatitis E virus replication requires an active ubiquitin-proteasome system. *J Virol*, 2012. **86**(10): p. 5948-52.

Chapter 12

Nederlandse Samenvatting

Dutch Summary

Samenvatting voor de leek

Het hepatitis E virus (HEV) is één van de belangrijkste oorzaken van virale hepatitis. Het HEV komt het bloed binnen via het maag-darm kanaal en kan zich uitstekend vermenigvuldigen in de lever. Het beloop van een acute HEV-infectie wordt gekenschetst door een aantal stadia: van subklinisch, naar acuut en uiteindelijk naar fulminant. De ziekte hepatitis E wordt in steeds grotere mate gezien als een “public health concern”. Ofschoon de mortaliteit van 0.2 – 1.0% relatief klein lijkt, kan deze bij zwangere vrouwen in het laatste trimester van de zwangerschap stijgen tot 20 - 25%. Daarnaast zijn er belangrijke zorgen over het risico van juist dit virus voor andere groepen patiënten en met name voor transplantatiepatiënten. Zulke patiënten krijgen immunosuppressieve medicijnen voorgeschreven die mogelijk de afweer tegen HEV zouden kunnen aantasten. Onfortuinlijker wijze is er weliswaar toch wel heel wat literatuur over de mechanismen waarmee het lichaam zichzelf verdedigt tegen HEV infectie, maar is deze goed samengevat noch afdoende geanalyseerd. Om deze deficiëntie te repareren voer ik in **hoofdstuk** 2 en **hoofdstuk** 3 een systematisch literatuuronderzoek uit, waar ik mij met name concentreer op de interferonen (inflammatoire hormonen belangrijk bij de virale afweer) alsook de zogenaamde ISGs (genproducten die van het DNA worden afgeschreven volgend op stimulatie van cellen door interferonen en die de uiteindelijke antivirale werking uitvoeren). Deze analyse vormt de basis van experimentele studies in de daarop volgende **hoofdstuk** ken.

In **hoofdstuk** 4 begin ik eerst met het karakteriseren van verschillende immuun relevante hormonen met betrekking tot hun invloed op HEV infectie. Deze studie kreeg een extra dimensie door de resultaten te vergelijken met de werking van deze hormonen op infectie door het hepatitis C virus. Ik laat hier zien dat met name interferon alfa een krachtig anti-HEV effect heeft en deze studie steunt dan ook het gebruik van interferon alfa in HEV-besmette patiënten.

In **hoofdstuk** 5 concentreer ik mij met name op de ISGs en karakteriseer welke van deze ISGs belangrijk bij het bestrijden van HEV. Het blijkt dat specifiek het RIG-I ISG hier belangrijk is (samen met andere) en ik besteed aandacht aan het moleculaire mechanisme van dit ISG in haar gevecht met het HEV. De hoop is dat zulke fundamentele studies van hulp kunnen zijn bij het ontwikkelen van nieuwe rationele therapie om het HEV te bestrijden. Omdat in mijn studies beschreven in **hoofdstuk** 5 ook bleek dat IRF1 een krachtige ISG is met

betrekking tot HEV infectie, besloot ik in **hoofdstuk** 6 ook op basaal niveau de werking van dit ISG te onderzoeken. Ook omdat ik een veelheid van modelsystemen gebruik in dit hoofdstuk geeft het resultaat een goed beeld van de betrokken moleculaire mechanismen. Bovendien onderzoek ik de interactie van IRF1 met ribivarine therapie (een belangrijk wapen van de geneesheer in het gevecht met het HEV), wat van belang kan zijn voor artsen die dergelijke therapie voor HEV-besmette patiënten willen inzetten. Gelijkaardig ga ik in **hoofdstuk** 7 het proinflammatoire hormoon TNF-alfa onderzoeken. Dit hormoon wordt meer geassocieerd met het bestrijden van bacteriële infectie, ik laat echter zien dat het ook de anti-virale afweer ondersteunt. Het mechanisme is nieuw: TNF alfa werkt door het stimuleren van de productie van ISGs. Een belangrijke implicatie is dat patiënten die anti-TNF alfa therapie krijgen verdacht moeten zijn op HEV infectie.

Ook zonder interferonen kan het lichaam het gevecht aan met het HEV virus. De mechanismen vragen weer productie van ISGs. In **hoofdstuk** 8 karakteriseer ik het moleculaire mechanisme die deze constitutieve afweer onderligt, verder inzicht verschaffend.

Een venster op verbeterde behandeling van hepatitis E in de toekomt wordt geopend in **hoofdstuk** 9. Hier bestudeer ik de importantie van de zogenaamde cellulaire proteïnet-vertalendemachinerie voor de infectie metn HEV. Ik laat zien dat het afremmen van elementen uit deze processen een sterke antivirale werking heeft, met name het inhiberen van eIF4E remt virale replicatie in sterke mate. Omdat deze remming onafhankelijk is van interferon alfa en ribavirine, zou het eIF4E dus een belangrijk nieuw doelwit kunnen zijn voor nieuwe antivirale therapie. Onfortuinlijker wijze lijkt dit niet het geval voor de proteosoom inhibitor MG132. Anderen hadden reeds gerapporteerd dat deze remmer effectief was was voor het bestrijden van HEV infectie. In **hoofdstuk** 10 helaas, laat ik zien dat deze observaties waarschijnlijk niet specifiek zijn en dat proteosoominhibitoren geen toekomst hebben in de behandeling van hepatitis E.

In het laatste hoofdstuk (**hoofdstuk** 11) van dit proefschrift tenslottega ik alle kennis die ik heb verzameld gedurende mijn promotieonderzoek duiden en integreren en inkaderen in de reeds beschikbare biomedische literatuur. Ik doe daar uitspraken over de mechanismen die worden aangezwengeld door het lichaam om het virus bestrijden. Samen hoop ik dat mijn studies een nieuwe bijdrage hebben in de strijd der mensheid tegen hepatitis E.

Appendix

Acknowledgements

Publications

PhD Portfolio

Curriculum Vitae

Acknowledgements

I would like to give my sincere gratitude to all those people who give their kindly help during my four-year Ph.D. study in Rotterdam. During this period, I have taken my efforts, but I could not complete this without all your help.

First, I would like to express my sincere gratitude to my promoter, Dr. Prof. Maikel Peppelenbosch and to my co-promoter, Dr. Qiuwei Pan.

Dr. Qiuwei Pan, thank you all the support and encouragement during my four-year study in Rotterdam. When I first met you, I was deeply inspired by your enthusiasm to scientific research. When you talk about scientific research, you are always full of passion. You always encourage me when I have problems in my research. I have learned a lot from you about how to general research questions, how to write a manuscript and how to present my research. I am so glad that have the opportunity to work with you and under your supervision during the past years.

Prof. Dr. Maikel P. Peppelenbosch, thank you for all the valuable suggestions for my research. You are such a knowledgeable and talent people who know almost everything in biological filed. I can always learn new knowledge and new techniques during the regular meeting we had. You innovative and creative ideas help me have a deeper and wider vision about my research. You are also a wisdom and humor person, you can always explain the difficult scientific question in an easy and interestingly way. Thank you for the critical reversion about the manuscript of my paper and this thesis.

Dr. Luc van der Laan, thank you for the discussion for my projects. You always encourage me every time when we have a discussion and when I got some good news. I am so glad that you will be in my promotion as an Inner Committee.

I would like to thank Dr. Ron Smits. You are very knowledgeable and kind person. You are always ready to help when we have problems during experiments. Thank you for being so patient and kind when teaching me different kinds of techniques.

Prof. Dr. Robbert de Man, I am honored to have you as Inner Committee for my promotion. Thank you!

Prof. Nassim Kamar, thank you for the valuable suggestion on our research. It is my honor to have the chance met and discussed with you at the International Liver Congress.

Dr. Dave Sprengers, thank you for all your suggestions during the regular meeting. You always rise up the question about what is the clinical implication of our research. This is very helpful for my research.

Dr. Gwenny Fuhler, thank you for your help during the last four years. You are so generous that always share your techniques and materials with us. In the Monday seminar, you gave me many valuable suggestions for my research.

Dr. Auke Verhaar, thank you for giving me so much help for ordering molecular stuff. Each time when we need something in the lab, you always provide them very quickly.

To Yuebang, we are very good friends. You are always being supportive and helpful. When I first arrived Holland, you gave me so much help in all kinds of things. You also helped so much with my experiments. You are always energetic and optimistic. We have spent countless memorable time together in the lab and visiting outside. I really appreciate we can be good friends and I believe this friendship will last forever!

To Wenshi, you are a very nice and smart person. You helped me so much for my experiments and gave some many valuable suggestions for my research. You always have creative ideas about research study and I had learned a lot from you. You invited me to your home many times and we spend lots of fun time together. I wish you have a bright future and have a happy marriage with Hongbo.

To Wenhui, we came to Rotterdam almost at the same time and soon became good friends. We shared one apartment for almost one year and you are a really nice person. Thank you for inviting me to you home so many times. All the best to you and your husband, Zhiyong and your son, Luhan.

To Xinying, thank you for showing me around the lab and teaching me to do different kinds of experiments when I first came to the lab. You organized a lot of interesting group activities and we really enjoy them.

To Yijin, you are a very smart and independent girl. Thank you for all the help for my experiments. Thank you for organizing a nice trip to Belgium.

To Wanlu, thank you for helping do the confocal microscope experiment and providing the important materials for my experiments. Thank you for all the encouragements. Wish you a bright future.

To Wen, thank you for all your help to my experiment. You always cook for us when we have a party or a trip. Good luck with your research.

To Pengyu, you are a knowledgeable and smart person. You always will to explore new research technologies and teach them to us. Thank you for your help to my research. Wish you a bright future.

To Shan, thank you for cooking us the best and delicious foods and we had lots of interesting time. Wish you have great achievement in your future research.

To Prof. Kairong Wang, you are like a big brother for me. Thank you for sharing us with your experience on research and life without reservation. Wish you all the best in China.

To Dr. Kan Chen, thank you for giving us interesting lectures about immunology. All best to you and your family.

To Dr. Menggang Liu, it is very interesting and eye-open to listen from you talk about the clinical and surgery knowledge. Wish you all the best in Rotterdam and back to China.

To Manzhi, thank you for your help on my research and bringing lots of food to us. Wish you all the best for you research and a happy marriage with Maoxing.

To Meng, Buyun and Changbo, thank you for inviting me to your place for interesting parties. I thank you for all the help you gave to me.

To Sunrui, Jiaye thank you for all the nice food you bring for us. Wish you have a nice stay in Rotterdam.

To Guoying, thank you for inviting me to your house and the nice party, wish you have a happy marriage with Tang Ying.

To Yingying, thank you for sharing food with us. I give my best wishes to you and your husband, Zhanmin and your lovely son Hengyu.

To Elmer, thank you for organizing so many interesting lab parties. To Rik and Wesley, we had a wonderful time that played basketball together. Wish all you guys good luck in the future.

To Petra, thank you for giving us working instruction and keeping us lab running in good condition.

To Sonja, thank you for organizing the regular Monday Seminar. I also thank you for all the suggestions you gave to my research.

To Hakim, thank you for the interesting discussion on my research.

To Monique, you are so kind and patient when teaching to culture organoids. Thank you for your kindly help for my experiments.

To Marieke, thank you for helping me with the flow cytometry experiments.

To Raymond and Leonie, thank you for all your help and assistance.

To my office members, Martijn, Lauke, Lisanne, Jasmine, Michiel, Juan Li and Zhouhong. I want to thank you all for your support during the past years. I really appreciate being in one office with all you guys and thanks for the great time we had together. My best wishes to all of you.

To all MDL members and some people whom may have left the lab, Hugo, Jaap, André, Marcel, Thomas, Wouter, Evelyne, Sergey, Pauline, Que, Xiaolei, Pratika, Vincent, Anthonie, Kim, Kostas, Aniek, Nadine, Alexander, Henk, Gertine, Paula, Jan, Shaoshi and so on. I want to thank you all your kindly help during my four-year stay in Rotterdam. My best wishes to all of you!

To my friends Bin Wu, Tao Lu, Shihao, Zhihao, Jinluan, Ling Huang, Ling Yan, and Changbin, thank you for your kindly helps, my best wishes to all of you!

To Dr. Prof. Yanming Zhang, my supervisor of Master research, thank you for your kindly help during my master study. You encouraged me to pursue a higher level of scientific research. Thank you!

I would like also give my great thanks to the financial support from the China Scholarship Council.

Last but not least, to Yang, my beloved wife, thank you for all your love and support. You always comfort and encourage me when I face difficulties. Without all your love and support, I could not finish my study. To my dear father, mother, young sister, grandfather, grandmother and all family members, you give me the biggest support during all my life. I give all my best wishes to you.

Publications list

1. **L. Xu,** W. Wang, Y. Li, X. Zhou, Y. Yin, Y. Wang, R. A. de Man, Luc J. W. van der Laan, F. Huang, N. Kamar, M. P. Peppelenbosch and Q. Pan (2017). RIG-I Is a Key Antiviral Interferon-Stimulated Gene Against Hepatitis E Virus Dispensable of Interferon Production. *Hepatology*. In Press

2. **L. Xu,** W. Wang, M. P. Peppelenbosch and Q. Pan (2017). Noncanonical Antiviral Mechanisms of ISGs: Dispensability of Inducible Interferons. *Trends Immunol*. 2017. 38(1):1-2

3. **L. Xu,** X. Zhou, W. Wang, Y. Wang, Y. Yin, L. J. Laan, D. Sprengers, H. J. Metselaar, M. P. Peppelenbosch and Q. Pan (2016). IFN regulatory factor 1 restricts hepatitis E virus replication by activating STAT1 to induce antiviral IFN-stimulated genes. *FASEB J.* 30(10): 3352-3367.

4. Wang, W., **L. Xu,** J. Su, M. P. Peppelenbosch and Q. Pan (2017). Transcriptional Regulation of Antiviral Interferon-Stimulated Genes. *Trends Microbiol*. In Press

5. W. Wang, Y. Yin, **L. Xu**, J. Su, F. Huang, Y. Wang, P. P C Boor, K. Chen, W. Wang, W Cao, X. Zhou, P. Liu, L. J. W. van der Laan, J. Kwekkeboom, M. P. Peppelenbosch and Q. Pan (2017). Unphosphorylated ISGF3 Drives Constitutive Expression of Interferon-stimulated Genes to Protect Against Viral Infections. *Sci Signal*. In Press.

6. Yin, Y., W. Dang, X. Zhou, **L. Xu,** W. Wang, W. Cao, S. Chen, J. Su, X. Cai, S. Xiao, M. P. Peppelenbosch and Q. Pan (2017). PI3K-Akt-mTOR axis sustains rotavirus infection via the 4E-BP1 mediated autophagy pathway and represents an antiviral target. *Virulence.* In Press.

7. Wang, W., Y. Wang, Y. Debing, X. Zhou, Y. Yin, **L. Xu**, E. Herrera Carrillo, J. H. Brandsma, R. A. Poot, B. Berkhout, J. Neyts, M. P. Peppelenbosch and Q. Pan (2017). Biological or pharmacological activation of protein kinase C alpha constrains hepatitis E virus replication. *Antiviral Res*. 140: 1-12.

8. Zhou, X., F. Huang, **L. Xu,** Z. Lin, F. M. S. d. Vrij, A. C. Ayo-Martin, M. v. d. Kroeg, M. Zhao, Y. Yin, W. Wang, W. Cao, Y. Wang, S. A. Kushner, J. M. Peron, L. Alric, R. A. d. Man, B. C. Jacobs, J. J. v. Eijk, E. M. A. Aronica, D. Sprengers, H. J. Metselaar, C. I. d. Zeeuw, H. R. Dalton, N. Kamar, M. P. Peppelenbosch and Q. Pan (2017). Hepatitis E virus infects neurons and brains. *J Infect Dis*. In Press.

9. Wang, W., **L. Xu,** J. H. Brandsma, Y. Wang, M. S. Hakim, X. Zhou, Y. Yin, G. M. Fuhler, L. J. van der Laan, C. J. van der Woude, D. Sprengers, H. J. Metselaar, R. Smits, R. A. Poot, M. P. Peppelenbosch and Q. Pan (2016). Convergent Transcription of Interferon-stimulated Genes by TNF-alpha and IFN-alpha Augments Antiviral Activity against HCV and HEV. *Sci Rep.* 6: 25482.

10. Wang, W., **L. Xu,** P. Liu, K. Jairam, Y. Yin, K. Chen, D. Sprengers, M. P. Peppelenbosch, Q. Pan and R. Smits (2016). Blocking Wnt Secretion Reduces Growth of Hepatocellular Carcinoma Cell Lines Mostly Independent of beta-Catenin Signaling. *Neoplasia*. 18(12): 711-723.

11. Zhou, X., **L. Xu**, W. Wang, K. Watashi, Y. Wang, D. Sprengers, P. E. de Ruiter, L. J. van der Laan, H. J. Metselaar, N. Kamar, M. P. Peppelenbosch and Q. Pan (2016). Disparity of basal and therapeutically activated interferon signalling in constraining hepatitis E virus infection. *J Viral Hepat*. 23(4): 294-304.

12. Wang, Y., W. Wang, **L. Xu,** X. Zhou, E. Shokrollahi, K. Felczak, L. J. van der Laan, K. W. Pankiewicz, D. Sprengers, N. J. Raat, H. J. Metselaar, M. P. Peppelenbosch and Q. Pan (2016). Cross Talk

between Nucleotide Synthesis Pathways with Cellular Immunity in Constraining Hepatitis E Virus Replication. *Antimicrob Agents Chemother.* 60(5): 2834-2848.

13. Zhou, X., **L. Xu**, Y. Wang, W. Wang, D. Sprengers, H. J. Metselaar, M. P. Peppelenbosch and Q. Pan (2015). Requirement of the eukaryotic translation initiation factor 4F complex in hepatitis E virus replication. *Antiviral Res*. 124: 11-19.

14. Yin, Y., M. Bijvelds, W. Dang, **L. Xu,** A. A. van der Eijk, K. Knipping, N. Tuysuz, J. F. Dekkers, Y. Wang, J. de Jonge, D. Sprengers, L. J. van der Laan, J. M. Beekman, D. Ten Berge, H. J. Metselaar, H. de Jonge, M. P. Koopmans, M. P. Peppelenbosch and Q. Pan (2015). Modeling rotavirus infection and antiviral therapy using primary intestinal organoids. *Antiviral Res*. 123: 120-131.

15. Yin, Y., Y. Wang, W. Dang, **L. Xu,** J. Su, X. Zhou, W. Wang, K. Felczak, L. J. van der Laan, K. W. Pankiewicz, A. A. van der Eijk, M. Bijvelds, D. Sprengers, H. de Jonge, M. P. Koopmans, H. J. Metselaar, M. P. Peppelenbosch and Q. Pan (2016). Mycophenolic acid potently inhibits rotavirus infection with a high barrier to resistance development. *Antiviral Res*. 133: 41-49.

16. **L. Xu,** X. Zhou, M. P. Peppelenbosch and Q. Pan (2015). Inhibition of hepatitis E virus replication by proteasome inhibitor is nonspecific. *Arch Virol.* 160(2): 435-439.

17. Wang, J., G. Hu, W. Gao, **L. Xu**, P. Ning and Y. Zhang (2014). Immortalized porcine intestinal epithelial cell cultures susceptible to porcine rotavirus infection. *J Virol Methods.* 202: 87-94.

18. Zhang, C., L. He, K. Kang, H. Chen, **L. Xu** and Y. Zhang (2014). Screening of cellular proteins that interact with the classical swine fever virus non-structural protein 5A by yeast two-hybrid analysis. *J Biosci.* 39(1): 63-74.

19. Wang, J., G. Hu, Z. Lin, L. He, **L. Xu** and Y. Zhang (2014). Characteristic and functional analysis of a newly established porcine small intestinal epithelial cell line. *PLoS One.* 9(10): e110916.

20. Ning, P., M. Guo, K. Guo, **L. Xu**, M. Ren, Y. Cheng and Y. Zhang (2013). Identification and effect decomposition of risk factors for Brucella contamination of raw whole milk in china. *PLoS One*. 8(7): e68230.

21. Ning, P., K. Guo, L. Cheng, **L. Xu**, C. Zhang, H. Cui, Y. Cheng, R. Xu, W. Liu and Q. Lv (2013). Pilot survey of raw whole milk in China for *Listeria monocytogenes* using PCR. *Food Control*. 31(1): 176-179.

22. Ning, P., K. Guo, **L. Xu**, R. Xu, C. Zhang, Y. Cheng, H. Cui, W. Liu, Q. Lv, W. Cao and Y. Zhang (2012). Short communication: evaluation of Brucella infection of cows by PCR detection of Brucella DNA in raw milk. *J Dairy Sci.* 95(9): 4863-4867.

PhD Portfolio

Name PhD Student Lei Xu

Erasmus MC Department Gastroenterology and Hepatology

Ph.D Period October 2013 - June 2017

Promotor Prof. Dr. Maikel P. Peppelenbosch

Copromotor Dr. Qiuwei Pan

General Courses

- 2014, the workshop on Photoshop and Illustrator CS5
- 2014, the Virology Course and Symposium
- 2014, Microscope Image Analysis: From Theory to Practice
- 2015, the Course Biomedical Research Techniques XIII

National and International Conferences

- 2015, Annual Day of the Molecular Medicine Postgraduate School, Rotterdam, the Netherlands. (Poster presentation)
- 2016, 51th the International Liver Congress™ (EASL, European Association for the Study of the Liver), Barcelona, Span (Oral presentation for Early morning workshop)
- 2016, 9th Dutch Experimental Gastroenterology and Hepatology (DEGH) meeting. Veldhoven, The Netherlands (2 Poster presentation)
- 2016, Annual Day of the Molecular Medicine Postgraduate School, Rotterdam, the Netherlands. (Poster presentation)
- 2017, 52th the International Liver Congress™ (EASL, European Association for the Study of the Liver), Amsterdam, the Netherlands (Oral presentation)

Academic Awards

- 2016, 51th the International Liver Congress™ (EASL, European Association for the Study of the Liver), Barcelona, Span (€650)
- 2013, China Scholarship Council (CSC) Scholarship (File No. 201306300027)

Curriculum Vitae

Lei Xu was born on October 10, 1987, in Yangling, Shaanxi Province, China. He attended primary, middle and high school in Yangling.

In 2005, he moved to Changchun City in Jilin Province and started his undergraduate study. He majored in Veterinary Medicine (5 years) in the College of Animal Science and Veterinary Medicine at Jilin University. During that time, he participated in a project aimed to develop a colloidal gold immunoassay strip for the rapid detection of Goose Paramyxovirus. He obtained his Bachelor degree in 2010. He started master research in the same year at Northwest Agriculture and Forest University, Yangling. He studied at the College of Veterinary Medicine under the supervision of Prof. Yanming Zhang. His main interest was to study the function of two unidentified viral proteins of Porcine Circovirus Type 2. He obtained his Master degree in 2013.

In 2013, with the support of China Scholarship Council, he got an opportunity to start his Ph.D research at the department of Gastroenterology and Hepatology, Erasmus Medical Center Rotterdam, the Netherlands. Under the supervision of Prof. Maikel P. Peppelenbosch and Dr. Qiuwei Pan, he mainly focused on the innate immunity and hepatitis E virus infection. He was dedicated to elucidating the important role of IFN pathway in defending HEV infection. He will continue his research on the interaction of innate immunity and pathogen infection at Northwest Agriculture and Forest University.